



**University of
Nottingham**
UK | CHINA | MALAYSIA

Emergent spacetime properties from entanglement

Candidate

Eugenia Colafranceschi

Thesis Advisors

Prof. Gerardo Adesso

Dr. Daniele Oriti

*Thesis submitted to the University of Nottingham
for the degree of Doctor of Philosophy*

July 2022

A nonna Franca e nonno Gino

Abstract

The last century saw the development of two revolutionary theories: Einstein’s general relativity, which taught us that spacetime is a physical system, i.e. the gravitational field; and quantum mechanics, which revealed properties of microscopic systems foreign to the way we perceive reality in our everyday life, such as non-locality. We are now trying to reach a new turning point: the formulation of a theory of quantum gravity, capable of reconciling these revolutionary discoveries from microscopic to macroscopic scales, i.e. describing physical scenarios in which both gravity and quantum mechanics do enter, and matching validated theories for those where only one (or none) of the two does.

Various background-independent approaches to the problem of quantum gravity postulate that, at the Planck scale, spacetime dissolves into a microstructure of discrete, pre-geometric quantum entities, leading to the picture of continuum spacetime and geometry emerging from their collective behaviour. Entanglement, and more generally all quantum correlations generated by the interactions of the fundamental entities, are thus expected to play a key role in this phenomenon; moreover, in such a background-independent hence purely relational setting, continuum spacetime and geometry have to be reconstructed from them. In recent years, several results supported this view by uncovering a close relationship between entanglement and spacetime geometry and topology. Furthermore, entanglement turned out to be deeply tied to a likely constitutive aspect of gravity: holography, which has been a guiding theme of research in quantum gravity since the formulation of the Bekenstein-Hawking area law for the black hole entropy. Understanding the origin of the threefold connection among gravity, holography and entanglement would therefore be a major step towards the formulation of a theory of quantum gravity.

The work we are going to present tackles this issue from an information-theoretic perspective, inspired by the cited view of spacetime properties emerging from the quantum information generated and transferred by the interactions among the fundamental entities. We specifically investigate the entanglement origin of the holographic behaviour of finite regions of quantum space modelled by spin networks. These are graphs coloured by quantum data encoding the geometric properties of elementary portions of space dual to their vertices, primarily known for providing a basis of the kinematic Hilbert space of loop quantum gravity. Our work starts with a characterization of spin networks as the entanglement skeleton of many-body states describing collections of “space quanta” in group field theory, a quantum gravity approach conceived to be a field theory *of* spacetime and interpreted as a second-quantization of loop quantum gravity. On the basis of the characterization of spin networks as graphs built up from the entanglement of space quanta, we establish a solid correspondence between this quantum gravity formalism and tensor networks, a quantum information language that realizes an efficient encoding of the entanglement structure of many-body states in the geometry of a network.

We rely on the correspondence we established between spin networks regarded as “entanglement graphs” and tensor networks to investigate the entanglement origin of holography in finite regions of space. On the basis of a bipartition of the quantum degrees of freedom associated to spin networks into bulk and boundary ones, we point out that every spin network state can be regarded as a map between these two sets, in the spirit of the Choi-Jamiołkowski isomorphisms of quantum information theory. This enables the translation of the “static” properties of a spin network state into the “dynamic” properties of the corresponding flow of information from the bulk to the boundary. In particular, we show that requiring such a flow to be an isometry - which is a necessary condition for holography - translates into the reduced bulk state maximising the entanglement entropy. The latter is computed by leveraging the tensor network reading of spin networks: assuming a random distribution of weights associated to the individual vertices, we exploit random tensor network techniques to map the computation of the entropy to the evaluation of the free energy of a classical Ising model defined on the spin network graph. The analysis of such a statistical model allows us to highlight the relation between the combinatorial structure and colouring of a spin network and the holographic character of the bulk-to-boundary flow of information it defines.

We deepen the investigation of holography on spin networks composed of random vertices by studying the impact of the bulk entanglement on the boundary entropy, with the latter computed through the random tensor network technique mentioned above. We highlight a regime (in terms of colouring and combinatorics of the spin network) in which the boundary entropy is determined by the area of a bulk surface (corresponding to the domain wall of the dual Ising model), with corrections given by the entropy of the bulk region enclosed by that surface. We also show that increasing the entanglement content of the bulk triggers a phase transition from such a “holographic regime” to a regime in which the boundary entropy satisfies a “area+volume” law, up to the emergence of a black hole like region in the bulk (in the dual statistical picture, a region the Ising domain wall cannot access).

The work described so far focuses on spacetime properties emergent from the quantum correlations of the space atoms at the level of quantum discrete geometry. The continuum, classical limit of the emergent spacetime scenario, a major issue in any quantum gravity approach, is not considered. The last part of this thesis is however dedicated to a comparable issue addressed in quantum information theory: the quantum-to-classical transition problem, i.e. how classical reality (i.e. what we perceive in our everyday life) emerges from the quantum microstructure of our world. We specifically study features of the emergence of objectivity of observables within the framework of quantum Darwinism, where multiple observers acquire information on a quantum system by probing fragments of its environment.

Non potevo lasciarti bandire da solo.
Senza di me, non bandiresti certo lontano.
Obelix

Acknowledgments

La frase di Obelix ad Asterix non è solo un omaggio alla metà migliore di me, la mia gemella Elena, ma anche a tutti coloro che hanno reso possibile il viaggio che mi ha portato fin qui.

Il mio primo ringraziamento va a Gerardo, per avermi dato fiducia e avermi seguito in questo percorso con un'attenzione e una premura eccezionali; per avermi supportato in ogni scelta, e avermi insegnato che la ricerca è sia curiosità che generosità. Un ringraziamento speciale va poi a Daniele, per essere stato una guida e un modello di ricerca nel senso più profondo e felice del termine: che non dà nulla per scontato, che dà valore ad ogni opinione, mai distruttiva ma sempre critica e propositiva.

Un ringraziamento affettuoso a Goffredo, per le tante discussioni stimolanti, per essere stato una presenza costante e un collaboratore speciale.

Sono poi moltissime le persone che vorrei ringraziare per tutto ciò che ho ricevuto, sul piano scientifico e personale, durante il mio percorso accademico all'università La Sapienza di Roma. Qui mi limiterò a citarne tre, che sono state per me dei mentori e dei punti di riferimento. Il Professor Giovanni Montani, le cui lezioni mi hanno fatto appassionare alla fisica gravitazionale, e i cui incoraggiamenti sono stati per me una risorsa preziosa. Il Professor Fabio Sciarrino, che ringrazio per avermi insegnato e fatto amare la fisica quantistica, e avermi consigliato e ispirato nelle scelte accademiche. Il Professor Giovanni Amelino Camelia, che con la sua profondità e schiettezza mi ha guidato e stimolato nei miei primi passi nel mondo della ricerca, e sui cui insegnamenti continuo a riflettere.

Vorrei ringraziare tutti gli amici e i colleghi di Nottingham, per avermi regalato momenti speciali; in particolare Carmine, per avermi accolto e coccolato fin dall'inizio, e Giulia, Nicola, Marco e Davide per avermi fatto sentire un po' a casa. Grazie al gruppo di Monaco, per avermi dato tanto sia dal punto di vista scientifico che umano. A Luca, per i momenti di confronto e condivisione. A Roukaya, per il suo affetto, la sua capacità di ascoltare e la sua energia positiva.

Grazie a Fabio, il mio amico geniale, per aver stravolto i miei schemi mentali più della fisica quantistica e gravitazionale. Grazie a Simen, per la sua amicizia sincera e premurosa. Grazie a Valeria, per avermi sempre incoraggiato e stimolato, e per essere la persona splendida che è.

Grazie alla mia compagna di viaggio, Francesca, per essermi sempre accanto e capirmi come solo un "pidocchio" sa fare.

Grazie, infine, alla mia famiglia, per essere il punto di partenza e arrivo del mio bandire.

Contents

List of Figures	xv
Preface	xix
1 Introduction	1
2 Spin networks for quantum geometry	5
2.1 Penrose's spin networks	5
2.2 Spin networks in lattice gauge theories	7
2.3 Loop quantum gravity and spin networks	10
2.3.1 Canonical formulation of general relativity in the Ashtekar-Barbero variables	10
2.3.2 Dirac quantization and structure of the kinematic sector of the theory . . .	12
2.3.3 Quantum operators and physical interpretation of spin networks	16
2.4 The GFT approach to quantum gravity	18
2.5 Entanglement and correlations on spin networks to probe and reconstruct geometry	21
2.5.1 On the horizon surface: correlations and bulk entropy	21
2.5.2 Distance from entanglement	22
2.5.3 Entanglement entropy and holographic spin networks	23
2.5.4 Gluing adjacent faces with entanglement	24
3 Spin networks as entanglement graphs: an information-theoretic characterization	25
3.1 Graphs and their adjacency matrix description	25
3.2 Labelled entanglement graphs	27
3.2.1 Embedding \mathcal{H}_γ into \mathcal{H}_N via group averaging	27
3.2.2 Entanglement graphs	28
3.2.3 Constructing entanglement graphs of arbitrary connectivity	29
3.2.4 Comparing graph states with the same number of vertices	30
3.2.5 Spin network states with individually weighted vertices	31
3.3 Unlabelled entanglement graphs	31
3.3.1 Unlabelled-graph states in the first-quantization language	31
3.3.2 Unlabelled-graph states in the second-quantization language	32
3.3.2.1 Unlabelled-graph states from individually weighted vertices	33
3.4 Combinatorial product	33
3.5 Effective distinguishability of vertices	35
3.6 The quantum information tool of Tensor Networks	36
3.6.1 Matrix Product States	37
3.6.2 Projected Entangles-Pair States	37

3.7	A simple realization of entanglement/topology and entanglement/geometry correspondences in GFT and TN	39
3.8	A dictionary between GFT states and (generalised) TN	41
3.9	Discussion	42
4	Holographic properties of random spin networks as entanglement graphs	45
4.1	Partitioning the degrees of freedom of spin networks: bulk and boundary subspaces	46
4.2	Random spin networks and dual statistical models	47
4.2.1	Random spin networks	47
4.2.2	Rényi entropy from Ising partition function	47
4.3	Holographic bulk-to-boundary maps from random spin networks	53
4.3.1	Spin network states as bulk-to-boundary maps	53
4.3.1.1	Fixed-spin case	53
4.3.1.2	General (spin-superposition) case	53
4.3.2	Isometry condition for bulk-to-boundary maps	54
4.3.3	Holographic character of bulk-to-boundary maps from random spin networks	55
4.3.3.1	Homogeneous case	56
4.3.3.2	Inhomogeneous case	58
4.3.4	Discussion	60
4.4	Holographic random spin network states and modelling of black hole horizons . . .	60
4.4.1	Homogeneous case	62
4.4.1.1	Non-dominant bulk entropy: Ryu–Takayanagi formula for homogeneous spin networks	62
4.4.1.2	Large bulk entropy and emergence of horizon-like regions in homogeneous spin networks	63
4.4.2	Inhomogeneous case	64
4.4.2.1	Non-dominant bulk entropy: Ryu–Takayanagi formula for inhomogeneous spin networks	65
4.4.2.2	Larger bulk entropy and emergence of horizon-like regions in inhomogeneous spin networks	66
5	Emergence of objectivity of observables	69
5.1	Improved bounds on the emergence of objectivity of observables	70
5.2	Testing optimality of the objectivity bound with an N -splitter	76
5.3	Quantum discord from local distribution of quantum correlations in infinite dimension	77
6	Conclusions	79
A	Notions of representation and recoupling theory	83
A.1	Algebra of representation functions	83
A.2	The Peter-Weyl decomposition	84
A.3	Intertwiner map and Schur’s lemma	84
A.4	Representation and recoupling theory of $SU(2)$	85
B	Average entropy from the Ising model	87
B.1	Randomization over the double copy of the vertex states	87
B.2	Contributions to the average entropy	87
B.2.1	Internal-link contribution	87
B.2.2	Boundary-edge contribution	88
B.2.3	Bulk contribution	88
B.2.4	Ising action	89

C	Supplemental material for the emergence of objectivity of observables	91
C.1	<i>f</i> -dependent objectivity bounds	91
C.2	Properties of the pure loss channel	95
C.2.1	Symmetry of the reduced dynamics	95
C.2.2	Lower bound for the objectivity range of a pure loss channel	96
C.3	Proof of Corollary 5.3.1	98

List of Figures

List of Figures

2.1	An example of Penrose’s spin network: every edge carries an integer corresponding to twice the angular momentum in units of \hbar	6
2.2	Subfigure (a) illustrates a graph edge e (black line) which punctures the surface S and is split by the intersection point into segments e_1 and e_2 ; the action of the operator $\hat{E}_i[S]$ on the holonomy $h_e[A]$ is given by Eq. (2.3.47). Subfigure (b) illustrates a sphere S containing just one spin network vertex v , and an elementary portion of it punctured only by the n -th edge of v , denoted as S_n . Since the spin network vertex is gauge invariant, the action of $\hat{E}_i[S]$ on it vanishes, see Eq. (2.3.49).	16
2.3	Excitation of the field $\phi(g^1, \dots, g^d) \in L^2(G^d/G)$ for the case $d = 4$. On the left, the simplicial representation as a tetrahedron with variables g^1, \dots, g^4 associated to the four faces, which are dual to the edges of a four-valent spin network vertex. On the right, the spin network vertex coloured by: spins j^1, \dots, j^4 on the edges, magnetic numbers n^1, \dots, n^4 at their free ends, and an intertwiner ι on the core.	19
2.4	Studying correlations between parts of the boundary (a) and between disjoint bulk regions (b). Both settings are equivalent to an intertwiner of the spins $\partial A \cup \partial B$, which can be unfolded as depicted in (c): two vertices corresponding to the subsystems ∂A and ∂B are connected by a “fictitious link” representing the correlations between them. For $j = 0$ the two subsystems are uncorrelated.	23
3.1	The gluing of the i -th edge of vertex v , denoted as e_v^i and depicted in red, to the i -th edge of vertex w , denoted as e_w^i and depicted in blue, gives rise to a link between v and w indicated as ℓ_{vw}^i	26
3.2	Gluing of two spin network vertices performed by acting on two open edges with the same group element and integrating over the latter. Group variables are depicted as large white disks (except for the element h through which the group acts, highlighted in red) and magnetic indices as small yellow disks; intertwiner tensors are instead represented by green squares. The group averaging is depicted in panel (a) and returns a pair of bivalent intertwiners contracting the magnetic indices of the two edges, as shown in panel (b).	28

4.1	Illustration of the replica trick in Eq. (4.2.5). In (a) the density matrix ρ on $\mathcal{H}_R \otimes \mathcal{H}_{\bar{R}}$ describing the state of the system: the black disks refer to the subsystems described by \mathcal{H}_R (top) and by $\mathcal{H}_{\bar{R}}$ (bottom), the white disks to the dual components. In (b) the l.h.s. of Eq. (4.2.5): the trace over \bar{R} (dashed green line) yields ρ_R ; the latter is then multiplied by itself (connection of internal disks) and traced over (dashed red line). In (c) the r.h.s. of Eq. (4.2.5): two copies of ρ_R are considered; the swap operator, whose action is denoted by a square, causes the trace to be performed across the two spaces. In (d) the factorization of the swap operator S for the single vertex on the intertwiner (large square in the center) and on each individual edge (small squares)	48
4.2	Relationship between a spin network state ρ_γ and the corresponding bulk-to-boundary superoperator Λ . The state $ \omega\rangle$ is a maximally entangled state of two copies of the bulk.	55
4.3	In the Ising action \mathcal{A}_0 , both the boundary spins μ (shown in red) and the bulk ones ν (shown in green) point up: $\mu_v = +1, \nu_v = +1 \forall v$	56
4.4	In the Ising action \mathcal{A}_1 , the boundary spins (in red) point up, but the bulk spins (in green) are flipped down: $\mu_v = -\nu_v = +1 \forall v$	56
4.5	For $\log D_j \gg \log d_j$ the minimal energy configuration for \mathcal{A}_1 is that with all Ising spins σ_v (shown in black) pointing down. Each pair of misaligned Ising- and boundary-spin carries a contribution to the free energy F_1 equal to $\log d_j$, so $F_1 = \partial\gamma \log d_j$	56
4.6	For $\log d_j \gg \log D_j$ the minimal energy configuration is that with all Ising spins σ_v (shown in black) pointing up. Each pair of misaligned Ising- and bulk-spin carries a contribution to the free energy F_1 equal to $\log D_j$, so $F_1 = N \log D_j$	56
4.7	Ising configuration with Ising spins (shown in black) pointing down in a region X , bulk spins (in green) $\nu_v = -1 \forall v$ and boundary spins (in red) $\mu_v = +1 \forall v$. The contributions to \mathcal{A}_1 derive from: misaligned Ising- and boundary-spins (∂X_{ext}), misaligned Ising- and bulk-spins (region outside X) and misaligned nearest-neighbor Ising spins (∂X_{int}).	57
4.8	Spin network state given by the gluing (symbolised by the dotted lines) of random vertex tensors $f_v \in \mathcal{H}^{\vec{v}}$ (the green disks). ζ is the input state for the bulk degrees of freedom (intertwiners), depicted as input lines; $\psi(\zeta)$ is the output state for the boundary edges, depicted as output lines. The boundary entanglement entropy is computed for a set A of the latter, shown in red.	61
4.9	The minimum of H_1 is degenerate; the corresponding surfaces Σ_a and Σ_b , with area $ \Sigma_a = \Sigma_b = 5$, are shown by dashed red lines.	64
4.10	If intertwiner entanglement is present in a region Ω of the bulk (highlighted in yellow in the figure, as well as the vertices within it), the degeneracy of the minimal energy is removed. In fact, $ \Sigma_a = 6$ and $ \Sigma_b = 7$	64
4.11	By increasing the dimension of the bulk disk Ω via refinement of vertices, the minimal-energy surface Σ_c is prevented from entering it.	65
4.12	Each shell r crosses radial links carrying spin j_r ; vertices between shells r and $r+1$ recouple three spins j_r (one on the radial inward direction, two on the edges tangent to shell r) and one spin j_{r+1} (outward radial direction).	66
4.13	In absence of bulk entanglement, the Ising domain wall (the dashed red line) moves towards the center of the spherical geometry.	67
4.14	When a bulk disk of radius R is in a random pure state, the Ising domain wall is prevented from entering it.	67
5.1	Case $f_j = j^2$. We plot the upper bound on $\ \Lambda_j - \mathcal{E}_j\ _{\diamond_{H,E}}$ for $E = 1$ and $\delta = 0.01$, obtained through numerical optimisation of Eq. (5.1.17) over the truncation dimension d	74

-
- 5.2 Case $f_j = j$. We compare the upper bound on $\|\Lambda_j - \mathcal{E}_j\|_{\diamond_{H,E}}$ for $E = 1$ and $\delta = 0.01$, obtained by numerical optimisation of Eq. (5.1.23) over d (red dots, lowermost curve), with the bound obtained by Knott *et al.* in [62] (blue dots, uppermost curve). 75

Preface

This thesis is based on material from the following publications, which are the result of the research I carried out as a PhD student at the University of Nottingham from October 2018 to March 2022.

- [1] Eugenia Colafranceschi and Daniele Oriti. “Quantum gravity states, entanglement graphs and second-quantized tensor networks”. In: *JHEP* 07 (2021), p. 052. DOI: [10.1007/JHEP07\(2021\)052](https://doi.org/10.1007/JHEP07(2021)052). arXiv: [2012.12622](https://arxiv.org/abs/2012.12622) [[hep-th](#)].
- [2] Eugenia Colafranceschi, Goffredo Chirco, and Daniele Oriti. “Holographic maps from quantum gravity states as tensor networks”. In: *Phys. Rev. D* 105.6 (2022), p. 066005. DOI: [10.1103/PhysRevD.105.066005](https://doi.org/10.1103/PhysRevD.105.066005). arXiv: [2105.06454](https://arxiv.org/abs/2105.06454) [[hep-th](#)].
- [3] Goffredo Chirco, Eugenia Colafranceschi, and Daniele Oriti. “Bulk area law for boundary entanglement in spin network states: Entropy corrections and horizon-like regions from volume correlations”. In: *Phys. Rev. D* 105.4 (2022), p. 046018. DOI: [10.1103/PhysRevD.105.046018](https://doi.org/10.1103/PhysRevD.105.046018). arXiv: [2110.15166](https://arxiv.org/abs/2110.15166) [[hep-th](#)].
- [4] Eugenia Colafranceschi and Gerardo Adesso. “Holographic entanglement in spin network states: a focused review”. In: *AVS Quantum Sci.* 4 (2022), p. 025901. DOI: [10.1116/5.0087122](https://doi.org/10.1116/5.0087122). arXiv: [2202.05116](https://arxiv.org/abs/2202.05116) [[hep-th](#)].
- [5] Eugenia Colafranceschi, Ludovico Lami, Gerardo Adesso, and Tommaso Tufarelli. “Refined diamond norm bounds on the emergence of objectivity of observables”. In: *J. Phys. A* 53.39 (2020), p. 395305. DOI: [10.1088/1751-8121/aba469](https://doi.org/10.1088/1751-8121/aba469). arXiv: [2003.08153](https://arxiv.org/abs/2003.08153) [[quant-ph](#)].

Entanglement, the presence of quantum correlations between physical systems that causes them to lose their individuality as the composite system acquires physical properties that are inaccessible at the level of the individual subsystems, deeply challenged our classical view of reality: it brings to light that the classical notion of local and isolated system is an idealisation, and that the physical properties of a system are actually *defined* by the interactions with its environment. The change in perspective on reality brought about by quantum mechanics becomes even more radical when combined with the discovery, with Einstein’s general relativity, that spacetime is a physical, dynamical entity: the gravitational field. In fact, as any other physical system, spacetime is expected to possess quantum properties, e.g. to be discrete and subject to entanglement. This scenario led to a major challenge for theoretical physics in the last century: the merging of quantum mechanics and Einstein’s general relativity in a theory of [Quantum Gravity \(QG\)](#), capable to describe physical scenarios in which strong gravity and quantum mechanics effects overlap, as we expect to occur, for example, inside black holes. Over the last century, the problem of QG has been approached from different angles and with different techniques [6], leading to the emergence of several candidate theories: string theory, [Loop Quantum Gravity \(LQG\)](#) [7–9], [Group Field Theory \(GFT\)](#) [10–12], spinfoam models [13–15], causal dynamical triangulations [16, 17] and asymptotic safety [18], to name a few. However, so far none turned out to be a complete and fully consistent theory of QG.

Most background-independent approaches to QG share the view of spacetime being composed, at the Plank scale, of discrete and pre-geometric quantum entities. We then expect the entanglement generated by the interactions among the latter to trigger the emergence of classical, continuous aspects of gravity; moreover, since the description of quantum spacetime has to be (due to the requirement of background independence) purely relational, continuum spacetime and geometric notions (such as distance) have to be reconstructed from the quantum correlations of these fundamental entities. The idea of entanglement as the “fabric of spacetime” is supported by several results in QG and beyond, most obtained within the duality between the gravitational theory of asymptotically [Anti de Sitter \(AdS\)](#) spacetime and a [Conformal Field Theory \(CFT\)](#) living on the boundary of the latter, known as the [AdS/CFT](#) correspondence [19–22]. The Ryu-Takayanagi (RT) formula [23, 24], for example, relates the entanglement entropy of the boundary CFT to the area of a codimension-2 surface in the dual bulk spacetime. The entanglement-geometry relation pointed out by the RT formula is further strengthened by the observation [25, 26] that entanglement of the boundary-theory degrees of freedom is a necessary condition for the connectivity of the dual bulk spacetime. Also worth mentioning in the [AdS/CFT](#) context is the derivation, from the entanglement “first law” in CFT, of Einstein’s equations linearised about the [AdS](#) background, which promotes the entanglement-geometry relation to a dynamic level [27, 28]. The connection between geometry and entanglement also appears in contexts not directly related to QG, for example in the proof that a geometric space can emerge from the entanglement of quantum degrees of freedom associated to an abstract Hilbert space [29]. Crucially, the mentioned results are all pointing in the same direction: the idea of *spacetime as a geometric representation of entanglement*.

In recent years, the concept of entanglement has become increasingly intertwined with a driving theme of research in QG: holography. Broadly understood as the physical scenario in which all properties of a system confined in a certain region of space are encoded in the boundary of that region, holography has played a pivotal role in classical and quantum gravity since the derivation of the Bekenstein-Hawking area law for black hole entropy[30, 31], the discovery of the Hawking radiation[32] and the formulation of the information loss paradox[33]. Indeed, black holes being peculiar configurations of the gravitational field, holography was recognised to be a key element in understanding spacetime and gravitational physics at a more fundamental level [34–36], and over the last 25 years it has been extensively studied at both the classical and quantum level. An instance of holography in QG is the cited AdS/CFT correspondence, with all its offspring; other relevant examples include work on the microscopic interpretation of the black hole entropy[37–40], on the recovering of gravitational dynamics from the thermodynamics of boundaries[41, 42] and on the modelling of quantum black holes [43] and the holographic hypothesis [44, 45] in LQG. The holographic behaviour of both gravitational and non-gravitational physical systems has been traced back, in several contexts, to the structure of quantum correlations (specifically entanglement) of the fundamental degrees of freedom living on the bulk and on the boundary. It is the case for the results obtained within the AdS/CFT correspondence, since the bulk kinematic (e.g. area of surfaces) and dynamic (Einstein’s equations) can be related to the entanglement properties of degrees of freedom in the boundary CFT, as mentioned above. But it happens also in Quantum Information Theory (QIT) and condensed matter physics, as the entanglement entropy of quantum many-body systems in their ground states has been proven to follow an area law [46].

As pointed out, the view of spacetime as a geometric representation of entanglement comes from various corners while holography, which is expected to be a defining feature of gravity, is intimately tied to the entanglement structure of the involved degrees of freedom. In this thesis we explore the threefold connection among gravity, holography and entanglement by importing in a truly QG context a quantum information language which has been found to be particularly suitable for modelling holographic entanglement: Tensor Networks (TN) [47–50]. It decomposes the entanglement structure of many-body states into interconnected one-body tensors, which are represented as nodes of a network. This language has been largely exploited in the AdS/CFT correspondence starting from [51], which showed that the entanglement renormalization of CFT boundary states carries out a TN decomposition of the latter, with the possibility to interpret the emerging network as a spatial slice of the AdS spacetime, upon definition of a metric from combinatorial ingredients. Exactly-solvable models of the AdS/CFT correspondence have then been constructed through perfect [52] and random [53] tensors. These works (and many others of similar nature) leverage the above analogy - spacetime as a geometric representation of entanglement on one hand, and many-body wave-functions with a geometric description of their entanglement structure on the other - at an “operational” level to construct explicit examples of AdS/CFT states in terms of TN. However, it is possible to implement that analogy beyond the AdS/CFT context, and at a deeper level; this is one of the main purposes of the work presented in this thesis. *What if the “bodies” of the tensor network (i.e. the many-body wavefunction) were themselves quanta of space, with entanglement expressing adjacency relations between them?* The connection between entanglement and geometry would be structural, and gravity would be a quantum phenomenon in its own right. Let us stress that the last feature is prompted by the success of the standard model, which describes the other fundamental interactions via Quantum Field Theory (QFT). However, due to the background independence of gravity (and the inconsistency of a description of gravity in terms of local degrees of freedom, signalled by black hole thermodynamics), a QFT describing it certainly cannot be defined *on* spacetime. The QG approach of GFT [10–12], introduced below, captures all these insights, being a field theory of “quanta of space” glued to each other by entanglement, defined on a group manifold which provides the mathematical support to describe the geometrical features of the field quanta.

In the GFT approach to QG [10–12] the fundamental excitations of the field are to be understood as quanta of space, entangled to each other to form *spatial* geometries, and whose interaction processes give rise to *spacetime* geometries. Therefore, as stressed before, the manifold on which the field lives is not a spacetime manifold (as in standard QFT), but an abstract one encoding

the geometric properties of the space quanta. Specifically, the field lives on four copies of a Lie group, usually $SU(2)$, and the field quanta are 3-simplices (i.e. tetrahedra) having a group variable associated to each face; a gauge-invariance constraint on these variables ensures that they truly encode the quantum geometry of a 3-simplex. In a dual representation, the 3-simplex is a vertex with four edges, one for each face, decorated with the corresponding group variable. Equivalently (by representation theory of compact Lie groups), each edge is decorated by a spin, and the vertex by an intertwiner arising from the gauge-invariant recoupling of the edge spins, in what is called a *spin network vertex* (mainly known for being the basic kinematic structure of LQG). The gluing of vertices builds up *spin networks* (graphs decorated by the aforementioned quantum geometric data) dual to simplicial complexes and is realized, as anticipated above, by entangling vertex degrees of freedom. The Hilbert space of the theory is thus a Fock space for the spin network vertices, and the entanglement structure of many-body states pertaining to it represents a spin network graph dual to a discrete geometry. In other words, spin networks (as defined e.g. in LQG) arise in GFT as *entanglement patterns of many-body states associated to spin network vertices*. The principle is thus the same as that of TN, which are collections of tensors connected to each other via index contraction representing entanglement between the corresponding degrees of freedom.

Both formalisms of GFT and TN therefore rely on graphical structures built up from entanglement. The first achievement of the work we are going to present is to make this shared feature explicit and more precise, building on previous work which had already pointed out the analogy between spin networks and particular TN decompositions in LQG [54, 55] and in the first-quantization formulation of the GFT framework [56]. In particular, we are going to promote that analogy to the proper second-quantization setting of GFT, where a crucial difference with the quantum information language arises: while the GFT quanta are indistinguishable, the nodes of a tensor network, as normally defined, are not. But in a QG model the indistinguishability of the building blocks of space is a necessary condition for background independence; in fact, it can be understood as a discrete counterpart of invariance under diffeomorphisms, as vertex labels play the role of “coordinates” over an abstract combinatorial pattern. We are going to show that spin networks, regarded as GFT entanglement graphs, are generalised TN that, in addition to having a direct simplicial-geometry interpretation, naturally satisfy (a discrete version of) invariance under diffeomorphisms. This reading thus takes us beyond the practical advantages of applying TN to the AdS/CFT context: a purely quantum information language, which performs a geometric encoding of entanglement, gets identified with a QG (purely background independent) language that makes the connection between entanglement and geometry its structural principle. That is, QG and QIT dialogue on an interpretive level, not just on an operational one.

Once this dictionary is in place, we investigate holography as a quasi-local property entering the description of finite spatial boundaries, i.e. spacetime corners. We outline a setting for studying holography on spin networks through a suitable splitting of their degrees of freedom into bulk and boundary, and the characterization of them as quantum channels transferring information from one to the other. We then adapt to our setting a tensor network technique for the computation of the entanglement entropy of random states, which is based on translating the average entropy to the partition function of a classical, statistical dual model. The class of spin network states to which this technique applies is the one obtained by gluing (i.e. entangling) individual vertices in a random state. We then study holography on finite regions of space described by that random spin network states from two different perspectives:

- (1) we analyse under which conditions on the combinatorics and colouring of the spin networks the corresponding bulk-to-boundary flow of information is an isometry (a property required for the expectation values of observables to be preserved from bulk to boundary);
- (2) we investigate to which extent the entanglement entropy of the boundary reflects/is affected by the bulk.

The analysis of point (2) aims to identify a holographic regime for the boundary entropy, namely the configurations of random spin networks which give rise to an analogue of the RT formula, i.e. a dependence of the boundary entropy on the area of a bulk surface. By varying the parameters

governing these configurations (combinatorics and link colouring of the spin networks) we then trigger a phase transition from the holographic regime to one in which the boundary entropy follows an “area+volume” law. We also show that further variation of parameters in this direction (more precisely, an increase in the entanglement content of the bulk) causes the emergence of a horizon-like surface, thereby providing a concrete realisation of the proposal made by Krasnov and Rovelli in Ref. [43] of defining a quantum black hole as the part of a spin network that does not influence observables at infinity.

We began by discussing the role of entanglement (and quantum mechanics more generally) in challenging the way we think about reality, space and time based on our everyday “classical” experience. The quantum picture applied to gravity leads to the hypothesis of spacetime dissolving, at the Planck scale, into pre-geometric quantum entities, and the consequent view of continuum and classical gravitational physics emerging from them in a suitable regime of the underlying theory. However, the problem of how classical reality emerges from the quantum realm presents itself even if we disregard the quantum nature of spacetime, e.g. consider a Newtonian spacetime. In QIT, this is commonly referred to as the *quantum-to-classical transition problem*, and turns out to be intimately tied with the theory of decoherence [57–60]. The latter indeed reveals the crucial role played in this transition by the environment, which acts on physical systems as a source of decoherence. A possible solution to the problem is however provided by the theory of quantum Darwinism, which promotes the environment from source of decoherence to carrier of information about the system. More specifically, quantum Darwinism aims to explain how our objective classical reality arises from the quantum world by analysing the distribution of information about a quantum system that is accessible to multiple observers, who probe the system by intercepting fragments of its environment. In the last chapter of this thesis, we focus on the objectivity of observables arising in the quantum-to-classical transition within the premises of quantum Darwinism. Going beyond recent studies for finite- and infinite-dimensional systems [61, 62], we present a unified approach to derive bounds on the emergence of such objectivity in quantum systems of arbitrary dimension. We also prove, building on the finite-dimensional setting of [61], that an infinite-dimensional system cannot share quantum correlations with asymptotically many observers, as the maximum correlation each observer can establish with the system is, on average, of purely classical nature.

Outline of the thesis

In chapter 2 we review the formalism of spin networks for describing quantum spatial geometries, from its first appearance in the discrete and relational modelling of space due to Penrose to the modern one present in lattice gauge theories and the QG approaches of LQG and GFT. We also give an overview of results on the study of entanglement on spin network states and its role in reconstructing geometry.

In chapter 3 we illustrate the characterization of spin networks as graphs of entanglement in the GFT framework, and the formulation in terms of second-quantized TN.

In chapter 4 we present the tensor network technique we employ to trace the computation of the average entropy of random spin network states back to the evaluation of the partition function of a classical statistical model. We then present the investigation on holography on random spin networks, by analysing (1) the flow of information from the bulk to the boundary, relying on the Choi-Jamiołkowski duality of QIT; and (2) the information content of the boundary and its relationship with the bulk.

In chapter 5 we present the work on the emergence of objectivity of observables for quantum systems of arbitrary dimension, in the non-gravitational setting of the quantum-to-classical transition problem of QIT.

2

Spin networks for quantum geometry

Spin networks defined as graphs decorated by quantum data appear in several contexts: quantum gauge theories, QG, topological quantum field theories and CFT. Here we are interested in their role in QG, where they provide an orthonormal basis of states for the quantum geometry of space; in this role they in fact enter the QG approaches of LQG [7–9], spin foam models [13–15] and GFT [10–12]. The work presented in chapters 3 and 4 indeed focuses on a characterization of spin networks modelling quantum spatial geometries from an information-theoretic perspective, and leverage the latter for the investigation of quasi-local holography. In this chapter we nevertheless introduce spin networks from a broader angle: we start by illustrating, in section 2.1, the first appearance of the concept, which is due to Penrose. We then present, in section 2.2, the definition of spin networks in lattice gauge theories. This can be considered a base example for the use of these objects in QG, as it highlights that spin networks enter the theory by virtue of the role played in it by the holonomy of a connection. Spin networks indeed appear in LQG as a (background independent) $SU(2)$ gauge theory; this is illustrated in section 2.3. In the latter we also explain in detail the structure of the kinematic sector of LQG, as it provides an important ground of comparison with our results in GFT. In section 2.4 we present the GFT framework and the way spin networks enter it. Finally, in section 2.5 we review several results on the possibility to probe and reconstruct quantum geometry from the entanglement structure of spin network states.

2.1 Penrose’s spin networks

As mentioned above, the first appearance of the notion of spin networks as a discrete and relational (thereby background independent) model of quantum geometry is due to Penrose, who formulates it along the view that *discreteness* lies at the core of spacetime and quantum mechanics, and in the effort of building them up simultaneously from combinatorial principles. In fact, Penrose’s idea is getting rid of the continuum not via an approximation of it, but via a reformulation of the theory where discrete concepts are used as *primary concepts*, as basic building blocks of the theory. Continuous concepts are then expected to emerge in a limit, as the complexity of the model increases.

Moved by this idea, Penrose reconstructs a combinatorial notion of space by taking the *total angular momentum* as primary discrete concept (the discreteness being in its spectrum). Note that, in order to reconstruct a background independent notion of space, only the *total* angular momentum, not its projection along a certain direction, can be taken as primary concept. In fact, there is no pre-existing notion of space directions.

The model is composed of a set of “units”, each one representing a system with a well-defined total angular momentum $j = n\frac{\hbar}{2}$, where $n \in \mathbb{N}$ is the *spin-number*; a unit with spin-number n is called an n -unit. The units are depicted as line segments that meet at nodes, forming diagrams like the one in figure 2.1, where three units come together at each node. These diagrams are called *spin networks*. Importantly, the units are not given the interpretation of particles, nor does the network express their relative motion; they are just systems that transfer angular momentum

▷ *Beyond Lie groups* This is not an exclusive property of Lie algebras: Hopf algebras, for example, also possess it, and a generalised class of spin networks indeed corresponds to them [63].

2.2 Spin networks in lattice gauge theories

We show that in the gauge theory for a compact Lie group G spin networks are gauge invariant observables with support on a graph, where the latter is decorated by an element of the gauge group on each edge or, in the dual (via the Peter-Weyl theorem) basis by an irreducible representation of G on each edge and an intertwiner on each vertex. We also show, following Ref. [64], that a lattice gauge theory for $G = SU(2)$ can be written as a “sum over histories” of spin networks, namely as a spin foam model.

We start by introducing the key elements of non-abelian gauge theories, and then present their formulation on a lattice. A gauge theory for the connection (gauge field) A_μ^α , where μ is a spacetime index and α an index in the Lie algebra of the gauge group G , has an action of the following form:

$$S(A) = \int d^4x F(A) \wedge \star F(A) \quad (2.2.1)$$

where \star is the Hodge operator and $F(A)$ is a 2-form, the *curvature* of the connection A : $F(A) = dA - i\lambda A \wedge A$, with λ the gauge coupling. The action is invariant under group-valued transformations $g(x) \in G$ in every spacetime point x , under which

$$A_\mu(x) \rightarrow g^{-1}(x)A_\mu(x)g(x) + \frac{1}{\lambda}g^{-1}(x)\partial_\mu g(x), \quad (2.2.2)$$

while $F_{\mu\nu}$ transforms as follows:

$$F_{\mu\nu}(x) \rightarrow g^{-1}(x)F_{\mu\nu}(x)g(x) \quad (2.2.3)$$

The “natural variable” of a gauge theory is the parallel transport of the connection along a path e ,

$$h_e[A] = \mathcal{P} \exp \left\{ i\lambda \int_e A \right\} \in G, \quad (2.2.4)$$

with \mathcal{P} denoting path-ordering; in fact, the holonomy h_e transforms smoothly under the action of the gauge group:

$$h_e \rightarrow g^{-1}(s_e)h_e g(t_e) \quad (2.2.5)$$

where s_e and t_e are, respectively, source and target points of path e . It follows that for a closed path, namely a *loop* l , the holonomy h_l transforms as

$$h_l \rightarrow g^{-1}h_l g \quad (2.2.6)$$

A gauge-invariant quantity of the connection can be constructed out of h_l by taking the trace of the matrix associated to it in a given representation ρ :

$$W_l^\rho = \text{Tr}_\rho(h_l[A]) \quad (2.2.7)$$

as follows from the cyclic property of trace. This quantity is called *Wilson loop*, and depends exclusively on the loop l and the representation ρ .

We now proceed to present the discretization of the theory on a lattice. We consider a hypercube lattice in \mathbb{R}^D with lattice spacing equal to 1, and denote by N_μ the lattice size in the μ -th direction, with $1 \leq \mu \leq D$. The *lattice points* are defined as follows:

$$\Lambda^0 = \{ \vec{i} = (i_1, \dots, i_D) : i_\mu \in \{1, \dots, N_\mu\}, 1 \leq \mu \leq D \} \quad (2.2.8)$$

Unit vectors along the axes of the lattice are denoted by $\hat{\mu} := (0, \dots, 1_{(\mu)}, \dots, 0)$ for $1 \leq \mu \leq D$, so that the neighbour of the point \vec{i} in the μ -direction is $\vec{i} + \hat{\mu}$. In the following, we refer to a lattice

point \vec{i} with the simplified notation i (i.e. we omit the vector symbol). The k -cells of the lattice, i.e. elementary k -dimensional subregions, are defined as follows:

$$\Lambda^k = \{(i, \hat{\mu}_1, \dots, \hat{\mu}_k), i \in \Lambda^0, 1 \leq \mu_1 \leq \dots \leq \mu_k \leq D\} \quad (2.2.9)$$

Among them we have *links* (or *edges*) $(i, \hat{\mu}) \in \Lambda^1$ and *plaquettes* (or *faces*) $(i, \hat{\mu}, \hat{\nu}) \in \Lambda^2$. To indicate that a k -cell contains a k' -cell (where $k > k'$) we write $k\text{-cell} \supset k'\text{-cell}$.

The configuration variables of the theory can be regarded as maps which associate to any link $(i, \hat{\mu}) \in \Lambda^1$ a group element $g_{(i, \hat{\mu})}$ corresponding to the parallel transport of the continuum connection A along that link:

$$\begin{aligned} g: \Lambda^1 &\rightarrow G \\ (i, \hat{\mu}) &\rightarrow g_{(i, \hat{\mu})} = \mathcal{P} \exp \left\{ i\lambda \int_{(i, \hat{\mu})} A \right\} \end{aligned} \quad (2.2.10)$$

From Eq. (2.2.1) we see that the action of the gauge theory depends on the connection only via its curvature. The discrete counterpart of the latter is the map associating to any plaquette $(i, \hat{\mu}, \hat{\nu}) \in \Lambda^2$ the holonomy of the connection around its boundary:

$$\begin{aligned} h: \Lambda^2 &\rightarrow G \\ (i, \hat{\mu}, \hat{\nu}) &\rightarrow h_{(i, \hat{\mu}, \hat{\nu})} \end{aligned} \quad (2.2.11)$$

with

$$h_{(i, \hat{\mu}, \hat{\nu})} = g_{(i, \hat{\mu})} g_{(i+\hat{\mu}, \hat{\nu})} g_{(i+\hat{\nu}, \hat{\mu})}^{-1} g_{(i, \hat{\nu})}^{-1} \quad (2.2.12)$$

The last ingredient we need for the lattice formulation of the gauge theory is the generating function of a gauge transformation. This is a map φ that associates to each vertex $i \in \Lambda^0$ an element of the gauge group $\varphi_i \in G$. Under a gauge transformation the configuration variables then transform as follows:

$$g_{(i, \hat{\mu})} \rightarrow g'_{(i, \hat{\mu})} = \varphi_i g_{(i, \hat{\mu})} \varphi_{i+\hat{\mu}}^{-1} \quad (2.2.13)$$

and for the holonomy we thus have that $h_{(i, \hat{\mu}, \hat{\nu})} \rightarrow \varphi_i h_{(i, \hat{\mu}, \hat{\nu})} \varphi_i^{-1}$. Any class function of the holonomy $h_{(i, \hat{\mu}, \hat{\nu})}$ is therefore gauge invariant.

Since the action of the lattice gauge theory depends on the configuration variables only via the discrete curvature, it can be discretized over faces:

$$S(h) = \sum_{f \in \Lambda^2} s(h_f) \quad (2.2.14)$$

where f refers to the generic face, $f := (i, \hat{\mu}, \hat{\nu})$, and $s(h_f)$ is the corresponding action. The path integral of the theory is then given by

$$Z = \int \mathcal{D}g \prod_{f \in \Lambda^2} e^{-s(h_f)} \quad (2.2.15)$$

where

$$\int \mathcal{D}g := \prod_{(i, \hat{\mu}) \in \Lambda^1} \int_G dg_{(i, \hat{\mu})} \quad (2.2.16)$$

is the integral over G for each lattice link with the Haar measure dg .

Generic gauge invariant observables of the theory can be constructed as follows. Let $\tau_{(i, \hat{\mu})} \in \mathcal{R}$ be an irreducible representation of G associated to the link $(i, \hat{\mu})$, and $V^{(i, \hat{\mu})}$ the corresponding representation space. At each lattice point $i \in \Lambda^0$ we can identify D incoming links, $(i - \hat{\mu}, \hat{\mu})$ with $\mu = 1, \dots, D$, and D outgoing links, $(i, \hat{\mu})$ with $\mu = 1, \dots, D$. Let I^{μ_i} be an intertwiner (see the definition in appendix A.3) from (the tensor product of) the incoming representations to (the tensor product of) the outgoing representations at $i \in \Lambda^0$:

$$I^{\mu_i} : \bigotimes_{\mu}^D V^{\tau_{(i-\hat{\mu}, \hat{\mu})}} \rightarrow \bigotimes_{\mu}^D V^{\tau_{(i, \hat{\mu})}}, \quad (2.2.17)$$

(to simplify the notation, the dependence of the map I^{ι_i} from the incoming and outgoing representations is left implicit). The *spin network* associated to the representations $\{\tau_{(i,\hat{\mu}) \in \Lambda^1}\}$ and intertwiners $\{\iota_i \in \Lambda^0\}$ is the gauge invariant quantity defined by

$$W_{\tau_\ell, \iota_i}(g_\ell) := \left(\prod_{\ell \in \Lambda^1} \sum_{m_\ell n_\ell} \right) \left(\prod_{\ell \in \Lambda^1} t_{m_\ell n_\ell}^{\tau_\ell}(g_\ell) \right) \left(\prod_{i \in \Lambda^0} I_{m_{(i,\hat{i})} \dots m_{(i,\hat{D})}, n_{(i-1,\hat{i})} \dots n_{(i-1,\hat{D})}}^{\iota_i} \right) \quad (2.2.18)$$

where ℓ refers to the generic link $(i, \hat{\mu})$ and, on the left hand side, τ_ℓ , ι_i and g_ℓ account for the set of analogous variables on the whole lattice, e.g. g_ℓ stands for $\{g_{\ell \in \Lambda^1}\}$. The expectation value of a spin network W_{τ_ℓ, ι_i} is then computed by

$$\langle W_{\tau_\ell, \iota_i} \rangle = \frac{1}{Z} \int \mathcal{D}g W_{\tau_\ell, \iota_i}(g_\ell) \prod_{f \in \Lambda^2} e^{-s(h_f)} \quad (2.2.19)$$

We now proceed to derive the dual (according to the Peter-Weyl theorem) of Eq. (2.2.15). The first step is to decompose the action into irreducible representations of the gauge group. Note that, since $s(h_f)$ is a class function, it decomposes into characters; by defining $w(h_f) := e^{-s(h_f)}$ we thus have that

$$Z = \int \mathcal{D}g \prod_{f \in \Lambda^2} \left(\sum_{\rho_f \in \mathcal{R}} w^{\rho_f} \chi^{\rho_f}(h_f) \right) = \int \mathcal{D}g \prod_{f \in \Lambda^2} \left(\sum_{\rho_f \in \mathcal{R}} w^{\rho_f} \sum_{m_f} t_{m_f m_f}^{\rho_f}(h_f) \right) \quad (2.2.20)$$

Note a first hint of the spin foam model: the path integral now contains an irreducible representation $\rho_f \in \mathcal{R}$ for each face f of the lattice. Given Eq. (2.2.4), the representation function $t_{mm}^\rho(h_f)$ can be written as product of representations functions of the group variables on the links bounding the face f :

$$\begin{aligned} t_{mm}^\rho(h_{(i,\hat{\mu},\hat{\nu})}) &= t_{mm}^\rho \left(g_{(i,\hat{\mu})} g_{(i+\hat{\mu},\hat{\nu})} g_{(i+\hat{\nu},\hat{\mu})}^{-1} g_{(i,\hat{\nu})}^{-1} \right) \\ &= \sum_{npq} t_{mn}^\rho(g_{(i,\hat{\mu})}) t_{np}^\rho(g_{(i+\hat{\mu},\hat{\nu})}) t_{pq}^{\rho^*}(g_{(i+\hat{\nu},\hat{\mu})}) t_{qm}^{\rho^*}(g_{(i,\hat{\nu})}) \end{aligned} \quad (2.2.21)$$

For every link $\ell \in \Lambda^1$ then there are $2(D-1)$ representation functions of g_ℓ in the path integral, one for each face f cobounding it (i.e. such that $f \supset \ell$). The integration over g_ℓ thus yields (see Eq. (A.3.4) in appendix A.3) the following contribution:

$$\int dg_\ell \prod_{f \supset \ell} t_{m_f n_f}^{\rho_f}(g_\ell) = \sum_{\iota_\ell} I_{\{m_f \supset \ell\}}^{\{\rho_f \supset \ell\}; \iota_\ell} I_{\{n_f \supset \ell\}}^{\{\rho_f \supset \ell\}; \iota_\ell} \quad (2.2.22)$$

where $I^{\{\rho_f \supset \ell\}; \iota_\ell}$ is the ι_ℓ -th projector from the tensor product of representations $\{\rho_f\}_{f \supset \ell}$ onto the trivial representation (i.e. an intertwiner operator). The path integral thus also contains an intertwiner label ι_ℓ for each link ℓ . In Eq. (2.2.22) the vector indices $\{m_f \supset \ell\}$ refer to the source point of ℓ (for link $(i, \hat{\mu})$, the point i), while $\{n_f \supset \ell\}$ refer to the target one (the point $i + \hat{\mu}$). As a consequence, the set of projectors emerging from the integral over the group variables associated to all links can be grouped by lattice points. Given $i \in \Lambda^0$, the contraction of all projectors corresponding to i defines the *gauge constraint factor*

$$C_i(\{\rho_f \supset i\}, \{k_{\ell \supset i}\}) := \sum_{\{m_f\}_{f \supset \ell}} \prod_{\ell \supset i} I_{\{m_f \supset \ell\}}^{\{\rho_f \supset \ell\}; k_{\ell \supset i}} \quad (2.2.23)$$

which depends on the representations associated to all faces incident on i , i.e. $\{\rho_f \supset i\}$, and on the intertwiner labels $\{k_{\ell \supset i}\}$ of the projectors (one for each link containing i). The final expression of the path integral is then the following:

$$Z = \left(\prod_{f \in \Lambda^2} \sum_{\rho_f \in \mathcal{R}} \right) \left(\prod_{\ell \in \Lambda^1} \sum_{\iota_\ell} \right) \left(\prod_{f \in \Lambda^2} w^{\rho_f} \right) \prod_{i \in \Lambda^0} C_i \quad (2.2.24)$$

The path integral thus contains, in addition to the Boltzmann weight $w^{\rho f}$ for each face $f \in \Lambda^2$, a gauge constraint factor C_i for each lattice point $i \in \Lambda^0$. The dual model therefore corresponds to a spin foam model, i.e. a 2-complex with faces coloured by irreducible representations of the gauge group G and links coloured by intertwiners, where each configuration has a probability amplitude that factorizes into amplitudes associated to the faces and amplitudes associated to the vertices.

2.3 Loop quantum gravity and spin networks

LQG is a canonical quantization of general relativity based on a 3 + 1 decomposition of spacetime, which relies on a formulation of it in $SU(2)$ variables (as opposed to standard metric ones), in terms of which the theory acquires the form of a background independent $SU(2)$ gauge theory. The states of the canonical hypersurface, i.e. the kinematical states which evolve in time via a Hamiltonian constraint, are spin networks to be interpreted as polymer-like excitations of the gravitational field. The main result of LQG is the definition of geometrical operators, specifically area and volume operators, and the prediction of the discreteness of their spectrum.

2.3.1 Canonical formulation of general relativity in the Ashtekar-Barbero variables

The Einstein-Hilbert action in metric variables reads

$$S[g_{\mu\nu}] = \frac{1}{2\kappa} \int d^4x \sqrt{-g} R \quad (2.3.1)$$

where $\kappa = 8\pi G/c^3 = 8\pi\ell_p^2/\hbar$. Given a spacetime foliation in terms of a three-dimensional space-like surface Σ , the spacetime metric $g_{\mu\nu}$ can be expressed in terms of the induced Riemannian metric of Σ , q_{ab} , a shift vector N_a and a lapse function N . The action of general relativity then reads

$$S[q_{ab}, \pi^{ab}, N_a, N] = \frac{1}{2\kappa} \int dt \int_{\Sigma} d^3x [\pi^{ab} \dot{q}_{ab} - N_a \mathcal{V}^a(q_{ab}, \pi^{ab}) - N \mathcal{S}(q_{ab}, \pi^{ab})] \quad (2.3.2)$$

where $\pi^{ab} = q^{-\frac{1}{2}} (K^{ab} - Kq^{ab})$, with K_{ab} extrinsic curvature of Σ , are the momenta canonically conjugate to the space metric q_{ab} ; $\mathcal{V}^a(q_{ab}, \pi^{ab})$ is the vector constraint which generates three-dimensional diffeomorphisms on Σ , and $\mathcal{S}(q_{ab}, \pi^{ab})$ is the scalar constraint which generates coordinate time evolution.

The space metric q_{ab} is then described in terms of a triad field e_a^i (with internal index $i = 1, 2, 3$ and space index $a = 1, 2, 3$) defining an orthogonal frame at each point of Σ : $q_{ab} = e_a^i e_b^j \delta_{ij}$. From it one defines the (inverse) *densitized triad*

$$E_i^a := \frac{1}{2} \varepsilon^{abc} \varepsilon_{ijk} e_b^j e_c^k \quad (2.3.3)$$

and its conjugate variable:

$$K_a^i := \frac{1}{\sqrt{\det(E)}} K_{ab} E_j^b \delta^{ij} \quad (2.3.4)$$

Note that the new variables contain some redundancy, as nine E_i^a are used to express the six independent components of the induced metric q_{ab} . This redundancy derives from the symmetry under $SO(3)$ rotations on the local frames e_a^i , and is removed by the imposition of the constraint

$$\mathcal{G}_i(E_j^a, K_a^j) := \varepsilon_{ijk} E^{aj} K_a^k = 0 \quad (2.3.5)$$

where $\mathcal{G}_i(E_j^a, K_a^j)$, called *Gauss constraint*, is the generator of the local gauge transformations. The action then acquires the following form:

$$S[E_j^a, K_a^j, N_a, N, N^j] = \frac{1}{\kappa} \int dt \int_{\Sigma} d^3x [E_i^a \dot{K}_a^i - N^i \mathcal{G}_i(E_j^a, K_a^j) - N_a \mathcal{V}^a(E_j^a, K_a^j) - N \mathcal{S}(E_j^a, K_a^j)] \quad (2.3.6)$$

Let us then introduce the *Ashtekar-Barbero connection*, which will play the role of configuration variable. Let Γ_a^i be the $\mathfrak{so}(3)$ connection (called *spin connection*) defining a covariant derivative compatible with the triad; the Ashtekar-Barbero connection is the $\mathfrak{so}(3)$ connection defined as follows:

$$A_a^i = \Gamma_a^i + \gamma K_a^i \quad (2.3.7)$$

where γ is the *Immirzi parameter*. Remarkably, the connection A_a^i is conjugate to E_i^a , with Poisson brackets

$$\{E_j^a(x), A_b^i(y)\} = \kappa\gamma\delta_b^a\delta_j^i\delta(x,y), \quad \{E_j^a(x), E_i^b(y)\} = \{A_a^j(x), A_b^i(y)\} = 0 \quad (2.3.8)$$

In terms of the Ashtekar-Barbero variables E_j^a and A_a^j the action finally reads

$$S[E_j^a, A_a^j, N_a, N, N^j] = \frac{1}{\kappa} \int dt \int_{\Sigma} d^3x [E_i^a \dot{A}_a^i - N^i \mathcal{G}_i(E_j^a, A_a^j) - N^b \mathcal{V}_b(E_j^a, A_a^j) - N \mathcal{S}(E_j^a, A_a^j)] \quad (2.3.9)$$

and the constraints are given by

$$\mathcal{G}_i(E_j^a, A_a^j) = D_a E_i^a \quad (2.3.10)$$

$$\mathcal{V}_b(E_j^a, A_a^j) = E_j^a F_{ab}^j - (1 + \gamma^2) K_b^i G_i \quad (2.3.11)$$

$$\mathcal{S}(E_j^a, A_a^j) = \frac{E_i^a E_j^b}{\sqrt{\det(E)}} \left(\epsilon_k^{ij} F_{ab}^k - 2(1 + \gamma^2) K_{[a}^i K_{b]}^j \right) \quad (2.3.12)$$

where F_{ab} is the curvature of the connection A_a and $D_a E_i^a$ is the covariant divergence of E_i^a .

The phase space variables

The Ashtekar-Barbero variables E_j^a and A_a^j take values in the Lie algebra of the local gauge group $SO(3)$. It is however preferable to work with the universal covering group of $SO(3)$, i.e. $SU(2)$, as the latter allows to introduce fermions into the theory (note that this is possible because both groups possess the same Lie algebra). In the following we therefore consider $A_a = A_a^i \tau_i \in \mathfrak{su}(2)$ and $E^a = E_i^a \tau^i \in \mathfrak{su}(2)$, with $\tau_i := i\frac{\sigma_i}{2}$ (where σ_i are the Pauli matrices) generators of the $\mathfrak{su}(2)$ algebra. Let us dwell on the properties of these variables.

The Gauss constraint of Eq. (2.3.10) generates local $SU(2)$ transformations. The finite version of such transformations is the following:

- Under a local (and finite) $SU(2)$ transformation generated by the Gauss constraint of Eq. (2.3.10) the connection A_a becomes

$$A'_a = g A_a g^{-1} + g \partial_a g^{-1} \quad (2.3.13)$$

A new variable, which transforms in a simpler way under the action of the local gauge group, can be constructed out of the connection: the holonomy $h_e(A) \in SU(2)$, which defines the parallel transport of $SU(2)$ spinors along a path $e \subset \Sigma$:

$$h_e[A] = \mathcal{P} \exp - \int_e A \quad (2.3.14)$$

where \mathcal{P} is the path-ordering operator. In fact, under a gauge transformation the holonomy $h_e[A]$ becomes

$$h'_e[A] = g(s_e) h_e[A] g^{-1}(t_e) \quad (2.3.15)$$

- The densitized triad E_i^a transforms, under the action of the local gauge group, as follows:

$$E^{a'} = g E^a g^{-1} \quad (2.3.16)$$

Since E_i^a encodes the spatial geometry of Σ , any geometrical quantity on Σ can thus be written in terms of it. Important examples are the area of a two-dimensional surface $S \subset \Sigma$,

$$A_S[E] := \int_S d\sigma^1 d\sigma^2 \sqrt{E_i^a E_j^b \delta^{ij} n_a n_b}, \quad (2.3.17)$$

and the volume of a three-dimensional region $R \subset \Sigma$:

$$V_R[E] = \int_R d^3x \sqrt{\left| \frac{1}{3!} \varepsilon_{abc} E_i^a E_j^b E_k^c \varepsilon^{ijk} \right|} \quad (2.3.18)$$

2.3.2 Dirac quantization and structure of the kinematic sector of the theory

The quantization of the theory is performed via the Dirac program. The first step thus consists in the representation of the phase space variables as operators in an auxiliary (kinematic) Hilbert space \mathcal{H}_{kin} . The constraints are then promoted to self-adjoint operators in \mathcal{H}_{kin} , and the space of solutions to them is going to define, with a suitable inner product, the physical Hilbert space $\mathcal{H}_{\text{phys}}$. We can identify in this procedure two intermediate steps, corresponding to the construction of the space of solutions to the Gauss constraint (i.e. gauge invariant functionals of the connection), \mathcal{H}^0 , and that of solutions to both the Gauss and the vector constraint, $\mathcal{H}_{\text{diff}}^0$. Schematically:

$$\mathcal{H}_{\text{kin}} \xrightarrow{\text{Gauss}} \mathcal{H}^0 \xrightarrow{\text{Diff}} \mathcal{H}_{\text{diff}}^0 \xrightarrow{\text{Scalar}} \mathcal{H}_{\text{phys}} \quad (2.3.19)$$

Since, in light of the results presented in chapters 3 and 4, we are mainly interested in the kinetic sector of the theory, i.e. in the solutions to the Gauss and the vector constraints, in the following we focus on the construction of \mathcal{H}_{kin} , \mathcal{H}^0 and $\mathcal{H}_{\text{diff}}^0$.

Kinematic Hilbert space \mathcal{H}_{kin}

LQG adopts the A -polarization, i.e. assigns to the connection A the role of configuration variable. The construction of \mathcal{H}_{kin} thus requires the definition of the vector space of functionals of the connection and of a suitable inner product on it. A basic functional of the connection is the holonomy defined in Eq. (2.3.14); in fact, it possesses several nice properties: it transforms in a simple way under the action of the local gauge group, see Eq. (2.3.15), as well as under the action of a diffeomorphism $\phi \in \text{diff}(\Sigma)$:

$$h_e[\phi^* A] = h_{\phi^{-1}(e)}[A] \quad (2.3.20)$$

That is, acting with a diffeomorphism on the connection ($\phi^* A$) corresponds to translating the path e with ϕ^{-1} . The holonomy is then promoted to fundamental observable via the introduction of the notion of *generalised connection*, which consists in the assignment of an element $h_e \in SU(2)$ to any path $e \subset \Sigma$. Kinematic states are then functions of generalised connections called *cylindrical functions*. More specifically, given a graph $\Gamma \subset \Sigma$ and a smooth function $f : G^N \rightarrow \mathbb{C}$, a cylindrical function corresponds to the functional of the connection

$$\psi_{\Gamma, f}[A] = f(h_{e_1}[A], \dots, h_{e_N}[A]) \quad (2.3.21)$$

where e_1, \dots, e_N are the edges of graph Γ . An example of cylindrical function which is also gauge invariant is given by the Wilson loop:

$$W_l[A] = \text{Tr}[h_l[A]] \quad (2.3.22)$$

The set of cylindrical functions for a given graph Γ is denoted by Cyl_Γ . The algebra of kinematical observables is then defined as follows:

$$\text{Cyl} = \cup_\Gamma \text{Cyl}_\Gamma \quad (2.3.23)$$

To complete the construction of the kinematical Hilbert space \mathcal{H}_{kin} one needs to provide the space of cylindrical functions Cyl with a scalar product. This is done via the Ashtekar-Lewandowski measure μ_{AL} , whose action on an element $\psi_{\Gamma, f} \in \text{Cyl}$ is

$$\mu_{AL}(\psi_{\Gamma, f}) = \int \prod_{e \in \Gamma} dh_e f(h_{e_1}, \dots, h_{e_L}) \quad (2.3.24)$$

with dh Haar measure of $SU(2)$. The kinematical scalar product between two cylindrical functions $\psi_{\Gamma,f}$ and $\psi_{\Gamma,g}$ is then given by

$$\mu_{AL}(\overline{\psi_{\Gamma,f}}\psi_{\Gamma,g}) = \int \prod_{e \in \Gamma} dh_e \overline{f(h_{e_1}, \dots, h_{e_L})} g(h_{e_1}, \dots, h_{e_L}) \quad (2.3.25)$$

This definition is extended to cylindrical functions associated to different graphs (having different ordering/orientation or different combinatorics) by using the fact that every function $\psi_{\Gamma,f}$ is equivalent to a function $\psi_{\Gamma',f'}$ on a “larger” graph Γ' with f' independent from the holonomies on the edges which pertain to Γ' but not to Γ ¹. In fact one defines

$$\langle \psi_{\Gamma,f} | \psi_{\Gamma'',g} \rangle := \mu_{AL}(\overline{\psi_{\Gamma',f'}}\psi_{\Gamma'',g'}) = \int \prod_{e \in \Gamma'} dh_e \overline{f'(h_{e_1}, \dots, h_{e_L})} g'(h_{e_1}, \dots, h_{e_L}) \quad (2.3.26)$$

where Γ' is any graph such that $\Gamma \subset \Gamma'$ and $\Gamma'' \subset \Gamma'$. Notably, this scalar product is invariant under diffeomorphisms and gauge transformations. The kinematical Hilbert space \mathcal{H}_{kin} is the Cauchy completion of Cyl in the norm defined by the scalar product of Eq. (2.3.26).

A discrete orthonormal basis of \mathcal{H}_{kin} is provided by the Peter-Weyl theorem, that applied to a cylindrical function $\psi_{\Gamma,f}[A]$ yields

$$\begin{aligned} \psi_{\Gamma,f}[A] &= f(h_{e_1}[A], \dots, h_{e_L}[A]) \\ &= \sum_{j_1 \dots j_L} f_{m_1 \dots m_L, n_1 \dots n_L}^{j_1 \dots j_L} \prod_e \sqrt{2j_e + 1} D_{m_e n_e}^{j_e}(h_e[A]) \end{aligned} \quad (2.3.27)$$

Note in fact that $f_{m_1 \dots m_L, n_1 \dots n_L}^{j_1 \dots j_L}$ is given by the scalar product (defined according to Eq. (2.3.25))

$$f_{m_1 \dots m_L, n_1 \dots n_L}^{j_1 \dots j_L} = \langle \Gamma, j_e, m_e, n_e | \psi_{\Gamma,f} \rangle, \quad (2.3.28)$$

where $|\Gamma, j_e, m_e, n_e\rangle := |j_{e_1}, m_{e_1}, n_{e_1}, \dots, j_{e_L}, m_{e_L}, n_{e_L}\rangle$ with

$$\langle h_e | j_e, m_e, n_e \rangle := \sqrt{2j_e + 1} D_{m_e n_e}^{j_e}(h_e). \quad (2.3.29)$$

Therefore, the states $|\Gamma, j_e m_e n_e\rangle$ for any possible graph $\Gamma \in \Sigma$ form a complete orthonormal basis of \mathcal{H}_{kin} .

Equivalent definitions of the Hilbert space \mathcal{H}_{kin} We have defined \mathcal{H}_{kin} as the completion of Cyl in the norm given by the scalar product of Eq. (2.3.26). In the following we list other equivalent definitions of \mathcal{H}_{kin} .

- ⊙ Consider the space of cylindrical functions with support on graph Γ : $\mathcal{H}_\Gamma := L^2(G^L)$, where L is the number of edges of Γ . Given a graph Γ' such that $\Gamma \subset \Gamma'$, the Hilbert space \mathcal{H}_Γ results to be a proper subspace of $\mathcal{H}_{\Gamma'}$ ². One can then define \mathcal{H}_{kin} as the limit of a family of such Hilbert spaces:

$$\mathcal{H}_{\text{kin}} = \lim_{\Gamma \rightarrow \infty} \mathcal{H}_\Gamma \quad (2.3.30)$$

where the limit denotes an infinite refinement of the graph.

- ⊙ The Hilbert space \mathcal{H}_{kin} can be defined as the direct sum of suitable Hilbert spaces with support on a graph. The observation underlying this definition is the following: given two graphs Γ and Γ' such that $\Gamma \subset \Gamma'$, the state $|\Gamma, j_e, m_e, n_e\rangle$ pertains to both \mathcal{H}_Γ and $\mathcal{H}_{\Gamma'}$, so it cannot be a basis of \mathcal{H}_{kin} ; in fact, all vectors in \mathcal{H}_Γ have spin zero on the edges that are in Γ' but not in Γ .

¹In the spin network basis, this corresponds to having that edges labelled with the trivial representation $j_e = 0$.

²As pointed out above, any function $\psi_{\Gamma,f} \in \mathcal{H}_\Gamma$ is equivalent to a function $\psi_{\Gamma',f'} \in \mathcal{H}_{\Gamma'}$ where f' is independent from the holonomies on the edges which are in Γ' but not in Γ and coincides with f on $\Gamma \cap \Gamma'$. Moreover, the scalar product on \mathcal{H}_Γ is the one induced from the embedding space $\mathcal{H}_{\Gamma'}$, and defined via the Ashtekar-Lewandowski measure of Eq. (2.3.24).

One hence considers the proper subspace of \mathcal{H}_Γ spanned by basis states with $j_l > 0$, that we denote by $\tilde{\mathcal{H}}_\Gamma$. The Hilbert space \mathcal{H}_{kin} can then be defined as follows:

$$\mathcal{H}_{\text{kin}} \sim \bigoplus_{\Gamma} \tilde{\mathcal{H}}_\Gamma \quad (2.3.31)$$

where the direct sum is over all possible graphs $\Gamma \in \Sigma$.

- ⊙ The Hilbert space \mathcal{H}_{kin} can be defined as the space of squared integrable functions in the Ashtekar-Lewandowski measure μ_{AL} for a suitable extension of the space of the smooth connection, to which we refer by \tilde{A} : $\mathcal{H}_{\text{kin}} \sim L^2[\tilde{A}, d\mu_{AL}]$. For more details see Ref. [65].

Hilbert space of gauge invariant states: $\mathcal{H}^0 := \mathcal{H}_{\text{kin}}^{\mathcal{G}}$

In the following we introduce the space of solutions of the Gauss constraint: $\mathcal{H}^0 := \mathcal{H}_{\text{kin}}^{\mathcal{G}}$. We recall that the Gauss constraint is the generator of local $SU(2)$ gauge transformations. The space \mathcal{H}^0 is thus composed of states of \mathcal{H}_{kin} which are gauge invariant, called spin network states.

Let $U_{\mathcal{G}}[g]$ be the operator generating a finite local gauge transformation $g(x) \in SU(2)$, i.e.

$$U_{\mathcal{G}}[g]D_{mn}^j(h_e) = D_{mn}^j(g_{s_e} h_e g_{t_e}^{-1}) \quad (2.3.32)$$

where $g_{s_e} := g(s_e)$ and $g_{t_e} := g(t_e)$, with s_e and t_e source and target vertices of e . The operator $P_{\mathcal{G}}$ projecting kinematical states of \mathcal{H}_{kin} onto \mathcal{H}^0 is constructed via the average over all possible $SU(2)$ transformations:

$$P_{\mathcal{G}} = \int D[g] U_{\mathcal{G}}[g] \quad (2.3.33)$$

Crucially, since the gauge transformation $U_{\mathcal{G}}[g]$ acts at the end points of the graph edges $e \subset \Gamma$, the action of $P_{\mathcal{G}}$ on a state $\psi_{\Gamma,f} \in \mathcal{H}_{\text{kin}}$ factorizes over vertices:

$$P_{\mathcal{G}}\psi_{\Gamma,f} = \prod_v P_{\mathcal{G}}^v \psi_{\Gamma,f} \quad (2.3.34)$$

with $P_{\mathcal{G}}^v$ acting only on vertex $v \subset \Gamma$. Within the Peter-Weyl decomposition of $\psi_{\Gamma,f}$ given in Eq. (2.3.27), the operator $P_{\mathcal{G}}^v$ acts as follows (to simplify the notation, the four edges $e \subset v$ are labelled by):

$$\begin{aligned} P_{\mathcal{G}}^v \prod_{e \subset v} D_{m_e n_e}^{j_e}(h_e) &= \int dg \prod_{e \subset v} D_{m_e n_e}^{j_e}(gh_e) \\ &= \left(\int dg \prod_{e \subset v} D_{m_e q_e}^{j_e}(g) \right) \prod_{e \subset v} D_{q_e n_e}^{j_e}(h_e) \\ &= \left(\sum_{\iota} I_{m_1 \dots m_4}^{\iota} I_{q_1 \dots q_4}^{\iota} \right) \prod_{e \subset v} D_{q_e n_e}^{j_e}(h_e) \end{aligned} \quad (2.3.35)$$

where $I_{m_1 \dots m_4}^{\iota} \in \text{Inv}_{SU(2)} \left[\bigotimes_{e \subset v} V^{j_e} \right]$ is an intertwiner operator recoupling the spins incident on the single vertex (see appendix A.4). A gauge invariant state associated to a closed graph Γ thus takes the following form:

$$\psi_{\Gamma,f}[A] := \sum_{j_1 \dots j_L} f^{\vec{j}_e, \vec{\iota}_v} s_{\Gamma, \vec{j}_e, \vec{\iota}_v}[A] \quad (2.3.36)$$

where

$$s_{\Gamma, \vec{j}_e, \vec{\iota}_v}[A] = \bigotimes_{v \subset \Gamma} \iota_v \bigotimes_{e \subset \Gamma} \sqrt{2j_e + 1} D^{j_e}(h_e[A]) =: \langle h_e[A] | \Gamma, \vec{j}_e, \vec{\iota}_v \rangle \quad (2.3.37)$$

are gauge invariant functionals of the connection called spin network states. The spin network states $|\Gamma, \vec{j}_e, \vec{\iota}_v\rangle$ for all possible graphs $\Gamma \in \Sigma$ form a complete orthonormal basis of \mathcal{H}^0 .

Hilbert space of diffeomorphism invariant states: $\mathcal{H}_{\text{diff}}$

Here we present the space of solutions of the vector constraint (the generator of three-dimensional diffeomorphisms on Σ): $\mathcal{H}_{\text{diff}}$. This is not a subspace of \mathcal{H}_{kin} : since the orbits of diffeomorphisms are not compact, diffeomorphism invariant states are not contained in \mathcal{H}_{kin} but in the dual of the space of cylindrical functions Cyl ; in fact, $\text{Cyl} \subset \mathcal{H}_{\text{diff}} \subset \text{Cyl}^*$, a relation known as Gelfand triple.

Let us start by introducing the operator $U[\phi]$ implementing a diffeomorphism $\phi \in \text{diff}(\Sigma)$ on elements of $\text{Cyl} \subset \mathcal{H}_{\text{diff}}$; it acts on $\psi_{\Gamma,f} \in \text{Cyl}$ as follows:

$$U[\phi]\psi_{\Gamma,f}[A] = \psi_{\phi^{-1}(\Gamma),f}[A] \quad (2.3.38)$$

i.e. by “moving” the graph Γ with ϕ^{-1} . Diffeomorphism invariant states are thus defined as elements $\langle[\psi_{\Gamma,f}]| \in \text{Cyl}^*$ given by

$$\langle[\psi_{\Gamma,f}]| = \sum_{\phi \in \text{diff}(\Sigma)} \langle\psi_{\Gamma,f}|U[\phi] \quad (2.3.39)$$

where $[\psi_{\Gamma,f}]$ denotes the equivalence class of $\psi_{\Gamma,f}$ under diffeomorphisms. The previous expression is a well defined element of Cyl^* because only a finite number of terms in the sum contribute (see below). The set of diffeomorphism invariant states is finally promoted to a Hilbert space $\mathcal{H}_{\text{diff}}$ via the definition of the following scalar product:

$$\langle[\psi_{\Gamma,f}]|[\psi_{\Gamma',g}]_{\text{diff}} := \langle[\psi_{\Gamma,f}]|\psi_{\Gamma',g}\rangle = \sum_{\phi \in \text{diff}(\Sigma)} \langle\psi_{\Gamma,f}|U[\phi]|\psi_{\Gamma',g}\rangle \quad (2.3.40)$$

Hilbert space of gauge and diffeomorphism invariant states: $\mathcal{H}_{\text{diff}}^0$

The space of solutions of both the Gauss and the vector constraint, denoted by $\mathcal{H}_{\text{diff}}^0$, can be constructed by restricting the above procedure to the space of gauge-invariant cylindrical functions Cyl^0 and its dual. In fact, gauge and diffeomorphism invariant states are elements $\langle P_{\text{diff}}\psi| \in \text{Cyl}^{0*}$, where ψ is a gauge invariant state (to simplify the notation we omit the explicit reference to the underlying graph) and $P_{\text{diff}} : \text{Cyl}^0 \rightarrow \text{Cyl}^{0*}$ is such that

$$\langle P_{\text{diff}}\psi|\psi'\rangle = \sum_{\phi \in \text{diff}(\Sigma)} \langle\psi|U[\phi]|\psi'\rangle \quad (2.3.41)$$

with $U[\phi]$ defined in Eq. (2.3.38). The scalar product is then given by

$$\langle[\psi]||[\psi']\rangle_{\text{diff}} = \langle\psi|P_{\text{diff}}|\psi'\rangle = \sum_{\phi \in \text{diff}(\Sigma)} \langle\psi|U[\phi]|\psi'\rangle \quad (2.3.42)$$

To see why the above sum is always finite consider that

- if the diffeomorphism ϕ changes the graph Γ underlying ψ , it takes ψ into a state orthogonal to itself;
- if the diffeomorphism ϕ does not change Γ , there are two possibilities:
 - (a) the state is invariant, hence no multiplicity factor enters the sum of Eq. (2.3.42),
 - (b) ϕ changes the ordering and/or orientation of the graph; these are discrete operations, so a discrete multiplicity enter the sum of Eq. (2.3.42).

A basis of $\mathcal{H}_{\text{diff}}^0$ is given by spin network states associated to the equivalence class of graphs under diffeomorphisms, called *s-knot states*.

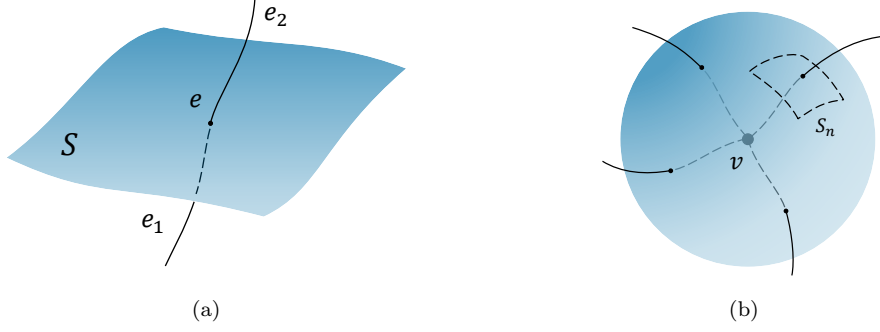


Figure 2.2. Subfigure (a) illustrates a graph edge e (black line) which punctures the surface S and is split by the intersection point into segments e_1 and e_2 ; the action of the operator $\hat{E}_i[S]$ on the holonomy $h_e[A]$ is given by Eq. (2.3.47). Subfigure (b) illustrates a sphere S containing just one spin network vertex v , and an elementary portion of it punctured only by the n -th edge of v , denoted as S_n . Since the spin network vertex is gauge invariant, the action of $\hat{E}_i[S]$ on it vanishes, see Eq. (2.3.49).

2.3.3 Quantum operators and physical interpretation of spin networks

We have seen that the Ashtekar-Barbero variables describing the geometry of the canonical hypersurface Σ are the $SU(2)$ -connection A_a^i and its canonical momentum, the densitized triad E_i^a . In the quantum theory, A_a^i becomes a multiplicative operator, while E_i^a becomes a derivative operator:

$$\hat{A}_a^i \psi[A] = A_a^i \psi[A] \quad (2.3.43)$$

$$\hat{E}_i^a \psi[A] = -i\hbar\kappa\gamma \frac{\delta}{\delta A_a^i} \psi[A] \quad (2.3.44)$$

where $\psi[A] \in \mathcal{H}_{\text{kin}}$. Both operators are not well defined in \mathcal{H}_{kin} , as they send $\psi[A]$ out of the kinematical space. Well defined operators on \mathcal{H}_{kin} can however be constructed by suitably smearing \hat{A}_a^i and \hat{E}_i^a on substructures of Σ . The holonomy $h_e[A]$, which is the smearing of (the path ordered exponential of) the connection along a one-dimensional path $e \subset \Sigma$, becomes in fact a well defined multiplicative operator in \mathcal{H}_{kin} . The densitized triad, instead, being a vector density can naturally be integrated over two-dimensional surfaces. Therefore, given a surface $S \subset \Sigma$ parametrized by coordinates σ^1, σ^2 one defines

$$\hat{E}_i[S] = \int_S d\sigma^1 d\sigma^2 n_a(\vec{\sigma}) \hat{E}_i^a = -i\hbar\kappa\gamma \int_S d\sigma^1 d\sigma^2 n_a(\vec{\sigma}) \frac{\delta}{\delta A_a^i} \quad (2.3.45)$$

where

$$n_a(\vec{\sigma}) := \varepsilon_{abc} \frac{\partial x^b(\vec{\sigma})}{\partial \sigma^1} \frac{\partial x^c(\vec{\sigma})}{\partial \sigma^2} \quad (2.3.46)$$

is the normal 1-form on S . The action of $\hat{E}_i[S]$ on the holonomy $h_e[A]$, in the case of e crossing the surface S only in one point as in figure 2.2(a), is given by

$$\hat{E}_i[S] h_e[A] = \pm i\hbar\kappa\gamma h_{e_1}[A] \tau_i h_{e_2}[A] \quad (2.3.47)$$

where e_1 and e_2 are the segments in which the intersection point splits e , τ_i with $i = 1, 2, 3$ are the generators of the $\mathfrak{su}(2)$ algebra, and the sign depends on the relative orientation of e and S . That is, the operator $\hat{E}_i[S]$ acts on the holonomy by inserting $\pm i\hbar\kappa\gamma \tau_i$ at the point of intersection. The action vanishes in the case $e \cap S = \emptyset$.

Given a spin network state $|\psi\rangle$, consider the action of $\hat{E}_i[S]$ on a spin network vertex v , where S is a sphere of radius ϵ centered at v . Then

$$\lim_{\epsilon \rightarrow 0} \sum_e \hat{E}_i[S] |\psi\rangle = \sum_n \hat{E}_i[S_n] |\psi\rangle \quad (2.3.48)$$

where S_n is the piece of the sphere punctured only by the n -th edge of the vertex v , as shown in figure 2.2(b). From Eq. (2.3.47) it follows that the effect of this transformation coincides with the first order of an infinitesimal gauge transformation. Therefore, the action of $\hat{E}_i[S]$ in Eq. (2.3.48) is the action of the quantum Gauss constraint on a spin network vertex. Due to the gauge invariance of the latter, we have that

$$\sum_n \hat{E}_i[S_n]|\psi\rangle = 0 \quad (2.3.49)$$

i.e. the total quantum flux for a spin network vertex vanishes.

Area operator The area of a two-dimensional surface $S \subset \Sigma$ is given, classically, by Eq. (2.3.17). Its quantum counterpart \hat{A}_S is constructed by considering a partition of S into N 2-cells, S_1, \dots, S_N , and expressing the area operator as the limit of a Riemann sum:

$$\hat{A}_S = \lim_{N \rightarrow \infty} \left(\sum_{n=1}^N \sqrt{\hat{E}_i[S_n] \hat{E}^i[S_n]} \right) \quad (2.3.50)$$

Given a path e which intersects S_n only once, from Eq. (2.3.47) it follows that

$$\hat{E}_i[S_n] \hat{E}^i[S_n] h_e[A] = i^2 (\hbar \kappa \gamma)^2 h_{e_1}[A] \tau_i \tau^i h_{e_2}[A] = (\hbar \kappa \gamma)^2 (-\tau_i \tau^i) h_e[A] \quad (2.3.51)$$

where we used the fact that $-\tau_i \tau^i$ is the Casimir operator. The action of the square of the flux through S_n is therefore diagonal on the holonomy along a path e intersecting S_n only once. In the representation space V^j , where the Casimir operator has eigenvalue $j(j+1)$, the previous expression takes the form

$$\hat{E}_i[S_n] \hat{E}^i[S_n] D_{mn}^j(h_e[A]) = (\hbar \kappa \gamma)^2 j(j+1) D_{mn}^j(h_e[A]) \quad (2.3.52)$$

It follows that the action of the area operator is diagonalized by spin network states, with

$$\hat{A}_S |\psi\rangle = \hbar \kappa \gamma \sqrt{j(j+1)} |\psi\rangle \quad (2.3.53)$$

when the surface S is punctured only once by the spin network $|\psi\rangle$, and

$$\hat{A}_S |\psi\rangle = \hbar \kappa \gamma \sum_p \sqrt{j_p(j_p+1)} |\psi\rangle \quad (2.3.54)$$

in the case of multiple intersection points³. The spectrum of the area operator is therefore discrete, and the area eigenvalues are determined by the spins attached to the edges of the spin network graph; in particular, an edge carrying a spin j is interpreted as being dual to an elementary surface of area $\hbar \kappa \gamma \sqrt{j(j+1)}$.

Volume operator The volume operator for a three-dimensional region R is analogously obtained by first writing the classical version (see Eq. (2.3.18)) as the limit of a Riemann sum defined on a decomposition of R into 3-cell, and then by quantizing the regularized expression. For simplicity, assume that R is decomposed in a cubic lattice, and let N be the number of 3-cell in the decomposition. The volume operator is given by

$$\hat{V}_R = \lim_{N \rightarrow \infty} \left(\sum_{k=1}^N \sqrt{\frac{1}{3!} \varepsilon_{abc} \hat{E}_i[S_n^a] \hat{E}_j[S_n^b] \hat{E}_k[S_n^c] \varepsilon^{ijk}} \right) \quad (2.3.55)$$

where S_n^a is the surface whose normal 1-form lies in the a -th direction. The limiting process is performed so that each vertex is contained in only one 3-cell. The volume operators turn out to be diagonalised by spin network states as well. We do not go into detail in the calculation of the spectrum of the volume operator, for which we refer to the literature. We just mention the

³There are other possible choices for the area spectrum in LQG, see Ref. [66, 67].

fundamental result of the volume spectrum being discrete, with eigenvalues determined by the intertwiner quantum numbers. The node of a spin network, which is coloured by the intertwiner label, can thus be interpreted as a “quantum of space”.

The resulting picture is that of spin networks representing the quantum version of a *twisted geometry* [68–70]. The latter is a collection of polyhedra in which adjacent faces possess the same area but have, in general, different shape and/or orientation. That is, only “neighbouring relations” are present in a twisted geometry: the planes of adjacent faces are not necessarily parallel. Twisted geometries thus differ from standard Regge triangulations in which faces of neighbouring polyhedra, having the same area, shape and orientation, perfectly adhere to each other.

Definition and properties of spin networks in LQG are summarised in box 2.1.

2.1 Spin networks in Loop Quantum Gravity

- ▷ A spin network is a graph $\Gamma \subset \Sigma$ with edges e labelled by irreducible representations of $SU(2)$, namely **spins** $j_e \in \frac{\mathbb{N}}{2}$, and vertices v labelled by $SU(2)$ **intertwiners** $\iota_v \in I_v$, i.e. $SU(2)$ -invariant tensors of (the tensor product of) the representations attached to all edges converging at a vertex.

- ▷ A spin network state $|\Gamma, \vec{j}_e, \vec{\iota}_v\rangle$ is the state corresponding to the following wavefunction on the space of generalised connections:

$$s_{\Gamma, \vec{j}_e, \vec{\iota}_v}(\vec{h}_e) = \bigotimes_{v \in \Gamma} \iota_v \bigotimes_{e \subset \Gamma} \sqrt{2j_e + 1} D^{j_e}(h_e) \quad (2.3.56)$$

where $h_e \in SU(2)$ is the holonomy of the Ashtekar connection A_a^i along the edge e of Γ . That is, a spin network is a wavefunction defining a probability amplitude on the holonomies.

- ▷ Spin network states (defined on closed graphs) are gauge invariant states and provide a basis of the space of solutions of the Gauss constraint, \mathcal{H}^0 .
- ▷ Spin network states diagonalise the area and the volume operator and can be understood as representing quantum twisted geometries: every link is dual to a surface $S \subset \Sigma$ intersecting it, and the spin attached to the link is related to the area of such surface according to Eq. (2.3.53); every node is dual to an elementary portion of space, and the intertwiner attached to it is related to its volume.
- ▷ Spin network states invariant under spatial diffeomorphisms are obtained by considering equivalence classes of labelled graphs on Σ under diffeomorphism (spin-knot states).
- ▷ Spin network states invariant under spatial diffeomorphisms and defined on closed graphs (thereby gauge invariant) represent kinematical states of the theory, whose evolution is implemented via the scalar constraint.

2.4 The GFT approach to quantum gravity

A **GFT** is the theory of a quantum field ϕ defined on d copies of a group manifold G , as follows:

$$\begin{aligned} \phi : G^d &\rightarrow \mathbb{C} \\ g^1, \dots, g^d &\phi(g^1, \dots, g^d) \end{aligned} \quad (2.4.1)$$

In the simplicial **GFT** model for **QG** $G = SU(2)$ and the field is required to satisfy the *closure condition*:

$$\phi(hg^1, \dots, hg^d) = \phi(g^1, \dots, g^d) \quad \forall h \in G \quad (2.4.2)$$

As a result, the excitations of the field can be interpreted as $(d - 1)$ -simplices, to be understood as “quanta of space”, whose geometric properties are encoded in the group variables g^1, \dots, g^d

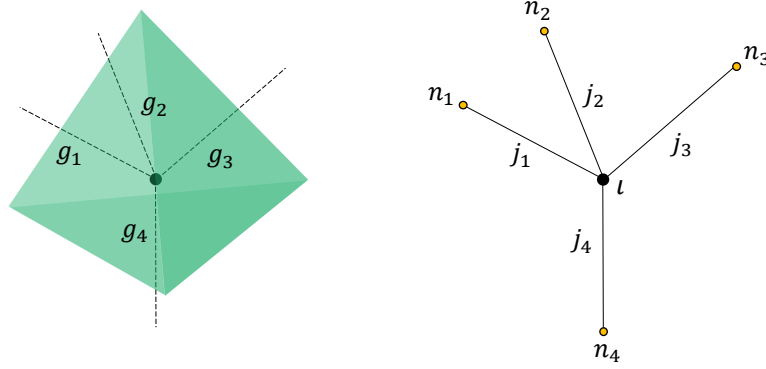


Figure 2.3. Excitation of the field $\phi(g^1, \dots, g^d) \in L^2(G^d/G)$ for the case $d = 4$. On the left, the simplicial representation as a tetrahedron with variables g^1, \dots, g^4 associated to the four faces, which are dual to the edges of a four-valent spin network vertex. On the right, the spin network vertex coloured by: spins j^1, \dots, j^4 on the edges, magnetic numbers n^1, \dots, n^4 at their free ends, and an intertwiner ι on the core.

associated to their d faces. Figure 2.3 shows an example of field excitation for $d = 4$: a tetrahedron; it also illustrates that the fundamental simplex can be represented as a d -valent vertex, with an open line (or *edge*) corresponding to each face and identified by the label $i = 1, \dots, d$ numbering the faces of the simplex: the edge with label i carries the group variable g^i . Through the Peter-Weyl decomposition one obtains

$$\phi(\vec{g}) = \sum_{\vec{j}, \vec{n}, \iota} \phi_{\vec{n}, \iota}^{\vec{j}} \left(\prod_{i=1}^4 \sqrt{2j^i + 1} D_{m^i n^i}^{j^i}(g^i) \right) I_{\vec{n}}^{\vec{j}; \iota} = \sum_{\vec{\xi}} \phi_{\vec{n}, \iota}^{\vec{j}} s_{\vec{n}, \iota}^{\vec{j}}(\vec{g}) \quad (2.4.3)$$

where $s_{\vec{n}, \iota}^{\vec{j}}(\vec{g})$ is the spin network basis wavefunction defined in Eq. (2.3.37) for the single vertex.

The GFT action takes the form

$$S_d[\phi, \phi^*] = \int d\vec{g} d\vec{q} \phi(\vec{g}) \mathcal{K}(g^i (q^i)^{-1}) \phi(\vec{q}) + \frac{\lambda}{d+1} \int \prod_{i \neq j=1}^{d+1} dg_i^j \mathcal{V}(g_i^j (g_j^i)^{-1}) \phi(\vec{g}_1) \dots \phi(\vec{g}_{d+1}) + c.c. \quad (2.4.4)$$

where $\vec{g} = \{g^1, \dots, g^d\}$, λ is a coupling constant and $\mathcal{K}(g^i (q^i)^{-1})$ and $\mathcal{V}(g_i^j (g_j^i)^{-1})$ are the kinetic and interaction kernels, respectively. The presence in the action of combinatorial non-local interactions (a crucial difference with respect to standard quantum field theories) is responsible for the gluing of GFT quanta into discrete geometric structures. In particular, the fundamental $(d-1)$ -simplices combine into d -complexes of arbitrary topology, interpreted as discrete substratum of the continuum spacetime that should emerge from them in some appropriate limit. These d -complexes are dual to the Feynman diagrams in the perturbative expansion of the GFT partition function:

$$Z = \int D\phi D\phi^* e^{-S_d[\phi, \phi^*]} = \sum_{\Gamma} \frac{\lambda^{N(\Gamma)}}{\text{sym}(\Gamma)} Z(\Gamma), \quad (2.4.5)$$

where Γ is the Feynman graph, $N(\Gamma)$ is the number of interaction vertices in Γ , $\text{sym}(\Gamma)$ is a symmetry factor and $Z(\Gamma)$ is the Feynman amplitude associated to Γ . At the boundary of the Feynman diagrams one finds spin networks as defined in LQG and the Feynman amplitudes coincide with spinfoam amplitudes [71], a feature made evident by the Peter-Weyl decomposition of the group functions. Notably, the entire expansion can be seen as the result of merging the strategy of quantum Regge calculus [72] (sum over discrete geometric data attached to a lattice) with that

of dynamical triangulations [73] (for given geometric data, sum over all possible lattices). Let us finally mention that **GFT** can be regarded as a generalization of random tensor models [74, 75], where the combinatorial structures of the latter are enriched with group-theoretic data. As we will clarify in the following chapter, these additional data are responsible for the characterization of the graphs associated to **GFT** states as patterns of entanglement among field quanta.

Despite sharing the same geometric combinatorial structure and algebraic data, the spin networks of **LQG** and **GFT** exhibit some differences with respect to their role and interpretation in the respective frameworks. We illustrate this point in detail in the next chapter. Here we only mention that, while spin networks are introduced in **LQG** as graphs embedded in a background manifold with fixed topology, spin networks considered in **GFT** (as well as in spin foam models) are *abstract spin networks* and the partition function of the theory allows transitions between different spatial topologies. Spin networks of **GFT** can in fact carry, in addition to the purely algebraic data, topological data.

The Fock space structure

The second-quantization formulation of **GFT** is based on field operators $\hat{\phi}$ and $\hat{\phi}^\dagger$ that satisfy the following (bosonic) commutation relations:

$$[\hat{\phi}(\vec{g}), \hat{\phi}^\dagger(\vec{q})] = \int dh \prod_{i=1}^d \delta(hg^i(q^i)^{-1}), \quad [\hat{\phi}(\vec{g}), \hat{\phi}(\vec{q})] = [\hat{\phi}^\dagger(\vec{g}), \hat{\phi}^\dagger(\vec{q})] = 0, \quad (2.4.6)$$

where the r.h.s. of the first equation is the gauge invariant Dirac delta distribution on G^d . The **GFT** Fock space is constructed from the repeated action of the creation operator on the vacuum state $|0\rangle$, defined as the state annihilated by all $\hat{\phi}(\vec{g})$. In the second-quantization settings the modes of the Peter-Weyl decomposition of Eq. (2.4.3), for which we use the notation $\phi_{\vec{\xi}} := \phi_{\vec{n}, \iota}^{\vec{j}}$ where $\vec{\xi} := \{\vec{j}, \vec{n}, \iota\}$, are similarly promoted to creation and annihilation operators which satisfy

$$[\hat{\phi}_{\vec{\xi}}, \hat{\phi}_{\vec{\xi}}^\dagger] = \delta_{\vec{\xi}, \vec{\xi}}, \quad [\hat{\phi}_{\vec{\xi}}, \hat{\phi}_{\vec{\xi}'}] = [\hat{\phi}_{\vec{\xi}}^\dagger, \hat{\phi}_{\vec{\xi}'}^\dagger] = 0 \quad (2.4.7)$$

As anticipated above, an excitation of the field corresponds to a $(d-1)$ -simplex dual to an open spin network vertex:

$$|1_{\vec{\xi}}\rangle = \hat{\phi}_{\vec{\xi}}^\dagger |0\rangle = |\vec{j}, \vec{n}, \iota\rangle \quad (2.4.8)$$

As we will make extensive use of the **GFT** formalism in the first-quantization language, let us present the derivation of the **GFT** Fock space from the Hilbert space associated to a single vertex, i.e. the one-particle sector of the theory, and the construction of a pre-Fock space. The single-vertex Hilbert space is given by

$$\mathcal{H} = L^2(G^d/G) = \bigoplus_{\vec{j}} \left(I^{\vec{j}} \otimes \bigotimes_{i=1}^d V^{j^i} \right). \quad (2.4.9)$$

where the right hand side is the result of applying the Peter-Weyl to the left hand side. Starting from the Hilbert space of the single vertex \mathcal{H} we can then consider the Hilbert space associated to a set of N (distinguishable) vertices:

$$\mathcal{H}_N := \underbrace{\mathcal{H} \otimes \cdots \otimes \mathcal{H}}_N \quad (2.4.10)$$

A generic “ N -particle” state thus takes the form

$$|\psi\rangle = \int \left(\prod_v d\vec{g}_v \right) \psi(\vec{g}_1, \dots, \vec{g}_N) |\vec{g}_1, \dots, \vec{g}_N\rangle, \quad (2.4.11)$$

where $\vec{g}_v = \{\vec{g}_v^1, \dots, \vec{g}_v^d\}$, and $|\vec{g}_v\rangle$ provides a basis for the Hilbert space of the v -th vertex. By taking the direct sum of the Hilbert spaces associated to all possible number of vertices N one

obtains the GFT pre-Fock space:

$$\text{pre-}\mathcal{F}(\mathcal{H}) = \bigoplus_{N=1}^{\infty} \mathcal{H}_N \quad (2.4.12)$$

The Fock space of the theory is then obtained by symmetrizing every term of the direct sum over the vertex labels:

$$\mathcal{F}(\mathcal{H}) = \bigoplus_{N=1}^{\infty} \text{sym} \left(\underbrace{\mathcal{H} \otimes \cdots \otimes \mathcal{H}}_N \right). \quad (2.4.13)$$

2.5 Entanglement and correlations on spin networks to probe and reconstruct geometry

In this section, which is based on Ref. [4], we give an overview of a series of results on the study of correlations and entanglement entropy on spin networks which, in the spirit of the work presented in chapters 3 and 4, are based on the interplay between QG and quantum information and/or condensed matter physics. Let us stress that, while our results in chapters 3 and 4 have been obtained within the GFT approach to QG, the ones we are going to present here mostly pertain to the LQG framework. Nevertheless, they provide a prominent example of how to probe and reconstruct geometry from the quantum correlation structure of spin networks, and provide a key term of comparison to our work. The results are grouped by theme and presented in mainly chronological order.

2.5.1 On the horizon surface: correlations and bulk entropy

We start with early results on spin networks describing finite regions of 3D space bounded by a causal horizon. On one hand, these results deal with the computation of the horizon entropy and the recognition of correlations between horizon subregions as responsible for corrections to the entropy area law [76]; on the other, they concern the introduction of the concept of bulk entropy and its relationship with the boundary area [77].

Black point model for the computation of the horizon entropy In Ref. [76] Livine and Terno modelled the horizon of a static black hole (at the kinematic level) as a two-sphere made by $2n$ elementary patches, each one punctured by an edge carrying the spin $\frac{1}{2}$ (the argument is as follows: since any representation space V^j can be decomposed into the symmetrised product of $2j$ spin- $\frac{1}{2}$ representations, the spin- $\frac{1}{2}$ patch can be considered as the “elementary patch”). We denote by R the black hole region, so that its boundary ∂R corresponds to the horizon two-sphere. The Hilbert space $\mathcal{H}_{\partial R}$ describing the set of boundary edges can be decomposed as

$$\mathcal{H}_{\partial R} = \bigotimes_{j=0}^{2n} V^{\frac{1}{2}} \cong \bigoplus_{j=0}^n V^j \otimes D_n^j \quad (2.5.1)$$

where D_n^j is the degeneracy space of states with spin j . The gauge-invariant subspace associated to the horizon is then given by the intertwiner space

$$\mathcal{H}_{\partial R}^{(0)} = \text{Inv}_{SU(2)} \left[\bigotimes_{j=0}^{2n} V^{\frac{1}{2}} \right] \cong D_n^0 \quad (2.5.2)$$

where the superscript (0) is used to denote the presence of gauge-invariance. In this description the bulk is thus coarse-grained to a single point (hence the name “black point model”), as depicted in figure 2.4(a). The assumption that the surface is a causal horizon implies complete ignorance of the bulk geometry, and the boundary state is therefore given by

$$\rho = \frac{1}{N} \sum_r |l^r\rangle \langle l^r| \quad (2.5.3)$$

where $\{|\iota^r\rangle\}$ is a basis of the intertwiner space $\mathcal{H}_{\partial R}^0$ and N the dimension of the latter. Note that the Boltzmann entropy of such state coincides with its von Neumann entropy, both being equal to $\log N$. The intertwiner-space dimension N is computed via random walk techniques, and the result for the entropy in the asymptotic limit $n \rightarrow \infty$ is an area law with a logarithmic correction. The latter is shown to be given by the total amount of correlations between two halves of the horizon surface. Let us show the methodology, as this will be useful for subsequent discussion and for comparing the results presented in chapters 3 and 4 to the LQG literature. Consider the splitting of the boundary into a set ∂A of $2k$ qubits and a complementary set ∂B of $2(n-k)$ qubits (see figure 2.4(a)). Then

$$\mathcal{H}_{\partial R} = \mathcal{H}_{\partial A} \otimes \mathcal{H}_{\partial B} \quad (2.5.4)$$

where $\mathcal{H}_{\partial A} = (V^{\frac{1}{2}})^{\otimes 2k}$ and $\mathcal{H}_{\partial B} = (V^{\frac{1}{2}})^{\otimes 2(n-k)}$ (note that such a factorisation does not hold for the gauge-invariant subspace $\mathcal{H}_{\partial R}^{(0)}$, see the discussion on Ref. [67]). When decomposing each subspace into a direct sum over irreducible representations j , e.g. $\mathcal{H}_{\partial A} = \bigoplus_{j=0} V_{\partial A}^j \otimes D_{\partial A}^j$, the intertwiner states of $\mathcal{H}_{\partial R}^{(0)} \subset \mathcal{H}_{\partial R}$ turn out to be singlet states on $V_{\partial A}^j \otimes V_{\partial B}^j$ with extra indices a_j and b_j labelling basis of the degeneracy spaces $D_{\partial A}^j$ and $D_{\partial B}^j$, respectively. This corresponds to unfolding the intertwiner as illustrated in figure 2.4(c). The horizon state then becomes the following:

$$\rho = \frac{1}{N} \sum_j \sum_{a_j b_j} |j, a_j, b_j\rangle \langle j, a_j, b_j| \quad (2.5.5)$$

It is found that, for $2k = n$ (symmetric splitting of the horizon surface), the mutual information $I_\rho(\partial A : \partial B)$, amounting to three times the entanglement between ∂A and ∂B (quantified e.g. by the entanglement of formation), equals the logarithmic correction to the horizon entropy.

A possible relationship of the entanglement between ∂A and ∂B (for $\partial A \ll \partial B$) with the evaporation process is also suggested, as the case $j = 0$ corresponds to the detachment of the surface patch ∂A from the rest of the horizon.

Bulk-topology contribution to the boundary entropy In Ref. [77] Livine and Terno generalised the computation of the horizon entropy performed in Ref. [76] by taking into account the non-trivial structure of the bulk graph. In particular, they promoted the boundary state counting of Ref. [76] to a bulk state counting performed by gauge-fixing the holonomies on internal loops to avoid over-estimating the number of states seen by an external observer (it is showed that, because of gauge invariance, the bulk degrees of freedom are truly carried by internal loops). The horizon entropy (evaluated as the logarithm of the number of states supported by a bulk flower-graph with fixed boundary conditions) then turned out to depend on the topology of the graph through its number of loops.

2.5.2 Distance from entanglement

Correlations between disjoint regions of a spin network In Ref. [67] Livine and Terno explored the correlations induced between two disjoint regions A and B of a spin network from the “outside geometry” R (i.e. the region of the spin network complementary to $A \cup B$, see figure 2.4(b)). Since $\partial A \cup \partial B = \partial R$, the gauge invariant state induced on the boundary of the two regions can be regarded as the result of coarse-graining R to a single intertwiner, as in the model of the previous paragraph. The presence of correlations between A and B can then be traced back to the fact that, because of the requirement of gauge invariance of ∂R , the Hilbert space $\mathcal{H}_{\partial R}^{(0)}$ is not isomorphic to $\mathcal{H}_{\partial A}^{(0)} \otimes \mathcal{H}_{\partial B}^{(0)}$. The intertwiner on ∂R can in fact be unfolded into two vertices connected by a “fictitious link” as in figure 2.4(c), and $\mathcal{H}_{\partial A}^{(0)} \otimes \mathcal{H}_{\partial B}^{(0)}$ is recovered as the subspace with internal link labelled by the trivial representation $j = 0$ (which effectively corresponds to the absence of connection). The internal link thus encodes the entanglement between regions A and B , induced from the complementary region R . This entanglement is then related to a notion of

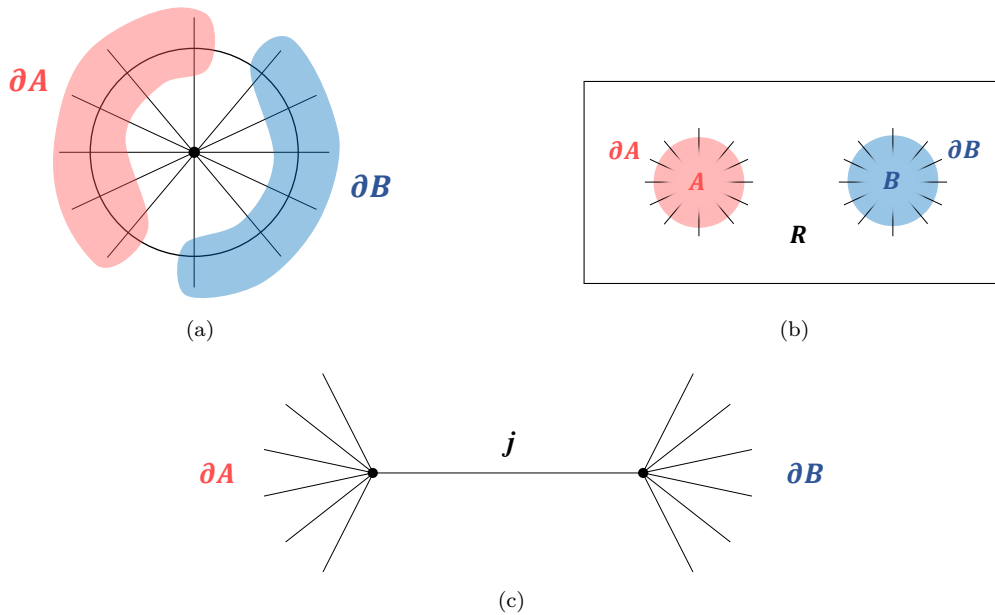


Figure 2.4. Studying correlations between parts of the boundary (a) and between disjoint bulk regions (b). Both settings are equivalent to an intertwiner of the spins $\partial A \cup \partial B$, which can be unfolded as depicted in (c): two vertices corresponding to the subsystems ∂A and ∂B are connected by a “fictitious link” representing the correlations between them. For $j = 0$ the two subsystems are uncorrelated.

distance between parts of the spin network, building on the idea that, in absence of a background geometry, such a notion can only be defined in term of correlations between the quantum degrees of freedom, and is expected to be induced from the algebraic and combinatorial structure of the “outside geometry”.

In the same spirit, Ref. [78] by Feller and Livine shows how a notion of distance can be reconstructed from spin network states whose correlations map onto the standard Ising model.

Let us finally mention that, as opposed to Ref. [67], the more recent Ref. [79] by Livine identifies the link entanglement of the unfolded intertwiner as unphysical, as deriving from looking at non-gauge invariant states.

2.5.3 Entanglement entropy and holographic spin networks

Gauge-invariant degrees of freedom are non-local: the Hilbert space of a spin network graph \mathcal{H}_γ , indeed, does not factorise into the tensor product of Hilbert spaces describing the subgraphs into which γ can be split. We mentioned that in Ref. [76] and Ref. [67] this issue is overcome by embedding the intertwiner space into the tensor product of Hilbert spaces which are *not* gauge-invariant (each one being the tensor product of representations attached to a subset of boundary edges and to a “fictitious” internal-link). Likewise, in Ref. [80] and Ref. [81] Donnelly showed how the entanglement entropy between an arbitrary region R of a spin network graph and its complement \bar{R} can be computed by embedding \mathcal{H}_γ into an extended Hilbert space that factorises over R and \bar{R} , with the gauge symmetry broken at the interface of the two regions. More specifically, Ref. [80] takes the complete graph in a spin network basis state: the reduced density matrix ρ_R is therefore completely mixed, and the entropy given by

$$S(\rho_R) = \sum_{e \in \partial R} (2j_e + 1) \quad (2.5.6)$$

An explanation of the agreement with the result obtained from the isolated horizon framework in the limit of a large number of punctures is then provided: the spin network states representing the

purification of ρ_R in the two frameworks have a Schmidt decomposition of the same rank (note that the result holds only asymptotically: the isolated-horizon entropy is less than Eq. (4.2.21), as it includes the gauge-invariance constraint on the boundary ∂R). Reference [81], instead, takes the whole graph in a completely generic state. The entropy of region R then turns out to be given by the sum of three positive terms: the Shannon entropy of the distribution of boundary representations, the weighted average of $\log(2j + 1)$ over all boundary representations j , and a term representing non-local correlations.

An alternative definition of entanglement entropy of regions of a spin network, similarly derived from the embedding of the Hilbert space of gauge-invariant states into an extended Hilbert space, is provided in Ref. [82], and relies on an extension procedure that is based on the excitation content of the theory instead of the underlying graph.

The computation of the entanglement entropy of spin network states and the study of a holographic regime via models and techniques from condensed matter physics is the methodology underlying the results on random spin networks to which this review is dedicated. It has been adopted in earlier work: in Ref. [83] Feller and Livine introduced a class of states inspired by the Kitaev’s toric code model which satisfy an area law for entanglement entropy and whose correlation functions between distant spins are non-trivial.

We close this subsection with a general result on boundaries in QG: in Ref. [84] Bianchi *et al.* showed that boundary states associated to finite portions of spacetime, representing local gravitational processes with certain initial and final data, are mixed, pointing out that such a feature can be regarded as the consequence of tracing over the correlations between the region and its exterior.

2.5.4 Gluing adjacent faces with entanglement

We finally recall recent results by Bianchi and collaborators on entanglement as a tool for gluing (in the sense specified below) elementary portions of space (spin network vertices). Crucially, this will allow us to differentiate between the various notions of gluing of spin network vertices, and to clarify which degrees of freedom are involved in the corresponding entangling procedures. The variety we refer to stems from the distinction between vector geometries, which are defined below, and twisted geometries, of which tensor networks provide a quantum version. In fact, as explained in section 2.3.3, a spin network describes a quantum twisted geometry in which “neighbouring relations” of quantum polyhedra are codified by links: two intertwiners connected by a link ℓ represent neighbouring polyhedra, whose adjacent faces have equal area (determined by the spin j_ℓ) but different shape and/or orientation, in general. Note that the absence of correlation between the polyhedra of a twisted geometry is translated, at the quantum level of the spin network, to the unentangled nature of the intertwiner degrees of freedom (i.e. the quantum geometry of neighbouring polyhedra has uncorrelated fluctuations). In a vector geometry the normals to the adjacent faces of neighbouring polyhedra are instead anti-parallel, i.e. the two faces adhere to each other, despite the possibly different shape.

In Ref. [85] it was shown that a quantum version of vector geometries can be obtained from a spin network graph by entangling the intertwiner degrees of freedom. They introduced a class of states, called *Bell-network states*, constructed by creating between intertwiners at nearest-neighbour nodes the analogous of the spin-spin correlations of a Bell singlet states. These correlations ensure that the normals to the adjacent faces of the corresponding quantum polyhedra are always back-to-back, i.e. that the face planes are parallel. Then, exactly as a Bell singlet state can be understood as a uniform superposition of back-to-back spins over all space directions, a Bell-network state at fixed spins represents a uniform superposition over all vector geometries. In Ref. [86] it was further shown that the entanglement entropy of Bell-network states obeys an area law.

3

Spin networks as entanglement graphs: an information-theoretic characterization

In this chapter, which is based on Ref. [1], we show that spin networks arise in GFT as entanglement patterns among space quanta, and establish a precise correspondence between them and tensor networks suitably generalised to a second-quantization framework.

In section 3.1 we present the encoding of combinatorial patterns into matrices and the related notions of labelled- and unlabelled-graphs, i.e. graphs made of distinguishable and indistinguishable vertices, respectively. We then outline how to construct GFT states associated to graphs with arbitrary connectivity: we first provide, in section 3.2, a basis-independent prescription to define states associated to labelled-graph, working in the pre-Fock space of the theory; in section 3.3 we then implement vertex-relabelling invariance, obtaining states of unlabelled-graphs in the GFT Fock space. In section 3.4 we define a scalar product which compares graph states independently of the vertex-labelling, with the criterion of maximising the overlap between their combinatorial structures. We conclude the analysis on graph states with section 3.5, where we show how an effective and relational notion of distinguishability of vertices can be recovered by adding new degrees of freedom (with the interpretation of discrete matter fields) to the GFT model. We then introduce, in section 3.6, the TN formalism and dedicate section 3.7 to highlight the relationship between entanglement and geometry and topology in the GFT and TN frameworks. We finally present, in section 3.8, the dictionary between GFT and TN, explaining how GFT (labelled- and unlabelled-)graph states can be read as precise classes of tensor network states.

3.1 Graphs and their adjacency matrix description

In this section we introduce the graph theory notions that we will use to differentiate between combinatorial patterns implemented on distinguishable and undistinguishable quanta (and thus to properly define the GFT entanglement graphs in first- and second-quantization, respectively). For these and other notions of graph theory, see e.g. Ref. [87].

Definition 3.1.1 (Labelled graph). A labelled graph γ is an ordered set of vertices $V = \{v \mid v = 1, \dots, N\}$ connected according to a certain pattern.

A labelled graph composed of N vertices can be described by a $N \times N$ matrix A , called *adjacency matrix*, whose entries encode the adjacency relations among vertices: A_{vw} takes value 1 if vertex v is connected to vertex w , and 0 otherwise. Since A encodes all information about γ (which simply consists of “who is glued to whom”) we refer to a graph by using both notations, i.e. $\gamma \equiv A$.

Two graphs which differ only for the labelling of their vertices are said to be *isomorphic*. Formally, two labelled graphs $\gamma = A$ and $\gamma' = A'$ with same number of vertices N are isomorphic if there exist a permutation π on N elements such that $A' = P_\pi A P_\pi^{-1}$, where P_π is the matrix obtained by permuting the columns of the identity matrix according to π .

Given an adjacency matrix A , we denote by $[A]$ the equivalence class of matrices obtained by permuting rows and columns of A :

$$[A] = \{A' \mid A' = P_\pi A P_\pi^{-1}, \pi \in S_N\}, \quad (3.1.1)$$

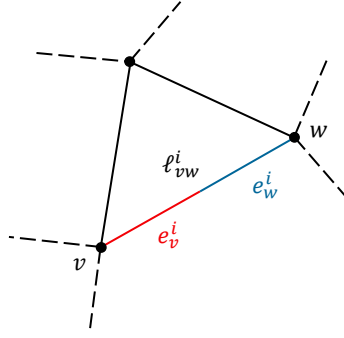


Figure 3.1. The gluing of the i -th edge of vertex v , denoted as e_v^i and depicted in red, to the i -th edge of vertex w , denoted as e_w^i and depicted in blue, gives rise to a link between v and w indicated as ℓ_{vw}^i .

where S_N is the set of possible permutations on N elements. Note that two isomorphic graphs belongs to the same equivalence class of adjacency matrices.

Definition 3.1.2 (Unlabelled graph). An unlabelled graph $[\gamma]$ is the combinatorial pattern represented by $[A]$, where $\gamma \equiv A$.

Two unlabelled graphs $[\gamma]$ and $[\gamma']$ are said to be isomorphic if and only if they have a common adjacency matrix. Moreover, two isomorphic graphs have exactly the same set of adjacency matrices.

The adjacency-matrix encoding of a graph can be easily generalised to the case in which edges departing from vertices are distinguished by a label $i = 1, \dots, d$, as is the case for spin network vertices. We denote by e_v^i the edge of label i departing from vertex v and by ℓ_{vw}^i the link formed by edges e_v^i and e_w^i , as shown in figure 3.1. Assuming the absence of 1-vertex loops, the generalised adjacency matrix takes the form

$$A = \begin{pmatrix} 0_{d \times d} & A_{12} & \dots & A_{1N} \\ & 0_{d \times d} & & \\ & & \ddots & \\ & & & 0_{d \times d} \end{pmatrix} \quad (3.1.2)$$

where A_{vw} is now a $d \times d$ matrix (and $0_{d \times d}$ stands for the null $d \times d$ matrix), with element $(A_{vw})_{ij} := A_{(v-1) \cdot d + i, (w-1) \cdot d + j}$ equal to 1 if vertices v and w are connected along edges labelled by i and j , respectively (i.e. e_v^i and e_w^j are glued together), and 0 otherwise. To simplify the notation, and since the edge labelling does not play any particular role, we assume that vertices can be connected only along edges carrying the same label. The matrix A_{vw} then takes a diagonal form:

$$A_{vw} = \begin{pmatrix} a_{vw}^1 & 0 & \dots & 0 \\ 0 & \ddots & & \\ \vdots & & \ddots & \\ 0 & & & a_{vw}^d \end{pmatrix} \quad (3.1.3)$$

with a_{vw}^i equal to 1 (0) if vertices v and w are connected (not connected) along their edges of colour i . We also define the following substructures of a labelled-graph γ described by such generalised adjacency matrix:

- * $L = \{\ell_{vw}^i \mid v, w \in V : (A_{vw})_{ii} = 1\}$ set of internal links of γ
- * $\partial\gamma = \{e_v^i \mid v \in V : (A_{vw})_{ii} = 0 \forall w \in V\}$ set of boundary edges of γ
- * $E = L \cup \partial\gamma$ set of all edges of γ

The generalised adjacency matrix defined by Eqs. (4.3.17) and (3.1.3) thus encodes the connectivity pattern γ of a set of N spin network vertices. Equivalence classes of these matrices under vertex relabelling can still be defined, and the notion of unlabelled spin network graphs naturally follows.

3.2 Labelled entanglement graphs

In this section:

- (a) we illustrate the embedding of \mathcal{H}_γ into \mathcal{H}_N ;
- (b) we show that the gluing in \mathcal{H}_N is defined by an entanglement relation, and spin network graphs are therefore entanglement graphs;
- (c) we outline a prescription to construct (labelled) entanglement graphs in the pre-Fock space of the theory, where the vertices are distinguishable.

3.2.1 Embedding \mathcal{H}_γ into \mathcal{H}_N via group averaging

Consider a generic state for a set of N open vertices: $\psi \in \mathcal{H}_N$. Starting from it, one can construct a special class of states in which the N vertices are connected according to a certain pattern γ . We restrict the analysis to the case in which the connection can be realized only between edges of the same label i^1 . By assigning an orientation to the edges, with the group element g^i associated to the outgoing direction, the gluing of two vertices shows up as follows: the vertices v and w are connected along a link of colour i if the multi-particle wavefunction $\psi(\vec{g}_1, \dots, \vec{g}_N)$ depends on the elements g_v^i and g_w^i only through the product $g_v^i (g_w^i)^{-1}$. The two vertices are then said to form an internal link ℓ_{vw}^i (where i is the colour of the link, v and w are the source and target vertices, respectively) which carries the group element $g_\ell = g_v^i (g_w^i)^{-1}$. It was showed in Ref. [88] that such gluing is realized by averaging through the right action of the group on the two open edges carrying g_v^i and g_w^i :

$$\int dh \psi(\dots, g_v^i h, \dots, g_w^i h, \dots) = \psi_\ell(\dots, g_v^i (g_w^i)^{-1}, \dots). \quad (3.2.1)$$

In fact, the convolution on the group element h forces $\psi(\vec{g}_1, \dots, \vec{g}_N)$ to depend on g_v^i and g_w^i through the product $g_v^i (g_w^i)^{-1}$ representing the group variable associated to the internal link ℓ_{vw}^i . The resulting wavefunction ψ_ℓ is therefore associated to a set of N spin network vertices with a link between v and w (for which we used the short notation ℓ). As a consequence, every state associated to a spin network graph γ and living in $\mathcal{H}_\gamma = L^2(G^L/G^N)$ (where L and N are the number of links and nodes of γ , respectively) can be seen as the result of gluing the arguments of a N -particle state $\psi \in \mathcal{H}_N$ according to the combinatorial pattern of γ :

$$\int \left(\prod_{\ell \in \gamma} dh_\ell \right) \psi(\dots, g_v^i h_\ell, \dots, g_w^i h_\ell, \dots) = \psi_\gamma(g_\ell = g_v^i (g_w^i)^{-1}) \quad (3.2.2)$$

where the argument of ψ_γ on the left hand side symbolises its dependence over all link variables.

Equation (3.2.2) thus represents the embedding of $\psi_\gamma \in \mathcal{H}_\gamma$ into \mathcal{H}_N , and shows that the Hilbert space \mathcal{H}_N contains, among its elements, states associated to the graph γ . Furthermore, the Hilbert space \mathcal{H}_γ is a Hilbert subspace of \mathcal{H}_N : the scalar product on the first is in fact the one induced by the latter. This result was proved in Ref. [88] as part of a broader analysis on the possibility to regard group field theory as a second quantization of loop quantum gravity: \mathcal{H}_γ is in fact the Hilbert space associated to a given graph γ in LQG.

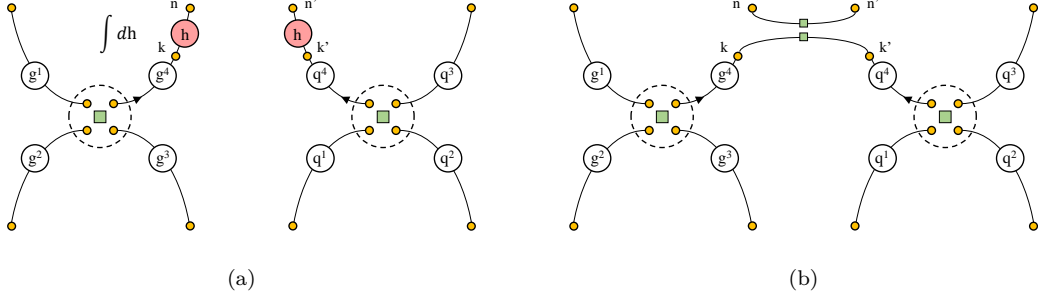


Figure 3.2. Gluing of two spin network vertices performed by acting on two open edges with the same group element and integrating over the latter. Group variables are depicted as large white disks (except for the element h through which the group acts, highlighted in red) and magnetic indices as small yellow disks; intertwiner tensors are instead represented by green squares. The group averaging is depicted in panel (a) and returns a pair of bivalent intertwiners contracting the magnetic indices of the two edges, as shown in panel (b).

3.2.2 Entanglement graphs

In the spin network basis, gluing edges corresponds to entangling the degrees of freedom attached to their free ends. We clarify this point with the following example. Consider the gluing of two four-valent spin network vertices described by the wavefunction ψ , and decompose the latter according to the Peter-Weyl theorem:

$$\int dh \psi(g^1, \dots, g^4 h, q^1, \dots, q^4 h) = \sum_{\vec{j}\vec{j}'} \sum_{\vec{n}\vec{n}', \vec{\nu}\vec{\nu}'} \psi_{\vec{n}\vec{n}', \vec{\nu}\vec{\nu}'}^{\vec{j}\vec{j}'} \int dh s_{\vec{n}, \vec{\nu}}^{\vec{j}}(g^1, \dots, g^4 h) s_{\vec{n}', \vec{\nu}'}^{\vec{j}'}(q^1, \dots, q^4 h) \quad (3.2.3)$$

where $s_{\vec{n}, \vec{\nu}}^{\vec{j}}$ is the spin network basis state for the open vertex introduced in the previous chapter:

$$s_{\vec{n}, \vec{\nu}}^{\vec{j}}(\vec{g}) := \left(\prod_{i=1}^4 \sqrt{2j^i + 1} D_{m^i n^i}^{j^i}(g^i) \right) I_{\vec{n}}^{\vec{j}; \vec{\nu}} \quad (3.2.4)$$

The integral of the spin network basis wavefunction on the r.h.s. of Eq. (3.2.3) is the factor implementing the gluing of the open edges with label 4. The integral is graphically represented in figure 3.2 and performed in the following. To simplify the notation, the label 4 is removed from all quantum numbers (e.g. j^4 is denoted just as j); we also adopt the notation $n^{123} = \{n^1, n^2, n^3\}$. By substituting to Eq. (3.2.3) the expression of Eq. (3.2.4) one obtains

$$\int dh \psi(g^1, \dots, g^4 h, q^1, \dots, q^4 h) = \sum_{\vec{j}\vec{j}'} \sum_{\vec{n}\vec{n}', \vec{\nu}\vec{\nu}'} \sum_{kk'} \psi_{\vec{n}\vec{n}', \vec{\nu}\vec{\nu}'}^{\vec{j}\vec{j}'} s_{n^{123k}, \vec{\nu}}^{\vec{j}}(\vec{g}) s_{n', 123k', \vec{\nu}'}^{\vec{j}'}(\vec{q}) \int dh D_{kn}^j(h) D_{k'n'}^{j'}(h) \quad (3.2.5)$$

The integral of the Wigner matrices on the r.h.s. yields (see Eq. (A.4.7) in appendix A)

$$\int dh D_{kn}^j(h) D_{k'n'}^{j'}(h) = \delta_{jj'} I_{kk'} I_{nn'} \quad (3.2.6)$$

where $I_{kk'}$ is a bivalent intertwiner in the space $V^j \otimes V^j$ attached to the free ends of the to-be-glued edges:

$$I_{kk'} := \frac{(-1)^{j+k}}{\sqrt{2j+1}} \delta_{k, -k'} \quad (3.2.7)$$

¹This restriction leads to d -colored graphs, as extensively studied in the random tensor models literature [74, 75].

By inserting Eq. (3.2.6) into Eq. (3.2.5) the latter becomes

$$\int dh \psi(g^1, \dots, g^4 h, q^1, \dots, q^4 h) = \sum_{\vec{j}j'} \sum_{\vec{n}\vec{n}', \ell\ell'} \sum_{kk'} \left(\psi_{\vec{n}\vec{n}', \ell\ell'}^{\vec{j}j'} \delta_{jj'} I_{nn'} \right) s_{n^{123k}, \ell}^{jj}(\vec{g}) s_{n^{123k'}, \ell'}^{j'j}(\vec{q}) I_{kk'} \quad (3.2.8)$$

In this expression, represented in figure 3.2(b), both the state coefficient and the spin network basis elements are contracted with a bivalent intertwiner. Crucially, this is equivalent to projecting $|\psi\rangle$ on the following state of $V^j \otimes V^j$:

$$|\ell\rangle := \sum_{kk'} I_{kk'} |j, k\rangle |j, k'\rangle = \sum_k \frac{(-1)^{j+k}}{\sqrt{2j+1}} |j, k\rangle |j, -k\rangle \quad (3.2.9)$$

which is a singlet state. The entanglement between the two edges composing the link can be quantified via the von Neumann entropy. Denoting by ρ_s and ρ_t the reduced density matrices of the edges attached to the source and target vertex of the link ℓ , respectively, one can easily check that

$$S(\rho_s) = S(\rho_t) = \log d_j \quad (3.2.10)$$

i.e. the entanglement entropy of the two subsystems reaches its maximum possible value: the state $|\ell\rangle$ is maximally entangled.

Therefore, starting from a set of open spin network vertices, the gluing of pairs of their edges is performed by entangling, in a singlet states, the spins on the corresponding free ends. *The connectivity pattern of a set of vertices can thus be understood as an entanglement pattern among the degrees of freedom attached to the free ends of their open edges.*

3.2.3 Constructing entanglement graphs of arbitrary connectivity

Here we provide a prescription to construct in \mathcal{H}_N spin network states with arbitrary combinatorial pattern, exploiting the adjacency-matrix description of graphs. We start by defining a class of operators on \mathcal{H}_N , called *link maps*, which glue different vertices by projecting open-edge states into a “link subspace”, i.e. the subspace invariant under the right action of the group on the open edges to be glued.

Definition 3.2.1 (Link map). The gluing of two vertices v and w along their open edges of label i is performed by a map

$$\mathbb{P}_\ell : L^2(G^2) \rightarrow L^2(G^2/RG), \quad (3.2.11)$$

where the two copies of the group G are attached to the edges e_v^i and e_w^i to be glued, ℓ is short notation for ℓ_{vw}^i and $/R$ is the factorization over the right action of the group. The link map \mathbb{P}_ℓ is defined as follows:

$$\mathbb{P}_\ell := \int dh dg_v^i dg_w^i |g_v^i\rangle \langle g_v^i h| \otimes |g_w^i\rangle \langle g_w^i h| \quad (3.2.12)$$

When acting on a multi-particle state $\psi \in \mathcal{H}_N$, the link map \mathbb{P}_ℓ realizes the convolution of Eq. (3.2.1):

$$\mathbb{P}_\ell |\psi\rangle = \int \prod_v d\vec{g}_v \int dh \psi(\dots, g_v^i h, \dots, g_w^i h, \dots) |\vec{g}_1, \dots, \vec{g}_N\rangle \quad (3.2.13)$$

We can then construct a spin network state with arbitrary combinatorial structure γ by applying to a multi-particle state in \mathcal{H}_N (with N greater or equal to the number of vertices of γ) the link maps according to the adjacency matrix A of γ :

$$\begin{aligned} |\psi_\gamma\rangle &= \left(\bigotimes_{a_{vw}^i=1} \mathbb{P}_{\ell_{vw}^i} \right) |\psi\rangle \\ &= \int \prod_v d\vec{g}_v \int \left(\prod_{a_{vw}^i=1} dh_{vc^i(v)} \right) \psi(\dots, g_v^i h_{vc^i(v)}, \dots) |\vec{g}_1, \dots, \vec{g}_N\rangle \end{aligned} \quad (3.2.14)$$

where $\vec{c}(v)$ is a vector encoding the connectivity of vertex v :

$$c^i(v) = \begin{cases} w & \text{if } a_{vw}^i = 1; \\ 0 & \text{if } a_{vw}^i = 0; \end{cases} \quad (3.2.15)$$

the gluing elements $h_{vc^i(v)}$ are such that $h_{vw} = h_{wv}$; and $h_{v0} = e$, where e is the identity element. The resulting state is thus a spin network state with support on γ , i.e. it pertains to the Hilbert subspace $\mathcal{H}_\gamma \subset \mathcal{H}_N$.

Note that, since the gluing operation is a projection from \mathcal{H}_N to \mathcal{H}_γ , given $\psi_\gamma \in \mathcal{H}_\gamma$ a multi-particle state in \mathcal{H}_N from which ψ_γ can be obtained via the link maps is not uniquely defined. Let us also stress that the provided prescription is basis-independent, as it is defined through the action of projection operators on the Hilbert spaces associated to the open vertices.

3.2.4 Comparing graph states with the same number of vertices

As mentioned before, in Ref. [88] it was showed that the scalar product on \mathcal{H}_γ is the one induced by \mathcal{H}_N . Following our generalised construction of graph states in \mathcal{H}_N , we show that the scalar product on \mathcal{H}_N allows also to compare graph states with the same number N of vertices but possibly different combinatorial structure². We start by decomposing the wavefunction $\psi_\gamma(g_\ell)$ in the spin network basis:

$$\begin{aligned} \psi_\gamma(g_\ell) &= \int \left(\prod_A dh \right) \psi(\dots, g_v^i h_{vc^i(v)}, \dots) \\ &= \int \left(\prod_A dh \right) \left(\prod_v \sum_{\vec{j}_v, \vec{n}_v, \vec{\iota}_v} \right) \psi_{\vec{n}_1 \dots \vec{n}_N, \vec{\iota}_1 \dots \vec{\iota}_N}^{\vec{j}_1 \dots \vec{j}_N} \prod_v I_{\vec{m}_v}^{\vec{j}_v; \vec{\iota}_v} \prod_{i=1}^4 d_{j_v^i} D_{m_v^i, n_v^i}^{j_v^i} (g_v^i h_{vc^i(v)}) \end{aligned} \quad (3.2.16)$$

where we introduced the short notation

$$\prod_A dh := \prod_{a_{vw}^i=1} dh_{vc^i(v)} \quad (3.2.17)$$

for the Haar measure on the gluing elements corresponding to the adjacency matrix A . By performing the integral over the gluing elements one obtains

$$\psi_\gamma(g_\ell) = \sum_{j_\gamma, n_\partial, \iota_V} (\psi_\gamma)_{n_\partial, \iota_V}^{j_\gamma} (\theta_\gamma)_{n_\partial, \iota_V}^{j_\gamma} (g_\ell) \quad (3.2.18)$$

where j_γ is the set of spins associated to the graph γ , n_∂ the magnetic numbers associated to its boundary, ι_V the set of intertwiners associated to its vertices;

$$(\psi_\gamma)_{n_\partial, \iota_V}^{j_\gamma} := \psi_{\vec{n}_1 \dots \vec{n}_N, \vec{\iota}_1 \dots \vec{\iota}_N}^{\vec{j}_1 \dots \vec{j}_N} \prod_{a_{vw}^i=1} \delta_{j_v^i, j_w^i} I_{n_v^i, n_w^i} \quad (3.2.19)$$

and

$$(\theta_\gamma)_{n_\partial, \iota_V}^{j_\gamma} (g_\ell) := \langle g_\ell | j_\gamma, n_\partial, \iota_V \rangle \quad (3.2.20)$$

with $|j_\gamma, n_\partial, \iota_V\rangle$ element of the spin network basis of \mathcal{H}_γ . To show that the natural scalar product in \mathcal{H}_N allows to compare states associated to graphs with same number of vertices N but possibly different connectivity, we can restrict the attention to the basis states. We obtain

$$\begin{aligned} \langle j'_{\gamma'}, n'_{\partial\gamma'}, \iota'_V | j_\gamma, n_\partial, \iota_V \rangle &= \left(\prod_v \delta_{j'_v, j_v} \delta_{n'_{c^i(v)}, n_{c^i(v)}} \right) \left(\prod_{v: c^i(v)=0 \wedge c'^i(v) \neq 0} \delta_{n_{c^i(v)}, n'_{c^i(v)}} \right) \\ &\cdot \left(\prod_{v: c^i(v) \neq 0 \wedge c'^i(v)=0} \delta_{n'_v, n_v} \right) \left(\prod_{v: c^i(v)=c'^i(v)=0} \delta_{n'_v, n_v} \right) \prod_v \delta_{\iota'_v, \iota_v} \end{aligned} \quad (3.2.21)$$

²Note that states associated to graphs with different number of vertices are necessarily orthogonal, due to the structure of the GFT (pre-)Fock space.

The above expression shows that graph states with different combinatorial structures are not necessarily orthogonal. Such feature derives from the fact that, in our framework, graphs do not underpin the definition of the kinematical Hilbert space, but arise as entanglement patterns among quanta, defined in a larger (with respect to the degrees of freedom associated to each graph) (pre-)Fock space. Let us also remark that, though given a graph state $\psi_\gamma \in \mathcal{H}_\gamma$ the multi-particle one $\psi \in \mathcal{H}_N$ of the pre-gluing phase is not uniquely defined, such an ambiguity does not affect the result of the scalar product.

3.2.5 Spin network states with individually weighted vertices

Here we consider a special class of states constructed out of a set of individually weighted vertices, namely of multi-particle states which factorize per vertex. The interest in these states is multiple: in addition to being the simplest generalization of condensate states used in cosmology [89, 90] where also space-connectivity information is encoded, and having been used in Ref. [91, 92] to model black hole geometries, they can be put in direct relation to tensor networks (see section 3.8).

Consider a multi-particle state that factorizes over the single-vertex Hilbert spaces:

$$|\psi^f\rangle = \bigotimes_v |f_v\rangle \quad (3.2.22)$$

where $f_v \in \mathcal{H}$ is the state of vertex v and f on the right hand side is a short notation for the whole set of single-vertex states: $f := \{f_1, \dots, f_N\}$. By applying to $|\psi^f\rangle$ the link maps according to the combinatorial pattern $\gamma \equiv A$ one obtains the spin network state

$$\begin{aligned} |\psi_\gamma^f\rangle &:= \left(\bigotimes_{a_{vw}^i=1} \mathbb{P}_{\ell_{vw}^i} \right) \bigotimes_v |f_v\rangle \\ &= \int \prod_v d\vec{g}_v \int \left(\prod_{a_{vw}^i=1} dh_{vc^i(v)} \right) \prod_v f_v(g_v^i h_{vc^i(v)}) \bigotimes_v |\vec{g}_v\rangle \end{aligned} \quad (3.2.23)$$

with support on γ and individually weighted vertices. Note that, given a state $\psi_\gamma \in \mathcal{H}_\gamma$, it is always possible to identify functions f_1, \dots, f_N that return it once glued according to the adjacency matrix of γ , i.e. $\psi_\gamma = \psi_\gamma^f$.

3.3 Unlabelled entanglement graphs

As we have shown, in GFT the discrete geometries resulting from the gluing of the fundamental simplices (the ‘‘quanta of space’’) are encoded in the entanglement structure of multi-particle states and represented by graphs whose vertices are dual to the fundamental simplices (spin network graphs). So far we considered the GFT vertices as *distinguishable*, i.e. we labelled them and worked in the pre-Fock space of the theory. However, the vertex labelling is just an auxiliary structure, which does not possess any physical meaning. In the following we show how to remove it from the labelled-graph states by symmetrizing over the vertex labels, thereby obtaining states associated to unlabelled graphs. This symmetrization projects the state into the proper (kinematic) Hilbert space of the underlying GFT, i.e. the Fock space, in which only wavefunctions symmetric under permutations of the vertex set appear.

3.3.1 Unlabelled-graph states in the first-quantization language

Given a state ψ_γ associated to a graph $\gamma = A$, we turn it into a state invariant under vertex-relabelling by symmetrizing over the vertex labels:

$$\psi_{[\gamma]} \left(g_\ell = g_v^i g_{c^i(v)}^{-1} \right) = \text{sym}_v \left\{ \psi_\gamma \left(g_\ell = g_v^i g_{c^i(v)}^{-1} \right) \right\} = \sum_\pi \int \left(\prod_A dh \right) \psi(\dots, g_{\pi(v)}^i h_{vc^i(v)}, \dots) \quad (3.3.1)$$

with π referring to a permutation over N elements. In $\psi_{[\gamma]}$, the vertex degrees of freedom are still entangled according to the pattern of the original labelled-graph state, but the vertices are *indistinguishable*; the state is thus associated to the unlabelled graph $[\gamma] = [A]$.

Denoting by \mathcal{P}_π the operator performing the relabelling $v \rightarrow \pi(v)$, i.e.

$$\langle \vec{g}_1, \dots, \vec{g}_N | \mathcal{P}_\pi | \psi_\gamma \rangle = \psi_\gamma(\vec{g}_{\pi(1)}, \dots, \vec{g}_{\pi(N)}), \quad (3.3.2)$$

we can write $\psi_{[\gamma]}$ as follows:

$$|\psi_{[\gamma]}\rangle = \sum_{\pi \in S_N} \mathcal{P}_\pi |\psi_\gamma\rangle = \mathcal{P}_{\text{inv}} |\psi_\gamma\rangle \quad (3.3.3)$$

where $\mathcal{P}_{\text{inv}} = \sum_{\pi \in S_N} \mathcal{P}_\pi$ is the operator projecting the labelled-graph state into the subspace invariant under vertex relabelling.

3.3.2 Unlabelled-graph states in the second-quantization language

The unlabelled graph state $|\psi_{[\gamma]}\rangle$ belongs, by definition, to the Fock space $\mathcal{F}(\mathcal{H})$, and can be written in the second-quantization formalism as follows:

$$|\psi_{[\gamma]}\rangle = \int \left(\prod_v d\vec{g}_v \right) \psi_\gamma \left(g_\ell = g_v^i g_{c^i(v)}^{-1} \right) \prod_v \hat{\phi}^\dagger(\vec{g}_v) |0\rangle \quad (3.3.4)$$

In fact, the symmetry of the wavefunction is ensured by the commutativity of the field operators, which “projects” ψ_γ to the Fock space.

So far we constructed unlabelled-graph states starting from labelled-graph ones and implementing invariance under vertex-relabelling. This is the most natural procedure as vertex labels, despite lacking a physical interpretation, are needed to define a graph. However, we could be interested in implementing an entanglement pattern directly in the Fock space. Let us then define the operator performing this task; given an unlabelled graph $[\gamma]$ with N vertices we introduce the following $N + N$ -body operator:

$$O_{[\gamma]} = \int \prod_v d\vec{g}_v \int \left(\prod_A dh \right) \prod_v \hat{\phi}^\dagger(g_v^i h_{vc^i(v)}) \prod_v \hat{\phi}(\vec{g}_v), \quad (3.3.5)$$

where $\hat{\phi}^\dagger(g_v^i h_{vc^i(v)})$ is a short notation for $\hat{\phi}^\dagger(g_v^1 h_{vc^1(v)}, \dots, g_v^A h_{vc^A(v)})$ and $\vec{c}(1), \dots, \vec{c}(N)$ are the vectors defined in Eq. (3.2.15) which encode the connectivity of the graph. When acting on a N -particle state the operator $O_{[\gamma]}$ entangles the vertex degrees of freedom according to the pattern $[\gamma]$:

$$O_{[\gamma]} \prod_v \hat{\phi}(\vec{g}_v)^\dagger |0\rangle = \int \left(\prod_A dh \right) \prod_v \hat{\phi}^\dagger(g_v^i h_{vc^i(v)}) |0\rangle \quad (3.3.6)$$

Note that, though the operator $O_{[\gamma]}$ generates an entanglement pattern directly in the Fock space, it is still dependent from the possibility to distinguish vertices; in fact, defining the vectors $\vec{c}(1), \dots, \vec{c}(N)$ requires assigning a vertex labelling to $[\gamma]$. Note also that $O_{[\gamma]}$ can be thought of as a second-quantized version of the link maps introduced in subsection 3.2.3. However, it is not a projection operator, as further applications of $O_{[\gamma]}$ on the state of Eq. (3.3.6) leaves the latter unchanged only if the pattern $[\gamma]$ is completely symmetric (completely connected or disconnected). In fact we have that

$$\begin{aligned} O_{[\gamma]}^2 \prod_v \hat{\phi}(\vec{g}_v)^\dagger |0\rangle &= \int \left(\prod_A dh dh' \right) \sum_\pi \prod_v \hat{\phi}^\dagger \left(g_{\pi(v)}^i h_{\pi(v)c^i(\pi(v))} h'_{vc^i(v)} \right) |0\rangle \\ &= \int \left(\prod_A dh dh' \right) \sum_\pi \prod_v \hat{\phi}^\dagger \left(g_v^i h_{vc^i(v)} h'_{\pi^{-1}(v)c^i(\pi^{-1}(v))} \right) |0\rangle, \end{aligned} \quad (3.3.7)$$

and, in order for the r.h.s of Eq. (3.3.7) to be proportional to the r.h.s of Eq. (3.3.6), all links in $[\gamma]$ must be glued (case $c^i(v) \neq 0 \forall v, i$) or open (case $c^i(v) = 0 \forall v, i$).

3.3.2.1 Unlabelled-graph states from individually weighted vertices

Here we introduce the unlabelled version of the graph states constructed out of individually weighted vertices, defined in subsection 3.2.5. Consider the labelled-graph state $|\psi_{[\gamma]}^f\rangle$ defined in Eq. (3.2.23); its unlabelled counterpart is given by

$$|\psi_{[\gamma]}^f\rangle = \int \left(\prod_v d\vec{g}_v \right) \psi_{[\gamma]}^f \left(g_\ell = g_v^i g_{c^i(v)}^{-1} \right) \bigotimes_v |\vec{g}_v\rangle \quad (3.3.8)$$

where

$$\psi_{[\gamma]}^f \left(g_\ell = g_v^i g_{c^i(v)}^{-1} \right) = \text{sym} \left\{ \psi_{[\gamma]}^f \left(g_\ell = g_v^i g_{c^i(v)}^{-1} \right) \right\} = \sum_{\pi} \int \left(\prod_{a_{vw}^i=1} dh_{vc^i(v)} \right) \prod_v f_v \left(g_{\pi(v)}^i h_{vc^i(v)} \right) \quad (3.3.9)$$

and f in $\psi_{[\gamma]}^f$ refers to the set of vertex wavefunctions ordered according to the adjacency matrix $A = \gamma$. Note that

$$\begin{aligned} \psi_{[\gamma]}^f(\vec{g}_{\pi(1)}, \dots, \vec{g}_{\pi(N)}) &= \int \left(\prod_A dh \right) \prod_v f_v \left(g_{\pi(v)}^i h_{vc^i(v)} \right) \\ &= \int \left(\prod_A dh \right) \prod_v f_{\pi^{-1}(v)} \left(g_v^i h_{\pi^{-1}(v)c^i(\pi^{-1}(v))} \right) \\ &= \int \left(\prod_{A'} dh' \right) \prod_v f_{\pi^{-1}(v)} \left(g_v^i h'_{vc^i(v)} \right) \\ &= \psi_{[\gamma']}^{f'}(\vec{g}_1, \dots, \vec{g}_N), \end{aligned} \quad (3.3.10)$$

where $f'_v := f_{\pi^{-1}(v)}$ and $h'_{vc^i(v)} := h_{\pi^{-1}(v)c^i(\pi^{-1}(v))}$. That is, $\mathcal{P}_{\pi}|\psi_{[\gamma]}^f\rangle = |\psi_{[\gamma']}^{f'}\rangle$ with $\gamma' \equiv A' = P_{\pi^{-1}}AP_{\pi}^{-1}$ and $f' = P_{\pi^{-1}}f = \{f_{\pi^{-1}(1)}, \dots, f_{\pi^{-1}(N)}\}$.

3.4 Combinatorial product

An unlabelled-graph state is defined by a combinatorial pattern $[\gamma]$ and a wavefunction of the variables attached to the graph elements (vertices and links) symmetric with respect to the vertex labels. As showed in the previous section, such a state can be thought of as built up from a set of labelled-graph states related to each other by vertex-relabelling. We have emphasized that quantum states associated to different graphs are not orthogonal, as to be expected since they simply correspond to different entanglement patterns of the same number of quanta. At the same time, we are interested in the possibility of comparing such states and defining a precise measure of their overlap that depends directly on the underlying combinatorial pattern.

Consider the scalar product between two unlabelled-graph states, written (in the pre-Fock space) as the result of summing over labelled-graph ones:

$$\langle \varphi_{[\gamma']} | \psi_{[\gamma]} \rangle = \langle \varphi_{\gamma'} | \mathcal{P}_{\text{inv}} \mathcal{P}_{\text{inv}} | \psi_{\gamma} \rangle = \langle \varphi_{\gamma'} | \mathcal{P}_{\text{inv}} | \psi_{\gamma} \rangle = \sum_{\pi \in S_N} \langle \varphi_{\gamma'} | \mathcal{P}_{\pi} | \psi_{\gamma} \rangle \quad (3.4.1)$$

On the basis of this expression, we define a ‘‘combinatorial product’’ which compares labelled-graph states giving relevance to the combinatorial aspect, independently on the specific vertex-labelling: it amounts to select, among the possible versions of two graph states corresponding to different labellings of the vertices, the ones which maximise the superposition of their combinatorial structures, and then compute the standard scalar product between them. As such, it is not a scalar product *per se*, e.g. it cannot be defined on a basis of the Hilbert space the states live in, as it inherently depends on the pair of states considered. This product can rather be seen as a prescription to align graphs in order to maximise their overlap, and then compute the (standard) scalar product between the corresponding states.

Definition 3.4.1 (Combinatorial product). Given two graph states $|\psi_\gamma\rangle$ and $|\varphi_{\gamma'}\rangle$ we define their combinatorial product as follows:

$$\langle\varphi_{\gamma'}|\psi_\gamma\rangle_{\text{comb}} := \langle\varphi_{\gamma'}|\mathcal{P}_{\bar{\pi}}|\psi_\gamma\rangle \quad (3.4.2)$$

where the permutation $\bar{\pi}$ is such that

$$|\langle\varphi_{\gamma'}|\mathcal{P}_{\bar{\pi}}|\psi_\gamma\rangle| = \max_{\pi \in S_{\min}} |\langle\varphi_{\gamma'}|\mathcal{P}_\pi|\psi_\gamma\rangle| \quad (3.4.3)$$

with

$$S_{\min} := \{\pi \in S_N : d(P_{\pi^{-1}}AP_{\pi^{-1}}^{-1}, B) = \min_{C \in [A]} d(C, B)\} \quad (3.4.4)$$

where $A \equiv \gamma$ and $B \equiv \gamma'$, and $d(\cdot, \cdot)$ is a notion of distance between matrices.

Note that $\langle\varphi_{\gamma'}|\psi_\gamma\rangle_{\text{comb}} = 1$ if the states $|\psi_\gamma\rangle$ and $|\varphi_{\gamma'}\rangle$ differ only for the labelling of their vertices, as expected in a setting where such a labelling is deprived of any physical meaning.

At this point, a question naturally arises: can we provide a similar prescription in the Fock space, i.e. define a scalar product which emphasizes the combinatorial structure of the states? Note that, when considering symmetric states, all permutations of the vertex labels produce the same value on the right hand side of Eq. (3.4.2). Therefore, selecting a particular alignment of vertices does not affect the result. Moreover, to define such a scalar product in the Fock space is simply not possible: aligning graphs as we have done requires vertex labels, and thus to break the symmetry which underpins the very definition of the Fock space. To clarify this point, in the following we translate the combinatorial product in the second-quantized formalism. We work with unlabelled-graph states written as in Eq. (3.3.4) in order to recover, when breaking the Fock space symmetry, the labelled-graph wavefunctions from which they were defined³. We start by rewriting Eq. (3.4.1) in a second-quantized formalism:

$$\begin{aligned} \langle\varphi_{[\gamma']}|\psi_{[\gamma]}\rangle &= \int \left(\prod_v d\vec{g}_v d\vec{q}_v \right) \varphi_{\gamma'}^*(\vec{q}_1, \dots, \vec{q}_N) \psi_\gamma(\vec{g}_1, \dots, \vec{g}_N) \langle 0 | \prod_v \hat{\phi}(\vec{q}_v) \prod_v \hat{\phi}^\dagger(\vec{g}_v) | 0 \rangle \\ &= \int \left(\prod_v d\vec{g}_v d\vec{q}_v \right) \varphi_{\gamma'}^*(\vec{q}_1, \dots, \vec{q}_N) \psi_\gamma(\vec{g}_1, \dots, \vec{g}_N) \sum_{\pi \in S_N} C_\pi(\vec{q}_1, \vec{g}_1, \dots, \vec{q}_N, \vec{g}_N), \end{aligned} \quad (3.4.5)$$

with

$$C_\pi(\vec{q}_1, \vec{g}_1, \dots, \vec{q}_N, \vec{g}_N) := \langle 0 | \prod_v [\hat{\phi}(\vec{q}_v), \hat{\phi}^\dagger(\vec{g}_{\pi(v)})] | 0 \rangle, \quad (3.4.6)$$

This formula makes explicit how the commutation properties of the field operators ensure that all the contributions coming from the various possible vertex-labellings are taken into account in the computation of the scalar product. At a combinatorial level, this means that every vertex v of one (labelled) graph overlaps with any vertex $\pi(v)$ of the other. In other words, each term C_π corresponds to a possible overlap configuration between two labelled versions of $[\gamma]$ and $[\gamma']$.

We note that C_π corresponds to a particular ordering of the ladder operators, and exploit this observation to write the combinatorial product of definition 3.4.1 in a second-quantization form. We start by defining the following ordering prescription:

$$: \prod_v \hat{\phi}(\vec{q}_v) \prod_v \hat{\phi}^\dagger(\vec{g}_v) :_\pi := \prod_v \hat{\phi}(\vec{q}_v) \hat{\phi}^\dagger(\vec{g}_{\pi(v)}) \quad (3.4.7)$$

³In doing this, we make a slight abuse of notation: in Eq. (3.3.4) the unlabelled-graph state $|\psi_{[\gamma]}\rangle$ is written in terms of the labelled-graph wavefunction ψ_γ , but the only readable information about the latter is its symmetrized version, namely $\psi_{[\gamma]}$; in fact, the commutativity of the creation operators $\hat{\phi}^\dagger$ hides any information content about ψ_γ which is not symmetric under vertex relabelling. Note also that, given $\psi_{[\gamma]}$, the choice of ψ_γ is not unique; however, this feature is not relevant for the present purpose.

We then point out that the unlabelled-graph state of Eq. (3.3.4) can be seen as the result of acting on the vacuum state with the operator

$$O_{\psi_{[\gamma]}} = \int \left(\prod_v d\vec{g}_v \right) \psi_{\gamma}(\vec{g}_1, \dots, \vec{g}_N) \prod_v \hat{\phi}^{\dagger}(\vec{g}_v) \quad (3.4.8)$$

In other terms, the information about the unlabelled-graph state can be equivalently encoded in an operator. By this line of reasoning, the Fock space scalar product can be seen as the vacuum expectation value of an observable constructed out of the states to be compared:

$$\langle \varphi_{[\gamma']} | \psi_{[\gamma]} \rangle = \langle 0 | O_{\varphi_{[\gamma']}}^{\dagger} O_{\psi_{[\gamma]}} | 0 \rangle \quad (3.4.9)$$

We might thus be tempted to define the combinatorial product between two unlabelled-graph states as the vacuum expectation value of an ordered version of that observable, using the prescription introduced in Eq. (3.4.7):

$$\langle \varphi_{[\gamma']} | \psi_{[\gamma]} \rangle_{\text{comb}} \stackrel{?}{=} \langle 0 | O_{\varphi_{[\gamma']}}^{\dagger} O_{\psi_{[\gamma]}} : \bar{\pi} | 0 \rangle \quad (3.4.10)$$

where the permutation $\bar{\pi}$ is such that

$$|\langle 0 | O_{\varphi_{[\gamma']}}^{\dagger} O_{\psi_{[\gamma]}} : \bar{\pi} | 0 \rangle| = \max_{\pi \in S_{\min}} |\langle 0 | O_{\varphi_{[\gamma']}}^{\dagger} O_{\psi_{[\gamma]}} : \pi | 0 \rangle| \quad (3.4.11)$$

with S_{\min} defined in Eq. (3.4.4). A first drawback of Eq. (3.4.10) is that it crucially depends on the form in which the unlabelled graph states (and so the corresponding observables) are expressed. But, more importantly, it selects a “preferred” vertex-labelling and thus leads out of the Fock space; therefore, it *cannot be* the scalar product induced by the Fock space on a given subset of states. These considerations makes it clear that an alignment prescription between graphs in the Fock space is prevented by the very definition of this space, i.e. by the vertex-label symmetry underlying it. Let us stress that we do not see this as a shortcoming, but as a feature of the formalism, which correctly indicates that the only physical information is to be label-independent, and that there is no special physical reason, in this context, to partition the Hilbert space into sectors associated to different combinatorial patterns. The situation changes if new physical ingredients are introduced, leading to a meaningful, i.e. physically characterized, labelling of the vertex set. We outline a situation in which this is the case in the following section.

3.5 Effective distinguishability of vertices

In a fundamental quantum gravity theory that possesses the same symmetries of classical General Relativity (even when not arising from its straightforward quantization), the only allowed reference frames are “physical rods and clocks”; in other words, the presence of a background structure respect to which define a notion of space/time locality is *a priori* excluded. This has led to the formulation of the relational strategy for the construction of diffeomorphism invariant observables in quantum gravity [93–99]⁴. In the same spirit, here we show how to attain an effective distinguishability of vertices by introducing in the theory additional degrees of freedom, interpreted as discretized (scalar) matter and to be used as a “physical reference frame”, without breaking the fundamental symmetries of the formalism, in particular the symmetry under permutations of vertex labels that we suggested to be a discrete analogue of diffeomorphism invariance. Operationally, we use these additional degrees of freedom to break the symmetry over the vertex-labels at an effective level only, achieving distinguishability only for a special class of quantum states and in a physically motivated approximation.

⁴The issue of defining and formulating physics in terms of quantum reference frames defined by suitable matter systems is also an important topic in the foundations of quantum mechanics, beside quantum gravity applications [100–102].

For simplicity we consider, as additional degrees of freedom, a minimally coupled free massless scalar field χ discretized along the geometric data on the graphs (and simplicial complexes) associated to GFT quantum states, in analogy with the approach of [90, 103] for defining a relational dynamics in the GFT condensate cosmology, and based on the analysis of scalar matter coupled to quantum gravity in GFT [104] and canonical LQG and spin foam models [105, 106]. The GFT field thus turns into $\phi(\vec{g}, \chi) \in L^2(G^d/G \times \mathbb{R})$, and the canonical commutation relations of Eq. (2.4.6) are modified as follows:

$$[\hat{\phi}(\vec{g}; \chi), \hat{\phi}^\dagger(\vec{g}'; \chi')] = \int dh \prod_{i=1}^d \delta(hg^i(q^i)^{-1}) \delta(\chi - \chi') \quad (3.5.1)$$

We focus on the simpler case of graph states with individually weighted vertices (the generalization to a non-separable graph wavefunction is straightforward). With the new dynamical variables given by the values of the scalar field χ , the unlabelled-graph state takes the following form:

$$|\psi_{[\gamma]}^f\rangle = \sum_{\pi} \int \prod_v d\chi_v d\vec{g}_v \int \left(\prod_A dh \right) \prod_v f_v \left(g_v^i h_{\pi(v)c^i(\pi(v))}; \chi_v \right) \prod_v \hat{\phi}^\dagger(\vec{g}_v; \chi_v) |0\rangle \quad (3.5.2)$$

The scalar product between two graph states of this type is thus given by

$$\langle \psi_{[\gamma']}^{f'} | \psi_{[\gamma]}^f \rangle = \sum_{\pi} \int \prod_v d\chi_v d\vec{g}_v \int \left(\prod_{A'} dh' \right) \left(\prod_A dh \right) \prod_v f'_v \left(g_v^i h'_{v c'^i(v)}; \chi_v \right) f_{\pi(v)} \left(g_v^i h_{\pi(v)c^i(\pi(v))}; \chi_v \right), \quad (3.5.3)$$

where we used the commutation relations of Eq. (3.5.1). We then make the following assumption: in a partial semiclassical limit of the theory, the vertex wavefunctions are peaked on non-equal values of the scalar field χ taken from the set $\{\chi_1^0, \dots, \chi_N^0\}$. Then the scalar field labels can be interpreted as defining an effective embedding of the abstract graphs to which the quantum states are associated (more precisely, of their vertices) into an auxiliary manifold; but more generally, they provide a physical (i.e. in terms of measurable quantities) way to distinguish the vertices in the associated graphs. As an example, consider the case in which f_v and f'_v are picked on χ_v^0 ; the main contribution to the scalar product then comes from the trivial permutation $\pi(v) = v$:

$$\langle \psi_{[\gamma']}^{f'} | \psi_{[\gamma]}^f \rangle \approx \int \prod_v d\vec{g}_v \int \left(\prod_{A'} dh' \right) \left(\prod_A dh \right) \prod_v f'_v \left(g_v^i h'_{v c'^i(v)}; \chi_v^0 \right) f_v \left(g_v^i h_{v c^i(v)}; \chi_v^0 \right) \quad (3.5.4)$$

More generally, if f'_v is peaked on $\chi_{\omega'(v)}^0$ and f_v is peaked on $\chi_{\omega(v)}^0$, where $\omega, \omega' \in S_N$, the permutation π providing the main contribution to the scalar product is the one which satisfies the condition $\omega'(v) = \omega(\pi(v))$. We therefore see that, if the vertex wavefunctions are peaked on values of the field taken from a discrete set $\{\chi_1^0, \dots, \chi_N^0\}$, the scalar product is effectively performed on two labelled versions of the original unlabelled graph states, and the set $\{\chi_1^0, \dots, \chi_N^0\}$ represents the effective vertex-labelling. As we noted already, peaking the wavefunctions on $\{\chi_1^0, \dots, \chi_N^0\}$ can be interpreted as embedding the graph into an auxiliary manifold via physically measurable quantities, thus justifying the resulting distinguishability.

It is important to stress that the recovered distinguishability is *effective*, obtained through a suitable choice of states and hence only in a suitable approximation of the fundamental theory, and *relational*, since it allows to align graph structures with respect to each other, as desired. In fact, we remark again that we cannot restore distinguishability of vertices at a structural level, as this is prevented from the very symmetric structure of the Fock space, and this impossibility is well grounded in the requirement of background independence of the fundamental theory.

3.6 The quantum information tool of Tensor Networks

A tensor $T_{n_1 \dots n_N}$ is an array of complex numbers: the indices n_i take values in a discrete set, whose dimension D_i is usually called *bond dimension*; the number N of indices is called *rank* of

the tensor. Each index n_i can be thought of as labelling a basis in a Hilbert space \mathcal{H}_{D_i} , and the tensor can then be regarded as a map between the Hilbert spaces associated to complementary set of indices. As an example, consider the rank-two tensor T_{ab} with input index a and output index b ; denoting by \mathcal{H}_{in} and \mathcal{H}_{out} the corresponding input and output Hilbert spaces, we can interpret the tensor as the following map [107]:

$$\begin{aligned} T : \mathcal{H}_{\text{in}} &\rightarrow \mathcal{H}_{\text{out}} \\ |a\rangle &\rightarrow \sum_b T_{ab}|b\rangle \end{aligned} \quad (3.6.1)$$

When regarding all the indices of a tensor $T_{n_1 \dots n_N}$ as output indices, that tensor accounts for the state of a quantum system described by the Hilbert space $\mathcal{H}_{D_1} \otimes \dots \otimes \mathcal{H}_{D_N}$:

$$|T\rangle = \sum_{n_1 \dots n_N} T_{n_1 \dots n_N} |n_1 \dots n_N\rangle \quad (3.6.2)$$

A *tensor network* is a set of tensors connected according to a certain pattern, where the connection is realized by the contraction of their indices. By representing a tensor as a node with open lines, one for each index, the tensor network acquires the structure of a graph. In the following subsections we present two of the most common tensor network structures.

3.6.1 Matrix Product States

Matrix Product States (MPS) for a system of spins s can be constructed by applying the Wilson renormalization group method [108, 109], as we are going to explain (see Ref. [110] for a detailed presentation of the topic). Let \mathcal{H}_1 be the single spin Hilbert space, having dimension $d_1 = 2s + 1$. Given two spins s_1 and s_2 , consider a subspace $\mathcal{H}_2 \subset \mathcal{H}_1 \otimes \mathcal{H}_1$ with $d_2 \leq d_1^2$. Proceed iteratively by adding spins and taking the subspace $\mathcal{H}_i \subset \mathcal{H}_{i-1} \otimes \mathcal{H}_1$ such that $d_i \leq d_{i-1}d_1$. A state of N spins in the subspace \mathcal{H}_N can then be written as follows:

$$|\psi\rangle = \sum_{s_1, \dots, s_N} A_1^{s_1} A_2^{s_2} \dots A_N^{s_N} |s_1, s_2, \dots, s_N\rangle \quad (3.6.3)$$

where $A_i^s \in M_{d_{i-1} \times d_i}$ for $i = 2, \dots, N-1$, A_1^s is a row vector of rank d_1 and A_N^s is a column vector of rank d_N . Explicitly:

$$|\psi\rangle = \sum_{s_1, \dots, s_N} (A_1^{s_1})_\alpha (A_2^{s_2})_{\alpha\beta} \dots (A_{N-1}^{s_{N-1}})_{\mu\nu} (A_N^{s_N})_\nu |s_1, s_2, \dots, s_N\rangle, \quad (3.6.4)$$

where $\alpha, \beta, \dots, \nu$ are the matrix indices. To each site i we thus associated a tensor $(A_i^s)_{\alpha\beta}$ that, in addition to the physical index s_i , has left and right virtual indices α and β connecting it with sites $i-1$ and $i+1$, respectively. The virtual indices can be thought of as describing the states of auxiliary systems added to each site.

3.6.2 Projected Entangled-Pair States

The MPS of Eq. (3.6.3) can be expressed as another type of tensor network decomposition: **Projected Entangled-Pair States (PEPS)**. Let $|\epsilon_i\rangle \in \mathcal{H}_i \otimes \mathcal{H}_i$ be a maximally entangled state between the right ancilla of site i and the left ancilla of site $i+1$. Consider the operator $P_i : \mathcal{H}_{i-1} \otimes \mathcal{H}_i \rightarrow \mathcal{H}_i$ projecting the ancilla states to the s -spin state:

$$P_i = \sum_s \sum_{\alpha\beta} (A_i^s)_{\alpha\beta} |s\rangle \langle \alpha\beta| \quad (3.6.5)$$

The matrix product state of Eq. (3.6.3) can then be written as follows:

$$|\psi\rangle = \sum_{s_1, \dots, s_N} A_1^{s_1} A_2^{s_2} \dots A_N^{s_N} |s_1, s_2, \dots, s_N\rangle = (P_1 \otimes \dots \otimes P_N) |\epsilon_1\rangle \otimes \dots \otimes |\epsilon_{N-1}\rangle \quad (3.6.6)$$

Such a tensor network decomposition is thus built up from maximally entangled ancilla pairs (making up the links of the network) which are projected to physical spins (the network sites). Here we considered a one-dimensional system, a spin chain, but the PEPS decomposition can be easily generalised to higher dimensional systems. Before illustrating this point, we show that in a simple one-dimensional PEPS, specifically the state of a translationally invariant system, entanglement entropy is bounded by an area law. To start note that, since the reduced density matrix $\rho_{1,2,\dots,M}$ for the first M spins has rank bounded by d_M , the entanglement entropy $S(\rho_{1,2,\dots,M})$ satisfies

$$S(\rho_{1,2,\dots,M}) \leq \log d_M. \quad (3.6.7)$$

We assume that all the auxiliary systems have dimension D , and site N is connected to site 1, i.e. $A_i^s \in M_{D \times D} \forall i$. The state of the translationally invariant spin chain thus takes the following form:

$$|\psi\rangle = \sum_{s_1, \dots, s_N} \text{Tr}(A_1^{s_1} A_2^{s_2} \dots A_N^{s_N}) |s_1, s_2, \dots, s_N\rangle. \quad (3.6.8)$$

Given an interval A of the spin chain the entanglement entropy S_A then satisfies

$$S_A \leq 2 \log D \quad (3.6.9)$$

which is an area law for the upper bound to S_A . In fact, denoting by c_A the curve bounding A , we have that

$$S_A \leq \min_{c_A} \{c_A \cap \text{network}\} \log D, \quad (3.6.10)$$

where $\{c_A \cap \text{network}\}$ is the number of intersections between the curve c_A and the spin chain.

We can introduce PEPS in dimension higher than one by considering network sites that, in addition to the physical spin s , have a number $d > 2$ of auxiliary spins which are maximally entangled with their neighbours. For simplicity we assume that each auxiliary spin has dimension D . The PEPS is then constructed by projecting the entangled auxiliary-spin pairs onto the physical spins with the following operators:

$$P_i = \sum_s \sum_{\alpha^1 \dots \alpha^d=1}^D (A_i^s)_{\alpha^1 \dots \alpha^d} |s\rangle \langle \alpha^1 \dots \alpha^d|, \quad (3.6.11)$$

where $\alpha^1 \dots \alpha^d$ are the virtual indices referring to the auxiliary spins. That is, the PEPS is given by

$$|\psi\rangle = (P_1 \otimes \dots \otimes P_N) \bigotimes_{\ell \in \mathcal{N}} |\epsilon_\ell\rangle \quad (3.6.12)$$

where we denoted by ℓ the generic link of the network \mathcal{N} , and by $|\epsilon_\ell\rangle$ the corresponding maximally entangled states of auxiliary spins.

Let A be a region of the network and c_A its boundary. Since every maximally entangled state between an auxiliary spin and its neighbour has dimension D , we have that

$$S_A \leq \min_{c_A} \{c_A \cap \text{network}\} \log D, \quad (3.6.13)$$

where $\{c_A \cap \text{network}\}$ corresponds to the number of entangled pairs across the boundary c_A of region A . Therefore, also in this case the entanglement entropy turns out to be bounded by an area law. Note that an area law for the upper bound to the entanglement entropy arises in tensor networks directly from their definition, as the contraction of indices generally induces entanglement between the corresponding degrees of freedom. However, only some tensor networks saturate this bound, thus exhibiting an holographic behaviour; among them, we can find tensor networks built up from perfect tensors (a special class of isometric tensors) [107] or random tensor networks in the limit of large bond dimensions [111].

It is possible to construct PEPS with completely arbitrary network geometries by varying the number of auxiliary spins of each site, and defining their entanglement relations by choosing appropriate ancilla-pair states. See Ref. [112] for an example of such construction: the vertices

possess the highest possible valence for a completely connected graph (namely $N - 1$ for a graph of N vertices), and separable ancilla states are introduced to account for the absence of links between vertices.

Let us finally mention that PEPS are used in the study of lattice gauge theories (LGT) via tensor networks techniques [113, 114]. In particular, in the LGT context they are provided with a gauge-invariance symmetry at each node, thus resembling also in this aspect the structure of GFT graphs. The second-quantized tensor networks that we are going to define in the GFT context can indeed be seen as a generalization of such construction.

3.7 A simple realization of entanglement/topology and entanglement/geometry correspondences in GFT and TN

Before presenting the map between group field theory states and tensor networks, we highlight some features which are highly relevant from a quantum gravity perspective.

Entanglement/connectivity correspondence A first one is the relation between entanglement and connectivity of the network/graph. As previously explained, both frameworks employ entanglement as the glue of these structures.

In the GFT context, due to the simplicial interpretation of the graph, this feature implies a relation between entanglement and connectivity of space. In fact, links made of entangled vertex-lines correspond to adjacency relations of the cells dual to the involved vertices. This means that entanglement determines the topology of the simplicial complex dual to the graph. We have, therefore, an explicit example of an entanglement/topology correspondence.

In the tensor network context, a simplicial-geometry interpretation of the network is possible when the latter is proved to reproduce a discretized manifold, as it happens for tensor networks modelling AdS/CFT states [111, 112]. There is however a crucial difference with respect to the GFT case: in the mentioned tensor network constructions, the geometric interpretation is induced “at a later stage”, by defining a metric through the graph distance. We showed that for GFT graphs, instead, the geometric characterization arises naturally thanks to the presence, on top of the combinatorial structure, of additional quantum geometric degrees of freedom.

Beyond these frameworks, a link between entanglement and space(time) connectivity has been clearly pointed out, for example, in the work by [115] in the AdS/CFT context. There it was shown, via a thought experiment, that disentangling two sets of degrees of freedom in the CFT corresponds to increasing the proper distance between the dual spacetime regions, while the area separating them decreases.

This is the combinatorial and topological side of the story. In fact, there is an additional geometric side of the same story, which is particularly interesting from the point of view of quantum gravity (including the GFT formalism and beyond it, in AdS/CFT applications, LQG etc.): the entanglement so established carries a straightforward geometric interpretation, and corresponding entanglement measures can be seen to be measuring geometric observables.

Primitive entanglement/area correspondence In the geometric interpretation of spin network graphs in the context of GFT (and LQG), a link of the graph is dual to a portion of surface on the shared boundary of the two simplices dual to the vertices sharing the link, and the spin attached to it labels the eigenvectors of the area operator associated to that surface. The spectrum of the area operator for such dual surface is (using symmetric ordering) $\sqrt{j(j+1)}$ in Planck units, and thus it scales like j for largish eigenvalues. This is also the scaling of the dimension of the Hilbert space of states associated to each link labeled by a given spin, i.e. a maximally entangled state, which is $d_j = 2j + 1$. In turn, this dimension gives a simple measure of the entanglement that we have seen being associated to the same link, thus establishing a sort of “primitive entanglement/area correspondence” in our quantum gravity states.

Primitive entanglement/volume correspondence An entanglement process can be identified as lying also at the origin of the intertwiner degrees of freedom attached to the vertices of the graph/network, when embedding the spin network states in a Hilbert space of open lines. In particular, the intertwiner arises from the “gluing” of open lines into a vertex, by means of the requirement of local gauge invariance. The spin network basis wavefunction can in fact be written, in the Hilbert space of d open lines

$$\mathcal{H}_d = \bigoplus_{\vec{j}} \left(\bigotimes_{i=1}^d V^{j^{i*}} \otimes \bigotimes_{i=1}^d V^{j^i} \right), \quad (3.7.1)$$

as follows:

$$\begin{aligned} s_{\vec{n},\iota}^{\vec{j}}(\vec{g}) &:= \sum_{\vec{m}} I_{\vec{m}}^{\vec{j};\iota} \prod_{i=1}^d d_{j^i} D_{m^i n^i}^{j^i}(g^i) \\ &= \langle \vec{g} | \sum_{\vec{m}} \left(\bigotimes_i \sqrt{d_{j^i}} |j^i n^i\rangle \langle j^i m^i| \right) \left(\sum_{\vec{p}} I_{\vec{p}}^{\vec{j};\iota} |j^1 p^1\rangle \otimes \cdots \otimes |j^d p^d\rangle \right) \end{aligned} \quad (3.7.2)$$

The second line of Eq. (3.7.2) shows that $s_{\vec{n},\iota}^{\vec{j}}$ can be seen as the result of contracting line states (round brackets on the left) with an entangled state of (equal-side) open ends of that lines (round brackets on the right). This is one more instance of a straightforward entanglement/geometry correspondence at the discrete (simplicial) geometry level. In fact, the entanglement structure is controlled by the degree of freedom ι , the intertwiner quantum number, which can be shown (in both simplicial quantum geometry of **GFT** and **LQG**) to label eigenvalues of the operator measuring the volume of the polyhedron dual to the spin network vertex. Thus, also volume information is a measure of the entanglement of quantum gravity degrees of freedom.

Entanglement/area laws A well known consequence of the entanglement origin of tensor networks is the fact that, as showed for the translationally invariant **MPS**, the entanglement entropy is bounded by an area law: given a region A of the network bounded by the curve c_A , and denoted by D the dimension of the Hilbert space associated to the links, we have that

$$S_A \leq \min_{c_A} \{c_A \cap \text{network}\} \log D \quad (3.7.3)$$

When interpreting $\log D$ as the area of an elementary surface dual to the network link, Eq. (3.7.3) turns into an area law for the upper bound to the entanglement entropy. In fact, $\{c_A \cap \text{network}\}$ counts the number of intersections between the boundary c_A and the network, i.e. the number of surface units in c_A , and $\{c_A \cap \text{network}\} \log D$ thus provides the area of the boundary surface c_A .

For tensor networks modelling holographic states in the **AdS/CFT** correspondence (as in Ref. [116], where the tensor network arises by entanglement renormalization, and in Ref. [117], where is constructed by entanglement distillation) Eq. (3.7.3) acquires precisely the connotation of an area law for the upper bound to the entanglement entropy.

In the spin network states of **GFT** the spins carried by a link are eigenvalues of an area operator associated to the surface dual to it. Therefore, the bound to the entanglement entropy of a link, and hence of an extended region of the spin network graph, naturally possesses an area-law interpretation⁵. Spin network states in **GFT** thus share with general tensor networks the feature of having an entanglement entropy bounded according to Eq. (3.7.3). Just as there are classes of tensor networks that saturate the bound (and therefore exhibit an holographic nature), certain classes of **GFT** states have proved to satisfy an entanglement area law [56]. Let us finally point out that the area bounding a region of the **GFT** complex depends on

⁵We are considering the simplest case of a graph with fixed spins, and ignoring for simplicity the contribution to the entropy deriving from the intertwiner degrees of freedom.

the entanglement entropy of the links crossing it, whose total number is determined by the combinatorial structure of the graph. That general area law is thus the result of the graph connectivity and of the local contributions to the entanglement entropy, in turn carrying a primitive entanglement/area correspondence.

3.8 A dictionary between GFT states and (generalised) TN

We are going to show that **GFT** labelled-graph states can be understood as generalised **PEPS** and that, consequently, unlabelled ones realize an analogous correspondence in a second-quantization setting, leading to the definition of second-quantized tensor networks.

As explained in subsection 3.6.2, **PEPS** are constructed by projecting maximally-entangled ancilla-pairs states onto “physical” states (attached to the nodes of the network). In the **GFT** context, the role of ancilla-pair states is played by link states, i.e. maximally entangled states of edge spins, and that of node degrees of freedom by intertwiners. We clarify this with an example, and then present the more general case.

Consider a set of N vertices, with vertex v in the generic state

$$|T_v\rangle = \sum_{\vec{j}, \vec{n}, \iota} (T_v)_{\vec{n}}^{\vec{j}, \iota} |\vec{j}, \vec{n}, \iota\rangle \quad (3.8.1)$$

As shown in subsection 3.2.2, edges of the vertices can be connected by projecting their state into the singlet state defined in Eq. (3.2.9) and reported below:

$$|\ell\rangle := \sum_k \frac{(-1)^{j+k}}{\sqrt{2j+1}} |j, k\rangle |j, -k\rangle \quad (3.8.2)$$

Given a combinatorial pattern γ of the N vertices which is completely connected (no open edges), consider a state of the form of Eq. (3.8.2) for each link of the graph, and perform the contraction with the vertex states:

$$\left(\bigotimes_{\ell \in \gamma} |\ell\rangle \right) \bigotimes_v |T_v\rangle = \sum_{\iota^1 \dots \iota^N} \text{tr}_\gamma \left[(T_1)^{\vec{j}_1, \iota_1} \dots (T_N)^{\vec{j}_N, \iota_N} \right] |\iota_1, \dots, \iota_N\rangle \quad (3.8.3)$$

where $j_v^i = j$ for all v and all i due to the projection onto the link states, A is the adjacency matrix which encodes the combinatorial pattern of γ and tr_A is the tensorial trace contracting the vertex tensors according to A with bivalent intertwiners:

$$\text{tr}_\gamma \left[(T_1)^{\vec{j}_1, \iota_1} \dots (T_N)^{\vec{j}_N, \iota_N} \right] = \left(\prod_v \sum_{\vec{j}_v, \vec{n}_v} \right) (T_1)^{\vec{j}_1, \iota_1} \dots (T_N)^{\vec{j}_N, \iota_N} \prod_{a_{vw}=1} \delta_{j_v^i, j} \delta_{j_w^i, j} I_{n_v^i, n_w^i} \quad (3.8.4)$$

The state defined by Eq. (3.8.6), associated by construction to the graph γ , is a tensor network of the form of Eq. (3.6.12), where the intertwiners ι_v play the role of “physical” indices and n_v^i that of “virtual” indices with bond dimension d_j ; in fact, in this simple example all links carry the same spin j .

A more general setting can be considered by taking, as **GFT** counterparts of the **TN** ancilla-pair states, link states in the direct sum of the Hilbert spaces associated to all group representations:

$$|\ell\rangle = \bigoplus_j \sum_k \frac{(-1)^{j+k}}{\sqrt{2j+1}} |j, k\rangle |j, -k\rangle \quad (3.8.5)$$

The contraction of the link states with the vertex states then yields

$$\left(\bigotimes_{\ell \in \gamma} |\ell\rangle \right) \bigotimes_v |T_v\rangle = \bigoplus_{\vec{j}_1 \dots \vec{j}_N} \sum_{\iota_1 \dots \iota_N} \text{tr}_\gamma \left[(T_1)^{\vec{j}_1, \iota_1} \dots (T_N)^{\vec{j}_N, \iota_N} \right] |\vec{j}_1, \iota_1, \dots, \vec{j}_N, \iota_N\rangle \quad (3.8.6)$$

where

$$\mathrm{tr}_\gamma \left[(T_1)^{\vec{j}_1, \ell_1} \dots (T_N)^{\vec{j}_N, \ell_N} \right] = \sum_{\vec{n}_1 \dots \vec{n}_N} (T_1)_{\vec{n}_1}^{\vec{j}_1, \ell_1} \dots (T_N)_{\vec{n}_N}^{\vec{j}_N, \ell_N} \prod_{a_{vw}^i=1} \delta_{j_v^i, j_w^i} I_{n_v^i, n_w^i} \quad (3.8.7)$$

Let us now move to the second-quantization framework. In particular, consider a **GFT** unlabelled-graph state constructed out of individually-weighted vertices, with the latter given by Eq. (3.8.1):

$$|\psi_{[\gamma]}^T\rangle = \bigoplus_{\vec{j}_1 \dots \vec{j}_N} \left(\prod_v \sum_{\vec{n}_{v\ell_v}} \right) \sum_{A' \in [A]} \left(\prod_v (T_v)_{\vec{n}_{\pi(v)}}^{\vec{j}_{\pi(v)}, \ell_{\pi(v)}} \right) \prod_{a_{vw}^i=1} \delta_{j_v^i, j_w^i} I_{n_v^i, n_w^i} I_{m_v^i, m_w^i} \prod_{v=1}^N \left(\hat{\phi}_{\vec{m}_v}^{\vec{j}_v, \ell_v} \right)^\dagger |0\rangle \quad (3.8.8)$$

We recognize within the round brackets a tensor network which is the symmetrized version of that in Eq. (3.8.7), and can be understood as a *second-quantized tensor network*. The argument can be extended to arbitrary **GFT** unlabelled-graph states, which take the form

$$|\psi_{[\gamma]}\rangle = \bigoplus_{\vec{j}_1 \dots \vec{j}_N} \left(\prod_v \sum_{\vec{n}_{v\ell_v}} \right) \sum_{A' \in [A]} \psi_{\vec{n}_{\pi(1)} \dots \vec{n}_{\pi(N)}}^{\vec{j}_{\pi(1)}, \ell_{\pi(1)} \dots \vec{j}_{\pi(N)}, \ell_{\pi(N)}} \prod_{a_{vw}^i=1} \delta_{j_v^i, j_w^i} I_{n_v^i, n_w^i} I_{m_v^i, m_w^i} \prod_{v=1}^N \left(\hat{\phi}_{\vec{m}_v}^{\vec{j}_v, \ell_v} \right)^\dagger |0\rangle \quad (3.8.9)$$

Note that this expression reduces to Eq. (3.8.8) for

$$\psi_{\vec{n}_{\pi(1)} \dots \vec{n}_{\pi(N)}}^{\vec{j}_{\pi(1)}, \ell_{\pi(1)} \dots \vec{j}_{\pi(N)}, \ell_{\pi(N)}} = \prod_v (T_v)_{\vec{n}_{\pi(v)}}^{\vec{j}_{\pi(v)}, \ell_{\pi(v)}} \quad (3.8.10)$$

Let us finally remark the features of **GFT** graph states which characterize them as *generalised* tensor networks. Some of them are already present at the first-quantized level. The bond dimensions of tensor indices, i.e. the spins associated to the links, are not fixed parameters, but truly dynamical variables; in fact, strictly speaking each Hilbert space associated to a link (before additional conditions are taken into account) is infinite dimensional, being isomorphic to $L^2(G)$. Moreover, the “physical” indices are not, in general, independent from the “virtual” ones. Note also that, as first pointed out by Chirco *et al.* in Ref. [56], even first-quantized **GFT** graph states can be regarded as tensor networks; this remains true at the second-quantization level. A feature which instead pertains more naturally to the second-quantization framework is the dynamical nature of the combinatorial structure: since the network arises from the dynamics of a field, vertices can be created or destroyed, and graph connectivity (deriving from the entanglement properties of the field excitations) can vary. We also point out that, as we noted in quantum gravity applications with a simplicial-geometry interpretation, the **GFT** quanta are endowed with a local gauge symmetry (invariance under the diagonal action of a Lie group), which makes their quantum states corresponding to symmetric tensor networks, of the type employed in applications to gauge theories.

3.9 Discussion

The **GFT** formalism describes entanglement graphs representing simplicial complexes which are understood as spatial portions of a quantum spacetime (or, more generally, codimension-one sub-manifolds). These structures naturally satisfy a discrete version of diffeomorphism invariance, as they are symmetric respect to permutations of the vertex-labelling used to define them⁶. In fact, a given vertex-labelling for an entanglement graph can be understood as a choice of coordinate system on the (discretized) spatial manifold it describes. Invariance under vertex-relabelling can thus be regarded as the discrete analogue of diffeomorphism invariance.

Entanglement graphs have been first defined in the pre-Fock space, where distinguishability of vertices enables to define a combinatorial pattern among them, then constrained with the aforementioned symmetry. The pre-Fock and Fock spaces of the theory allow (in fact, make mandatory)

⁶Note that the links of the graph, as adjacency relations among vertices, are defined by the vertex labels themselves.

to consider also superpositions of labelled and unlabelled entanglement graphs, respectively. The two are conceptually quite different.

In the pre-Fock space of distinguishable vertices, graphs in quantum superposition can be aligned according to the given vertex labelling. In a discrete-gravity perspective, we could say that superposing labelled entanglement graphs amounts to superposing discrete metrics (to the extent in which they are encoded in the combinatorial pattern only). A notion of graph superposition has recently been provided in Ref. [118] through the definition of an Hilbert space for coloured graphs, where colours are generic field data. When the latter have a geometric interpretation, that coloured graphs coincide, at a formal/descriptive level, with our labelled entanglement graphs. At a structural level, the difference is in taking graphs as basic structures, decorated with some data “at a later stage” (case of [118]), or having them emergent from the quantum behaviour of a many-body system (GFT case). The first setting naturally implies an orthogonality relation among different graphs, which, instead, is not necessarily satisfied in the second: the scalar product between labelled-graph states in the GFT pre-Fock space can be non-vanishing even for non equal graphs, precisely because the latter are just *features* of the many-body states and, specifically, manifestations of their entanglement content. Note that, though the Hilbert spaces describing graphs in the two contexts have a different structure, a robust notion of graph superposition naturally derives from both of them.

Once it has been established that vertex labelling does not possess any physical meaning, comparing graphs independently on it becomes particularly relevant. In Ref. [118] Arrighi *et al.* stressed that, if vertex labels were *a priori* not observable, the scalar product between coloured graphs differing only for that labels would be 1; as it is not the case (the result is actually zero) invariance under vertex relabelling must be enforced. In the GFT pre-Fock space the scalar product between isomorphic entanglement graphs, though *a priori* not zero, is not necessarily equal to 1. We defined an alternative scalar product which gets such an outcome, as compares entanglement graphs with the goal of maximising their overlap, regardless of the vertex labelling.

In addition to the pre-Fock space of labelled-graph states and their superpositions, our framework includes the space of properly physical, i.e. “diffeomorphism invariant”, states: the Fock space. Within it, we have naturally superpositions of unlabelled entanglement graphs, which can be understood, at a discrete-gravity level, as superpositions of geometries (i.e. equivalence classes of metrics). Note that a simple alignment prescription is not possible among unlabelled graphs, exactly as a notion of locality is not available when working with geometries. It could be possible, in principle, to define topological observables that capture the purely combinatorial, label-independent pattern encoded in a graph, i.e. associated to its entire equivalence class under graph isomorphisms. However, we leave this possibility for further work. Beside this possibility, we highlighted that a straightforward alignment prescription can be recovered when new degrees of freedom, interpreted as discretized matter, are added to the fundamental model, in the same spirit of the construction of relational (and diffeomorphism-invariant) observables in quantum gravity. In particular, we have shown that certain states allow to restore an effective (and relational) distinguishability of vertices thanks to their semi-classical behaviour with respect to the additional degrees of freedom.

4

Holographic properties of random spin networks as entanglement graphs

The main question we are going to tackle in this chapter, which is based on Refs. [2, 3], is the following: *given bounded regions of quantum space described by spin network states, under which conditions on the latter information on the bulk can be read from the boundary?* We rely on the following (basis-dependent) splitting of the degrees of freedom associated to (open) spin networks:

- * boundary: spins and corresponding magnetic numbers on open edges;
- * bulk: intertwiners on vertices (depending on spins of both internal and boundary edges).

We show that a generic spin network state can be understood as defining a *map* between these two sets: boundary states can be seen as the result of applying a graph-dependent map to certain bulk states, and vice versa. Entanglement enters this picture at two levels:

- (i) connectivity of the graph, i.e. the entanglement pattern among spin network vertices;
- (ii) quantum correlations among intertwiners.

While (i) underlies the definition of the map, (ii) determines both the input of the bulk-to-boundary map and (part of) the properties of the output boundary state. We then tackle the question stated above by two methods:

- (1) We analyse under which conditions the bulk-to-boundary map is an isometry (necessary condition for the expectation values of observables to be preserved from bulk to boundary).
- (2) We investigate to which extent the entanglement entropy of the boundary reflects/is affected by the bulk, by analysing the boundary states produced by the map upon varying the bulk input state.

We focus on a specific class of quantum states: the ones constructed out of individually weighted vertices, whose wavefunctions are randomly distributed. The quantum properties of such states, including the isometry of the associated bulk-to-boundary map, are thus fully determined by the combinatorial structure of their entanglement graph, the dimension of the degrees of freedom attached to it and the probability distribution of the vertex wavefunctions. To study these class of states we exploit the random tensor networks techniques employed in [53], adapting them to our context and generalizing them to account for the more general type of tensor networks our states correspond to.

In section 4.1 we explain in detail the bipartition of degrees of freedom of open spin networks into bulk and boundary. In section 4.2 we present the class of states we focus on, i.e. spin networks of random vertices, and the procedure to compute their Rényi-2 entropy via a dual Ising model. In section 4.3 we introduce the bulk-to-boundary map perspective on spin networks and perform point (1). In section 4.4 we perform point (2) and derive an analogue of the Ryu–Takayanagi formula for the boundary entropy; we also propose a toy model for the emergence of black hole horizons.

4.1 Partitioning the degrees of freedom of spin networks: bulk and boundary subspaces

Starting from $\psi \in \mathcal{H}_N$, we glue vertices according to $\gamma \equiv A$ and obtain

$$|\psi_\gamma\rangle := \left(\bigotimes_{a_{vw}^i=1} \mathbb{P}_{\ell_{vw}^i} \right) |\psi\rangle = \bigoplus_{j_\gamma} \sum_{n_\partial, \iota_V} (\psi_\gamma)_{n_\partial, \iota_V}^{j_\gamma} |j_\gamma, n_\partial, \iota_V\rangle \quad (4.1.1)$$

where

$$(\psi_\gamma)_{n_\partial, \iota_V}^{j_\gamma} := \psi_{\vec{n}_1 \dots \vec{n}_N, \iota_1 \dots \iota_N}^{\vec{j}_1 \dots \vec{j}_N} \prod_{a_{vw}^i=1} \delta_{j_v^i, j_w^i} I_{n_v^i, n_w^i} \quad (4.1.2)$$

The state ψ_γ pertains to the Hilbert subspace $\mathcal{H}_\gamma \subset \mathcal{H}_N$ that via the Peter-Weyl decomposition reads:

$$\mathcal{H}_\gamma = \bigoplus_{j_\gamma} \left(\bigotimes_v \mathcal{I}^{j_v} \otimes \bigotimes_{e \in \partial\gamma} V^{j_e} \right) \quad (4.1.3)$$

where we denoted by j_γ the set of spins associated to all edges of the graph: $j_\gamma = \{j_e \mid e \in E\}$.

The degrees of freedom described by ψ_γ are the following:

- (a) spins j_v^i and corresponding magnetic numbers n_v^i associated to the boundary edges $e_v^i \in \partial\gamma$;
- (b) spins j_{vw}^i associated to the internal links $\ell_{vw}^i \in L$;
- (c) intertwiner quantum numbers ι_v associated to the vertices $v \in V$, collectively indicated as $\dot{\gamma}$.

The set (a) corresponds to the *boundary degrees of freedom*, while sets (b) and (c) constitute the *bulk degrees of freedom*; in particular, the set (b) contains information on the combinatorial structure of the bulk and the dimension of the internal links, while (c) can be interpreted as a set of “internal” degrees of freedom anchored to the vertices. From the simplicial-geometry perspective, in fact, the intertwiners determine the volume of the simplices dual to the graph vertices, while the spin labels carry information about areas of surfaces, dual to the graph edges, which can be in the bulk or in the boundary. Since (c) is not independent from (a) and (b), the graph Hilbert space does not factorize into bulk and boundary Hilbert spaces. However, as can be seen from Eq. (4.1.3) such a factorization takes place in every fixed-spins subspace. We then define, for every spin- j_γ sector, a bulk Hilbert space:

$$\mathcal{H}_\dot{\gamma}^{j_\gamma} := \bigotimes_v \mathcal{I}^{j_v}, \quad (4.1.4)$$

given by the tensor product of the intertwiner-spaces attached to the vertices of γ (collectively denoted by $\dot{\gamma}$); and a boundary Hilbert space:

$$\mathcal{H}_\partial^{j_\partial} := \bigotimes_{e \in \partial\gamma} V^{j_e}, \quad (4.1.5)$$

where $j_\partial \subset j_\gamma$ is the subset of spins attached to the boundary edges. The spin- j_γ sector of the Hilbert space \mathcal{H}_γ , given by the tensor product of the bulk and boundary Hilbert spaces defined above, is denoted as $\mathcal{H}_\gamma^{j_\gamma}$:

$$\mathcal{H}_\gamma^{j_\gamma} := \mathcal{H}_\dot{\gamma}^{j_\gamma} \otimes \mathcal{H}_\partial^{j_\partial} \quad (4.1.6)$$

To emphasize this factorization, in the following we write basis states of $\mathcal{H}_\gamma^{j_\gamma}$ as

$$|j_\gamma, n_\partial, \iota_V\rangle \equiv \bigotimes_v |\vec{j}_v \iota_v\rangle \bigotimes_{e \in \partial\gamma} |j_e n_e\rangle \quad (4.1.7)$$

i.e. as tensor product of the basis states of the bulk Hilbert space, $\bigotimes_v |\vec{j}_v \iota_v\rangle$, and of the boundary Hilbert space, $\bigotimes_{e \in \partial\gamma} |j_e n_e\rangle$.

For a certain assignment of spins to the graph γ the corresponding Hilbert space thus factorizes into a bulk and a boundary Hilbert space. In the next section we show that spin network states in $\mathcal{H}_\gamma^{j_\gamma}$ (for arbitrary γ) naturally define maps between the bulk and boundary degrees of freedom, and that such a feature extends to completely generic (i.e. involving superposition of spin-sectors) states, upon embedding the graph Hilbert space \mathcal{H}_γ into the tensor product of generalized bulk and boundary Hilbert spaces.

4.2 Random spin networks and dual statistical models

The computation of the entanglement entropy of spin network states can be highly simplified by the use of random tensor network techniques. This clearly requires to restrict the attention to spin network states given by (superpositions of) random tensor networks. We introduce such a class of states in the following subsection, and dedicate subsection 4.2.2 to illustrate how random tensor network techniques can be used to translate their Rényi entropies into partition functions of a classical Ising model.

4.2.1 Random spin networks

We consider spin network states constructed out of the gluing of individually weighted vertices, introduced in the subsection 3.2.5, thereby corresponding to tensor networks. We also assume that the states are peaked on specific values j_γ of the edge spins of the underlying graph γ . This assumption allows us to work in a fixed spin-sector of $\mathcal{H}_N \supset \mathcal{H}_\gamma$ and thus largely simplifies the calculation. The attention is therefore restricted to states of the form

$$|\psi\rangle = \left(\bigotimes_{\ell \in \gamma} |\ell\rangle \right) \bigotimes_v |f_v\rangle \quad (4.2.1)$$

where $|\ell\rangle$ is the link state of Eq. (3.2.9) and f_v is a single-vertex wavefunction peaked on \vec{j}_v (we implicitly assumed compatibility among the spins $\vec{j}_1, \dots, \vec{j}_N$ on which f_1, \dots, f_N are peaked, the combinatorial pattern γ and the choice of spins of the corresponding link states).

The randomness we consider is local, i.e. inherent to the vertices separately: every state f_v , which is a tensor in a spin-sector of the single-vertex Hilbert space, i.e.

$$(f_v)_{\vec{n}_v \ell_v}^{\vec{j}_v} \in \mathcal{H}^{\vec{j}_v} := \mathcal{I}^{\vec{j}_v} \otimes \bigotimes_{i=1}^d V^{j_i}, \quad (4.2.2)$$

is picked randomly from its Hilbert space according to the uniform probability distribution. More specifically, the tensor $(f_v)_{\vec{n}_v \ell_v}^{\vec{j}_v}$ is regarded as a vector of dimension

$$D_v := D_{\vec{j}} \times d_{j_1} \times \dots \times d_{j_d}, \quad (4.2.3)$$

and the computation of typical values of functions of it is performed by setting $|f_v\rangle = U|f_v^0\rangle$, where $|f_v^0\rangle$ is a reference state and $U \in SU(D_v)$, and integrating over U with the Haar measure.

4.2.2 Rényi entropy from Ising partition function

In this section we show how to compute, for a random spin network state with fixed spins, the second-order Rényi entropy of an arbitrary region of the graph, which may include part of the bulk (intertwiners attached to the vertices) and/or of the boundary (spin states on open edges of the graph). The analysis is performed by adapting the technique of [53] to the GFT framework.

Let us start by illustrating the replica trick for the computation of the second-order Rényi entropy. Given a system whose Hilbert space admits the factorization $\mathcal{H}_R \otimes \mathcal{H}_{\bar{R}}$, let ρ be the

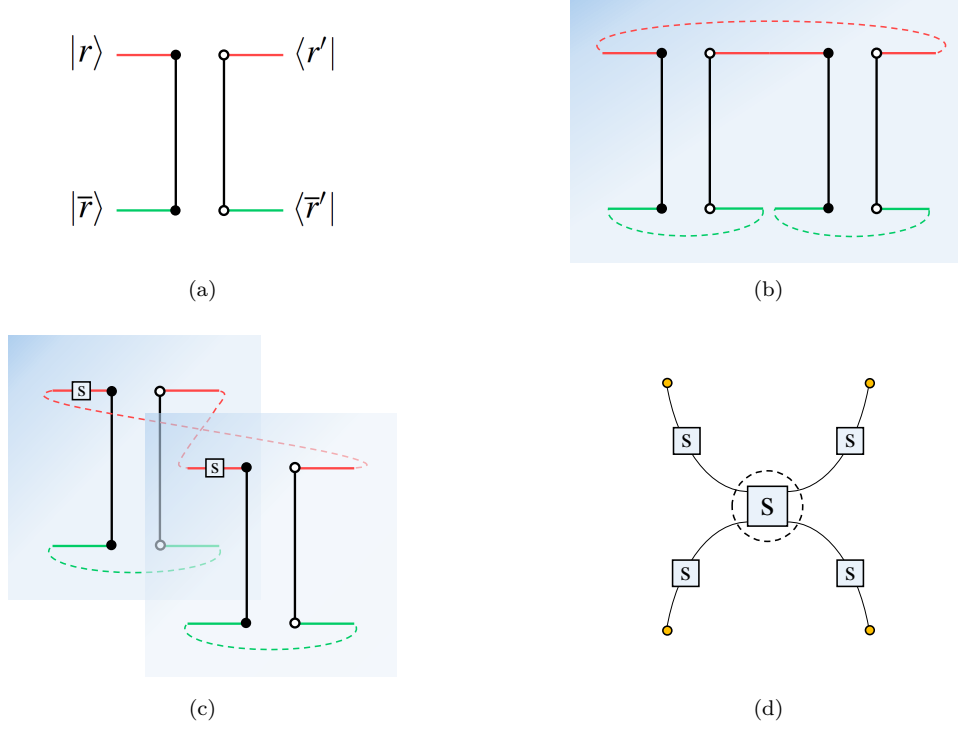


Figure 4.1. Illustration of the replica trick in Eq. (4.2.5). In (a) the density matrix ρ on $\mathcal{H}_R \otimes \mathcal{H}_{\bar{R}}$ describing the state of the system: the black disks refer to the subsystems described by \mathcal{H}_R (top) and by $\mathcal{H}_{\bar{R}}$ (bottom), the white disks to the dual components. In (b) the l.h.s. of Eq. (4.2.5): the trace over \bar{R} (dashed green line) yields ρ_R ; the latter is then multiplied by itself (connection of internal disks) and traced over (dashed red line). In (c) the r.h.s. of Eq. (4.2.5): two copies of ρ_R are considered; the swap operator, whose action is denoted by a square, causes the trace to be performed across the two spaces. In (d) the factorization of the swap operator S for the single vertex on the intertwiner (large square in the center) and on each individual edge (small squares)

density matrix on $\mathcal{H}_R \otimes \mathcal{H}_{\bar{R}}$ describing the state of the system and consider its reduction to subsystem R : $\rho_R = \text{Tr}_{\bar{R}}(\rho)$. The Rényi-2 entropy of ρ_R is given by

$$S_2(\rho_R) := -\log \text{Tr}(\rho_R^2) \quad (4.2.4)$$

The replica trick for the computation of this quantity is based on the possibility to express the trace of a reduced density matrix ρ_R as a trace over two copies of the density matrix ρ associated to the entire system (here we assume ρ to be normalised, i.e. $\text{Tr}(\rho) = 1$):

$$\text{Tr}(\rho_R^2) = \text{Tr}[(\rho \otimes \rho) S_R] \quad (4.2.5)$$

where the trace on the r.h.s. is performed over all degrees of freedom of ρ and the operator S_R , called *swap operator*, acts on the two copies of the Hilbert space \mathcal{H}_R associated to R as follows:

$$S_R |r\rangle \otimes |r'\rangle = |r'\rangle \otimes |r\rangle \quad (4.2.6)$$

with $|r\rangle$ and $|r'\rangle$ elements of an orthonormal basis of \mathcal{H}_R (while it acts as the identity on the two copies of the Hilbert space $\mathcal{H}_{\bar{R}}$). An illustration of the replica trick of Eq. (4.2.5) is given in figure 4.1.

Our goal is to compute the Rényi-2 of the random spin network state of Eq. (4.2.1) for an arbitrary portion R of the underlying graph γ . By applying the replica trick to the Rényi-2

entropy of $\rho_R = \text{Tr}_{\overline{R}}(\rho)$, where $\rho = |\psi\rangle\langle\psi|$, we can write

$$S_2(\rho_R) = -\log\left(\frac{Z_1}{Z_0}\right), \quad Z_1 := \text{Tr}_{\dot{\gamma}\cup\partial}[(\rho \otimes \rho) S_R], \quad (4.2.7)$$

$$Z_0 := \text{Tr}_{\dot{\gamma}\cup\partial}[\rho \otimes \rho],$$

where $\text{Tr}_{\dot{\gamma}\cup\partial}$ denotes a trace over all bulk and boundary degrees of freedom, the presence of the denominator Z_0 in the logarithm takes into account the possible non-normalisation of ρ , and where the swap operator S_R acts on two copies of the Hilbert space

$$\mathcal{H}_R = \left(\bigotimes_{v \in R} \mathcal{I}^{\vec{j}_v}\right) \otimes \left(\bigotimes_{e \in R} V^{j_e}\right), \quad (4.2.8)$$

associated to the spin network region R .

Crucially, by exploiting the tensor network form of Eq. (4.2.1) the density matrix $\rho = |\psi\rangle\langle\psi|$ can be written as follows:

$$\rho = \text{Tr}_L \left(\bigotimes_{\ell \in \gamma} |\ell\rangle\langle\ell| \bigotimes_v |f_v\rangle\langle f_v| \right), \quad (4.2.9)$$

where Tr_L denotes the trace over the degrees of freedom associated to edges forming internal links, i.e. magnetic momenta associated to the free ends of to-be-glued edges. We are thus exploiting the embedding of the spin network state in \mathcal{H}_N to write it as a set of open vertices (the $|f_v\rangle\langle f_v|$ terms) glued to each other by the trace with the set of link states $|\ell\rangle\langle\ell|$. By inserting Eq. (4.2.9) into the expression of Z_1 (Z_0 can be derived from the latter by simply replacing the swap operator with the identity) we then obtain

$$Z_1 := \text{Tr}_{\dot{\gamma}\cup\partial}[(\rho \otimes \rho) S_R]$$

$$= \text{Tr} \left[\left(\bigotimes_{\ell} \rho_{\ell}^{\otimes 2} \right) \left(\bigotimes_v \rho_v^{\otimes 2} \right) S_R \right] \quad (4.2.10)$$

where $\rho_{\ell} := |\ell\rangle\langle\ell|$ and $\rho_v := |f_v\rangle\langle f_v|$. Notably, the trace in the second line is performed over all degrees of freedom in the embedding space \mathcal{H}_N , i.e. that of a set of N open vertices. In the following, we omit the explicit reference to the bulk ($\dot{\gamma}$), boundary (∂) and internal link (L) subsets and denote this total trace simply by Tr .

Given the random character of the state, our objective is to compute the average value of the Rényi-2 entropy $S_2(\rho_R)$ with respect to the uniform probability distribution of the single-vertex states ρ_v . As we are going to show, the key point of the average entropy calculation is that the randomization over the vertex states can be implemented *before* performing the trace in Eq. (4.2.10), due to the linearity of such operations. As a first step, note that Z_1 and Z_0 are quadratic functions of the random vertex states ρ_v , and their average is therefore easier to compute than the average of the entropy. This observation motivated the proposal[53] of expanding the latter in powers of the fluctuations $\delta Z_1 = Z_1 - \overline{Z_1}$ and $\delta Z_0 = Z_0 - \overline{Z_0}$ (the overline is used to denote average value under randomisation of the vertex states):

$$\overline{S_2(\rho_R)} = -\log\left(\frac{\overline{Z_1}}{\overline{Z_0}}\right) + \sum_{n=1}^{\infty} \frac{(-1)^{n-1}}{n} \left(\frac{\overline{\delta Z_0^n}}{\overline{Z_0}^n} - \frac{\overline{\delta Z_1^n}}{\overline{Z_1}^n} \right) \quad (4.2.11)$$

In Ref. [53] Hayden *et al.* showed that for large enough bond dimensions, which in the present framework correspond to the edge spins, the fluctuations are suppressed, i.e.

$$\overline{S_2(\rho_R)} \simeq -\log\left(\frac{\overline{Z_1}}{\overline{Z_0}}\right), \quad (4.2.12)$$

where \simeq refers to asymptotic equality as the edge spins go to infinity. In particular they proved that, for a tensor network with homogeneous bond dimensions equal to D , given an arbitrary small parameter $\delta > 0$ it holds

$$|S_2(\rho_R) - \overline{S_2(\rho_R)}| < \delta \quad (4.2.13)$$

with probability $P(\delta) = 1 - \frac{D_c}{D}$, where D_c is a critical bond dimension depending on δ and on the number N of vertices as $D_c \propto \delta^{-2} e^{cN}$, with c a constant factor.

Thanks to Eq. (4.2.12) the computation of the average entropy can thus be traced back to the computation of the average quantities \overline{Z}_1 and \overline{Z}_0 . Let us focus on \overline{Z}_1 , as \overline{Z}_0 is simply given by the latter upon reducing the swap operator to the identity operator:

$$\overline{Z}_1 = \text{Tr} \left[\left(\bigotimes_{\ell} \rho_{\ell}^{\otimes 2} \right) \left(\bigotimes_v \overline{\rho_v^{\otimes 2}} \right) S_R \right], \quad (4.2.14)$$

For each vertex v , the average over the two copies of the state ρ_v can be computed via the Schur's lemma, as we illustrate in appendix A.3. The result is the following:

$$\overline{\rho_v^{\otimes 2}} = \frac{\mathbb{I} + S_v}{D_v(D_v + 1)}, \quad (4.2.15)$$

where D_v is the dimension of the single-vertex Hilbert space $\mathcal{H}^{\vec{j}_v}$ given in Eq. (4.2.3) and S_v is the swap operator on the two copies of it. Once Eq. (4.2.15) is inserted into Eq. (4.2.14), the latter can be written as

$$\overline{Z}_1 = c \sum_{\vec{\sigma}} \text{Tr} \left[\left(\bigotimes_{\ell} \rho_{\ell}^{\otimes 2} \right) \left(\bigotimes_v S_v^{\frac{1-\sigma_v}{2}} \right) S_R \right], \quad (4.2.16)$$

where $\sigma_v = \pm 1$ is a two-level variable associated to vertex v , $\vec{\sigma} = \{\sigma_1, \dots, \sigma_N\}$ and

$$c := \prod_v \frac{1}{D_v(D_v + 1)} \quad (4.2.17)$$

is a constant factor. That is, \overline{Z}_1 has been written as a sum of 2^N terms, each one involving the identity (\mathbb{I}) or the swap operator (S_v) for each of the N vertices, depending on the value of the corresponding variable σ_v : \mathbb{I} for $\sigma_v = +1$ and S_v for $\sigma_v = -1$. The quantity \overline{Z}_1 thus acquires the form of a partition function:

$$\overline{Z}_1 = \sum_{\vec{\sigma}} e^{-\mathcal{A}_1(\vec{\sigma})} \quad (4.2.18)$$

where

$$\mathcal{A}_1(\vec{\sigma}) := -\log c - \log \text{Tr} \left[\left(\bigotimes_{\ell} \rho_{\ell}^{\otimes 2} \right) \left(\bigotimes_{\sigma_v=-1} S_v \right) S_R \right] \quad (4.2.19)$$

Given the form of the single-vertex Hilbert space $\mathcal{H}^{\vec{j}_v}$, the swap operator S_v factorises as follows:

$$S_v = \bigotimes_{i=0}^d S_v^i, \quad (4.2.20)$$

i.e. into a swap operator S_v^0 for (the double copy of) the intertwiner Hilbert space $\mathcal{L}^{\vec{j}_v}$ and a swap operator S_v^i for (the double copy of) the representation space $V^{j_v^i}$ on each edge e_v^i , as shown in figure 4.1(d). Crucially, the same applies to the swap operator S_R ; by writing $R = A \cup \Omega$, where $A \subset \partial\gamma$ is a region of the boundary and $\Omega \subset \dot{\gamma}$ a region of the bulk, we have that

$$S_R = \left(\bigotimes_{e_v^i \subset A} S_v^i \right) \left(\bigotimes_{v \subset \Omega} S_v^0 \right) \quad (4.2.21)$$

To every boundary edge $e_v^i \subset A$ we then attach a two-level variable $\mu_v^i = \pm 1$ encoding whether ($\mu_v^i = -1$) or not ($\mu_v^i = +1$) it belongs to the boundary region $A \subset R$. We do the same for

every vertex $v \in \dot{\gamma}$: we introduce a two-level variable $\nu_v = \pm 1$ encoding whether ($\nu_v = -1$) or not ($\nu_v = +1$) the vertex v is contained in $\Omega \subset R$. These additional variables, called *pinning fields* [53] to model the effect of presence, on the bulk and boundary of γ , of the swap operators deriving from the decomposition of Eq. (4.2.21). The trace in Eq. (4.2.19) can then be written as follows:

$$\begin{aligned} & \text{Tr} \left[\left(\bigotimes_{\ell} \rho_{\ell}^{\otimes 2} \right) \left(\bigotimes_{\sigma_v = -1} S_v \right) S_R \right] \\ &= \text{Tr}_L \left[\left(\bigotimes_{\ell} \rho_{\ell}^{\otimes 2} \right) \bigotimes_{e_v^i \in L: \sigma_v = -1} S_v^i \right] \text{Tr}_{\dot{\gamma}} \left[\bigotimes_{\sigma_v \nu_v = -1} S_v^0 \right] \text{Tr}_{\partial} \left[\bigotimes_{e_v^i \in \partial \gamma: \sigma_v \mu_v^i = -1} S_v^i \right] \end{aligned} \quad (4.2.22)$$

Consider in fact a generic vertex v : if $\sigma_v = -1$ and $\nu_v = -1$, there are two swap operators acting on its intertwiner, which cancel each other out (as $S^2 = \mathbb{I}$); if, instead, $\sigma_v = -1$ and $\nu_v = +1$, or $\sigma_v = +1$ and $\nu_v = -1$ (a situation codified by the condition $\nu_v \sigma_v = -1$) there is just one swap operator acting on its intertwiner. A similar argument holds for the boundary edges.

By performing the traces in Eq. (4.2.22) one finally obtains the action of a classical Ising model defined on the graph γ , with additional pinning fields on the bulk and boundary degrees of freedom (see appendix B.2 for details on the derivation of the various terms):

$$\mathcal{A}_1(\vec{\sigma}) = \sum_{\ell_{vw}^i \in \gamma} \frac{1 - \sigma_v \sigma_w}{2} \log d_{j_{vw}^i} + \sum_{e_v^i \in \partial \gamma} \frac{1 - \sigma_v \mu_v^i}{2} \log d_{j_v^i} + \sum_v \frac{1 - \sigma_v \nu_v}{2} \log D_{j_v} + \text{const} , \quad (4.2.23)$$

We can indeed observe that Eq. (4.2.23) involves interactions between nearest neighbours Ising spins, where the adjacency relationship is determined by γ (two Ising spins interact only if the corresponding vertices are connected by a link); every Ising spin also interacts with the pinning fields located at its vertex (e.g. the Ising spin σ_v of a vertex v on the boundary interacts with the pinning field ν_v on the intertwiner of v and with the pinning field μ_v^i on the open edge e_v^i of v).

As far as \overline{Z}_0 is concerned, we pointed out that it corresponds to \overline{Z}_1 with $R = \emptyset$ (in fact $S_{\emptyset} = \mathbb{I}$). Therefore it holds that $\overline{Z}_0 = \sum_{\vec{\sigma}} e^{-\mathcal{A}_0(\vec{\sigma})}$, where \mathcal{A}_0 is given by Eq. (4.2.23) with all pinning fields equal to $+1$:

$$\mathcal{A}_0(\vec{\sigma}) = \sum_{\ell_{vw}^i \in \gamma} \frac{1 - \sigma_v \sigma_w}{2} \log d_{j_{vw}^i} + \sum_{e_v^i \in \partial \gamma} \frac{1 - \sigma_v}{2} \log d_{j_v^i} + \sum_v \frac{1 - \sigma_v}{2} \log D_{j_v} + \text{const} . \quad (4.2.24)$$

Note also that, since \overline{Z}_0 and \overline{Z}_1 enter $\overline{S}_2(\rho_R)$ only via their ratio, in the computation of the entropy the constant factors in Eq. (4.2.23) and Eq. (4.2.24) are irrelevant; we therefore omit them in the following.

By defining the free energies $F_1 := -\log \overline{Z}_1$ and $F_0 := -\log \overline{Z}_0$, the average entropy given by Eq. (4.2.12) can be expressed as

$$\overline{S}_2(\rho_R) \simeq F_1 - F_0, \quad (4.2.25)$$

namely as the energy cost of flipping down the pinning fields in the region R .

To study the properties of the partition function \overline{Z}_1 it is useful to rewrite the Ising action $\mathcal{A}_1(\vec{\sigma})$ in the form $\mathcal{A}_1(\vec{\sigma}) = \beta H_1(\vec{\sigma})$, where $\beta := d_j$ with j the average spin on γ , and

$$H_1(\vec{\sigma}) = \sum_{\ell_{vw}^i \in \gamma} \frac{1 - \sigma_v \sigma_w}{2} \frac{\log d_{j_{vw}^i}}{\beta} + \sum_{e_v^i \in \partial \gamma} \frac{1 - \sigma_v \mu_v^i}{2} \frac{\log d_{j_v^i}}{\beta} + \sum_v \frac{1 - \sigma_v \nu_v}{2} \frac{\log D_{j_v}}{\beta}. \quad (4.2.26)$$

The parameter β then plays the role of inverse temperature of the Ising model. The large-spins regime therefore corresponds to the Ising temperature going to zero, and the system dropping to the lowest energy configuration, which provides the main contribution to the partition function \overline{Z}_1 :

$$\overline{Z}_1 \simeq e^{-\beta \min_{\vec{\sigma}} H_1(\vec{\sigma})}, \quad (4.2.27)$$

which leads to the free energy

$$F_1 \simeq \beta \min_{\vec{\sigma}} H_1(\vec{\sigma}). \quad (4.2.28)$$

The same applies to $\overline{Z_0}$. Note that H_0 is given by Eq. (4.4.24) with all pinning fields pointing up: $\mu_v^i = \nu_v = +1 \forall v, i$; its minimum is therefore reached when all Ising spins are aligned to them (so that the bulk and boundary terms in Eq. (4.4.24) vanish) and aligned to each other (so that the internal-links term also vanishes). The only Ising configuration satisfying these requirements is that with all spins pointing up:

$$\min_{\vec{\sigma}} H_0(\vec{\sigma}) = H_0(\sigma_{\uparrow}) = 0 \quad (4.2.29)$$

where $\sigma_{\uparrow} := \{\sigma_v = +1 \forall v\}$. As a consequence,

$$F_0 \simeq \beta \min_{\vec{\sigma}} H_0(\vec{\sigma}) = 0 \quad (4.2.30)$$

Therefore, the average entropy can be finally computed via the following formula:

$$\overline{S_2(\rho_R)} \simeq \beta \min_{\vec{\sigma}} H_1(\vec{\sigma}), \quad (4.2.31)$$

with β the average dimension of the edge spins and $H_1(\vec{\sigma})$ the Ising-like Hamiltonian defined in Eq. (4.4.24). We thus shown that random tensor network techniques, specifically (a generalization of) that presented in [53], enable us to map the computation of the average Rényi entropy of a spin network to the evaluation of the energy of a classical Ising model living on that network. The principal features of such a mapping are summarised in box 4.1.

4.1 Random spin networks and the dual Ising model

Via the replica trick, the average Rényi-2 entropy of spin network states given by the gluing of (uniformly distributed) random spin network vertices - Eq. (4.2.1) - is given by two interacting copies of the spin networks themselves - Eq. (4.2.7) - with interaction scheme given by a classical Ising model on the underlying graph - Eq. (4.2.23). The key aspects of the calculation leading to the Ising model are the following:

Randomization and Ising spins The randomization over uniformly distributed vertex tensors yields an Ising spin σ_v for every vertex v , which can be $+1$ or -1 . Effectively, each edge e_v^i of the vertex, as well as the intertwiner degree of freedom, carries a copy of the spin σ_v . Note that all such copies have the same value; in fact, σ_v expresses an “Ising state” of the vertex, which is “transmitted” to all its edges and to the intertwiner.

Probed region and pinning fields A set of virtual spins called “pinning fields” keeps track of the boundary region $A \subset \gamma$ respect to which the entropy is computed. In particular, a spin $\mu_{e_v^i}$ is attached to every boundary edge $e_v^i \in \partial\gamma$, and takes value -1 if $e_v^i \in A$, and $+1$ otherwise.

Interaction of Ising spins and pinning fields The Ising spin σ_v on a boundary edge e_v^i interacts to the pinning field $\mu_{e_v^i}$ living on the same edge (with strength of the interaction proportional to $\log d_{j_v^i}$). Moreover, the Ising spin σ_v on a semi-link e_v^i interacts to the Ising spin σ_w on the complementary semi-link e_w^i , and the strength of interaction is proportional to $\log d_{j_{vw}^i}$. Equivalently, we could say that the Ising spins (when regarded as pertaining to the vertex in its entirety, not split in copies attached to the vertex substructures) interact to their nearest neighbours: σ_v interacts with σ_w if v and w are connected by a link.

4.3 Holographic bulk-to-boundary maps from random spin networks

4.3.1 Spin network states as bulk-to-boundary maps

In this section we show that spin network states naturally define maps between the bulk and the boundary of the graph underlying them, according to the bulk/boundary bipartition of degrees of freedom illustrated in the previous section.

4.3.1.1 Fixed-spin case

Consider a generic state in $\mathcal{H}_\gamma^{j_\gamma}$:

$$|\varphi\rangle = \sum_{n_{\partial\iota\nu}} \varphi_{n_{\partial\iota\nu}} \bigotimes_v |\vec{j}_{v\iota\nu}\rangle \bigotimes_{e \in \partial\gamma} |j_e n_e\rangle \quad (4.3.1)$$

where we adopted the notation of Eq. (4.1.7) emphasizing the factorization of the Hilbert space into bulk and boundary. Our claim is the following: by regarding the bulk subspace as *input* and the boundary subspace as *output* the state of Eq. (4.3.1) naturally defines a map from the first to the second,

$$\mathcal{M}_\varphi : \mathcal{H}_\gamma^{j_\gamma} \rightarrow \mathcal{H}_\partial^{j_\partial}, \quad (4.3.2)$$

which acts on a generic bulk (input) state $\zeta \in \mathcal{H}_\gamma^{j_\gamma}$ as follows:

$$\begin{aligned} \mathcal{M}_\varphi|\zeta\rangle &:= \langle \zeta | \varphi \rangle \\ &= \sum_{n_\partial} \left(\sum_{\iota\nu} \zeta_{\iota\nu}^* \varphi_{n_{\partial\iota\nu}} \right) \bigotimes_{e \in \partial\gamma} |j_e n_e\rangle =: |\varphi(\zeta)\rangle \end{aligned} \quad (4.3.3)$$

That is, by evaluating the spin network state φ on ζ (or, in tensor network language, by feeding the bulk input indices with ζ) and returning a boundary (output) state. In fact, the components of \mathcal{M}_φ in the bulk and boundary basis simply coincide with that of φ :

$$\langle \alpha | \mathcal{M}_\varphi | \beta \rangle = \varphi_{\alpha\beta} \quad (4.3.4)$$

where we collected in α and β the quantum numbers of the bulk and boundary basis elements, respectively; i.e.

$$|\alpha\rangle := \bigotimes_{e \in \partial\gamma} |j_e n_e\rangle \quad |\beta\rangle := \bigotimes_v |\vec{j}_{v\iota\nu}\rangle \quad (4.3.5)$$

This observation holds for any spin network state in $\mathcal{H}_\gamma^{j_\gamma}$, for any underlying graph γ and assignment of spins j_γ . The map associated to a spin network state acts by establishing correlations between the intertwiner degrees of freedom, which end up in the input configuration (in the example given above, ζ). As we shall see, the purpose of changing the perspective on spin networks from states to maps is that of studying the relationship between their bulk and boundary. In this respect, note that between the same bulk and boundary Hilbert spaces there is a family of maps defined by all possible states associated to all possible graphs having the same bulk and boundary of γ (i.e. same number of vertices and same boundary edges).

4.3.1.2 General (spin-superposition) case

We introduce the generalised bulk and boundary spaces:

$$\mathcal{H}_\gamma := \bigoplus_{j_\gamma} \mathcal{H}_\gamma^{j_\gamma}, \quad \mathcal{H}_{\partial\gamma} := \bigoplus_{j_\partial} \mathcal{H}_\partial^{j_\partial} \quad (4.3.6)$$

which are such that $\mathcal{H}_\gamma \subset \mathcal{H}_{\vec{j}_\gamma} \otimes \mathcal{H}_{\partial\gamma}$. Given a generic state in \mathcal{H}_γ ,

$$|\Psi\rangle = \bigoplus_{j_\gamma} \sum_{n_{\partial\gamma}} \Psi_{n_{\partial\gamma}}^{j_\gamma} \bigotimes_v |\vec{j}_{v\ell v}\rangle \bigotimes_{e \in \partial\gamma} |j_e n_e\rangle, \quad (4.3.7)$$

the contraction with an element of the generalised bulk space, $Z \in \mathcal{H}_{\vec{j}_\gamma}$, yields

$$\begin{aligned} |\Psi(Z)\rangle &= \langle Z | \Psi \rangle \\ &= \bigoplus_{j_\partial} \sum_{n_\partial} \left(\sum_{\ell_V} (Z_{\ell_V}^{j_\gamma})^* \Psi_{n_{\partial\gamma}}^{j_\gamma} \right) \bigotimes_{e \in \partial\gamma} |j_e n_e\rangle \end{aligned} \quad (4.3.8)$$

which is a state in the generalised boundary space. Crucially, we can regard Eq. (4.3.8) as the output of a map

$$M_\Psi : \mathcal{H}_{\vec{j}_\gamma} \rightarrow \mathcal{H}_{\partial\gamma} \quad (4.3.9)$$

that evaluates the state Ψ associated to γ on a certain state Z of the bulk degrees of freedom, i.e. the intertwiners, returning a boundary state $\Psi(Z)$. Note that the latter pertains to the subspace of $\mathcal{H}_{\partial\gamma}$ characterised by gauge invariance with respect to the left action of the group on boundary edges pertaining to the same vertex (the state being instead covariant under right action of the group on the boundary edges).

By considering the most general bulk and boundary Hilbert spaces we are thus able to regard *every* spin network state (involving arbitrary superposition of spins) as a map between them. The correlation between bulk and boundary degrees of freedom in the state translates into a correlation between the input and output subspaces connected by the map, as

$$\langle \alpha | M_\Psi | \beta \rangle = \Psi_{\alpha\beta} \quad (4.3.10)$$

with $|\alpha\rangle$ and $|\beta\rangle$ being, respectively, the boundary and bulk basis elements defined in Eq. (4.3.4), and with j_∂ in $|\alpha\rangle$ coinciding to the boundary-spins subset of j_γ in $|\beta\rangle$, for all possible spin sectors.

Let us remark that, despite the possibility of reading a generic graph state as a bulk-to-boundary map in the sense specified above, the graph Hilbert space itself cannot be factorized into boundary and bulk spaces due to the sharing of degrees of freedom between these two substructures (the intertwiner degree of freedom depend on the incident spins, which possibly pertain to the boundary). Note however that, in order to make the bulk degrees of freedom independent from the boundary ones, it is sufficient to fix the spins $\vec{j}_{\partial\gamma}$ of the boundary. The generalised bulk Hilbert space $\mathcal{H}_{\vec{j}_\gamma}$ is then redundant, as the effective bulk Hilbert space is a direct sum of j_γ -sectors with the boundary portion of j_γ given by $\vec{j}_{\partial\gamma}$.

4.3.2 Isometry condition for bulk-to-boundary maps

We proceed to determine the conditions under which the bulk-to-boundary map associated to a spin network state is an isometry. We restrict the attention to the fixed-spins case, but the analysis can be straightforwardly generalised to states involving spin superposition.

As explained in Section 4.3.1, a state $\varphi \in \mathcal{H}_{\vec{j}_\gamma}$ can be thought of as a map \mathcal{M}_φ acting on an a bulk state ζ as follows: $\mathcal{M}_\varphi|\zeta\rangle = \langle \zeta | \varphi \rangle$, thereby returning a state in the boundary Hilbert space. To simplify the notation, in the following we omit for the bulk-to-boundary map \mathcal{M}_φ the explicit reference to the state φ from which it is defined. The map \mathcal{M} is an isometry if and only if it satisfies

$$\mathcal{M}^\dagger \mathcal{M} = \mathbb{I}, \quad (4.3.11)$$

where \mathbb{I} is the identity operator. We are going to show that this condition is equivalent to the bulk reduction of the spin network state being completely mixed.

To start, note that the spin network state φ can be written in terms of the corresponding bulk-to-boundary map \mathcal{M} as follows:

$$|\varphi\rangle = \sum_{\beta} (\mathcal{M} \otimes \mathbb{I}) |\beta\rangle \otimes |\beta\rangle \quad (4.3.12)$$

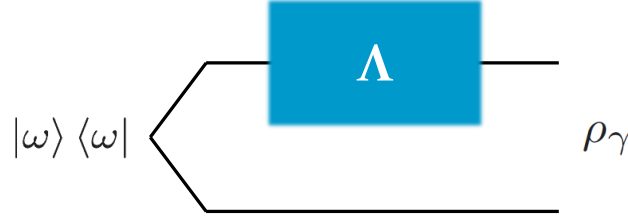


Figure 4.2. Relationship between a spin network state ρ_γ and the corresponding bulk-to-boundary superoperator Λ . The state $|\omega\rangle$ is a maximally entangled state of two copies of the bulk.

where $|\beta\rangle$ is the bulk basis element, see Eq. (4.3.4). That is, the state $|\varphi\rangle$ can be obtained by applying the map \mathcal{M} to a branch of two maximally entangled copies of the bulk, as depicted in figure 4.2. The reduced (and normalised) bulk state then takes the form

$$\begin{aligned}\rho_\gamma &:= \frac{1}{D_\gamma} \text{Tr}_\partial [\rho_\gamma] \\ &= \frac{1}{D_\gamma} \sum_{\beta\beta'} (\mathcal{M}^\dagger \mathcal{M})_{\beta'\beta} |\beta\rangle\langle\beta'| \end{aligned} \quad (4.3.13)$$

where $\rho_\gamma = |\varphi\rangle\langle\varphi|$ and D_γ is the dimension of the bulk Hilbert space. From this expression it is immediate to realize that the isometry condition $\mathcal{M}^\dagger \mathcal{M} = \mathbb{I}$ translates into the requirement that ρ_γ is maximally mixed, i.e.

$$\rho_\gamma = \frac{\mathbb{I}}{D_\gamma}, \quad (4.3.14)$$

Crucially, this condition can be checked by verifying that ρ_γ has maximum entropy.

Note finally that, when \mathcal{M} is an isometry, the corresponding superoperator on the space of bulk operators, $\Lambda(\cdot) := \mathcal{M} \cdot \mathcal{M}^\dagger$, is a CPTP map with Choi-Jamiołkowski state

$$J(\Lambda) = \Lambda \otimes \mathbb{I} \left(\frac{|\omega\rangle\langle\omega|}{D_\gamma} \right) = \frac{\rho_\gamma}{D_\gamma} \quad (4.3.15)$$

where

$$|\omega\rangle = \sum_{\beta} |\beta\rangle \otimes |\beta\rangle \quad (4.3.16)$$

is a maximally entangled state of two copies of the bulk (see figure 5.2.1).

4.3.3 Holographic character of bulk-to-boundary maps from random spin networks

The goal of this section is to determine under which conditions the flow of information from the bulk to the boundary of regions of quantum space described by the random spin network states introduced in section 4.2.1 exhibits a holographic behaviour, which corresponds to the bulk-to-boundary map associated to that class of states being an isometry. We showed that this isometry condition can be verified by computing the entanglement entropy content of the reduced bulk state ρ_γ . As illustrated in section 4.2, given the random character of the vertex weights the Rényi-2 entropy can be computed via the partition function of a classical Ising model having the following action:

$$\mathcal{A}(\vec{\sigma}) := -\frac{1}{2} \left[\sum_{\ell_{vw}^i \in L} (\sigma_v \sigma_w - 1) \log d_{j_{vw}^i} + \sum_{e_v^i \in \partial\gamma} (\sigma_v \mu_v^i - 1) \log d_{j_v^i} + \sum_v (\sigma_v \nu_v - 1) \log D_{j_v} \right] \quad (4.3.17)$$

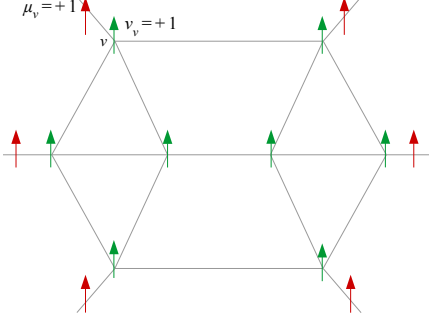


Figure 4.3. In the Ising action \mathcal{A}_0 , both the boundary spins μ (shown in red) and the bulk ones ν (shown in green) point up: $\mu_v = +1$, $\nu_v = +1 \forall v$.

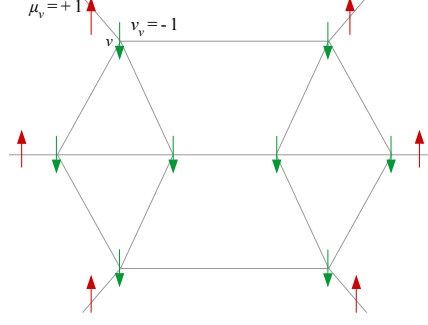


Figure 4.4. In the Ising action \mathcal{A}_1 , the boundary spins (in red) point up, but the bulk spins (in green) are flipped down: $\mu_v = -\nu_v = +1 \forall v$.

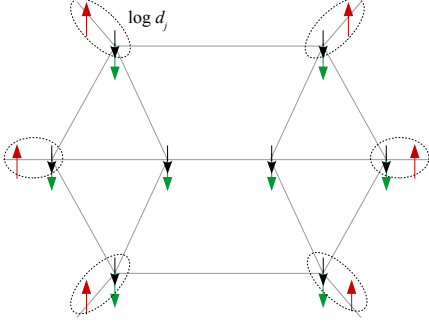


Figure 4.5. For $\log D_j \gg \log d_j$ the minimal energy configuration for \mathcal{A}_1 is that with all Ising spins σ_v (shown in black) pointing down. Each pair of misaligned Ising- and boundary-spin carries a contribution to the free energy F_1 equal to $\log d_j$, so $F_1 = |\partial\gamma| \log d_j$.

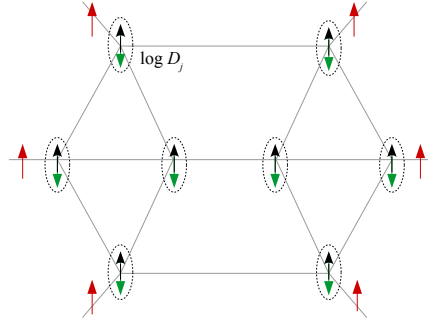


Figure 4.6. For $\log d_j \gg \log D_j$ the minimal energy configuration is that with all Ising spins σ_v (shown in black) pointing up. Each pair of misaligned Ising- and bulk-spin carries a contribution to the free energy F_1 equal to $\log D_j$, so $F_1 = N \log D_j$.

where σ_v are the Ising spins associated to the vertices of the graph, μ_v^i and ν_v pinning fields associated to boundary spins and intertwiners, respectively. In particular, the average entropy corresponds to the energy cost of flipping down the pinning fields of the bulk $\hat{\gamma}$ (see Figure 4.3 and Figure 4.4):

$$\overline{S_2(\rho_{\hat{\gamma}})} \simeq F_1 - F_0, \quad (4.3.18)$$

In the following we consider different possible configurations of the edge spins associated to the spin network graph, in order to gain insights on the behaviour of the entropy.

4.3.3.1 Homogeneous case

In the homogeneous case, i.e. with all edge spins equal to the same value j , the Ising action takes the form

$$\mathcal{A}(\vec{\sigma}) = -\frac{1}{2} \log d_j \left[\sum_{\ell_{vw}^i \in L} (\sigma_v \sigma_w - 1) + \sum_{e_v^i \in \partial\gamma} (\sigma_v \mu_v - 1) \right] - \frac{1}{2} \log D_j \sum_v (\sigma_v \nu_v - 1) \quad (4.3.19)$$

where we indicated as D_j the dimension of the intertwiner recoupling d j -spins. As discussed in subsection 4.2.2, in the large spins regime the free energy can be estimated by the minimum of

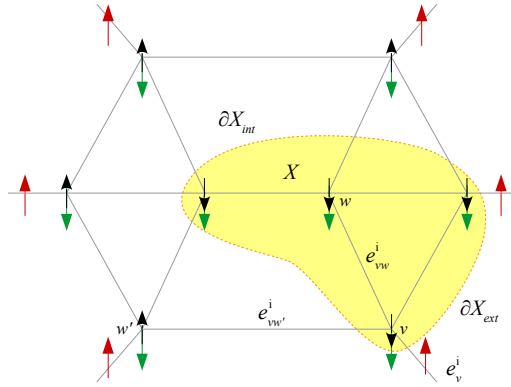


Figure 4.7. Ising configuration with Ising spins (shown in black) pointing down in a region X , bulk spins (in green) $\nu_v = -1 \forall v$ and boundary spins (in red) $\mu_v = +1 \forall v$. The contributions to \mathcal{A}_1 derive from: misaligned Ising- and boundary-spins (∂X_{ext}), misaligned Ising- and bulk-spins (region outside X) and misaligned nearest-neighbor Ising spins (∂X_{int}).

the Ising action and F_0 turns out to be zero: in \mathcal{A}_0 all pinning fields point up, and it is easy to see that its minimum is reached when also the Ising spins point up, so that all interaction terms vanish. We can then restrict the attention to the free energy F_1 .

The value of F_1 , approximated by the minimum of \mathcal{A}_1 (Ising action in which the bulk fields are flipped down), depends on the relative strength of the interactions, specifically by the ratio of $\log d_j$ (interaction strength between Ising spins σ_v and boundary spins μ_v) to $\log D_j$ (interaction strength between Ising spins σ_v and bulk spins ν_v). Let us focus on the following two regimes, which are the counterpart of the asymptotic regimes considered in [53]:

- $\log D_j \gg \log d_j$: the interaction with bulk spins is predominant, and the minimal energy configuration is thus the one with all Ising spins pointing down (see Figure 4.5). The contributions to the energy come from the misalignment of Ising spins with boundary spins, and amounts to $\log d_j$ for each boundary edge. The result is $F_1 = |\partial\gamma| \log d_j$, where $|\partial\gamma|$ is the number of boundary edges.
- $\log d_j \gg \log D_j$: the interaction with boundary spins is predominant, and the minimal energy configuration is thus the one with all Ising spins pointing up (see Figure 4.6). The contributions to the energy come from the misalignment of Ising spins with bulk spins, and amounts to $\log D_j$ for each vertex. The result is $F_1 = N \log D_j$, which is the maximum possible value for the entropy of the reduced bulk state, as $(D_j)^N$ is the bulk-space dimension.

We therefore found that, when the configuration that minimises \mathcal{A}_1 is the one with all Ising spins pointing up, the entropy reaches its maximum value, since $\overline{S_2(\rho_\gamma)} \approx F_1 - F_0 = N \log D_j$; this corresponds to ρ_γ being completely mixed, namely to the bulk-to-boundary map being isometric. The isometry condition for the map can thus be translated to the requirement of stability of the all-up configuration: for every $\vec{\sigma}$ it must hold that $\mathcal{A}_1(\vec{\sigma}) > N \log D_j$. Given an Ising configuration $\vec{\sigma}$, let $X(\vec{\sigma})$ be the region in which the Ising spins point down; by using Eq. (4.3.19) the stability condition can then be written as

$$|\partial X(\vec{\sigma})| \log d_j > |X(\vec{\sigma})| \log D_j \quad \forall \vec{\sigma} \quad (4.3.20)$$

where $|\partial X(\vec{\sigma})| = \#e \in \partial X(\vec{\sigma})$, and $|X(\vec{\sigma})| = \#v \in X(\vec{\sigma})$.

The significant cases are the ones with vertex valence $d \geq 4$ (for $d \leq 3$ the intertwiner degree of freedom is suppressed). The dimension of the intertwiner space is given by

$$D_j = \frac{2}{\pi} \int_0^\pi d\theta \sin^2 \left(\frac{\theta}{2} \right) \left(\frac{\sin \left((j + \frac{1}{2})\theta \right)}{\sin \left(\frac{\theta}{2} \right)} \right)^d \quad (4.3.21)$$

and the condition in Eq. (4.3.20) thus becomes the following:

$$e^{\frac{|\partial X(\vec{\sigma})|}{|\bar{X}(\vec{\sigma})|}} d_j > \frac{2}{\pi} \int_0^\pi d\theta \sin^2 \left(\frac{\theta}{2} \right) \left(\frac{\sin \left(d_j \frac{\theta}{2} \right)}{\sin \left(\frac{\theta}{2} \right)} \right)^d. \quad (4.3.22)$$

The interesting case for 4D quantum gravity models is $d = 4$. In this case the dimension of the intertwiner space is simply given by $D_j = 2j + 1 = d_j$ [119], i.e. it corresponds to the dimension of the edge spins, and the stability condition becomes

$$|\partial X(\vec{\sigma})| > |X(\vec{\sigma})| \quad \forall \vec{\sigma} \quad (4.3.23)$$

For the class of graphs we are considering (that is, at most one boundary link for each vertex) Eq. (4.3.23) cannot be satisfied by the configuration with all Ising spins pointing down; the bulk-to-boundary map thus cannot be isometric.

4.3.3.2 Inhomogeneous case

We then consider the situation in which the spin assignment to the graph is not homogeneous. We recall that, since $F_0 \simeq 0$, the entropy can be estimated via F_1 , and thus by the minimum of \mathcal{A}_1 . The key observation is, once again, the fact that when the all-up configuration is stable, namely minimises the action, $\overline{S_2(\rho_\gamma)}$ is maximised. In fact,

$$\mathcal{A}_1(\sigma_\uparrow) = \sum_v \log D_{\vec{j}_v} = \log D_\gamma, \quad (4.3.24)$$

which is the maximum possible value for the entropy of the reduced bulk state. We thus need to require that, for any Ising configuration $\vec{\sigma}$, it holds that $\mathcal{A}_1(\vec{\sigma}) > \log D_\gamma$. By identifying a configuration $\vec{\sigma}$ through its spin-down region $X(\vec{\sigma})$ (also indicated just as X , when the explicit reference to the corresponding vector $\vec{\sigma}$ is unnecessary) we can write $\mathcal{A}_1(\vec{\sigma})$ as follows:

$$\mathcal{A}_1(\vec{\sigma}) = \sum_{\ell_{vw}^i \in \partial X_{\text{int}}} \log d_{j_{vw}^i} + \sum_{e_v^i \in \partial X_{\text{ext}}} \log d_{j_v^i} + \sum_{v \in \bar{X}} \log D_{\vec{j}_v} \quad (4.3.25)$$

where $\partial X_{\text{int}} = L \cap \partial X$ is the internal boundary of X , $\partial X_{\text{ext}} = \partial \gamma \cap \partial X$ the external one (see Figure 4.7) and \bar{X} the complement of X ; the inequality $\mathcal{A}_1(\vec{\sigma}) > \log D_\gamma$ then reads

$$\sum_{\ell_{vw}^i \in \partial X_{\text{int}}} \log d_{j_{vw}^i} + \sum_{e_v^i \in \partial X_{\text{ext}}} \log d_{j_v^i} > \sum_{v \in X} \log D_{\vec{j}_v}, \quad (4.3.26)$$

namely, in a more compact form,

$$\sum_{e_v^i \in \partial X} \log d_{j_v^i} > \sum_{v \in X} \log D_{\vec{j}_v}, \quad (4.3.27)$$

which implies

$$\prod_{e_v^i \in \partial X} d_{j_v^i} > \prod_{v \in X} D_{\vec{j}_v}. \quad (4.3.28)$$

Therefore, for every spin-down region X the dimension of the boundary must be greater than the dimension of the bulk.

Let us focus on the case of valence $d = 4$. The dimension of the intertwiner space is given by the following expression [119]:

$$D_{\vec{j}} = \min\{j^1 + j^2, j^3 + j^4\} - \max\{|j^1 - j^2|, |j^3 - j^4|\} + 1 \quad (4.3.29)$$

Note that when the spin assignment reduces to the homogeneous one, the dimension of the intertwiner space is $D_{\vec{j}} = 2j + 1 = d_j$ and we recover from Eq. (4.3.28) the inequality $|\partial X| > |X|$ found in the homogeneous case, which is clearly false.

Before moving to the general case, we consider the simplified scenario of graphs made of vertices with spins pairwise equal: $j_v^i \in \{j_v^{\min}, j_v^{\max}\} \forall e_v^i \in \gamma$. For each vertex it thus holds that

$$D_{\vec{j}_v} = d_{j_v^{\min}}. \quad (4.3.30)$$

Combining Eq. (5.3.4) with Eq. (4.3.30) we then obtain

$$\sum_{\partial X} \log d_{j_v^i} > \sum_{v \in X} \log d_{j_v^{\min}}, \quad (4.3.31)$$

which is violated when, for example, the spin-down region X is such that all its vertices have a link $e_v^i \in \partial X$ carrying the minimum spin j_v^{\min} . Therefore, also in the case of vertices with spins pairwise equal the map is not an isometry.

We now consider the generic case. For vertex spins $j^{\min} = j^a \leq j^b \leq j^c \leq j^d = j^{\max}$ the dimension of the intertwiner space is

$$D_{j^a j^b j^c j^d} = \min\{j^a + j^d, j^b + j^c\} - \Delta + 1 \quad (4.3.32)$$

where $\Delta = j^{\max} - j^{\min}$. Combining Eq. (4.3.32) with Eq. (5.3.4) we obtain the inequality

$$\sum_{e_v^i \in \partial X} \log d_{j_v^i} > \sum_{v \in X} \log (\min\{j_v^a + j_v^d, j_v^b + j_v^c\} - \Delta_v + 1) \quad (4.3.33)$$

Let us stress that the key factors for the condition of Eq. (4.3.33) to be satisfied are the following:

- Combinatorial structure of the graph (number of links on the boundary ∂X and number of vertices inside ∂X).
- Dimensions (equivalently, spins) of the links; note that Δ “measures” the difference with the homogeneous case, which corresponds to $\Delta = 0$, and for which the isometry condition cannot be satisfied.

From Eq. (4.3.33) we see that, for a given combinatorial structure, increasing Δ , namely reducing the dimension of the bulk space, favours the attainment of the isometry condition. Since $j^d \leq j^a + j^b + j^c$ [119], it follows that $\Delta \leq j^b + j^c$. For the maximum possible value $\Delta^{\max} := j^b + j^c$ the dimension of the intertwiner space is equal to 1 (since $\Delta = j^d - j^a = j^b + j^c$ implies $j^a + j^d = j^b + j^c + 2j^a$, therefore $\min\{j^a + j^d, j^b + j^c\} = j^b + j^c$), which means that the bulk degrees of freedom are suppressed; Eq. (4.3.33) in fact becomes trivial:

$$\sum_{e_v^i \in \partial X} \log d_{j_v^i} > 0. \quad (4.3.34)$$

The largest possible value of Δ which does not trivialize the bulk degrees of freedom, $\Delta = \Delta_{\max} - 1$, corresponds to an intertwiner space of dimension 2; when $\Delta = \Delta_{\max} - 1$ for all vertices the stability condition for the all-up configuration becomes

$$\sum_{e_v^i \in \partial X(\vec{\sigma})} \log d_{j_v^i} > |X(\vec{\sigma})| \log 2 \quad \forall \vec{\sigma}, \quad (4.3.35)$$

which, for a given combinatorial pattern¹, is satisfied for sufficiently high values of the edge spins.

Let us compare the above analysis with that of Hayden et al. [53] for random tensor networks. In [53] the dimensions of links (“bond dimensions” in the tensor network language) are equal; this corresponds to our homogeneous case. Moreover, in [53] the dimension of the bulk degrees of freedom is independent from the bond dimensions (in contrast to the intertwiner space, which depends on the spins attached to the vertex links) and can be chosen small enough to make the isometry condition satisfied. In our framework the link dimensions can differ, and the homogeneous

¹We are considering graphs whose vertices can have at most one open edge, and in which two vertices cannot share more than one link.

configuration turns out to be the furthest from being isometric. This is a result of the correlation between bond dimensions and bulk degrees of freedom. In [53], where such a correlation is absent, the homogeneous configuration can meet the isometry condition with a suitable choice of the bulk dimension.

Let us finally stress the following points:

- * When spins are assigned to the links randomly, Δ measures the spread of the corresponding probability distribution. A growing spread Δ corresponds to an increasingly uniform probability distribution. This could be seen also as a condition on generic states in which spins are superposed, a class of which we are going to consider in the following.
- * Increasing Δ increases the “disorder” of the vertex structure, but decreases the dimension of the intertwiner space and thus the value of the maximum possible entropy of the bulk state.
- * From the perspective of the effective Ising model, increasing Δ corresponds to reducing the minimum possible free energy.

4.3.4 Discussion

We found that spin network graphs made of four-valent vertices (dual to 3D spatial geometries) with an homogeneous assignment of edge spins do not realise an isometric mapping of data from the bulk to boundary. Coherently, increasing the inhomogeneity of the spins assigned to a spin network with four-valent vertices increases the “isometry degree” of the corresponding bulk-to-boundary map.

Let us comment on the comparison of this work with Ref. [120], where the idea of interpreting spin network states as maps from the bulk to the boundary first appeared. In Ref. [120], Chen and Livine pointed out that spin network wavefunctions with support on an open graph can be regarded as linear forms on the boundary Hilbert space (the space of spin states living on the open edges of the spin network), and that coarse-graining the bulk, i.e. integrating over the bulk holonomies, then induces a probability distribution for the boundary degrees of freedom. Based on that, they proved the following: any boundary density matrix can be obtained, via the bulk-to-boundary coarse-graining procedure, from a pure bulk state with support on a graph composed of a single vertex connecting all boundary edges to a single bulk loop. A crucial difference between the map of Ref. [120] and \mathcal{M} is that the latter does not perform a coarse graining of the bulk (intended as tracing out the bulk holonomies); instead, it *evaluates* the (pure) spin network state on a given bulk configuration (specifically, a given state for the intertwiner degrees of freedom), thereby yielding a boundary state. Consequently, the latter is a pure state if the bulk input state is pure. By contrast, the boundary density matrix resulting from the bulk-to-boundary coarse-graining of Ref. [120] applied to a pure spin network state is typically mixed.

4.4 Holographic random spin network states and modelling of black hole horizons

Here we study how the entanglement entropy of the boundary of a random spin network is affected by the bulk, specifically by its combinatorial structure and quantum correlations among intertwiners. To this end, we exploit the bulk-to-boundary map perspective on spin network states introduced in section 4.3.1: given a random state (in the sense specified in subsection 4.2.1) $\psi \in \mathcal{H}_\gamma^{j_\gamma}$, we look at the boundary state produced by the corresponding bulk-to-boundary map \mathcal{M}_ψ applied to a certain bulk input state $\zeta \in \mathcal{H}_{\zeta_\gamma}^{j_\gamma}$, upon varying the latter. That is, we look at the “process”

$$|\zeta\rangle \quad \rightarrow \quad \mathcal{M}_\psi |\zeta\rangle := \langle \zeta | \psi \rangle = |\psi(\zeta)\rangle \quad (4.4.1)$$

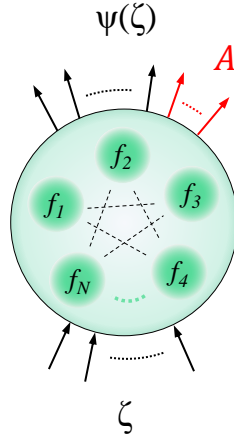


Figure 4.8. Spin network state given by the gluing (symbolised by the dotted lines) of random vertex tensors $f_v \in \mathcal{H}^{\vec{j}_v}$ (the green disks). ζ is the input state for the bulk degrees of freedom (intertwiners), depicted as input lines; $\psi(\zeta)$ is the output state for the boundary edges, depicted as output lines. The boundary entanglement entropy is computed for a set A of the latter, shown in red.

and analyse the entropy of the boundary output $\psi(\zeta)$ in relation to the bulk input ζ . In particular, we focus on the Rényi-2 entropy of a portion A of the boundary:

$$S_2(\rho_A) = -\log \text{Tr}(\rho_A^2) \quad (4.4.2)$$

where $\rho_A := \text{Tr}_{\bar{A}}(\rho)$ with $\rho = |\psi(\zeta)\rangle\langle\psi(\zeta)|$ and \bar{A} is the set of boundary edges complementary to A . The setting is outlined in figure 4.8. We compute the average value of $S_2(\rho_A)$ via the random tensor network techniques presented in section 4.2, which map it into the free energy of a classical Ising model defined on γ . The difference with respect to the analysis of section 4.2 is that the parent state ρ is not the “total” (bulk+boundary) spin network state given by the gluing of individually weighted vertices of Eq. (4.2.9), but a *boundary* state obtained by contracting the latter with a bulk state ζ , i.e.

$$\rho = \text{Tr}_L \left(|\zeta\rangle\langle\zeta| \bigotimes_{\ell \in \gamma} |\ell\rangle\langle\ell| \bigotimes_v |f_v\rangle\langle f_v| \right), \quad (4.4.3)$$

The average value of the entropy is then given by

$$\overline{S_2(\rho_A)} \simeq -\log \frac{\overline{Z_1}}{\overline{Z_0}}, \quad (4.4.4)$$

with

$$\begin{aligned} \overline{Z_1} &= \text{Tr} \left[\rho_\zeta^{\otimes 2} \left(\bigotimes_\ell \rho_\ell^{\otimes 2} \right) \left(\bigotimes_v \overline{\rho_v^{\otimes 2}} \right) S_A \right] \\ \overline{Z_0} &= \text{Tr} \left[\rho_\zeta^{\otimes 2} \left(\bigotimes_\ell \rho_\ell^{\otimes 2} \right) \left(\bigotimes_v \overline{\rho_v^{\otimes 2}} \right) \right] \end{aligned} \quad (4.4.5)$$

where $\rho_\zeta = |\zeta\rangle\langle\zeta|$, $\rho_\ell = |\ell\rangle\langle\ell|$ and $\rho_v = |f_v\rangle\langle f_v|$. The calculation is then analogous to that presented in section 4.2, with the exception of the following aspects:

- Since ρ is a boundary state, the pinning fields ν_v introduced in section 4.2 for the intertwiner degrees of freedom do not enter the calculation of the entropy. The Ising spins interact (besides with each other) with the boundary pinning fields μ_v^i , which point up in the Ising action associated to $\overline{Z_0}$, and are flipped down in that associated to $\overline{Z_1}$.

- The presence of the bulk state ζ leads to an additional contribution to the entropy: $S_2(\rho_{\zeta\downarrow})$, where $\rho_{\zeta\downarrow}$ is the reduced bulk state of the region with Ising spins pointing down.

By performing the traces in Eq. (4.4.5) we in fact obtain for \bar{Z} the expression of a partition function with the following Ising-like action:

$$\mathcal{A}(\vec{\sigma}) = -\frac{1}{2} \sum_{\ell_{vw}^i \in L} (\sigma_v \sigma_w - 1) \log d_{j_{vw}^i} - \frac{1}{2} \sum_{e_v^i \in \partial\gamma} (\sigma_v \mu_{e_v^i} - 1) \log d_{j_v^i} + S_2(\rho_{\zeta\downarrow}) \quad (4.4.6)$$

where $S_2(\rho_{\zeta\downarrow})$ is the Rényi-2 entropy of the bulk state reduced to the region with Ising spins $\sigma_v = -1$. We first analyse the simpler case of spin network states with homogeneous assignment of the edge spins, and tackle the general case (inhomogeneous spins) in subsection 4.4.2.

4.4.1 Homogeneous case

In the homogeneous case, where all spins take the same value j , we can define $\beta := \log d_j$ and write

$$\bar{Z} = \sum_{\vec{\sigma}} e^{-\beta H(\vec{\sigma})} \quad (4.4.7)$$

where

$$H(\vec{\sigma}) = -\frac{1}{2} \left[\sum_{\ell_{vw}^i \in L} (\sigma_v \sigma_w - 1) + \sum_{e_v^i \in \partial\gamma} (\sigma_v \mu_{e_v^i} - 1) \right] + \beta^{-1} S_2(\rho_{\zeta\downarrow}) \quad (4.4.8)$$

We recognise in $H(\vec{\sigma})$ the Hamiltonian function of a standard Ising model defined on γ (squared brackets), which involve internal-link and boundary-edge degrees of freedom, and a term deriving from the entanglement entropy of the bulk degrees of freedom, i.e. intertwiners. As observed in section 4.2 the quantity $\beta = \log d_j$ plays the role of an inverse temperature. The large-spins regime thus corresponds to the low temperature regime, in which the partition function is dominated by the lowest energy configuration. Since $\log \bar{Z}_0 \simeq 0$ (see the discussion of section 4.2) we have that

$$\overline{S_2(\rho_A)} \simeq -\log \frac{\bar{Z}_1}{\bar{Z}_0} \simeq \beta \min_{\vec{\sigma}} H_1(\vec{\sigma}) \quad (4.4.9)$$

where $H_1(\vec{\sigma})$ is given by Eq. (4.4.8) with $\mu_{e_v^i}^i = -1$ for $e_v^i \in A$ and $\mu_{e_v^i}^i = +1$ for $e_v^i \in \bar{A}$ (boundary pinning fields pointing down only in region A). In the following we consider the two regimes corresponding to having the Ising-Hamiltonian term dominant with respect to the bulk Rényi entropy and vice versa.

4.4.1.1 Non-dominant bulk entropy: Ryu–Takayanagi formula for homogeneous spin networks

In the case $S_2(\rho_{\zeta\downarrow}) = 0$ the Hamiltonian is given by

$$H_1(\vec{\sigma}) = -\frac{1}{2} \left[\sum_{\ell_{vw}^i \in L} (\sigma_v \sigma_w - 1) + \sum_{e_v^i \in \partial\gamma} (\sigma_v \mu_{e_v^i} - 1) \right] \quad (4.4.10)$$

Every pair of linked vertices with anti-parallel spins ($\sigma_v \sigma_w = -1$) carries a contribution to the energy equal to 1, and the same happens for pairs composed of a Ising-spin and a pinning field ($\sigma_v \mu_{e_v^i}^i = -1$). The value of $H_1(\vec{\sigma})$ thus coincides with the size of the domain wall $\Sigma(\vec{\sigma})$ between the spin-up and the spin-down regions², quantified by the number of links crossing it: $|\Sigma(\vec{\sigma})| = H_1(\vec{\sigma})$. We thereby obtain

$$\overline{S_2(\rho_A)} \simeq \log d_j \min_{\vec{\sigma}} |\Sigma(\vec{\sigma})| \quad (4.4.11)$$

²Here the pinning fields $\vec{\mu}$ are treated at the same level of the Ising spins.

where the left hand side, in which $\log d_j$ multiplies the number of links across the minimal $\Sigma(\vec{\sigma})$, provides the *area* of the latter ($\log d_j$ is in fact proportional to the area of the surface dual to a link). Equation (4.4.11) can thus be regarded as a version of the Ryu–Takayanagi formula for homogeneous spin networks. Let us also provide a “dynamic” picture of Eq. (4.4.11): in the $\overline{Z_0}$ configuration all Ising spins point up; when switching to the $\overline{Z_1}$ one, the Ising spins in the immediate proximity of A are induced to flip down; from there the spin-down region spreads, stopping when $H_1(\vec{\sigma})$, namely the size of the domain wall, is minimized.

If $S_2(\rho_{\zeta_\downarrow})$ is not null, but still negligible respect to the contribution to H_1 deriving from the interactions of Ising spins to each other and to pinning fields, the average Rényi-2 entropy continues to satisfy the Ryu–Takayanagi formula, with $S_2(\rho_{\zeta_\downarrow})$ a small correction to the area-law term:

$$\overline{S_2(\rho_A)} \simeq \log d_j \left(\min_{\vec{\sigma}} |\Sigma(\vec{\sigma})| \right) + S_2(\rho_{\zeta_\downarrow}) \quad (4.4.12)$$

where the minimization over $\vec{\sigma}$ is performed independently from the bulk term, and the spin-down region entering the latter is the one selected by this minimization procedure.

4.4.1.2 Large bulk entropy and emergence of horizon-like regions in homogeneous spin networks

We now consider the case in which the bulk entanglement contribution to $H_1(\vec{\sigma})$ is comparable to that of internal and boundary edges. This happens, for example, when the bulk is in a random pure state, namely has Rényi-2 entropy given by

$$S_2(\rho_{\zeta_\downarrow}) = \log \frac{D_j^N + 1}{D_j^{|\sigma_\downarrow|} + D_j^{|\sigma_\uparrow|}} \quad (4.4.13)$$

where σ_\downarrow (σ_\uparrow) is the region with Ising spins pointing up (down), and $|\sigma_\downarrow|$ ($|\sigma_\uparrow|$) the corresponding size. For vertices of valence 4 the intertwiner dimension is $D_j = d_j = e^\beta$, and for $\beta \gg 1$ it holds that³ $S_2(\rho_{\zeta_\downarrow}) \simeq \beta \min\{|\sigma_\uparrow|, |\sigma_\downarrow|\}$. The Hamiltonian thus takes the following form:

$$H_1(\vec{\sigma}) = -\frac{1}{2} \left[\sum_{\ell_{vw}^i \in L} (\sigma_v \sigma_w - 1) + \sum_{e_v^i \in \partial\gamma} (\sigma_v \mu_{e_v^i} - 1) \right] + \min\{|\sigma_\uparrow|, |\sigma_\downarrow|\} \quad (4.4.15)$$

In this case, the minimization of $H_1(\vec{\sigma})$, namely the behaviour of the minimum-size domain wall, strongly depends on the bulk entanglement contribution. We illustrate such an effect with an example; in particular, we show that the bulk entanglement can remove the degeneration between equal-energy configurations (i.e. equal-size domain walls) and, when sufficiently high in a given region, forces the domain wall to stay outside of it.

Consider the homogeneous graph depicted in figure 4.9. Since it is made of four-valent vertices, the dimension of the intertwiner degrees of freedom is equivalent to that of the edges: $D_j = d_j = 2j + 1$. The boundary region A we look at, together with its pointing-down pinning fields, is illustrated in figure 4.9. We first assume that the bulk state is a separable state of all intertwiners, therefore its entanglement entropy contribution is zero and $H(\vec{\sigma}) = |\Sigma(\vec{\sigma})|$. The minimal energy $H_1 = 4$ is then reached by two configurations (denoted as $\vec{\sigma}_a$ and $\vec{\sigma}_b$) whose corresponding surfaces $\Sigma_a := \Sigma(\vec{\sigma}_a)$ and $\Sigma_b := \Sigma(\vec{\sigma}_b)$ are depicted in figure 4.9.

We now switch on the intertwiner correlations in a bulk disk Ω , which is illustrated in figure 4.10; in particular, we assume Ω to be in a random pure state $|\zeta_\Omega\rangle$, with the complementary part of the bulk being in a direct product state:

$$|\zeta\rangle = |\zeta_\Omega\rangle \otimes \bigotimes_{v: r_v > 1} |\xi_v\rangle \quad (4.4.16)$$

³In fact

$$\frac{e^{\beta N} + 1}{e^{\beta|\sigma_\uparrow|} + e^{\beta|\sigma_\downarrow|}} \simeq \frac{e^{\beta N}}{e^{\beta|\sigma_\uparrow|}(1 + e^{\beta(|\sigma_\downarrow| - |\sigma_\uparrow|)})} \simeq e^{\beta(N - \max\{|\sigma_\uparrow|, |\sigma_\downarrow|\})} = e^{\beta \min\{|\sigma_\uparrow|, |\sigma_\downarrow|\}}. \quad (4.4.14)$$

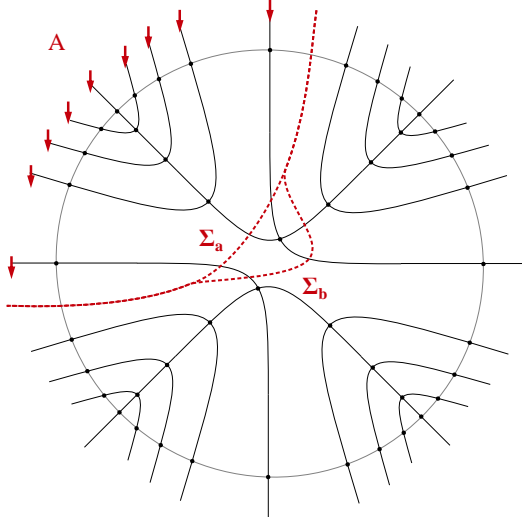


Figure 4.9. The minimum of H_1 is degenerate; the corresponding surfaces Σ_a and Σ_b , with area $|\Sigma_a| = |\Sigma_b| = 5$, are shown by dashed red lines.

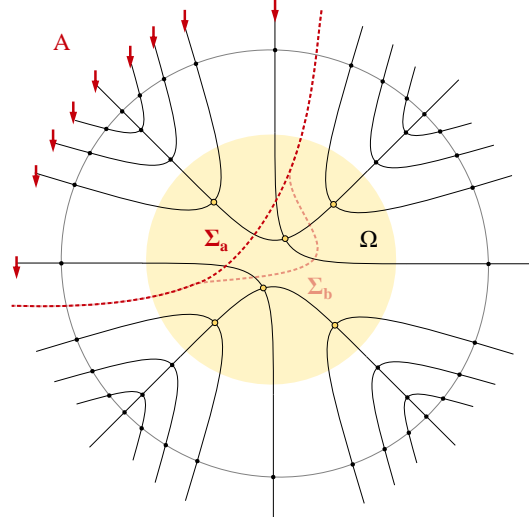


Figure 4.10. If intertwiner entanglement is present in a region Ω of the bulk (highlighted in yellow in the figure, as well as the vertices within it), the degeneracy of the minimal energy is removed. In fact, $|\Sigma_a| = 6$ and $|\Sigma_b| = 7$.

The Hamiltonian thus takes the form (see Eq. (4.4.15))

$$H_1(\vec{\sigma}) = -\frac{1}{2} \left[\sum_{\ell_{vw}^i \in L} (\sigma_v \sigma_w - 1) + \sum_{e_v^i \in \partial\gamma} (\sigma_v \mu_{e_v^i} - 1) \right] + \min\{|\Omega_\uparrow|, |\Omega_\downarrow|\} \quad (4.4.17)$$

where $\Omega_\downarrow := \Omega \cap \sigma_\downarrow$ and $\Omega_\uparrow := \Omega \cap \sigma_\uparrow$. For the two configurations $\vec{\sigma}_a$ and $\vec{\sigma}_b$ we then have that

$$H_1(\vec{\sigma}_a) = 4 + \beta^{-1} \log \frac{e^{9\beta} + 1}{e^{2\beta} + e^{7\beta}} \approx 4 + \beta^{-1} \log e^{2\beta} = 6 \quad (4.4.18)$$

$$H_1(\vec{\sigma}_b) = 4 + \beta^{-1} \log \frac{e^{9\beta} + 1}{e^{3\beta} + e^{6\beta}} \approx 4 + \beta^{-1} \log e^{3\beta} = 7 \quad (4.4.19)$$

When the bulk correlations are switched on, the degeneracy of the minimum of H_1 is thus removed. Note that the lowest-energy configuration, $\vec{\sigma}_a$, has a domain wall that enters the bulk disk Ω . However, upon increasing the dimension of the latter, the domain wall ends up being pushed out of it. To show this, we just have to refine vertices of the bulk disk Ω as shown in figure 4.11. The Ising energy of $\vec{\sigma}_a$ then increases to $H_1(\vec{\sigma}_a) = 14$, and the domain wall settles down outside Ω , with $H_{1\min} = 8$.

4.4.2 Inhomogeneous case

We consider here the more general case in which each link ℓ of the graph carries an arbitrary spin j_ℓ . From the Ising model point of view, this means that we are considering Ising spins with inhomogeneous couplings. Nevertheless, in order to define a Boltzmann weight for the partition function, we introduce a uniform β to be understood as an average inverse temperature, i.e. $\beta = \log d_j$ where d_j is the average edge dimension; then $\bar{Z} = \sum_{\vec{\sigma}} e^{-\beta H(\vec{\sigma})}$ with

$$H(\vec{\sigma}) = -\frac{1}{2} \sum_{\ell_{vw}^i \in L} (\sigma_v \sigma_w - 1) J_{vw}^i - \frac{1}{2} \sum_{e_v^i \in \partial\gamma} (\sigma_v \mu_{e_v^i} - 1) J_v^i + \beta^{-1} S_2(\rho_{\zeta_\downarrow}) \quad (4.4.20)$$

where $J_{vw}^i := \frac{\log d_{j_{vw}^i}}{\beta}$ and $J_v^i := \frac{\log d_{j_v^i}}{\beta}$ are the (normalised) strengths of the interaction. In the low-temperature (large-spins) regime the leading contribution to the partition function is that of

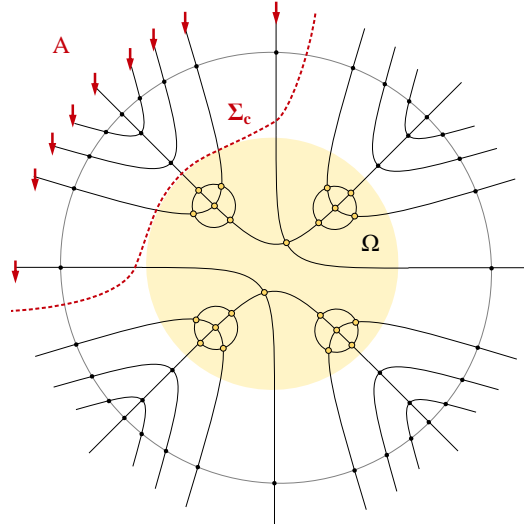


Figure 4.11. By increasing the dimension of the bulk disk Ω via refinement of vertices, the minimal-energy surface Σ_c is prevented from entering it.

the minimum energy configuration and $\log \overline{Z_0} \simeq 0$; in fact, when $\mu_v^i = +1 \forall e_v^i \in \partial\gamma$, the lowest energy configuration is that with all Ising spins pointing up, for which all terms in Eq. (4.4.20) are zero. When, instead, $\mu_v^i = -1$ for $e_v^i \in A$ and $\mu_v^i = +1$ for $e_v^i \notin A$ (boundary condition for $H_1(\vec{\sigma})$), a spin-up region (with external boundary \bar{A}) and a spin-down region (with external boundary A) arise, and the domain wall settles down in order to minimize $H_1(\vec{\sigma})$:

$$\overline{S_2(\rho_A)} \simeq -\log \frac{\overline{Z_1}}{\overline{Z_0}} \simeq \beta \min_{\vec{\sigma}} H_1(\vec{\sigma}) \quad (4.4.21)$$

We proceed to consider the alternative regimes characterized by the Ising-Hamiltonian/bulk-entropy term being dominant.

4.4.2.1 Non-dominant bulk entropy: Ryu–Takayanagi formula for inhomogeneous spin networks

For null bulk entanglement entropy we have the Ising Hamiltonian

$$H_1(\vec{\sigma}) = -\frac{1}{2} \sum_{\ell_{vw}^i \in L} (\sigma_v \sigma_w - 1) J_{vw}^i - \frac{1}{2} \sum_{e_v^i \in \partial\gamma} (\sigma_v \mu_{e_v^i} - 1) J_v^i \quad (4.4.22)$$

that provides the *area* of the domain wall, determined by both combinatorial and dimensional properties of the entanglement graph. In fact, it not just the number of open-edges/links that matters: every open-edge e_v^i (link e_{vw}^i) is weighted by a factor J_v^i (J_{vw}^i) proportional to (the logarithm of) its dimension (which, in turns, gives the area of the surface topologically dual to the link). An analogue of the Ryu-Takayanagi formula therefore holds and, due to the (quantum) discrete geometric nature of the degrees of freedom carried by the entanglement graphs, it involves a properly geometric notion of area (i.e. the spin degrees of freedom concur to the definition of the discrete geometry, and the discrete metric is not simply given by the graph distance). Similarly to the homogeneous counterpart, the presence of small bulk entanglement entropy represents a (not negligible, but small) correction to the area term:

$$\overline{S_2(\rho_A)} \simeq \log d_j \left(\min_{\vec{\sigma}} |\Sigma(\vec{\sigma})| \right) + S_2(\rho_{\zeta\downarrow}) \quad (4.4.23)$$

with $|\Sigma(\vec{\sigma})|$ given by Eq. (4.4.22).

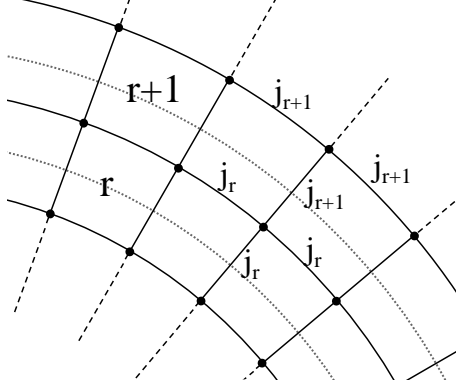


Figure 4.12. Each shell r crosses radial links carrying spin j_r ; vertices between shells r and $r+1$ recouple three spins j_r (one on the radial inward direction, two on the edges tangent to shell r) and one spin j_{r+1} (outward radial direction).

4.4.2.2 Larger bulk entropy and emergence of horizon-like regions in inhomogeneous spin networks

When the contribution of the bulk entanglement entropy is not small with respect to the Ising part, we need to minimize the whole Hamiltonian:

$$H_1(\vec{\sigma}) = -\frac{1}{2} \sum_{\ell_{vw}^i \in L} (\sigma_v \sigma_w - 1) J_{vw}^i - \frac{1}{2} \sum_{e_v^i \in \partial\gamma} (\sigma_v \mu_{e_v^i} - 1) J_v^i + \beta^{-1} S_2(\rho_{\zeta_\downarrow}) \quad (4.4.24)$$

Note that an internal link ℓ_{vw}^i carries a contribution (J_{vw}^i) to the energy only if the Ising spins σ_v and σ_w are misaligned; a boundary edge in A carries a contribution (J_v^i) only if the Ising spin σ_v points up, while a boundary edge in \bar{A} carries a contribution (J_v^i) only if the Ising spin σ_v points down. As a result, the first two terms of H_1 are minimized by the configuration whose spin-down region σ_\downarrow has external boundary A and internal boundary $|\Sigma(\vec{\sigma})|$ of smallest possible size. Then, the region σ_\downarrow contributes to H_1 with the (β -rescaled) Rényi-2 entropy of its reduced bulk state ρ_{ζ_\downarrow} . In the end, the minimization of H_1 is achieved when the spin-down region σ_\downarrow has the minimum possible area and volume correlations.

We illustrate the properties of this mechanism with an example. Consider the (spherically symmetric) graph of figure 4.12, with a radial gradient of edge spins: $j_{r+1} > j_r$. We assume that the bulk is in a random pure state inside a disk Ω of radius R and in a product state outside. Therefore,

$$S_2(\rho_{\zeta_\downarrow}) = \log \frac{\prod_{v \in \Omega} D_{j_v} + 1}{\prod_{v \in \Omega_\downarrow} D_{j_v} + \prod_{v \in \Omega_\uparrow} D_{j_v}} \quad (4.4.25)$$

We express the intertwiner dimensions D_{j_v} in Eq. (C.3.2) as local intertwiner inverse temperatures $\beta'_v = \log D_{j_v}$; we then consider the large spins regime and assume that the variance of intertwiner dimensions within Ω is small, i.e. $\beta'_v \approx \beta'$ for all $v \in \Omega$. Then Eq. (C.3.2) simplifies to⁴ $S_2(\rho_{\zeta_\downarrow}) =$

⁴In the large spins regime

$$\log \left(\frac{\prod_{v \in \Omega} D_{j_v} + 1}{\prod_{v \in \Omega_\downarrow} D_{j_v} + \prod_{v \in \Omega_\uparrow} D_{j_v}} \right) \approx \log \left(\frac{\prod_{v \in \Omega} e^{\beta'_v}}{\prod_{v \in \Omega_\downarrow} e^{\beta'_v} + \prod_{v \in \Omega_\uparrow} e^{\beta'_v}} \right) = \sum_{v \in \Omega} \beta'_v - \log \left(\prod_{v \in \Omega_\downarrow} e^{\beta'_v} + \prod_{v \in \Omega_\uparrow} e^{\beta'_v} \right) \quad (4.4.26)$$

If we assume that $\beta'_v \approx \beta'$ for all v then

$$\prod_{v \in \Omega_\downarrow} e^{\beta'_v} + \prod_{v \in \Omega_\uparrow} e^{\beta'_v} \approx e^{\beta' \max\{|\Omega_\uparrow|, |\Omega_\downarrow|\}} \left[1 + e^{-\beta' (\max\{|\Omega_\uparrow|, |\Omega_\downarrow|\} - \min\{|\Omega_\uparrow|, |\Omega_\downarrow|\})} \right] \approx e^{\beta' \max\{|\Omega_\uparrow|, |\Omega_\downarrow|\}} \quad (4.4.27)$$

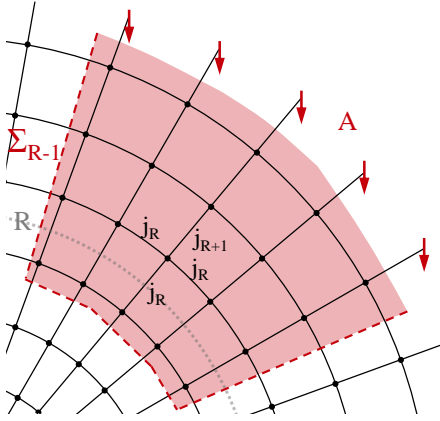


Figure 4.13. In absence of bulk entanglement, the Ising domain wall (the dashed red line) moves towards the center of the spherical geometry.

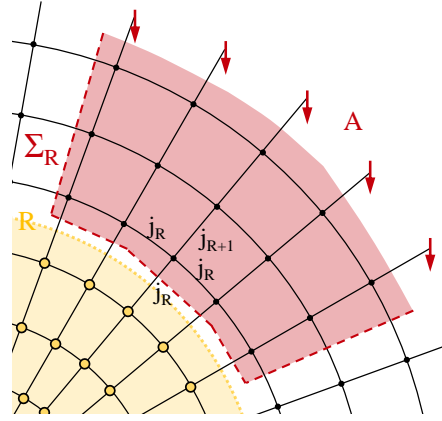


Figure 4.14. When a bulk disk of radius R is in a random pure state, the Ising domain wall is prevented from entering it.

$\beta' \min\{|\Omega_\uparrow|, |\Omega_\downarrow|\}$ and

$$H(\vec{\sigma}) \approx -\frac{1}{2} \sum_{\ell_{vw}^i \in L} (\sigma_v \sigma_w - 1) J_{vw}^i - \frac{1}{2} \sum_{e_v^i \in \partial\gamma} (\sigma_v \mu_{e_v^i} - 1) J_v^i + \frac{\beta'}{\beta} \min\{|\Omega_\uparrow|, |\Omega_\downarrow|\} \quad (4.4.29)$$

Note that, with respect to the homogeneous case of Eq. (4.4.17), the smallest number of aligned spins in the bulk region Ω is now weighted by the ratio of the intertwiner inverse temperature β' to the link inverse temperature β .

We are going to show how the presence of intertwiner entanglement in a disk Ω of the spherically symmetric graph in figure 4.13 affects the entanglement entropy of a portion A of the boundary. Note that, as we want $D_{j_r j_r j_r j_{r+1}} = 3j_r - j_{r+1} + 1 > 1$ inside Ω , we must have $j_r < j_{r+1} < 3j_r$ for $r \leq R$. Let $\mathcal{A}(r)$ be the Ising action of a configuration whose domain wall Σ_r lies between shell r and shell $r-1$ (see figure 4.13). When the bulk entanglement is not present, we have that

$$\mathcal{A}(r) = (|A| + 2) \log d_{j_r} + 2 \sum_{k=r+1}^{r_{\max}} \log d_{j_k} \quad (4.4.30)$$

The minimal-energy surface drops from shell $r+1$ to shell r if $\mathcal{A}(r+1) > \mathcal{A}(r)$. By using (4.4.30), the latter becomes

$$|A| \log d_{j_{r+1}} > (|A| + 2) \log d_{j_r} \quad , \quad (4.4.31)$$

which is satisfied by

$$d_{j_{r+1}} > d_{j_r}^{\frac{|A|+2}{|A|}} \quad , \quad (4.4.32)$$

that, for $|A| \gg 1$, is always true. We therefore have that, in absence of bulk entanglement, the minimal-energy surface moves toward the innermost shells.

When switching on the bulk entanglement within Ω (specifically, when assuming that Ω is in a random pure state), the value of the Ising action for the domain wall at $r=R$ is no more given by Eq. (4.4.30). Instead we have

$$\mathcal{A}(R) = (|A| + 2) \log d_{j_R} + 2 \sum_{k=R+1}^{r_{\max}} \log d_{j_k} + |A| \log \left(\frac{d_{j_R} + d_{j_{R+1}}}{2} \right) \quad (4.4.33)$$

and we get

$$\sum_{v \in \Omega} \beta'_v - \log \left(\prod_{v \in \Omega_\downarrow} e^{\beta'_v} + \prod_{v \in \Omega_\uparrow} e^{\beta'_v} \right) \approx \beta' \left(\Omega - \max\{|\Omega_\uparrow|, |\Omega_\downarrow|\} \right) = \beta' \min\{|\Omega_\uparrow|, |\Omega_\downarrow|\} \quad (4.4.28)$$

where we used the fact that $D_{j_r j_r j_r j_{r+1}} = 3j_r - j_{r+1} + 1 = \frac{d_{j_r} + d_{j_{r+1}}}{2}$. The condition for the domain wall to enter Ω , i.e. $\mathcal{A}(R+1) - \mathcal{A}(R) > 0$, thus leads to

$$|A| \log d_{j_{R+1}} > (|A| + 2) \log d_{j_R} + |A| \log \left(\frac{d_{j_R} + d_{j_{R+1}}}{2} \right) \quad (4.4.34)$$

which can be written as follows:

$$d_{j_{R+1}} \left(2 - d_{j_R}^{\frac{|A|+2}{A}} \right) > d_{j_R}^{1 + \frac{|A|+2}{A}} \quad . \quad (4.4.35)$$

Since $d_j \geq 2$ for $j > 0$, the left hand side of (4.4.35) is negative, and (4.4.35) is therefore never satisfied: the minimal-energy surface is prevented from entering the disk Ω , as shown in figure 4.14. We thus found that the presence of (large) intertwiner entanglement within the disk Ω makes its boundary (the shell of radius R) a horizon-like region.

5

Emergence of objectivity of observables

Quantum theory has proven to be extremely successful in describing the physical laws of microscopic objects. However, assuming the general validity of quantum theory, the apparent absence of quantum features (such as non-locality and superposition effects) in our everyday classical reality raises the issue of the quantum-to-classical transition: how do physical systems lose their “quantumness” with increasing scales and become effectively classical?

The theory of decoherence [57–60], which developed significantly over the past decades, has pointed out the key role played in this transition by the interaction of the system with its environment: due to this interaction the two become entangled, and the quantum correlations so established between the two parties cannot be observed at the level of the system alone. The entanglement with the environment thus *defines* the physical properties we can observe at the level of the system. In particular, only those states that are robust in spite of the interaction with the environment are observable in practice. The environmental monitoring therefore leads to the selection of preferred states (known as *pointer states* [121–123]) which represent the natural candidates for the classical states that are compatible with our everyday experience. However, decoherence alone does not explain how the striking contrast between classical and quantum states is overcome in the emergence of classicality. In fact, while classical states can be detected and agreed upon by initially ignorant observers without being perturbed, and thus exist objectively, quantum states are generally affected by the measurement process. It is therefore necessary to clarify how the information about pointer states becomes objective.

The theory of Quantum Darwinism [124–129] provides a possible solution by promoting the environment from source of decoherence to carrier of information about the system. In fact, Quantum Darwinism points out that a fundamental consequence of the system-environment interaction is the presence of information about the system encoded in the environment. By intercepting fragments of the environment, it is possible to acquire such information indirectly. In particular, Quantum Darwinism explains how information about the pointer states proliferates in the environment, allowing multiple observers to detect these states without perturbing their existence.

The Quantum Darwinism approach to the emergence of classicality has been explored theoretically in various specific models [130–142] and has also been the subject of recent experimental tests [143–145]. However, the range of applicability of such framework still represents an open issue in the quantum-to-classical transition problem. A recent result by Brandão *et al.* [61] made a significant contribution to it, showing how some classical features emerge in a model-independent way from the quantum formalism alone. Such result relies on the splitting of the objectivity notion into the following statements:

- ▶ *Objectivity of observables*: multiple observers probing the same system can at most acquire classical information about one and the same measurement;
- ▶ *Objectivity of outcomes*: the observers will agree on the result obtained from the preferred measurement.

Brandão *et al.* modelled the information flow from a (finite-dimensional) quantum system to

the fragments of its environment via quantum channels, i.e., completely positive trace-preserving (cptp) maps. They showed that, when the number of fragments N becomes large enough, most of these channels are well approximated by specific cptp maps, called “measure-and-prepare”. The form of such channels ensures the objectivity requirements. This is formalised by a bound on the distance (induced by the so-called diamond norm) between the system-environment channels and the measure-and-prepare ones. It is found that such distance goes to zero as $N \rightarrow \infty$, leading to convergence to objectivity of observables (in the following, we will refer to such a bound as *objectivity bound*). In [62], Knott *et al.* overcame the finite-dimension restriction by showing that also infinite-dimensional systems, under appropriate energy constraints, exhibit objectivity of observables. Another interesting result in this context was recently obtained by Qi and Ranard [146]: they showed that, for finite-dimensional systems, the set of channels which do not converge to objectivity is of fixed size $O(1)$, instead of scaling with the number of environmental fragments N , as in [61, 62].

In this chapter, which is based on Ref. [5], we extend the infinite-dimensional analysis of [62] and provide a unified approach to the emergence of the *objectivity of observables* in the interaction between a quantum system of *arbitrary* dimension and a large number of fragments of its environment. Specifically, we first prove that the objectivity of observables holds true for a wide class of (energy-constrained) infinite-dimensional systems. For such class we obtain tighter bounds on the emergence of this classical feature, compared to those available in the literature. Moreover, our framework can act as a bridge between the finite- and infinite-dimensional scenarios. Our results rely on an infinite-dimensional version of the Choi–Jamiołkowski isomorphism, adapted to our set of energy-constrained states. This generalises what was done in [62] for a specific choice of the energy constraint. Moreover, our analysis exploits novel bounds relating the diamond-norm distance of two channels with the distance between their respective Choi–Jamiołkowski states – see Aubrun *et al.* [147]. Such results are presented in Section 5.1.

We also tackle a relevant issue for the emergence of objectivity of observable, not considered in Refs [61, 62], which is the optimality of the rates at which the convergence to objectivity takes place. In fact, objectivity of observables is regarded as emergent whenever the upper bound on the distance between channels representing the system-environment information flow and the measure-and-prepare ones goes to zero asymptotically. But this does not give information on how well the objectivity bound approximates the considered diamond norm distance. To perform such optimality check, a possible strategy is to derive a *lower bound* for that diamond norm, which turns out to be an upper bound on the speed at which the emergence of objectivity of observables takes place. In Section 5.2 we perform this analysis for the specific model of a system-environment dynamics given by a pure loss channel, and show that for such model the rate of convergence to objectivity of observables scales at least as the inverse of the number of environmental fragments.

The final point we address regards the extension to an infinite-dimensional scenario of the operational interpretation of *quantum discord* [148, 149] derived for finite-dimensional systems by Brandão *et al.* [61]. In particular, it was proven that when information is distributed to many parties on one side of a bipartite system, the minimal average loss in correlations corresponds to the quantum discord. In Section 5.3 we generalise this result to the infinite-dimensional case by exploiting the objectivity bounds proved in Section 5.1.

5.1 Improved bounds on the emergence of objectivity of observables

The scenario we consider consists of a system A , generally infinite-dimensional, and its environment B , which is described as a collection of N (possibly infinite-dimensional) subsystems B_1, \dots, B_N , namely the environment fragments. We assume that the system of interest A is initially decorrelated from B_1, \dots, B_N , and that the corresponding state has bounded mean energy (defined via an appropriate Hamiltonian – see below). The information flow from the system to the whole environment is modelled as a quantum channel, i.e., a cptp map $\Lambda : \mathcal{D}(A) \rightarrow \mathcal{D}(B_1 \otimes \dots \otimes B_N)$, where $\mathcal{D}(Z)$ denotes the set of density matrices associated with a physical system Z . The transfer

of quantum information from A to the single environmental fragment B_j is therefore described by the “subchannel” $\Lambda_j = \text{Tr}_{B \setminus B_j} \circ \Lambda$. Objectivity of observables then arises whenever the maps Λ_j become arbitrarily close to measure-and-prepare channels, which allow observers to acquire only classical information about one and the same measurement. These channels are defined as $\mathcal{E}_j(X) := \sum_l \text{Tr}(M_l X) \tau_{j,l}$, where $\{M_l\}_l$ is a positive operator-valued measure (POVM) – crucially independent of the index j – and $\{\tau_{j,l}\}_l$ is a set of states for subsystem B_j .

We shall quantify distinguishability in the space of channels via a distance called *energy-constrained diamond norm* [150, 151]. This is a modification of the standard diamond norm [152–154], designed to implement a restriction on the average (initial) energy of the quantum system under examination. This is measured by a Hamiltonian, which we take to be an arbitrary self-adjoint operator H with spectrum bounded from below. Without loss of generality, we assume its ground state energy to be positive, i.e.

$$\inf_{\lambda \in \text{sp}(H)} \lambda = E_0 > 0, \quad (5.1.1)$$

where $\text{sp}(H)$ is the spectrum of H .

Definition 5.1.1. Let A' be a quantum system equipped with a Hamiltonian $H_{A'}$ that satisfies Eq. (5.1.1), and pick $E > E_0$. Then the energy-constrained diamond norm of an arbitrary Hermiticity-preserving linear map $\Lambda : \mathcal{D}(A') \rightarrow \mathcal{D}(B)$ is defined by

$$\|\Lambda\|_{\diamond, H, E} := \sup_{\text{Tr}[\rho_{H_{A'}}] \leq E} \|(\text{id}_A \otimes \Lambda_{A'})[\rho_{AA'}]\|_1, \quad (5.1.2)$$

where A is an arbitrary ancillary system, and $\|\cdot\|_1$ is the one-norm. A recent result by Weis and Shirokov [155] ensures that the input state $\rho_{AA'}$ in Eq. (5.1.2) can be taken to be pure.

In our analysis, we assume that the Hamiltonian admits a countable set of eigenvectors forming an orthonormal basis $\{|j\rangle, j = 0, 1, \dots\}$ of the Hilbert space. The index j is allowed to go to infinity, and the case of a finite-dimensional system will be treated by a suitable choice of the Hamiltonian eigenvalues (see below).

We want to stress that the assumption that a Hamiltonian H has discrete spectrum and is bounded from below is physically well motivated; in fact, it is contained in the so-called Gibbs hypothesis [156]:

Gibbs hypothesis. A (possibly unbounded) self-adjoint operator H is said to satisfy the Gibbs hypothesis if for every $\beta > 0$ the partition function $Z(\beta) := \text{Tr} e^{-\beta H}$ is finite. As a consequence, the state $\frac{1}{Z(\beta)} e^{-\beta H}$ has finite entropy. Moreover, for every eigenvalue E of the Hamiltonian H , the (unique) maximiser ρ of the entropy subjected to the constraint $\text{Tr} \rho H \leq E$ is the Gibbs state

$$\gamma(E) = \frac{1}{Z(\beta(E))} e^{-\beta(E)H}, \quad (5.1.3)$$

where $\beta = \beta(E)$ is the solution to the equation $\text{Tr} e^{-\beta H} (H - E) = 0$.

By setting

$$H = \sum_j f_j |j\rangle\langle j|, \quad (5.1.4)$$

we also require that the (increasing) sequence of eigenvalues f_j diverges sufficiently rapidly, in formula

$$\left| \sum_j \frac{1}{f_j} \log \frac{1}{f_j} \right| < \infty. \quad (5.1.5)$$

In the following, we will refer to the entire spectrum $\{f_j\}_j$ by using the short notation $f = \{f_j\}_j$. Eq. (5.1.5) clearly implies that $\sum_j \frac{1}{f_j} < \infty$. Notably, this excludes the physically relevant case $f_j = j$, corresponding to the canonical Hamiltonian on the Hilbert space of a harmonic oscillator. In spite of this drawback, our technical assumption allows us to explore a rich family of constraints

that effectively extend and interpolate between previously known bounds. Moreover, a slight modification of our proof technique allows us to deal with the excluded case $f_j = j$ as well; for details, see the end of this section.

Before proceeding with the presentation of our results, we want to clarify that the positive operator H and the scalar threshold E do not actually have any dynamical characterization. In fact, their role in our framework is simply to confine the bulk of a state's probability mass to a finite-dimensional subspace in a smooth and well-defined way.

We now introduce some technical elements and definitions that will enter our main results on the emergence of objectivity of observables, stated in Theorem 5.1.1. We start by considering a special class of entangled states featuring an f -dependent tail in the Hamiltonian eigenbasis:

$$|\phi\rangle := c_f \sum_{j=0}^{\infty} \phi_j |j, j\rangle_{AA'}, \quad (5.1.6)$$

with $\phi_j^2 := 1/f_j$ and $c_f := \left(\sum \frac{1}{f_j}\right)^{-\frac{1}{2}}$. In our derivation, an important role will be played by the local von Neumann entropy of $|\phi\rangle$, given by

$$\sigma := S(\mathrm{Tr}_{A'} |\phi\rangle\langle\phi|_{AA'}) = - \sum_j \frac{c_f^2}{f_j} \log \left(\frac{c_f^2}{f_j} \right) < \infty, \quad (5.1.7)$$

where the last inequality follows from Eq. (5.1.5).

A useful technical tool in our work is the d -dimensional truncation of our entangled state $|\phi\rangle$, which can be obtained as $(\Pi_d \otimes \mathrm{id})|\phi\rangle = (\mathrm{id} \otimes \Pi_d)|\phi\rangle = c_f \sum_{j=0}^{d-1} \phi_j |j, j\rangle$, where $\Pi_d = \sum_{j=0}^{d-1} |j\rangle\langle j|$. The ‘approximation error’ associated with this truncation can be quantified as follows:

Definition 5.1.2. The tail of our entangled state $|\phi\rangle$, dependent on the truncation dimension d , is defined as

$$\epsilon_d := \left\| ((\mathrm{id} - \Pi_d) \otimes \mathrm{id}) |\phi\rangle \right\| = c_f \sqrt{\sum_{j=d}^{\infty} \frac{1}{f_j}} \quad (5.1.8)$$

The f -dependent entangled state $|\phi\rangle$ allows us to consider a modified version of the Choi–Jamiołkowski states [62, 157] (*f-Choi states* for brevity – see below), that will be crucial to prove Theorem 5.1.1:

Definition 5.1.3. The *modified Choi–Jamiołkowski state* of a cptp map $\Lambda : \mathcal{D}(A') \rightarrow \mathcal{D}(B)$, for a given sequence of Hamiltonian eigenvalues $f = \{f_j\}_j$, is defined as

$$J_f(\Lambda) := \mathrm{id}_A \otimes \Lambda_{A'} [|\phi\rangle\langle\phi|], \quad (5.1.9)$$

where $|\phi\rangle$ is given in Eq. (5.1.6).

Having introduced all the required ingredients, we can now state the following theorem.

Theorem 5.1.1. *Let A be a quantum system equipped with a Hamiltonian H_A which satisfies the Gibbs hypothesis and which, when written as in Eq. (5.1.4), also satisfies Eq. (5.1.5). Consider an arbitrary cptp map $\Lambda : \mathcal{D}(A) \rightarrow \mathcal{D}(B_1 \otimes \dots \otimes B_N)$, and define the effective dynamics from $\mathcal{D}(A)$ to $\mathcal{D}(B_j)$ as $\Lambda_j := \mathrm{Tr}_{B \setminus B_j} \circ \Lambda$. For an arbitrary number $0 < \delta < 1$, there exists a POVM $\{M_l\}_l$ and a set $S \subseteq \{1, \dots, N\}$, with $|S| \geq (1 - \delta)N$, such that, for all $j \in S$ and for any integer truncation dimension $d \geq 0$, we have that*

$$\|\Lambda_j - \mathcal{E}_j\|_{\diamond, H, E} \leq \frac{\zeta}{\delta}, \quad (5.1.10)$$

where the measure-and-prepare channel \mathcal{E}_j is given by

$$\mathcal{E}_j(X) := \sum_l \mathrm{Tr}(M_l X) \tau_{j,l} \quad (5.1.11)$$

for some family of states $\tau_{j,l} \in \mathcal{D}(B_j)$, and

$$\zeta = \kappa d \left(\frac{E^2 \sigma}{N c_f^4} \right)^{1/3} + \frac{4E}{c_f^2} \epsilon_d, \quad (5.1.12)$$

where c_f is the normalization factor introduced in Eq. (5.1.6); ϵ_d is given in Definition 5.1.2; σ is defined by Eq. (5.1.7) and $\kappa := 3(16 \ln(2))^{1/3}$ is a universal constant.

The complete proof is detailed in C.1. In what follows we provide the key ideas behind it.

Outline of the proof of Theorem 5.1.1. We start by proving that the 1-norm of an operator L , given by the difference between two f -Choi states, can be bounded as follows:

$$\|L\|_1 \leq 4d^{\frac{3}{2}} \max_{\mathcal{M}} \|\text{id} \otimes \mathcal{M}[L]\|_1 + 4\epsilon_d. \quad (5.1.13)$$

Here, \mathcal{M} is an arbitrary measurement, thought of as a quantum-to-classical channel, d is the truncation dimension and ϵ_d is given in Definition 5.1.2. We then show that the distance between two channels is bounded by that between their f -Choi states:

$$\|\Lambda_0 - \Lambda_1\|_{\diamond H, E} \leq \frac{E}{c_f^2} \|J_f(\Lambda_0) - J_f(\Lambda_1)\|_1. \quad (5.1.14)$$

The key ingredient of the proof is a result (Lemma C.1.3 in C.1) which introduces a set of quantum-to-classical channels $\{\mathcal{M}_j | j \in J\}$ acting on a subset J of the environment fragments B_1, \dots, B_N . Let z be the outcome of such set of measurements, then the state $\mathbb{E}_z \rho_A^z \otimes \rho_{B_j}^z$ can be proved to be the modified Choi–Jamiołkowski state of a measure-and-prepare channel \mathcal{E}_j with POVM independent of $j \notin J$. The Lemma bounds the quantity

$$\mathbb{E}_{j \notin J} \max_{\mathcal{M}_j} \left\| \text{id} \otimes \mathcal{M}_j \left[\rho_{AB_j} - \mathbb{E}_z \rho_A^z \otimes \rho_{B_j}^z \right] \right\|_1 \quad (5.1.15)$$

through a function of the entropy for system A ; in (5.1.15), the expectation value is with respect to the uniform distribution over $\{1, \dots, N\} \setminus J$, and the maximum is taken over all quantum-to-classical channels.

Since $\rho_{AB_j} = J_f(\Lambda_j)$ and $\mathbb{E}_z \rho_A^z \otimes \rho_{B_j}^z = J_f(\mathcal{E}_j)$, by combining Lemma C.1.3 with the previous inequalities we find a bound for the quantity $\mathbb{E}_{j \notin J} \|\Lambda_j - \mathcal{E}_j\|_{\diamond H, E}$. We then easily obtain $\mathbb{E}_j \|\Lambda_j - \mathcal{E}_j\|_{\diamond H, E} \leq \zeta$, where the index j has uniform probability distribution over $\{1, \dots, N\}$, and ζ is given by Eq. (5.1.12).

We conclude the proof by applying Markov's inequality. In fact, the statement of the theorem is equivalent to the following one:

$$\text{P} \left(\|\Lambda_j - \mathcal{E}_j\|_{\diamond H, E} \geq \frac{\zeta}{\delta} \right) \leq \delta. \quad (5.1.16)$$

□

The result of Theorem 5.1.1 can be interpreted as follows. Fixing $0 < \delta < 1$ and E , and letting the number of environmental fragments N tend to infinity, we have that the dynamical maps connecting the system to each of the fragments become indistinguishable from measure-and-prepare channels. This statement is true for at least a fraction $1 - \delta$ of the sub-environments. Moreover, the measure-and-prepare channels involved are all defined by the same POVM $\{M_l\}_l$. For $\delta \ll 1$ this means that almost all observers probing the system by intercepting fragments of the environment can at most acquire classical information about one and the same measurement $\{M_l\}_l$ – i.e., objectivity of observables holds for such observers.

To illustrate the application of the results derived in this section to concrete physical models, we now consider some relevant examples.

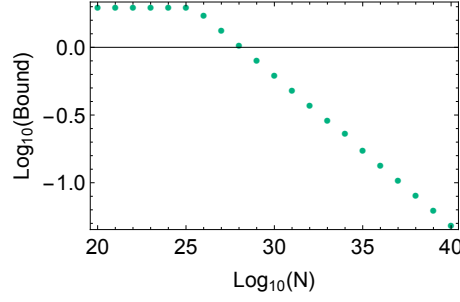


Figure 5.1. Case $f_j = j^2$. We plot the upper bound on $\|\Lambda_j - \mathcal{E}_j\|_{\diamond, H, E}$ for $E = 1$ and $\delta = 0.01$, obtained through numerical optimisation of Eq. (5.1.17) over the truncation dimension d .

Case $f_j = j^2$, with $j \geq 1$ (particle in a box). A quantum particle of mass m confined in a box of length L has Hamiltonian eigenvalues $f_j = \gamma j^2$, where γ is a constant given by $\gamma = \frac{\hbar^2 \pi^2}{2mL^2}$. Choosing units such that $\gamma = 1$ we have that $f_j = j^2$, and Theorem 5.1.1 turns out to hold for

$$\zeta = \alpha \left(\frac{\sigma d^3 E^2}{N} \right)^{1/3} + \beta E \sqrt{\psi^{(d)}(1)}, \quad (5.1.17)$$

where $\psi^{(n)}(z)$ is the n^{th} derivative of the digamma function $\psi(z)$, $\sigma \approx 2.4$ and α, β are universal constants: $\alpha := (12\pi^4)^{\frac{1}{3}}$, $\beta := \sqrt{\frac{8\pi^2}{3}}$. In Figure 5.1 we plot the objectivity bound ζ provided by a numerical optimisation of Eq. (5.1.17) over d , with $E = 1$ and $\delta = 0.01$.

Case of a D -dimensional system. In this example, we show that our methods can bridge finite and infinite dimensions. Specifically, let us consider the sequence of Hamiltonian eigenvalues

$$f_j = \begin{cases} 1 & j \leq D - 1, \\ \frac{e^{\omega j}}{1 - e^{-\omega}} & j \geq D, \end{cases} \quad (5.1.18)$$

where D is a parameter that will turn out to be the actual Hilbert space dimension when $\omega \rightarrow \infty$. We assume $d \geq D$ for convenience. We obtain that

$$\zeta = \left(\frac{432E^2(D + e^{-\omega D})^2 d^3 s}{N} \right)^{\frac{1}{3}} + 4E \sqrt{\frac{D + e^{-\omega D}}{e^{\omega d}}} \quad (5.1.19)$$

where

$$\begin{aligned} s &:= \ln(2)\sigma \\ &= \ln(D + e^{-\omega D}) + \frac{\omega(1 - D + De^{\omega})}{(e^{\omega} - 1)(De^{\omega D} + 1)} - \frac{\ln(1 - e^{-\omega})}{(1 + De^{\omega D})} \end{aligned}$$

(see Example C.1 in C.1 for details). Taking the limit $\omega \rightarrow \infty$ we have that

$$\lim_{\omega \rightarrow \infty} \zeta = \left(\frac{432E^2 D^2 d^3 \ln D}{N} \right)^{1/3}. \quad (5.1.20)$$

In this scenario, $\text{Tr}[\rho H] \leq E$ translates into the condition $\text{Tr}[\rho] \leq 1$, plus the additional constraint that the support of ρ is contained in the D -dimensional subspace spanned by $\{|0\rangle, |1\rangle, \dots, |D-1\rangle\}$. Physically, the considered limit corresponds to raising all the Hamiltonian eigenvalues with $j \geq D$ to unattainably high energies, so that only levels with $j < D$ can be populated.

In the finite-dimensional scenario, the tightest objectivity bound to date has been recently obtained by Qi and Ranard [146]. The Qi–Ranard result can be compared to ours by making the substitution $|R| = 1$, $|Q| = N\delta$ in Eq. (12) of Ref. [146]. For the present comparison, we have to

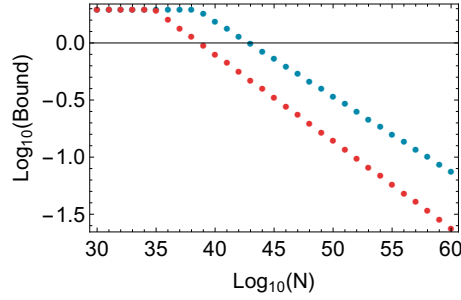


Figure 5.2. Case $f_j = j$. We compare the upper bound on $\|\Lambda_j - \mathcal{E}_j\|_{\diamond_{H,E}}$ for $E = 1$ and $\delta = 0.01$, obtained by numerical optimisation of Eq. (5.1.23) over d (red dots, lowermost curve), with the bound obtained by Knott *et al.* in [62] (blue dots, uppermost curve).

consider two possible expressions for the parameter Ω (which appears in Eq. (13) of Ref. [146]): $\Omega = D^2$ and $\Omega = 4D^{3/2}$, where D is the dimension of system A ; the corresponding expressions for the Qi–Ranard bound are the following:

$$\Omega = D^2 : \quad b_1 = \left(\frac{2D^6 \ln D}{N\delta} \right)^{1/2} \quad (5.1.21)$$

$$\Omega = 4D^{3/2} : \quad b_2 = 4 \left(\frac{2D^5 \ln D}{N\delta} \right)^{1/2} \quad (5.1.22)$$

Expressions b_1 and b_2 can be directly compared with our bound $b := \frac{\zeta}{\delta}$, with ζ given by Eq. (5.1.20), by taking $d = D$ (which clearly gives us the tightest bound for the range $d \geq D$) and by choosing $E = 1$. The comparison is meaningful only in the regime in which the bounds are non-trivial, namely smaller than 2. By applying this requirement to our bound b we obtain a threshold value for N which depends on D : $N > \frac{54D^5 \ln D}{\delta^3}$. We find that our bound b is never stronger than b_2 in its non-triviality regime. Note that b_2 was derived by the authors of [146] on the basis of our suggestion to exploit the Aubrun *et al.* result [147] in this context. Hence b_2 , which is the tightest known objectivity bound in finite dimensions, is a synthesis of independent insights from the analysis of Qi and Ranard and our work. The less tight bound b_1 was instead obtained by Qi and Ranard independently of the present work. There exists a regime in which our bound b is non-trivial and stronger than b_1 ; however, this regime may be of little relevance in experimental contexts, as it requires a very large threshold for N , e.g. rising above Avogadro’s number for $\delta < 0.1$.

We now return to the case $f_j = j$, in which the condition $\sum \frac{1}{f_j} < \infty$ is not satisfied. In this case the f -Choi states cannot be defined, and we replace them with truncated (standard) ones. To derive the objectivity bound we go through the same conceptual steps followed by Knott *et al.* in [62]. However, we bound the distance between truncated Choi–Jamiołkowski states more restrictively, by exploiting a result by Aubrun *et al.* [147, Corollary 9]. We are then able to derive an objectivity bound that, for $d > 16$, is tighter than the one obtained in [62]. In particular, we find that Theorem 5.1.1 holds for $f_j = j$ with

$$\zeta = \lambda \left(\frac{d^5 \log(d)}{N} \right)^{1/3} + 4\sqrt{\frac{E}{d}}, \quad (5.1.23)$$

where $\lambda := 3(16 \ln(2))^{1/3}$. In Figure 5.2 we compare the mean energy bound provided in [62] (blue dots, uppermost curve) with the refined one we obtain from Eq. (5.1.23) (red dots, lowermost curve). Both bounds are numerically optimised over d by setting $E = 1$ and $\delta = 0.01$.

5.2 Testing optimality of the objectivity bound with an N -splitter

The emergence of objectivity of observables, as explored in the previous section as well as in [61, 62], is expressed by an upper bound on the distance between the effective dynamics Λ_j and the measure-and-prepare channels \mathcal{E}_j , which goes to zero as the number N of environment fragments gets large. We now probe the optimality of such statement by looking at a lower bound for the distance between Λ_j and \mathcal{E}_j in a specific example. This gives information on the speed at which the emergence of objectivity of observables takes place. We carry out this analysis for a system-environment interaction modelled by a pure loss channel. In detail, both our system A and each of its sub-environments B_1, \dots, B_N will be single bosonic modes with associated annihilation operators a_0 and a_1, \dots, a_N , respectively. The canonical commutation relations read $[a_j, a_k^\dagger] = \delta_{jk}$. We consider the quantum channel

$$\Lambda_{A \rightarrow B_1, \dots, B_N}(\cdot) := U \left((\cdot)_A \otimes \bigotimes_{j=2}^N |0\rangle\langle 0|_{B_j} \right) U^\dagger, \quad (5.2.1)$$

where U is the symplectic unitary which implements a N -splitter from $\mathcal{D}(A \otimes B_2 \otimes \dots \otimes B_N)$ to $\mathcal{D}(B_1 \otimes \dots \otimes B_N)$. In terms of bosonic operators (in the Heisenberg picture) this transformation takes the explicit form $U^\dagger a_l U = \sum_m V_{lm} a_m$, with $V_{lm} = \frac{1}{\sqrt{N}} \exp \frac{2\pi i l m}{N}$. Since the initial environment state is the vacuum, the map in Eq. (5.2.1) corresponds to a pure loss channel of parameter $\frac{1}{N}$ [158]. Varying the environment state one obtains instead a general attenuator [159–164]. The reduced map $\Lambda_j : \mathcal{D}(A) \rightarrow \mathcal{D}(B_j)$ is given by $\Lambda_j = \text{Tr}_{B \setminus B_j} \circ \Lambda$ and has the same form for all j , as shown in C.2.1. As in the previous section, we assume that system A has bounded mean energy. As is typically the case in optical systems, the relevant Hamiltonian is obtained by setting $f_j = j$ (where j may be interpreted as the number of photons). We show that, for a maximum energy threshold E on system A satisfying $E \geq \frac{2}{N}$, the channels Λ_j approach the measure-and-prepare ones no faster than $\sim N^{-1}$. In particular, we can prove the following proposition.

Proposition 5.2.1. Consider the ctp map $\Lambda : \mathcal{D}(A) \rightarrow \mathcal{D}(B_1 \otimes \dots \otimes B_N)$ given by Eq. (5.2.1), and define $\Lambda_j := \text{Tr}_{B \setminus B_j} \circ \Lambda$ as the effective dynamics from $\mathcal{D}(A)$ to $\mathcal{D}(B_j)$. Let E be the energy bound for system A , which is assumed to satisfy $E \geq \frac{2}{N}$. Then, for all POVMs $\{M_l\}_l$ and states $\{\tau_{j,l}\}_l \in \mathcal{D}(B_j)$, it holds that

$$\min_{j=1, \dots, N} \|\Lambda_j - \mathcal{E}_j\|_{\diamond_{H,E}} \geq \frac{1}{2N}, \quad (5.2.2)$$

where the measure-and-prepare channel \mathcal{E}_j is given by Eq. (5.1.11).

Remark. The assumption $E \geq \frac{2}{N}$ in Proposition 5.2.1 is not strictly necessary yet it significantly simplifies the calculation.

Outline of the proof of Proposition 5.2.1. We look at the quantity

$$\mu(\Lambda) := \inf_{M, \tau_j} \|\Lambda_j - \mathcal{E}_{M, \tau_j}\|_{\diamond_{H,E}}, \quad (5.2.3)$$

where the infimum is over the set of possible POVMs $M = \{M_l\}_l$ and states $\tau_j = \{\tau_{j,l}\}_l$ entering the definition of the measure-and-prepare channel \mathcal{E}_j . We start by restricting the evaluation of the diamond norm to two-mode squeezed vacuum states: $|\psi_r\rangle = \frac{1}{\cosh(r)} \sum_n \tanh(r)^n |nn\rangle$. Since the channels \mathcal{E}_j are entanglement-breaking, the infimum on M and τ_j translates into an infimum on the set of separable states (with respect to the bipartition $C : B_j$, where C is the ancillary system entering the definition of the diamond norm): $(\text{id} \otimes \mathcal{E}_j)[\psi_r] = \omega \in \text{SEP}$, with $\psi_r := |\psi_r\rangle\langle\psi_r|$. We thus obtain that

$$\mu(\Lambda) \geq \inf_{\omega \in \text{SEP}} \sup_{r: \sinh(r)^2 \leq E} \|\text{id} \otimes \Lambda_j[\psi_r] - \omega\|_1. \quad (5.2.4)$$

A lower bound for the 1-norm in Eq. (5.2.4) is estimated through the inequality $\|X\|_1 \geq 2\|X\|_\infty$, which holds true for any operator X with $\text{Tr } X = 0$. The operator norm on the r.h.s. is bounded from below by looking at the matrix entries with respect to a second set of two-mode squeezed vacuum states. Upon straightforward calculations, one obtains Eq. (5.2.2). Details are provided in C.2.2. \square

It is interesting to compare the lower bound in Eq. (5.2.2) with the upper bounds on the convergence rate we have found so far, with the goal of estimating the rate at which emergence of objectivity actually takes place. To estimate an upper bound for the distance $\|\Lambda_j - \mathcal{E}_j\|_{\diamond_{H,E}}$ we optimise Eq. (5.1.23) over d by using the inequality $\ln(d) \leq d$, and exploit the fact that, for the model we are considering, all the reduced maps Λ_j have the same form. We thus obtain the following range:

$$\frac{1}{2N} \leq \|\Lambda_j - \mathcal{E}_j\|_{\diamond_{H,E}} \leq \mu \left(\frac{E^6}{N} \right)^{\frac{1}{15}}, \quad (5.2.5)$$

where $\mu < 10$ is a constant.

5.3 Quantum discord from local distribution of quantum correlations in infinite dimension

Quantum discord [148, 149] is regarded as a measure of the purely quantum part of correlations between systems [165, 166]. Consider two systems A and B , collectively described by a state ρ ; the total amount of correlations between them is quantified by the mutual information $I(A:B) = S(A) + S(B) - S(AB)$, where S denotes the von Neumann entropy: $S(A) = -\text{Tr}[\rho_A \log \rho_A]$. The quantum discord between A and B (from the perspective of subsystem B) is then defined by

$$D(A|B)_\rho := I(A:B)_\rho - \max_{\Gamma \in QC} I(A:B)_{(\text{id} \otimes \Gamma)(\rho)}, \quad (5.3.1)$$

where QC refers to quantum-to-classical channels having the form $\Gamma(X) := \sum_k \text{Tr}[N_k X] |k\rangle\langle k|$, with POVM $\{N_k\}_k$. The quantum discord $D(A|B)_\rho$ thus represents the amount of correlations that is inevitably lost when B is subject to a minimally disturbing local measurement, or, in other words, when B encodes its part of information into a classical system; in this respect, $D(A|B)_\rho$ can be thought of as the purely quantum part of correlations between A and B in the state ρ . In [61] Brandão *et al.* derived an interesting operational interpretation of quantum discord in terms of redistribution of quantum information to many parties. In particular they showed that

$$\lim_{N \rightarrow \infty} \max_{\Lambda_N} \mathbb{E}_j I(A:B_j)_{(\text{id} \otimes \Lambda_N)(\rho)} = \max_{\Gamma \in QC} I(A:B)_{(\text{id} \otimes \Gamma)(\rho)} \quad (5.3.2)$$

where the maximisation is over all maps $\Lambda_N : \mathcal{D}(B) \rightarrow \mathcal{D}(B_1 \otimes \dots \otimes B_N)$, and $\mathbb{E}_j I(A:B_j)$ is the average mutual information between A and B_j for the uniform probability distribution over j . Equation (5.3.2) shows that, when the share of correlations of B is redistributed to infinitely many parties $\{B_j\}$, the maximum *average* mutual information accessible through each one of the parties B_j corresponds to the purely classical part of correlations. This result is at the heart of the operational characterisation of quantum discord provided by Brandão *et al.* [61]. In fact, from Eq. (5.3.2) it follows that

$$D(A|B)_\rho = \lim_{N \rightarrow \infty} \min_{\Lambda_N} \mathbb{E}_j \left(I(A:B)_\rho - I(A:B_j)_{(\text{id} \otimes \Lambda_N)(\rho)} \right), \quad (5.3.3)$$

i.e., $D(A|B)_\rho$ is characterised as the minimal average loss in mutual information when B locally redistributes its share of correlations. Brandão *et al.* derived Eq. (5.3.2) as a corollary of the theorem through which they proved emergence of objectivity of observables in finite dimensions [61, Corollary 4]. In that context, B can be interpreted as the environment of system A , which splits into fragments $\{B_j\}$.

We generalise the above result to an infinite-dimensional scenario, for systems subjected to generic energy constraints. In particular, as infinite-dimensional counterpart of [61, Corollary 4], we prove the following corollary of our Theorem 5.1.1:

Corollary 5.3.1. *Let A be a quantum system equipped with a Hamiltonian H_A , and B a quantum system equipped with Hamiltonian H_B , both satisfying the Gibbs hypothesis. We also assume that H_B , when written as in Eq. (5.1.4), satisfies Eq. (5.1.5). Let $\Lambda_N : \mathcal{D}(B) \rightarrow \mathcal{D}(B_1 \otimes \dots \otimes B_N)$ be a cptp map, and define $\Lambda_j := \text{Tr}_{B \setminus B_j} \circ \Lambda_N$ as the effective dynamics from $\mathcal{D}(B)$ to $\mathcal{D}(B_j)$. Then for every $\delta > 0$ there exists a set $S \subseteq \{1, \dots, N\}$ with $|S| \geq (1 - \delta)N$ such that for all $j \in S$ and all states $\rho \in \mathcal{D}(A \otimes B)$ with $\text{Tr}[\rho H_A] \leq E_A, \text{Tr}[\rho H_B] \leq E_B$,*

$$\begin{aligned} I(A : B_j)_{(\text{id} \otimes \Lambda_j)(\rho)} &\leq \max_{\Gamma \in \text{QC}} I(A : B)_{(\text{id} \otimes \Gamma)(\rho)} \\ &\quad + (2\epsilon' + 4\Delta)S(\gamma(E_A/\Delta)) \\ &\quad + (1 + \epsilon')h\left(\frac{\epsilon'}{1 + \epsilon'}\right) + 2h(\Delta), \end{aligned} \tag{5.3.4}$$

where $\epsilon' = \frac{\zeta}{\delta}$, $\Delta = \frac{1}{2} \frac{\epsilon'}{1 + \epsilon'}$, $\gamma(E)$ is the Gibbs state for system A defined in Eq. (5.1.3), and the maximum on the r.h.s. is over quantum-to-classical channels $\Gamma(X) := \sum_l \text{Tr}(N_l X) |l\rangle\langle l|$, with $\{N_l\}_l$ a POVM and $\{|l\rangle\}_l$ a set of orthonormal states. As a consequence,

$$\lim_{N \rightarrow \infty} \max_{\Lambda_N} \mathbb{E}_j I(A : B_j)_{(\text{id} \otimes \Lambda_N)(\rho)} = \max_{\Gamma \in \text{QC}} I(A : B)_{(\text{id} \otimes \Gamma)(\rho)} \tag{5.3.5}$$

Outline of the proof of Corollary 5.3.1. We follow the conceptual steps of the proof of [61, Corollary 4], adapting them to our infinite-dimensional framework. In particular, our argument relies on a continuity bound for the conditional entropy of infinite-dimensional systems subjected to energy constraints [156, Lemma 17]. We apply it to the states $\tau = (\text{id} \otimes \Lambda_j)(\rho)$ and $\sigma = (\text{id} \otimes \mathcal{E}_j)(\rho)$, which are close in 1-norm by virtue of Theorem 5.1.1. Since the reduced entropies on the A subsystems are the same for τ and σ , the continuity bound for the conditional entropy holds true for the mutual information as well. We then obtain Eq. (5.3.4). To prove Eq. (5.3.5), we exploit Eq. (5.3.4) to show that the l.h.s. is no larger than the r.h.s.; this concludes the proof, as the reverse (r.h.s. no larger than l.h.s.) is trivial. The complete proof is given in C.3. \square

Remark. The result of Corollary 5.3.1 also applies to a Hamiltonian H_B that takes the form (5.1.4) with $f_j = j$, and therefore does not satisfy Eq. (5.1.5). In fact, the proof remains valid when the objectivity bound of Theorem 5.1.1 is replaced with the one given by (5.1.23).

As mentioned before, Eq. (5.3.5) implies that quantum discord can be interpreted as the minimal average loss in mutual information when one of the two parties asymptotically redistributes its share of correlations. In the framework of Quantum Darwinism this means that, when the number of environment fragments grows significantly, the correlations established between the (infinite-dimensional) system of interest A and each of the observers (who in turn has access only to a fragment B_j of the environment) can be at most classical.

In recent years, an intriguing connection between gravity, holography and entanglement has come to light. On one hand, various results point to entanglement as the “glue” of spacetime, and several background-independent approaches to QG indeed regard the latter as a many-body system, where entanglement is responsible for the connectivity of the different parts [167]. On the other, the entanglement structure of many-body systems, efficiently modelled by TN, is at the origin of their holographic behaviour [46]. The circle closes with the recognition that gravity manifests, in several contexts, a holographic nature. Understanding the origin of the gravity/holography/entanglement threefold connection would be a crucial step towards the formulation of a theory of QG [168]. This challenge requires bridging the fields of QIT and condensed matter physics with QG, for a fruitful exchange of tools and insights among them. The research presented in this thesis takes its cue from this: *it imports languages and techniques from the above fields into QG models, explores through them the entanglement origin of emergent features of quantum spacetime and aims to extract continuum classical physics from the quantum microstructure of our world.*

More specifically, we established a solid correspondence between the QG formalism of spin networks for the modelling of discrete quantum geometries and the information-theoretic language of TN, building up a dictionary to enhance the exchange of insights and techniques between the respective research areas. We then leverage that correspondence to study the emergence of holographic features of finite regions of spacetime from the entanglement structure of the underlying spin network states, mapped by our dictionary to random TN. Setting aside the quantum aspects of gravity, we also investigated the emergence of classical phenomena, specifically objectivity of observables, from the quantum world. Let us summarise in the following these three branches of our work, and provide outlook for their further development.

A dictionary between spin networks and tensor networks

The work on the information-theoretic characterization of spin networks started from the precise construction, within the GFT formalism, of QG states associated to spin network graphs, with the concrete characterization of such graphs as patterns of entanglement, whose combinatorial structure is encoded into (suitable generalised) adjacency matrices. This was a key open issue not only in GFT, but also in the QG approaches related to its formalism, including random tensor models, lattice quantum gravity, spin foam models and canonical LQG. We clarified it and turn it into the starting point of much further development.

In fact, the next step was establishing a solid correspondence between such QG states and random TN, generalized to arbitrary and dynamical dimension for each tensor leg, and to a second quantized setting, with a probability amplitude possibly dictated by an underlying QG model. Such a contribution represents an immediate conceptual and technical improvement over the standard tensor network modelling of QG states, exemplified by the work of B. Swingle [51] in which TN are identified with spatial slices of AdS spacetime *upon definition of a metric from the network combinatorics*. By contrast, within the correspondence we established, TN acquire an intrinsic geometric characterisation, as they possess additional degrees of freedom with a clear and rigorous

interpretation in terms of quantum simplicial geometry. In turn, this leads to a richer and more precise entanglement/geometry (and topology) correspondence, instantiated in several geometric quantities; indeed, in our context several conjectures put forward also in the AdS/CFT context about the correspondence between entanglement measures and geometric quantities find a precise realization. Moreover, providing TN with a Fock space setting enabled the attainment of (a discrete version of) diffeomorphism invariance for the structures involved, a necessary condition for background independence required by QG theories. This represents a further improvement on tensor network models like [51]: in fact, without a suitable invariance under relabelling of the nodes of the random TN, the interpretation of the latter as geometries appears incomplete. Since a possible way out is to give the labels associated to tensor network nodes some physical characterization, we also tackled such issue and illustrated a concrete realization for it: we showed how distinguishability of vertices can be recovered at a relational and effective level by coupling the GFT field to an additional degree of freedom playing the role of a physical reference frame, in the spirit of the relational strategy typically employed in the QG context to define physical (thus, diffeomorphism invariant) observables in absence of preferred notions of space, time and locality.

Bulk-to-boundary quantum channels and holographic entanglement entropy

As pointed out, when regarding spin networks as states of the GFT Fock space, the spin network graph is recognised to be the entanglement skeleton of the many-body system given by the collection of individual vertices. We exploited this feature to study the relationship between the quantum-correlation structure of open spin networks and their holographic character. Based on a bipartition of the quantum-geometric degrees of freedom into bulk (intertwiners) and boundary ones (spins on open edges), we showed that every spin network state can be regarded as a map between these two sets, in the spirit of the Choi-Jamiołkowski isomorphisms of QIT. In this way, the “static” properties of a spin network state are translated into “dynamic” properties of the corresponding map, representing the flow of information from the bulk to the boundary, and *vice versa*. In particular, requiring such a map to be an isometry - as it must be in presence of holography - translates into the reduced bulk state being maximally mixed, i.e. having maximum entropy. By assuming a random distribution of weights associated to the individual vertices, we performed the entropy calculation via (suitably generalised) random tensor network techniques; more specifically, we adapted to our framework the ones used by Hayden *et al.* in [53], combining the technical generalisations to the crucial (with respect to the QG interpretation) change in perspective pointed out before. The average entropy then turned out to be given by the free energy cost of shifting the domain wall of an Ising model defined on the spin network itself; the analysis of such statistical model enabled us to identify the role played by the edge spins of a spin network in the isometric character of the corresponding bulk-to-boundary information flow, highlighting the positive correlation between the latter and spin inhomogeneity.

We investigated further the properties of the bulk-to-boundary flow of information in spin network states in terms of entanglement entropy of boundary degrees of freedom. By focusing on spin networks made of random vertices and studying the free energy function of the Ising model dual to it, we determined the conditions for the validity of the Ryu–Takayanagi formula, and provided corrections to the latter induced by the bulk entanglement (in the double form of internal-links entanglement, defining the bulk combinatorial structure, and entanglement among the intertwiner degrees of freedom). We then showed how increasing the entanglement-entropy content of a bulk region can alter the area-scaling of the boundary entropy, up to the emergence of a horizon-like surface in the bulk (the boundary of the said region), so offering a concrete example of the definition of quantum black holes given in Ref. [43].

Emergence of objectivity of observables in a non-gravitational setting

In the last chapter we focused on phenomena emerging from the quantum realm in a different, non-gravitational setting: we investigated generic features of the emergence of objectivity of observables via the theory of quantum Darwinism, according to which information about a quantum system becomes objective as multiple observers indirectly probe it by measuring fragments of

the environment. Previous work [61, 62] had showed that, when the number of environmental fragments grows, the quantum channels modelling the information flow from system to observers become arbitrarily close - in terms of diamond norm distance - to “measure-and-prepare” channels, ensuring objectivity of observables; the convergence was formalised by an upper bound on the diamond norm distance, which decreases with increasing number of fragments. In chapter 5 we derived tighter diamond norm bounds on the emergence of objectivity of observables for quantum systems of infinite dimension, providing an approach which can bridge between the finite- and the infinite-dimensional cases. Furthermore, we probe the tightness of our bounds by considering a specific model of a system-environment dynamics given by a pure loss channel: for the latter we derived lower and upper bounds on the rate at which objectivity of observables emerges as a function of the number of environmental fragments. Finally, we generalised to infinite dimensions a result obtained by Brandão *et al.* [61], which provides an operational characterisation of quantum discord in terms of one-sided redistribution of correlations to many parties.

Outlook

We plan to develop further the information-theoretic approach to QG illustrated in this thesis, and tackle with it open issues on black hole physics and on the holographic nature of gravity. In the following, we provide a list of possible short-term extensions of this work, as well as long-term goals inspired by it.

In [2, 3] holography has been investigated for spin network states on a fixed (generic) graph. To promote the presented results to the dynamic level, a generalization to states involving a superposition of different graphs is required. We plan to implement it by enriching the spin network structure with data encoding the amount of link-entanglement between vertices, and using such data to manipulate the combinatorial structure of the graph, analogously to what has been done for random TN in Ref. [169].

With the aim of achieving an information-theoretic characterisation of black hole horizons, we plan to derive a “threshold condition” for the emergence of horizon-like surfaces in finite regions of quantum space by generalising, via the tensor network approach, the result of Ref. [170], where that condition is obtained via the typicality approach to the study of the local behaviour of spin networks with fixed homogeneous spins.

We are also interested in identifying microscopic states of black holes in the tensor/spin network language. A starting point can be found in the set of condensed states used in Refs. [171, 172] to model spherically symmetric geometries. In fact, being composed of individual vertex wavefunctions, that states resemble the TN considered in the aforementioned works [2, 3]. A generalization of them and a study of their holographic properties, which are necessary for a solid description of quantum black holes, can then be performed by taking advantage of quantum information techniques.

On a broader scale, an objective of our future research is the study and modelling of gravitational holography in a full dynamical context; taking as reference works such as [173] and [174] that, starting from fundamental aspects of gravity derive general guidelines on the holographic encoding of information in gravitational physics, we are keen to pursue this objective by implementing the approach of the aforementioned works in the context of spin network dynamics. We also aim at a local formulation of holography in QG, potentially making use of recent results on corner symmetry charges [175] and edge modes [176].

Finally, we would like to stress that QIT can contribute to the QG research far beyond the possibilities listed so far. In fact, quantum mechanics is an essential ally in overcoming the lack of guidelines in QG free from the bias of our classical view of the world. A purpose of the work collected in this thesis is to highlight the existing (but not yet exploited) parallelism between open issues and related possible strategies in the quantum-to-classical transition problem and the spacetime-emergence scenario. In this respect, a direction we intend to explore concerns the study of the emergence of classical spacetime from pre-geometric quantum entities via the theory of decoherence and quantum Darwinism.

A

Notions of representation and recoupling theory

A.1 Algebra of representation functions

Let G be a finite group or a compact Lie group. A *representation* ρ of G on a finite-dimensional complex vector space V^ρ is a group homomorphism

$$\rho : G \rightarrow \text{Aut}[V^\rho] \quad (\text{A.1.1})$$

where $\text{Aut}[V^\rho]$ is the automorphism group of V^ρ . An *invariant subspace* for the representation ρ is a vector subspace U such that, for all $u \in U$, $\rho(g)u \in U$ for all $g \in G$. A representation is *irreducible* if its only closed invariant subspaces are \emptyset and V^ρ . A representation is *unitary* if, for every $g \in G$, $\rho(g)$ is unitary. Two representations ρ and ρ' are *equivalent* if there exist an isomorphism $E : V^\rho \rightarrow V^{\rho'}$ such that $E\rho(g) = \rho'(g)E$ for all $g \in G$. We denote by $\rho = 0$ the *trivial representation* which maps every element of G to 1 (hence $V^0 \cong \mathbb{C}$).

Every finite-dimensional representation is equivalent to a unitary representation; we can hence restrict the attention to a set $\tilde{\mathcal{R}}$ of unitary representations, one for each equivalence class of finite-dimensional representations of G . A corollary of this result is that every finite-dimensional representation ρ of G can be decomposed into a direct sum of irreducible representations ρ_1, \dots, ρ_k :

$$V^\rho = V^{\rho_1} \oplus \dots \oplus V^{\rho_k} \quad (\text{A.1.2})$$

We denote by $\mathcal{R} \subset \tilde{\mathcal{R}}$ the subset of irreducible representations. The latter thus play the role of elementary “building blocks” of generic representations.

Let $V^{\rho*}$ be the vector space dual to V^ρ . Given $\rho \in \tilde{\mathcal{R}}$, the dual representation

$$\rho^* : G \rightarrow \text{Aut}[V^{\rho*}] \quad (\text{A.1.3})$$

is such that, for $\eta \in V^{\rho*}$,

$$(\rho^*(g)\eta)(v) = \eta(\rho(g^{-1})v) \quad \forall v \in V^\rho \quad (\text{A.1.4})$$

The representation spaces V^ρ , where $\rho \in \tilde{\mathcal{R}}$, are equipped with a standard scalar product $\langle \cdot | \cdot \rangle$, and the duality between two orthonormal basis $\{b_i\}$ of V^ρ and $\{\beta^i\}$ of $V^{\rho*}$ is defined by the following equations:

$$\langle b_i | b_j \rangle = \beta^i(b_j) = \delta_{ij}, \quad \langle \beta^i | \beta^j \rangle = \beta^j(b_i) = \delta_{ji} \quad (\text{A.1.5})$$

For $\rho \in \tilde{\mathcal{R}}$, $v \in V^*$ and $\eta \in V^{\rho*}$, the functions

$$t_{\eta,v}^\rho : G \rightarrow \mathbb{C} \\ g \rightarrow t_{\eta,v}^\rho(g) := \langle \eta | \rho(g)v \rangle \quad (\text{A.1.6})$$

are called *representation functions* of G and form a commutative and associative unital algebra over \mathbb{C} , denoted by $C_{\text{alg}}(G)$, with the operations

$$\left(t_{\eta,v}^\rho + t_{\eta',v'}^{\rho'} \right) (g) := t_{\eta+\eta',v+v'}^{\rho \oplus \rho'}(g), \quad (\text{A.1.7})$$

$$\left(t_{\eta,v}^\rho \cdot t_{\eta',v'}^{\rho'} \right) (g) := t_{\eta \otimes \eta', v \otimes v'}^{\rho \otimes \rho'}(g), \quad (\text{A.1.8})$$

null element given by $t_{0,0}^{(0)}$ (such that $t_{0,0}^{(0)}(g) = 0 \forall g \in G$) and unit element given by $t_{\eta,v}^{(0)}$ (such that $t_{\eta,v}^{(0)}(g) = 1 \forall g \in G$). The representation functions obtained from vectors of the orthonormal basis are simply the coefficients of the representation matrices $\rho(g)$ in that basis:

$$t_{mn}^\rho(g) := t_{\beta^m, b_n}^\rho(g) = \langle \beta^m | \rho(g) b_n \rangle \quad (\text{A.1.9})$$

A.2 The Peter-Weyl decomposition

The Peter-Weyl theorem sets out a Fourier analysis for compact groups. In fact, according to the Peter-Weyl theorem the matrix coefficients $t_{mn}^\rho(g)$ of all irreducible unitary representations $\rho \in \mathcal{R}$ of G form an orthogonal basis of $L^2(G)$, with

$$\langle t_{mn}^\rho | t_{m'n'}^{\rho'} \rangle = \int_G dg \overline{t_{mn}^\rho(g)} t_{m'n'}^{\rho'}(g) = \frac{1}{\dim V^\rho} \delta_{\rho\rho'} \delta_{mm'} \delta_{nn'} \quad (\text{A.2.1})$$

where dg is the Haar measure on G . Any function $f \in L^2(G)$ can therefore be written as

$$f(g) = \sum_{\rho \in \mathcal{R}} \sum_{mn} f_{mn}^\rho t_{mn}^\rho(g) \quad (\text{A.2.2})$$

where

$$f_{mn}^\rho = \dim V^\rho \int_G dg f(g) \overline{t_{mn}^\rho(g)} \quad (\text{A.2.3})$$

Equivalently,

$$L^2(G) \cong \bigoplus_{\rho \in \mathcal{R}} (V^{\rho*} \otimes V^\rho) \quad (\text{A.2.4})$$

where the closure of the right hand side to $L^2(G)$ is left implicit.

Class functions A function $w \in L^2(G)$ such that $w(hgh^{-1}) = w(g)$ for all $h \in G$ is called *class function* and has the Peter-Weyl decomposition

$$w(g) = \sum_{\rho \in \mathcal{R}} w^\rho \chi^\rho(g) \quad (\text{A.2.5})$$

where $\chi^\rho(g) = \text{Tr}(t^\rho(g))$ and

$$w^\rho = \dim V^\rho \int_G dg \overline{\chi^{(\rho)}(g)} w(g) \quad (\text{A.2.6})$$

A.3 Intertwiner map and Schur's lemma

Given a representation $\sigma \in \tilde{\mathcal{R}}$ with the orthogonal decomposition

$$V^\sigma \cong \bigoplus_{i=1}^q V^{\tau_k} \quad \tau_k \in \mathcal{R}, q \in \mathbb{N} \quad (\text{A.3.1})$$

where the first p components τ_1, \dots, τ_p , with $0 \leq p \leq q$, are equivalent to the trivial representation, it holds that

$$\int_G dg t_{mn}^\sigma(g) = \sum_{k=1}^p \overline{P_m^{\sigma;k}} P_n^{\sigma;k} \quad (\text{A.3.2})$$

where $P^{\sigma;k}$ is the projector $P^{\sigma;k} : V^\sigma \rightarrow V^{\tau_k}$ and $P_m^{\sigma;k} := P^{\sigma;k} | b_m \rangle$; the right hand side is thus the orthogonal decomposition of the identity in the subspace of V^σ of invariant vectors. The above formula can be generalised to the tensor product of representations. In fact,

$$V^{\rho_1} \otimes \dots \otimes V^{\rho_N} \cong \bigoplus_{i=1}^q V^{\tau_k} \quad \tau_k \in \mathcal{R}, q \in \mathbb{N} \quad (\text{A.3.3})$$

and, if τ_1, \dots, τ_p (with $0 \leq p \leq q$) are equivalent to the trivial representation, then

$$\int_G dg t_{m_1 n_1}^{\rho_1}(g) \dots t_{m_N n_N}^{\rho_N}(g) = \sum_{k=1}^p \overline{P_{m_1 \dots m_N}^{\rho_1 \dots \rho_N; k}} P_{n_1 \dots n_N}^{\rho_1 \dots \rho_N; k} \quad (\text{A.3.4})$$

where $P^{\rho_1 \dots \rho_N; k}$ is the projector from $V^{\rho_1} \otimes \dots \otimes V^{\rho_N}$ onto $\text{Inv}_G [V^{\rho_1} \otimes \dots \otimes V^{\rho_N}]$, i.e. the subspace of G -invariant tensors, also called *intertwiner space* (see below). The right hand side of Eq. (A.3.4) is thus the identity on such interwtiner space:

$$\int_G dg t_{m_1 n_1}^{\rho_1}(g) \dots t_{m_N n_N}^{\rho_N}(g) = \mathbb{I} \in \text{Inv}_G [V^{\rho_1} \otimes \dots \otimes V^{\rho_N}] \quad (\text{A.3.5})$$

Note that the properties of Eq. (A.3.3) and Eq. (A.3.4) underly the definition of spin networks.

Intertwiner map Given two representations ρ and σ , a linear map $I : V^\rho \rightarrow V^\sigma$ such that

$$I\rho(g) = \sigma(g)I \quad (\text{A.3.6})$$

is called *intertwiner*. We also says that I *intertwines* the two representations. Note that, if the map I is bijective, then Eq. (A.3.6) provides the definition of equivalence of the representations ρ and σ . Note also that, since $V^{\rho^*} \cong V^\rho$, the intertwiner can be regarded as a map $I : V^\rho \otimes V^\sigma \rightarrow V^0 \cong \mathbb{C}$, i.e. as an *invariant tensor* on $V^\rho \otimes V^\sigma$; the projector $P^{\rho_1 \dots \rho_N; k}$ defined in Eq. (A.3.4) is indeed an intertwiner.

Schur's lemma The Schur's lemma states the following:

- (i) Given two irreducible representations ρ and σ , let I be an intertwiner between them. Then I either vanishes or is an isomorphism (in which case the representations are equivalent).
- (ii) Given an irreducible representation ρ , let $M : V^\rho \rightarrow V^\rho$ be a linear map which satisfies

$$M\rho(g) = \rho(g)M \quad \forall g \in G \quad (\text{A.3.7})$$

Then there exist $\lambda \in \mathbb{C}$ such that $M = \lambda\mathbb{I}$, where \mathbb{I} is the identity operator on V^ρ .

A.4 Representation and recoupling theory of $SU(2)$

$SU(2)$ is a 3-dimensional compact Lie group corresponding to the group of 2×2 unitary matrices with determinant equal to +1. A generic element $h \in SU(2)$ can thus be written as follows:

$$h = \begin{pmatrix} a & -\bar{b} \\ b & \bar{a} \end{pmatrix} \quad |a|^2 + |b|^2 = 1 \quad a, b \in \mathbb{C} \quad (\text{A.4.1})$$

The Lie algebra of $SU(2)$, $\mathfrak{su}(2)$, has generators $\tau_i := i\frac{\sigma_i}{2}$ (where σ_i are the Pauli matrices) which satisfy

$$[\tau_i, \tau_j] = -\varepsilon_{ijk}\tau_k \quad (\text{A.4.2})$$

The representations of $SU(2)$ are labelled by a half-integer $j \in \frac{\mathbb{N}}{2}$ called *spin*. The representation space V^j is a Hilbert space of dimension $d_j := 2j+1$. Consider the angular momentum observables $\hat{J}_i := \frac{\sigma_i}{2}$ with brackets

$$[\hat{J}_i, \hat{J}_j] = i\varepsilon_{ijk}\hat{J}_k \quad (\text{A.4.3})$$

The standard basis of V^j is composed of the eigenstates of both the $\mathfrak{su}(2)$ Casimir $\hat{J}^2 := \hat{J}_i\hat{J}^i$ and the generator \hat{J}_3 , labelled by the spin j and the magnetic momentum m :

$$\hat{J}^2|jm\rangle = j(j+1)|jm\rangle \quad (\text{A.4.4})$$

$$\hat{J}_3|jm\rangle = m|jm\rangle \quad (\text{A.4.5})$$

with $m = -j, \dots, j$. The j -representation matrix of $g \in SU(2)$ is denoted by $D^j(g)$, and has coefficients

$$D_{mn}^j(g) := \langle jm|g|jn \rangle \quad (\text{A.4.6})$$

(compare to Eq. (A.1.9)). The representation matrices $D^j(g)$ are called *Wigner matrices*. By virtue of Eq. (A.3.4) we have that

$$\int_G dg D_{m_1 n_1}^{j_1}(g) D_{m_2 n_2}^{j_2}(g) D_{m_3 n_3}^{j_3}(g) D_{m_4 n_4}^{j_4}(g) = \sum_{\iota} I_{m_1 m_2 m_3 m_4}^{j_1 j_2 j_3 j_4; \iota} I_{n_1 n_2 n_3 n_4}^{j_1 j_2 j_3 j_4; \iota} \quad (\text{A.4.7})$$

where $I^{j_1 j_2 j_3 j_4; \iota}$ is a $SU(2)$ intertwiner recoupling the four representations j_1, \dots, j_4 , i.e. an element of the space $\text{Inv}_{SU(2)} [V^{j_1} \otimes \dots \otimes V^{j_4}]$.

B

Average entropy from the Ising model

B.1 Randomization over the double copy of the vertex states

A detailed proof of the result given by Eq. (4.2.15) can be found in [177]; we sketch here the same argument, adapted to our framework. The first step is to recognize that the space $\mathcal{H}_D \otimes_{\text{sym}} \mathcal{H}_D$, where \mathcal{H}_D is a D -dimensional Hilbert space and \otimes_{sym} is the symmetric tensor product, carries an irreducible representation of the group of $D \times D$ unitary matrices, under the map associating to any such matrix U the double copy $U^{\otimes 2}$. Then, given $|f\rangle \in \mathcal{H}_D$, consider the density matrix

$$\rho := \mathbb{E}_f (|f\rangle\langle f| \otimes |f\rangle\langle f|), \quad (\text{B.1.1})$$

where $\mathbb{E}_f(\cdot)$ is the average over f according to an arbitrary probability distribution. Since ρ commutes with all $U^{\otimes 2}$, by Schur's lemma (see e.g. [178] for a formulation of the latter which fits the present argument) it must be proportional to the identity operator on $\mathcal{H}_D \otimes_{\text{sym}} \mathcal{H}_D$, which is given by

$$\sum_{\pi \in S_2} P(\pi) = \mathbb{I} + S, \quad (\text{B.1.2})$$

where S_2 is the symmetric group on 2 objects and $P(\pi)$ is the operator permuting vectors in $\mathcal{H}_D^{\otimes 2}$ according to the permutation $\pi \in S_2$, which is \mathbb{I} for the trivial one (identity), and S for the swapping.

B.2 Contributions to the average entropy

B.2.1 Internal-link contribution

The trace

$$\text{Tr}_L \left[\left(\bigotimes_{\ell} \rho_{\ell}^{\otimes 2} \right) \bigotimes_{e_v^i \in L: \sigma_v = -1} S_v^i \right] \quad (\text{B.2.1})$$

factorizes over single-link contributions. There are two different possibilities for the term related to a generic link ℓ_{vw}^i , since it can contain

(i) no swap operators ($\sigma_v \sigma_w = +1$):

$$\begin{aligned} \text{Tr} [|\ell\rangle\langle\ell| \otimes |\ell\rangle\langle\ell|] &= \text{Tr} \left[\frac{1}{d_j^2} \sum_{mm'nn'pp'qq'} I_{mm'} I_{nn'} I_{pp'} I_{qq'} |m\rangle_v |m'\rangle_w \langle n|_v \langle n'|_w \otimes |p\rangle_v |p'\rangle_w \langle q|_v \langle q'|_w \right] \\ &= \frac{1}{d_j^2} \left(\sum_m \delta_{mm} \right)^2 = 1; \end{aligned} \quad (\text{B.2.2})$$

the contribution to the average entropy is then zero.

(ii) just one swap operator ($\sigma_v \sigma_w = -1$):

$$\begin{aligned} \text{Tr} [|\ell\rangle\langle\ell| \otimes |\ell\rangle\langle\ell| S_v^i] &= \text{Tr} \left[\frac{1}{d_j^2} \sum_{mm'nn'pp'qq'} I_{mm'} I_{nn'} I_{pp'} I_{qq'} |m\rangle_v \langle m'|_w \langle n|_v \langle n'|_w \otimes |p\rangle_v \langle p'|_w \langle q|_v \langle q'|_w S_v^i \right] \\ &= \text{Tr} \left[\frac{1}{d_j^2} \sum_{mm'nn'pp'qq'} I_{mm'} I_{nn'} I_{pp'} I_{qq'} |p\rangle_v \langle p'|_w \langle n|_v \langle n'|_w \otimes |m\rangle_v \langle m'|_w \right] \\ &= \frac{1}{d_j^2} \sum_m \delta_{mm} = \frac{1}{d_j}; \end{aligned} \tag{B.2.3}$$

the contribution to the average entropy is therefore $\log d_j$.

B.2.2 Boundary-edge contribution

The trace

$$\text{Tr}_{\partial} \left[\bigotimes_{e_v^i \in \partial\gamma: \sigma_v \mu_v^i = -1} S_v^i \right] \tag{B.2.4}$$

factorizes over contributions coming from single boundary-edges. The trace term for an edge e_v^i can contain

(i) no swap operators ($\sigma_v \mu_v = 1$):

$$\text{Tr} \left[(S_v^i)^2 \right] = \text{Tr} [\mathbb{I} \otimes \mathbb{I}] = d_j^2 \tag{B.2.5}$$

(ii) only one swap operator ($\sigma_v \mu_v^i = -1$):

$$\text{Tr} [S_v^i] = \text{Tr} \left[\sum_{mn} |m\rangle_v \langle m|_v \otimes |n\rangle_v \langle n|_v S_v^i \right] = \text{Tr} \left[\sum_{mn} |n\rangle_v \langle m|_v \otimes |m\rangle_v \langle n|_v \right] = \sum_m \delta_{mm} = d_j \tag{B.2.6}$$

The contribution of the boundary edge e_v^i to the average entropy can thus be expressed as follows:

$$-\log \text{Tr}_{\partial} \left[\bigotimes_{e_v^i \in \partial\gamma: \sigma_v \mu_v^i = -1} S_v^i \right] = - \sum_{e_v^i \in \partial\gamma} \frac{1}{2} (3 + \sigma_v \mu_v) \log d_{j_v^i}. \tag{B.2.7}$$

B.2.3 Bulk contribution

The trace

$$\text{Tr}_{\dot{\gamma}} \left[\bigotimes_{\sigma_v \nu_v = -1} S_v^0 \right] \tag{B.2.8}$$

factorizes over the intertwiners associated to the various vertices; the computation of the contribution for each vertex v is analogous to the one presented in the previous section for boundary edges, the only difference being the dimension of the Hilbert space under consideration, i.e. $D_{\dot{\gamma}_v}$ instead of $d_{j_v^i}$. The bulk contribution to the entropy thus takes the following form:

$$-\log \text{Tr}_{\dot{\gamma}} \left[\bigotimes_{\sigma_v \nu_v = -1} S_v^0 \right] = - \sum_v \frac{1}{2} (3 + \sigma_v \nu_v) \log D_{\dot{\gamma}_v}. \tag{B.2.9}$$

B.2.4 Ising action

We finally obtain

$$\begin{aligned} \mathcal{A}_1(\vec{\sigma}) &= \sum_v \log(D_v^2 + D_v) \\ &\quad - \frac{1}{2} \left[\sum_{e_{vw}^i \in L} (\sigma_v \sigma_w - 1) \log d_{j_{vw}^i} + \sum_{e_v^i \in \partial\gamma} (3 + \sigma_v \mu_v) \log d_{j_v^i} + \sum_v (3 + \sigma_v \nu_v) \log D_{\vec{j}_v} \right] \end{aligned} \quad (\text{B.2.10})$$

The first term on the r.h.s. of Eq. (B.2.10) can be decomposed into edge and intertwiner dimensions as follows:

$$\sum_v \log(D_v^2 + D_v) = 2 \sum_v \log D_v + \sum_v \log(1 + D_v^{-1}) = 2 \sum_{e_v^i \in \gamma} \log d_{j_v^i} + 2 \sum_v \log D_{\vec{j}_v} + \sum_v \log(1 + D_v^{-1}) \quad (\text{B.2.11})$$

and Eq. (B.2.10) then becomes

$$\mathcal{A}_1(\vec{\sigma}) = -\frac{1}{2} \left[\sum_{e_{vw}^i \in L} (\sigma_v \sigma_w - 1) \log d_{j_{vw}^i} + \sum_{e_v^i \in \partial\gamma} (\sigma_v \mu_v - 1) \log d_{j_v^i} + \sum_v (\sigma_v \nu_v - 1) \log D_{\vec{j}_v} \right] + k \quad (\text{B.2.12})$$

where k is a constant contribution given by

$$k = 2 \sum_{e_v^i \in \gamma / \partial\gamma} \log d_{j_v^i} + \sum_v \log(1 + D_v^{-1}). \quad (\text{B.2.13})$$

The action $\mathcal{A}_0(\vec{\sigma})$ takes the same form but, as mentioned before, with all pinning fields equal to +1.

C

Supplemental material for the emergence of objectivity of observables

C.1 f -dependent objectivity bounds

The proof of Theorem 5.1.1 involves a generalisation of the concept of Choi–Jamiołkowski isomorphism, which relies on a class of infinite-dimensional entangled states depending on the underlying system’s Hamiltonian. For clarity, we recall here the definition of modified Choi–Jamiołkowski state associated to such class of states.

Definition C.1.1 (Restatement). The *modified Choi–Jamiołkowski state* of a ctp map $\Lambda : \mathcal{D}(A') \rightarrow \mathcal{D}(B)$, for a given sequence of Hamiltonian eigenvalues $f = \{f_j\}_j$, is defined as

$$J_f(\Lambda) := \text{id}_A \otimes \Lambda_{A'}[|\phi\rangle\langle\phi|], \quad (\text{C.1.1})$$

where the entangled state $|\phi\rangle$ reads

$$|\phi\rangle := c_f \sum_{j=0}^{\infty} \phi_j |j, j\rangle_{AA'}, \quad (\text{5.1.6})$$

with $\phi_j^2 := 1/f_j$ and $c_f := \left(\sum \frac{1}{f_j}\right)^{-\frac{1}{2}}$.

We start by proving Lemma C.1.1, which bounds the distance between two f -Choi states as a function of d (the truncation dimension), and Lemma C.1.2, which relates the distance between two channels to that between their f -Choi states. Our preparations are completed by the rather technical Lemma C.1.3: there we show that a crucial inequality exploited in Ref. [61], whose original formulation explicitly relies on finite-dimensional techniques, may be suitably modified to fit our infinite-dimensional scenario. To achieve the latter result, we exploit the assumption that the f -Choi states have finite local entropy. Once all the above ingredients are in place, we present the proof of Theorem 5.1.1. We conclude the section by presenting additional details on the calculations behind Eq. (5.1.19), obtained for the sequence $\{f_j\}$ which bridges the finite- and infinite-dimensional cases.

Lemma C.1.1 is a generalised and refined version of Lemma S5 in the supplemental material of [62]. The first property comes from our definition of modified Choi–Jamiołkowski states, which relies on generic Hamiltonian eigenvalues $\{f_j\}$ (whilst in [62] the latter take an exponential form). The second one arises from applying a result by Aubrun *et al.* [147, Corollary 9].

Lemma C.1.1. *Given $L = \tau - \sigma$, where $\tau = J_f(\Lambda_1)$ and $\sigma = J_f(\Lambda_2)$ are modified Choi–Jamiołkowski states for the ctp maps Λ_1 and Λ_2 , we have that*

$$\|L\|_1 \leq 4d^{\frac{3}{2}} \max_{\mathcal{C}} \|\text{id} \otimes \mathcal{C}[L]\|_1 + 4\epsilon_d, \quad (\text{C.1.2})$$

where ϵ_d is given in Definition 5.1.2, d is the corresponding truncation dimension, and the maximum on the r.h.s. is over quantum-to-classical channels $\mathcal{C}(Y) = \sum_l \text{Tr}(N_l Y) |l\rangle\langle l|$, with POVM $\{N_l\}_l$ and orthonormal states $\{|l\rangle\}_l$.

Proof. By writing L in the form $L = \sum_{ij=0}^{\infty} |i\rangle\langle j| \otimes L_{ij}$ we have that

$$\begin{aligned}
\|L\|_1 &\stackrel{1}{\leq} \|(\Pi_d \otimes \text{id})[L]\|_1 + \|((\text{id} - \Pi_d) \otimes \text{id})[L]\|_1 \\
&= \|(\Pi_d \otimes \text{id})[L]\|_1 + \left\| \sum_{\min\{i,j\} \geq d} |i\rangle\langle j| \otimes L_{ij} \right\|_1 \\
&\stackrel{2}{\leq} 4d^{\frac{3}{2}} \max_{\mathcal{C}} \|(\Pi_d \otimes \mathcal{C})[L]\|_1 + \left\| \sum_{\min\{i,j\} \geq d} |i\rangle\langle j| \otimes L_{ij} \right\|_1 \\
&\stackrel{3}{\leq} 4d^{\frac{3}{2}} \max_{\mathcal{C}} \|(\text{id} \otimes \mathcal{C})[L]\|_1 + \left\| \sum_{\min\{i,j\} \geq d} |i\rangle\langle j| \otimes L_{ij} \right\|_1.
\end{aligned} \tag{C.1.3}$$

Note that in 1 we used the triangle inequality. In 2, instead, we applied a result by Aubrun *et al.* [147, Corollary 9]: in fact, for an arbitrary bipartite operator Z , it holds that

$$\max_{\mathcal{C}} \|(I \otimes \mathcal{C})[Z]\|_1 = \|Z\|_{\text{LOCC}_+} \geq \|Z\|_{\text{LO}},$$

where the maximization on the l.h.s. is as usual over local measurements, while the quantities (a) $\|\cdot\|_{\text{LOCC}_+}$ and (b) $\|\cdot\|_{\text{LO}}$ are the distinguishability norms [179, 180] associated with the sets of (a) local operations assisted by classical communication from the second system to the first; and (b) local operations alone. By [147, Eq. (40)], it holds that $\|Z\|_{\text{LO}} \geq \frac{1}{4n^{3/2}} \|Z\|_1$, where n denotes the smaller of the local dimensions. The inequality in 2 is just an application of this, with $Z := (\Pi_d \otimes \text{id})[L]$ and hence $n \leq d$. Furthermore, in 3 we applied the pinching theorem [181, Eq. (IV.52)], or, alternatively, the data processing inequality for the trace distance – note that $X \mapsto \Pi X \Pi + (\text{id} - \Pi)X(\text{id} - \Pi)$ is a ctp map for every projector Π . Finally, multiple applications of the triangle inequality yield

$$\begin{aligned}
\left\| \sum_{\min\{i,j\} \geq d} |i\rangle\langle j| \otimes L_{ij} \right\|_1 &= \|L - (\Pi_d \otimes \text{id})L(\Pi_d \otimes \text{id})\|_1 \\
&= \|(\tau - \sigma) - (\Pi_d \otimes \text{id})(\tau - \sigma)(\Pi_d \otimes \text{id})\|_1 \\
&= \|\tau - \tau_d - (\tau - \sigma_d)\|_1 \\
&\leq \|\tau - \tau_d\|_1 + \|\sigma - \sigma_d\|_1
\end{aligned}$$

where $\tau_d := (\Pi_d \otimes \text{id})\tau(\Pi_d \otimes \text{id})$ and $\sigma_d := (\Pi_d \otimes \text{id})\sigma(\Pi_d \otimes \text{id})$. The 1-norms on the r.h.s. can be bounded from above by exploiting the result of Proposition S2 in the supplemental material of [62], suitably adapted to our modified Choi–Jamiołkowski states. In particular, by replacing the coefficients $\phi_j = e^{-\frac{\omega_j}{2}}$ in [62, Proposition S2] with our $\phi_j = f_j^{-\frac{1}{2}}$ we have that, for $\rho = J_f(\Lambda)$,

$$\|\rho - \rho_d\|_1 \leq 2\epsilon_d, \tag{C.1.4}$$

where $\rho_d := (\Pi_d \otimes \text{id})\rho(\Pi_d \otimes \text{id})$. We then obtain

$$\left\| \sum_{\min\{i,j\} \geq d} |i\rangle\langle j| \otimes L_{ij} \right\|_1 \leq 4\epsilon_d.$$

□

Before proceeding with the proof, we restate for clarity the definition of energy-constrained diamond norm (see Definition 5.1.1 in the main text) for the specific case of a Hamiltonian which satisfies the Gibbs hypothesis and is written as in Eq. (5.1.4).

Definition C.1.2. Let A' be a quantum system equipped with a Hamiltonian $H_{A'}$ satisfying the Gibbs hypothesis and written as in Eq. (5.1.4), and pick $E > E_0 = f_0$. Then the energy-constrained diamond norm of an arbitrary Hermiticity-preserving linear map $\Lambda : \mathcal{D}(A') \rightarrow \mathcal{D}(B)$ is defined by

$$\|\Lambda\|_{\diamond_{H,E}} := \sup_{\sum_j f_j \langle j | \rho_{A'} | j \rangle \leq E} \|(\text{id}_A \otimes \Lambda_{A'}) (\rho_{AA'})\|_1, \quad (\text{C.1.5})$$

where A is an arbitrary ancillary system, and $\|\cdot\|_1$ is the one-norm. A recent result by Weis and Shirokov [155] ensures that the input state $\rho_{AA'}$ in Eq. (C.1.5) can be taken to be pure.

Lemma C.1.2 (Generalisation of Lemma S6 in the supplemental material of [62] for a Hamiltonian given by Eq. (5.1.4) and Eq. (5.1.5)). *For cptp maps Λ_0 and Λ_1 whose input system is equipped with a Hamiltonian H which satisfies the Gibbs hypothesis, takes the form as in Eq. (5.1.4) and satisfies Eq. (5.1.5), we have that*

$$\|\Lambda_0 - \Lambda_1\|_{\diamond_{H,E}} \leq \frac{E}{c_f^2} \|J_f(\Lambda_0) - J_f(\Lambda_1)\|_1, \quad (\text{C.1.6})$$

where the modified Choi–Jamiołkowski state $J_f(\Lambda)$ of Λ is constructed as in Definition 5.1.3.

Proof. Lemma C.1.2 can be proved by adapting the argument in the proof of [62, Lemma S6] to our choice of the input system’s Hamiltonian, i.e., by replacing the definition of modified Choi–Jamiołkowski states used there with the one given in Definition 5.1.3. \square

Lemma C.1.3 (Adapted from Eq. (16) in the supplementary notes of [61]). *Let Λ be a cptp map, and let the corresponding modified Choi–Jamiołkowski state given by Definition 5.1.3 be denoted with $\rho_{AB_1 \dots B_N} := \text{id}_A \otimes \Lambda_{A'}(|\phi\rangle\langle\phi|)$, where $|\phi\rangle$ is given in Eq. (5.1.6). Fix an integer $m \leq N$. Then there exists a set of indices $J := (j_1, \dots, j_{q-1})$, where $q \leq m$, and quantum-to-classical channels $\mathcal{C}_{j_1}, \dots, \mathcal{C}_{j_{q-1}}$ such that*

$$\mathbb{E}_{j \notin J} \max_{\mathcal{C}_j} \left\| \text{id} \otimes \mathcal{C}_j \left[\rho_{AB_j} - \mathbb{E}_z \rho_A^z \otimes \rho_{B_j}^z \right] \right\|_1 \leq \sqrt{\frac{2 \ln(2) \sigma}{m}}, \quad (\text{C.1.7})$$

where: σ is given in Eq.(5.1.7); the expectation value is with respect to the uniform distribution over $\{1, \dots, N\} \setminus J$; the maximum runs over all quantum-to-classical channels; z is a random variable that represents the outcome of the measurements $\mathcal{C}_{j_1}, \dots, \mathcal{C}_{j_{q-1}}$ on $\rho_{AB_1 \dots B_N}$; and $\rho_A^z, \rho_{B_j}^z$ are the corresponding post-measurement states.

Proof. It suffices to adapt the derivation of Eq.(16) in the supplementary notes of [61] to our infinite-dimensional scenario: the Choi–Jamiołkowski state of Λ is replaced with the f -Choi state of Definition 5.1.3, and the entropy $\log d_A$ with $S(\rho_A)$. Since Λ is trace preserving, $\rho_A = \text{Tr}_{A'}[|\phi\rangle\langle\phi|_{AA'}]$, and $S(\rho_A) = \sigma$ by definition of σ . \square

Theorem C.1.1 (Restatement). *Let A be a quantum system equipped with a Hamiltonian H_A which satisfies the Gibbs hypothesis and which, when written as in Eq. (5.1.4), also satisfies Eq. (5.1.5). Consider an arbitrary cptp map $\Lambda : \mathcal{D}(A) \rightarrow \mathcal{D}(B_1 \otimes \dots \otimes B_N)$, and define the effective dynamics from $\mathcal{D}(A)$ to $\mathcal{D}(B_j)$ as $\Lambda_j := \text{Tr}_{B \setminus B_j} \circ \Lambda$. For an arbitrary number $0 < \delta < 1$, there exists a POVM $\{M_l\}_l$ and a set $S \subseteq \{1, \dots, N\}$, with $|S| \geq (1 - \delta)N$, such that, for all $j \in S$ and for any integer truncation dimension $d \geq 0$, we have that*

$$\|\Lambda_j - \mathcal{E}_j\|_{\diamond_{H,E}} \leq \frac{\zeta}{\delta}, \quad (\text{5.1.10})$$

where the measure-and-prepare channel \mathcal{E}_j is given by

$$\mathcal{E}_j(X) := \sum_l \text{Tr}(M_l X) \tau_{j,l} \quad (\text{5.1.11})$$

for some family of states $\tau_{j,l} \in \mathcal{D}(B_j)$, and

$$\zeta = \kappa d \left(\frac{E^2 \sigma}{N c_f^4} \right)^{1/3} + \frac{4E}{c_f^2} \epsilon_d, \quad (5.1.12)$$

where c_f is the normalization factor introduced in Eq. (5.1.6); ϵ_d is given in Definition 5.1.2; σ is defined by Eq. (5.1.7) and $\kappa := 3(16 \ln(2))^{1/3}$ is a universal constant.

Proof. As we will see below, the states ρ_{AB_j} and $\mathbb{E}_z \rho_A^z \otimes \rho_{B_j}^z$ defined in Lemma C.1.3 are modified Choi–Jamiołkowski states. By applying Lemma C.1.1 to them we have that

$$\left\| \rho_{AB_j} - \mathbb{E}_z \rho_A^z \otimes \rho_{B_j}^z \right\|_1 \leq 4d^{3/2} \max_{c_j} \left\| \text{id}_A \otimes C_j \left[\rho_{AB_j} - \mathbb{E}_z \rho_A^z \otimes \rho_{B_j}^z \right] \right\|_1 + 4\epsilon_d. \quad (C.1.8)$$

By combining Eq. (C.1.8) with Lemma C.1.3 we then obtain

$$\begin{aligned} \mathbb{E}_{j \notin J} \left\| \rho_{AB_j} - \mathbb{E}_z \rho_A^z \otimes \rho_{B_j}^z \right\|_1 &\leq 4d^{3/2} \mathbb{E}_{j \notin J} \max_{c_j} \left\| \text{id}_A \otimes C_j \left[\rho_{AB_j} - \mathbb{E}_z \rho_A^z \otimes \rho_{B_j}^z \right] \right\|_1 + 4\epsilon_d \\ &\leq 4d^{3/2} \sqrt{\frac{2 \ln(2) \sigma}{m}} + 4\epsilon_d. \end{aligned} \quad (C.1.9)$$

We now show that $\mathbb{E}_z \rho_A^z \otimes \rho_{B_j}^z$ is the modified Choi–Jamiołkowski state of a quantum-to-classical channel, explicitly given by

$$\mathcal{E}_j(X) := c_f^{-2} \mathbb{E}_z \text{Tr} \left[(\rho_A^z)^\top H^{\frac{1}{2}} X H^{\frac{1}{2}} \right] \rho_{B_j}^z. \quad (C.1.10)$$

In fact,

$$\begin{aligned} (\text{id}_A \otimes \mathcal{E}_j)(|\phi\rangle\langle\phi|) &= c_f^2 \sum_{j,k} \frac{1}{f_j^{1/2}} \frac{1}{f_k^{1/2}} |j\rangle\langle k| \otimes \mathcal{E}_j(|j\rangle\langle k|) \\ &= \mathbb{E}_z \sum_{j,k} \langle j | \rho_A^z | k \rangle |j\rangle\langle k| \otimes \rho_{B_j}^z \\ &= \mathbb{E}_z \rho_A^z \otimes \rho_{B_j}^z. \end{aligned}$$

Note that the measurement appearing in Eq. (C.1.10) is independent of $j \notin J$. In fact, calling $N_{B_{j_1} \dots B_{j_{q-1}}}^z$ the POVM element corresponding to the outcome z of the measurement $C_{j_1} \otimes \dots \otimes C_{j_{q-1}}$, the POVM appearing in Eq. (C.1.10) can be expressed as $\left\{ c_f^{-2} p(z) H^{\frac{1}{2}} (\rho_A^z)^\top H^{\frac{1}{2}} \right\}_z$, where $p(z) = \text{Tr} \left[\rho_{AB_1 \dots B_N} N_{B_{j_1} \dots B_{j_{q-1}}}^z \right]$. Now the claim follows because

$$p(z) (\rho_A^z)^\top = \text{Tr}_{B_1 \dots B_N} \left[\rho_{AB_1 \dots B_N} N_{B_{j_1} \dots B_{j_{q-1}}}^z \right] \quad (C.1.11)$$

is independent of $j \notin J$.

Since ρ_{AB_j} is, by definition, the modified Choi–Jamiołkowski state of Λ_j , from Lemma C.1.2 it follows that

$$\|\Lambda_j - \mathcal{E}_j\|_{\diamond_{H,E}} \leq \frac{E}{c_f^2} \left\| \rho_{AB_j} - \mathbb{E}_z \rho_A^z \otimes \rho_{B_j}^z \right\|_1. \quad (C.1.12)$$

This, combined with Eq. (C.1.9), gives

$$\begin{aligned} \mathbb{E}_{j \notin J} \|\Lambda_j - \mathcal{E}_j\|_{\diamond_{H,E}} &\leq \frac{E}{c_f^2} \mathbb{E}_{j \notin J} \left\| \rho_{AB_j} - \mathbb{E}_z \rho_A^z \otimes \rho_{B_j}^z \right\|_1 \\ &\leq \frac{E}{c_f^2} \left(4d^{3/2} \sqrt{\frac{2 \ln(2) \sigma}{m}} + 4\epsilon_d \right) \\ &= \sqrt{\frac{32 \ln(2) E^2 d^3 \sigma}{m c_f^4}} + \frac{4E}{c_f^2} \epsilon_d. \end{aligned}$$

From the previous result we then find that

$$\begin{aligned} \mathbb{E}_j \|\Lambda_j - \mathcal{E}\|_{\diamond H, E} &\leq \mathbb{E}_{j \notin J} \|\Lambda_j - \mathcal{E}_j\|_{\diamond H, E} + \frac{m}{N} \mathbb{E}_{j \in J} \|\Lambda_j - \mathcal{E}_j\|_{\diamond H, E} \\ &\leq \sqrt{\frac{32 \ln(2) E^2 d^3 \sigma}{m c_f^4}} + \frac{4E}{c_f^2} \epsilon_d + \frac{2m}{N}. \end{aligned}$$

The right-hand-side, minimised with respect to m , gives the quantity

$$\zeta = \kappa d \left(\frac{E^2 \sigma}{N c_f^2} \right)^{1/3} + \frac{4E}{c_f^2} \epsilon_d, \quad (\text{C.1.13})$$

where $\kappa = 3(16 \ln(2))^{1/3}$. To complete the proof, we apply Markov's inequality: $P(X \geq a) \leq \frac{\mathbb{E}(X)}{a}$, where X is a non-negative random variable, $\mathbb{E}(X)$ its expectation value, and $a > 0$. In our case, $X = \|\Lambda_j - \mathcal{E}\|_{\diamond H, E}$, with j being uniformly distributed, and $a = \frac{\zeta}{\delta}$, which leads us to

$$P \left(\|\Lambda_j - \mathcal{E}_j\|_{\diamond H, E} \geq \frac{\zeta}{\delta} \right) \leq \delta, \quad (\text{C.1.14})$$

completing the proof. \square

Example (Case study: bridging finite and infinite dimensions). We calculate the quantity given by Eq. (5.1.12) for the sequence of Hamiltonian eigenvalues

$$f_j = \begin{cases} 1 & j \leq D - 1, \\ \frac{e^{\omega j}}{1 - e^{-\omega}} & j \geq D. \end{cases} \quad (\text{C.1.15})$$

We have that

$$c_f = (D + e^{-\omega D})^{-\frac{1}{2}}, \quad (\text{C.1.16})$$

$$\epsilon_d = \left(\frac{e^{-\omega d}}{D + e^{-\omega D}} \right)^{\frac{1}{2}} = e^{-\omega d/2} c_f, \quad (\text{C.1.17})$$

$$s := \ln(2)\sigma = \ln(D + e^{-\omega D}) + \frac{\omega(1 - D + D e^\omega)}{(e^\omega - 1)(D e^{\omega D} + 1)} - \frac{\ln(1 - e^{-\omega})}{(1 + D e^{\omega D})}, \quad (\text{C.1.18})$$

where we assumed $d \geq D$. We then obtain

$$\zeta = \left(\frac{432 E^2 (D + e^{-\omega D})^2 d^3 s}{N} \right)^{\frac{1}{3}} + 4E \sqrt{\frac{D + e^{-\omega D}}{e^{\omega d}}}, \quad (\text{C.1.19})$$

which is valid for any $d \geq D$.

C.2 Properties of the pure loss channel

C.2.1 Symmetry of the reduced dynamics

We show that, when the dynamics from system A to the environment fragments B_1, \dots, B_N is given by

$$\Lambda_{A \rightarrow B_1, \dots, B_N}(\cdot) := U \left((\cdot)_A \otimes \bigotimes_{j=2}^N |0\rangle\langle 0|_{B_j} \right) U^\dagger, \quad (\text{C.2.1})$$

with U the symplectic unitary implementing a N -splitter, the reduced dynamics $\Lambda_j = \text{Tr}_{B \setminus B_j} \circ \Lambda$ have the same form for all j . We start by introducing the Weyl displacement operator:

$$D(\vec{\alpha}) := \exp \left[\sum_j \left(\alpha_j a_j^\dagger - \alpha_j^* a_j \right) \right], \quad (\text{C.2.2})$$

where $\vec{\alpha}$ denotes a complex vector in \mathbb{C}^N , with N the number of modes. A quantum state ρ can be described in terms of the characteristic function

$$\chi_\rho(\vec{\alpha}) := \text{Tr}[\rho D(\vec{\alpha})], \quad (\text{C.2.3})$$

by means of which the state ρ can be reconstructed as

$$\rho = \int \frac{d^{2N}\alpha}{\pi^N} \chi_\rho(\vec{\alpha}) D(-\vec{\alpha}). \quad (\text{C.2.4})$$

We will describe the channel in Eq. (C.2.1) as the unitary operation on $\mathcal{D}(A \otimes B_2 \otimes \dots \otimes B_N)$ given by

$$\rho_{\text{in}} \rightarrow \rho_{\text{out}} = U \rho_{\text{in}} U^\dagger, \quad (\text{C.2.5})$$

with

$$\rho_{\text{in}} = \rho_A \otimes \bigotimes_{j=2}^N |0\rangle\langle 0|_{B_j}. \quad (\text{C.2.6})$$

The characteristic function for the input state is given by

$$\chi_{\rho_{\text{in}}}(\vec{\alpha}) = \text{Tr}[\rho_{\text{in}} D(\vec{\alpha})] = \chi_{\rho_A}(\alpha_1) \chi_{|0\rangle\langle 0|}(\alpha_2) \dots \chi_{|0\rangle\langle 0|}(\alpha_N) = \chi_{\rho_A}(\alpha_1) \exp\left[-\frac{1}{2}(\|\vec{\alpha}\|^2 - |\alpha_1^2|)\right] \quad (\text{C.2.7})$$

and for the output state we have

$$\chi_{\rho_{\text{out}}}(\vec{\alpha}) = \text{Tr}[\rho_{\text{out}} D(\vec{\alpha})] = \text{Tr}[U \rho_{\text{in}} U^\dagger D(\vec{\alpha})] = \text{Tr}[\rho_{\text{in}} U^\dagger D(\vec{\alpha}) U]. \quad (\text{C.2.8})$$

Since $U^\dagger D(\vec{\alpha}) U = D(V^\dagger \vec{\alpha})$, we obtain that

$$\chi_{\rho_{\text{out}}}(\vec{\alpha}) = \text{Tr}[\rho_{\text{in}} D(V^\dagger \vec{\alpha})] = \chi_{\rho_A}\left(\frac{\alpha_1 + \alpha_2 + \dots + \alpha_N}{\sqrt{N}}\right) \exp\left[-\frac{1}{2}\left(\sum_j |\alpha_j|^2 - \frac{1}{N}\left|\sum_j \alpha_j\right|^2\right)\right]. \quad (\text{C.2.9})$$

The characteristic function of the output state $\rho_{\text{out}_j} = \text{Tr}_{B \setminus B_j}[\rho_{\text{out}}]$ is obtained by setting $\alpha_{i \neq j} = 0$:

$$\chi_{\rho_{\text{out}_j}}(\alpha_j) = \chi_{\rho_A}\left(\frac{\alpha_j}{\sqrt{N}}\right) \exp\left[-\frac{1}{2}\left(\frac{N-1}{N}\right)|\alpha_j|^2\right]. \quad (\text{C.2.10})$$

It has the same form for all j , and the same property is therefore true for the reduced channel $\Lambda_j = \text{Tr}_{B \setminus B_j} \circ \Lambda$.

C.2.2 Lower bound for the objectivity range of a pure loss channel

The statement

$$\exists\{M_l\}_l : \forall j \in S, \exists\{\tau_{j,l}\}_l : \|\Lambda_j - \mathcal{E}_{M,\tau_j}\|_{\diamond H,E} \leq \frac{1}{\delta}\zeta, \quad (\text{C.2.11})$$

is equivalent to the inequality

$$\inf_M \sup_{1 \leq j \leq N} \inf_{\tau_j} \|\Lambda_j - \mathcal{E}_{M,\tau_j}\|_{\diamond H,E} \leq \frac{1}{\delta}\zeta. \quad (\text{C.2.12})$$

Note that we made explicit the dependence of the measure-and-prepare channels from POVM $M = \{M_l\}_l$ and set of states $\tau_j = \{\tau_{j,l}\}_l$ through the notation $\mathcal{E}_{M,\tau_j}(X) := \sum_l \text{Tr}(M_l X) \tau_{j,l}$. To investigate the optimality of the objectivity bound in Eq. (C.2.11) we thus need to estimate a *lower* bound for the l.h.s. of Eq. (C.2.12). We will perform this analysis for the channel in Eq. (C.2.1). Since the reduced dynamics Λ_j have the same form for all j we can get rid of the supremum on j and look at a lower bound for the quantity

$$\mu(\Lambda) := \inf_{M,\tau_j} \|\Lambda_j - \mathcal{E}_{M,\tau_j}\|_{\diamond H,E}. \quad (\text{C.2.13})$$

By substituting the definition of diamond norm we obtain

$$\mu(\Lambda) = \inf_{M, \tau_j} \|\Lambda_j - \mathcal{E}_{M, \tau_j}\|_{\diamond H, E} = \inf_{M, \tau_j} \sup_{\rho: \text{Tr}[\rho H_A] \leq E} \|\text{id}_C \otimes (\Lambda_j - \mathcal{E}_{M, \tau_j})_A[\rho]\|_1, \quad (\text{C.2.14})$$

where C is an arbitrary ancillary system (see Definition 5.1.1 in the main text). To simplify the notation, in the following we suppress the explicit reference to the bipartition $C : A$. We can choose $\rho = \psi_r := |\psi_r\rangle\langle\psi_r|$ with $|\psi_r\rangle := \frac{1}{\cosh(r)} \sum_n \tanh(r)^n |nn\rangle$, which is a two-mode squeezed vacuum state, and (noting that $\text{Tr}[\rho H_A] = \sinh(r)^2$) find the inequality

$$\mu(\Lambda) \geq \inf_{M, \tau_j} \sup_{r: \sinh(r)^2 \leq E} \|\text{id} \otimes (\Lambda_j - \mathcal{E}_{M, \tau_j})[\psi_r]\|_1. \quad (\text{C.2.15})$$

The channel \mathcal{E}_{M, τ_j} is entanglement breaking, so $\text{id} \otimes \mathcal{E}_{M, \tau_j}[\psi_r]$ is a separable state: $\text{id} \otimes \mathcal{E}_{M, \tau_j}[\psi_r] = \omega \in \text{SEP}$. Since $\|X\|_1 \geq 2\|X\|_\infty$ if $\text{Tr}[X] = 0$, we have that

$$\begin{aligned} \mu(\Lambda) &\geq 2 \inf_{\omega \in \text{SEP}} \sup_{r: \sinh(r)^2 \leq E} \|\text{id} \otimes \Lambda_j[\psi_r] - \omega\|_\infty \\ &= 2 \inf_{\omega \in \text{SEP}} \sup_{r: \sinh(r)^2 \leq E} \sup_{\phi} |\langle \phi | \text{id} \otimes \Lambda_j[\psi_r] | \phi \rangle - \langle \phi | \omega | \phi \rangle|, \end{aligned} \quad (\text{C.2.16})$$

where we substituted the definition of the infinity norm. We can choose, as $|\phi\rangle$, a two-mode squeezed vacuum state $|\phi_s\rangle = \frac{1}{\cosh(s)} \sum_n \tanh(s)^n |nn\rangle$, and get rid of the modulus to obtain

$$\mu(\Lambda) \geq 2 \inf_{\omega \in \text{SEP}} \sup_{r: \sinh(r)^2 \leq E} \sup_s (\langle \phi_s | \text{id} \otimes \Lambda_j[\psi_r] | \phi_s \rangle - \langle \phi_s | \omega | \phi_s \rangle). \quad (\text{C.2.17})$$

For a separable state ω , $|\langle \phi | \omega | \phi \rangle| \leq \lambda_{\max}$, where λ is defined by the Schmidt decomposition: $|\phi\rangle = \sum_i \sqrt{\lambda_i} |e_i f_i\rangle$. Hence $\langle \phi_s | \omega | \phi_s \rangle \leq \lambda_{\max}(\phi_s) = \frac{1}{\cosh(s)^2}$, and we have that

$$\mu(\Lambda) \geq 2 \sup_{r: \sinh(r)^2 \leq E} \sup_s \left(\langle \phi_s | \text{id} \otimes \Lambda_j[\psi_r] | \phi_s \rangle - \frac{1}{\cosh(s)^2} \right). \quad (\text{C.2.18})$$

A calculation of the quantity $\langle \phi_s | \text{id} \otimes \Lambda_j[\psi_r] | \phi_s \rangle$ can be found in [182]. By exploiting that result we find

$$\mu(\Lambda) \geq 2 \sup_s \left[\left(\sup_{r: \sinh(r)^2 \leq E} \frac{N}{(\sqrt{N} \cosh(r) \cosh(s) - \sinh(r) \sinh(s))^2} \right) - \frac{1}{\cosh(s)^2} \right]. \quad (\text{C.2.19})$$

For a given s , the supremum of the function

$$\frac{N}{(\sqrt{N} \cosh(r) \cosh(s) - \sinh(r) \sinh(s))^2} \quad (\text{C.2.20})$$

is reached for $r = \bar{r}$ such that $\bar{E} := \sinh(\bar{r})^2 = \frac{\tanh(s)^2}{N - \tanh(s)^2}$. Since $\bar{E} \leq \frac{1}{N-1} \leq \frac{2}{N}$ for $N \geq 2$ (and noting that $N \geq 2$ by definition of the channel Λ), we can choose $E \geq \frac{2}{N}$ in order to have $\bar{E} \leq E$ satisfied for all possible values of N . This is equivalent to evaluate an unconstrained supremum, for which we can use the calculation performed in [182] to obtain

$$\begin{aligned} \mu(\Lambda) &\geq 2 \sup_s \left[\frac{N}{N \cosh(s)^2 - \sinh(s)^2} - \frac{1}{\cosh(s)^2} \right] = 2 \sup_s \frac{\tanh(s)^2}{N \cosh(s)^2 - \sinh(s)^2} \\ &\geq \frac{1}{2N-1} \geq \frac{1}{2N}. \end{aligned} \quad (\text{C.2.21})$$

Our analysis therefore led to the following result: when the dynamics from A to B_1, \dots, B_N is given by Eq. (C.2.1) and the maximum energy of system A satisfies $E \geq \frac{2}{N}$, for all j and for all POVM $\{M_l\}_l$ and sets $\{\tau_{j,l}\}$ entering the definition of \mathcal{E}_j it holds that

$$\|\Lambda_j - \mathcal{E}_j\|_{\diamond H, E} \geq \frac{1}{2N}. \quad (\text{C.2.22})$$

C.3 Proof of Corollary 5.3.1

To prove Corollary 5.3.1, it suffices to adapt to our infinite-dimensional setting the argument in the proof of [61, Corollary 4]. The success of this programme depends crucially on a fundamental result by Winter [156, Lemma 17], reported below as Lemma C.3.1, which expresses a continuity bound for the conditional entropy of infinite-dimensional systems subjected to energy constraints.

Lemma C.3.1 ([156, Lemma 17]). *For a Hamiltonian H on A satisfying the Gibbs hypothesis and any two states τ and σ on the bipartite system $A \otimes B$ with $\text{Tr}(\tau H), \text{Tr}(\sigma H) \leq E$, $\frac{1}{2}\|\tau - \sigma\|_1 \leq \epsilon < \epsilon' \leq 1$ and $\Delta = \frac{\epsilon' - \epsilon}{1 + \epsilon'}$,*

$$|S(A|B)_\tau - S(A|B)_\sigma| \leq (2\epsilon' + 4\Delta)S(\gamma(E/\Delta)) + (1 + \epsilon')h\left(\frac{\epsilon'}{1 + \epsilon'}\right) + 2h(\Delta). \quad (\text{C.3.1})$$

Proof of Corollary 5.3.1. Let $0 < \delta < 1$ be a fixed number. Theorem 5.1.1 allows us to construct a POVM $\{M_l\}_l$, a set $S \subseteq \{1, \dots, N\}$ of cardinality at least $|S| \geq (1 - \delta)N$, and ensembles of states $\{\tau_{j,l}\}_l$ such that the corresponding measure-and-prepare channels \mathcal{E}_j defined in Eq. (5.1.11) satisfy Eq. (5.1.10) and (5.1.12) for all $j \in S$. Now, consider the states $\tau = (\text{id} \otimes \Lambda_j)(\rho)$ and $\sigma = (\text{id} \otimes \mathcal{E}_j)(\rho)$. By definition of f -diamond norm it follows that

$$\begin{aligned} \frac{1}{2}\|\tau - \sigma\|_1 &= \frac{1}{2}\|(\text{id} \otimes \Lambda_j)(\rho) - (\text{id} \otimes \mathcal{E}_j)(\rho)\|_1 \\ &\leq \frac{1}{2}\|\Lambda_j - \mathcal{E}_j\|_{\diamond_{H_B, E_B}} \\ &\leq \epsilon < \epsilon' \leq 1, \end{aligned}$$

where the inequalities in the last line follow from Theorem 5.1.1, and we set $\epsilon' := 2\epsilon := \frac{\zeta}{\delta}$, with ζ given in Eq. (5.1.12).

Applying Lemma C.3.1 to states τ and σ , we deduce that

$$|S(A|B)_{\text{id} \otimes \Lambda_j(\rho)} - S(A|B)_{\text{id} \otimes \mathcal{E}_j(\rho)}| \leq (2\epsilon' + 4\Delta)S(\gamma(E_A/\Delta)) + (1 + \epsilon')h\left(\frac{\epsilon'}{1 + \epsilon'}\right) + 2h(\Delta) \quad (\text{C.3.2})$$

where $\Delta := \frac{1}{2}\frac{\epsilon'}{1 + \epsilon'}$. Since the reduced entropies on the A subsystems are the same for τ and σ , this translates to

$$\begin{aligned} &|I(A : B)_{(\text{id} \otimes \Lambda_j)(\rho)} - I(A : B)_{(\text{id} \otimes \mathcal{E}_j)(\rho)}| \\ &\leq (2\epsilon' + 4\Delta)S(\gamma(E_A/\Delta)) + (1 + \epsilon')h\left(\frac{\epsilon'}{1 + \epsilon'}\right) + 2h(\Delta), \end{aligned}$$

and therefore

$$\begin{aligned} &I(A : B)_{\text{id} \otimes \Lambda_j(\rho)} \\ &\leq I(A : B)_{\text{id} \otimes \mathcal{E}_j(\rho)} + (2\epsilon' + 4\Delta)S(\gamma(E_A/\Delta)) + (1 + \epsilon')h\left(\frac{\epsilon'}{1 + \epsilon'}\right) + 2h(\Delta) \\ &\leq \max_{\Gamma \in \text{QC}} I(A : B)_{(\text{id} \otimes \Gamma)(\rho)} + (2\epsilon' + 4\Delta)S(\gamma(E_A/\Delta)) + (1 + \epsilon')h\left(\frac{\epsilon'}{1 + \epsilon'}\right) + 2h(\Delta), \end{aligned}$$

where the last inequality follows because any measure-and-prepare channel can be obtained by post-processing from a quantum-to-classical channel, and the mutual information obeys the data processing inequality.

We now move on the proof of Eq. (5.3.5). The fact that the right hand side is no larger than the left hand side is well known; to prove it, it suffices to choose as Λ the quantum-to-classical map that attains the accessible information $I(A : B_a) := \max_{\Gamma \in \text{QC}} I(A : B)_{(\text{id} \otimes \Gamma)(\rho)}$, makes N copies of the classical result, and stores it in N registers $B_1 \dots B_N$.

As it turns out, we only have to prove that the l.h.s. of Eq. (5.3.5) is no larger than the the r.h.s. . By using Eq. (5.3.4) we can write

$$\begin{aligned} \mathbb{E}_j I(A : B_j) & \tag{C.3.3} \\ & \leq \frac{1}{N} \left[(1 - \delta) N \left(I(A : B_a) + (2\epsilon' + 4\Delta) S(\gamma(E_A/\Delta)) + (1 + \epsilon') h\left(\frac{\epsilon'}{1+\epsilon'}\right) + 2h(\Delta) \right) + \delta N 2S(A) \right] \\ & = (1 - \delta) \left(I(A : B_a) + (2\epsilon' + 4\Delta) S(\gamma(E_A/\Delta)) + (1 + \epsilon') h\left(\frac{\epsilon'}{1+\epsilon'}\right) + 2h(\Delta) \right) + \delta 2S(A) , \end{aligned}$$

where we used the notation $I(A : B_j) := I(A : B)_{\text{id} \otimes \Lambda_j(\rho)}$. We can choose $\delta = \sqrt{\zeta}$, then

$$\epsilon' = 2\epsilon = \frac{\zeta}{\delta} \xrightarrow{N \rightarrow \infty} 0 , \tag{C.3.4}$$

and therefore

$$\Delta = \frac{1}{2} \frac{\epsilon'}{1 + \epsilon'} \xrightarrow{N \rightarrow \infty} 0 . \tag{C.3.5}$$

Moreover, since $S(\gamma(E_A)) = o(E_A)$ [156], we have that $\Delta S(\gamma(E_A/\Delta)) \xrightarrow{\Delta \rightarrow 0} 0$, as well as $\epsilon' S(\gamma(E_A/\Delta)) \xrightarrow{\epsilon', \Delta \rightarrow 0} 0$ (since $\epsilon' = O(\Delta)$). As a consequence, for our choice of δ ,

$$\begin{aligned} \mathbb{E}_j I(A : B_j) & \\ & \leq (1 - \delta) \left(I(A : B_a) + (2\epsilon' + 4\Delta) S(\gamma(E_A/\Delta)) + (1 + \epsilon') h\left(\frac{\epsilon'}{1+\epsilon'}\right) + 2h(\Delta) \right) + \delta 2S(A) \\ & \xrightarrow{N \rightarrow \infty} I(A : B_a) , \end{aligned} \tag{C.3.6}$$

independently of the choice of $\Lambda = \Lambda_{B \rightarrow B_1 B_2 \dots B_N}$. By considering the maximum of $\mathbb{E}_j I(A : B_j)$ over $\Lambda_{B \rightarrow B_1 B_2 \dots B_N}$ and then the limit $N \rightarrow \infty$ we therefore obtain that

$$\lim_{N \rightarrow \infty} \max_{\Lambda_{B \rightarrow B_1 B_2 \dots B_N}} \mathbb{E}_j I(A : B_j) \leq I(A : B_a) . \tag{C.3.7}$$

□

Bibliography

- [1] Eugenia Colafranceschi and Daniele Oriti. “Quantum gravity states, entanglement graphs and second-quantized tensor networks”. In: *JHEP* 07 (2021), p. 052. DOI: [10.1007/JHEP07\(2021\)052](https://doi.org/10.1007/JHEP07(2021)052). arXiv: [2012.12622](https://arxiv.org/abs/2012.12622) [[hep-th](#)].
- [2] Eugenia Colafranceschi, Goffredo Chirco, and Daniele Oriti. “Holographic maps from quantum gravity states as tensor networks”. In: *Phys. Rev. D* 105.6 (2022), p. 066005. DOI: [10.1103/PhysRevD.105.066005](https://doi.org/10.1103/PhysRevD.105.066005). arXiv: [2105.06454](https://arxiv.org/abs/2105.06454) [[hep-th](#)].
- [3] Goffredo Chirco, Eugenia Colafranceschi, and Daniele Oriti. “Bulk area law for boundary entanglement in spin network states: Entropy corrections and horizon-like regions from volume correlations”. In: *Phys. Rev. D* 105.4 (2022), p. 046018. DOI: [10.1103/PhysRevD.105.046018](https://doi.org/10.1103/PhysRevD.105.046018). arXiv: [2110.15166](https://arxiv.org/abs/2110.15166) [[hep-th](#)].
- [4] Eugenia Colafranceschi and Gerardo Adesso. “Holographic entanglement in spin network states: a focused review”. In: *AVS Quantum Sci.* 4 (2022), p. 025901. DOI: [10.1116/5.0087122](https://doi.org/10.1116/5.0087122). arXiv: [2202.05116](https://arxiv.org/abs/2202.05116) [[hep-th](#)].
- [5] Eugenia Colafranceschi, Ludovico Lami, Gerardo Adesso, and Tommaso Tufarelli. “Refined diamond norm bounds on the emergence of objectivity of observables”. In: *J. Phys. A* 53.39 (2020), p. 395305. DOI: [10.1088/1751-8121/aba469](https://doi.org/10.1088/1751-8121/aba469). arXiv: [2003.08153](https://arxiv.org/abs/2003.08153) [[quant-ph](#)].
- [6] *Approaches to Quantum Gravity: Toward a New Understanding of Space, Time and Matter*. Cambridge University Press, 2009. DOI: [10.1017/CBO9780511575549](https://doi.org/10.1017/CBO9780511575549).
- [7] Carlo Rovelli. *Quantum gravity*. Cambridge, UK: Univ. Pr., 2004.
- [8] Abhay Ashtekar and Eugenio Bianchi. “A short review of loop quantum gravity”. In: *Rept. Prog. Phys.* 84.4 (2021), p. 042001. DOI: [10.1088/1361-6633/abed91](https://doi.org/10.1088/1361-6633/abed91). arXiv: [2104.04394](https://arxiv.org/abs/2104.04394) [[gr-qc](#)].
- [9] Thomas Thiemann. *Modern canonical quantum general relativity*. Cambridge University Press, 2008. ISBN: 9780521741873, 9780521842631, 9780511363788. arXiv: [gr-qc/0110034](https://arxiv.org/abs/gr-qc/0110034) [[gr-qc](#)]. URL: <http://www.cambridge.org/catalogue/catalogue.asp?isbn=9780521842631>.
- [10] Daniele Oriti. “The microscopic dynamics of quantum space as a group field theory”. In: *Foundations of Space and Time: Reflections on Quantum Gravity*. Oct. 2011. arXiv: [1110.5606](https://arxiv.org/abs/1110.5606) [[hep-th](#)].
- [11] Thomas Krajewski. “Group field theories”. In: *PoS QGQGS2011* (2011). Ed. by John Barrett, Kristina Giesel, Frank Hellmann, Larisa Jonke, Thomas Krajewski, Jerzy Lewandowski, Carlo Rovelli, Hanno Sahlmann, and Harold Steinacker, p. 005. DOI: [10.22323/1.140.0005](https://doi.org/10.22323/1.140.0005). arXiv: [1210.6257](https://arxiv.org/abs/1210.6257) [[gr-qc](#)].
- [12] Sylvain Carrozza. “Flowing in Group Field Theory Space: a Review”. In: *SIGMA* 12 (2016), p. 070. DOI: [10.3842/SIGMA.2016.070](https://doi.org/10.3842/SIGMA.2016.070). arXiv: [1603.01902](https://arxiv.org/abs/1603.01902) [[gr-qc](#)].
- [13] Alejandro Perez. “Spin foam models for quantum gravity”. In: *Class. Quant. Grav.* 20 (2003), R43. DOI: [10.1088/0264-9381/20/6/202](https://doi.org/10.1088/0264-9381/20/6/202). arXiv: [gr-qc/0301113](https://arxiv.org/abs/gr-qc/0301113) [[gr-qc](#)].

- [14] Alejandro Perez. “The Spin Foam Approach to Quantum Gravity”. In: *Living Rev. Rel.* 16 (2013), p. 3. DOI: [10.12942/lrr-2013-3](https://doi.org/10.12942/lrr-2013-3). arXiv: [1205.2019](https://arxiv.org/abs/1205.2019) [gr-qc].
- [15] Marco Finocchiaro and Daniele Oriti. “Spin foam models and the Duflo map”. In: *Class. Quant. Grav.* 37.1 (2020), p. 015010. DOI: [10.1088/1361-6382/ab58da](https://doi.org/10.1088/1361-6382/ab58da). arXiv: [1812.03550](https://arxiv.org/abs/1812.03550) [gr-qc].
- [16] Jan Ambjorn, J. Jurkiewicz, and R. Loll. “Dynamically triangulating Lorentzian quantum gravity”. In: *Nucl. Phys. B* 610 (2001), pp. 347–382. DOI: [10.1016/S0550-3213\(01\)00297-8](https://doi.org/10.1016/S0550-3213(01)00297-8). arXiv: [hep-th/0105267](https://arxiv.org/abs/hep-th/0105267).
- [17] R. Loll. “Quantum Gravity from Causal Dynamical Triangulations: A Review”. In: *Class. Quant. Grav.* 37.1 (2020), p. 013002. DOI: [10.1088/1361-6382/ab57c7](https://doi.org/10.1088/1361-6382/ab57c7). arXiv: [1905.08669](https://arxiv.org/abs/1905.08669) [hep-th].
- [18] Astrid Eichhorn. “Status of the asymptotic safety paradigm for quantum gravity and matter”. In: *Found. Phys.* 48.10 (2018), pp. 1407–1429. DOI: [10.1007/s10701-018-0196-6](https://doi.org/10.1007/s10701-018-0196-6). arXiv: [1709.03696](https://arxiv.org/abs/1709.03696) [gr-qc].
- [19] Juan Martin Maldacena. “The Large N limit of superconformal field theories and supergravity”. In: *Int. J. Theor. Phys.* 38 (1999), pp. 1113–1133. DOI: [10.1023/A:1026654312961](https://doi.org/10.1023/A:1026654312961). arXiv: [hep-th/9711200](https://arxiv.org/abs/hep-th/9711200) [hep-th].
- [20] Edward Witten. “Anti-de Sitter space, thermal phase transition, and confinement in gauge theories”. In: *Adv. Theor. Math. Phys.* 2 (1998). Ed. by L. Bergstrom and U. Lindstrom, pp. 505–532. DOI: [10.4310/ATMP.1998.v2.n3.a3](https://doi.org/10.4310/ATMP.1998.v2.n3.a3). arXiv: [hep-th/9803131](https://arxiv.org/abs/hep-th/9803131).
- [21] S. S. Gubser, Igor R. Klebanov, and Alexander M. Polyakov. “Gauge theory correlators from noncritical string theory”. In: *Phys. Lett. B* 428 (1998), pp. 105–114. DOI: [10.1016/S0370-2693\(98\)00377-3](https://doi.org/10.1016/S0370-2693(98)00377-3). arXiv: [hep-th/9802109](https://arxiv.org/abs/hep-th/9802109).
- [22] Edward Witten. “Anti-de Sitter space and holography”. In: *Adv. Theor. Math. Phys.* 2 (1998), pp. 253–291. DOI: [10.4310/ATMP.1998.v2.n2.a2](https://doi.org/10.4310/ATMP.1998.v2.n2.a2). arXiv: [hep-th/9802150](https://arxiv.org/abs/hep-th/9802150).
- [23] Shinsei Ryu and Tadashi Takayanagi. “Holographic derivation of entanglement entropy from AdS/CFT”. In: *Phys. Rev. Lett.* 96 (2006), p. 181602. DOI: [10.1103/PhysRevLett.96.181602](https://doi.org/10.1103/PhysRevLett.96.181602). arXiv: [hep-th/0603001](https://arxiv.org/abs/hep-th/0603001).
- [24] Shinsei Ryu and Tadashi Takayanagi. “Aspects of Holographic Entanglement Entropy”. In: *JHEP* 08 (2006), p. 045. DOI: [10.1088/1126-6708/2006/08/045](https://doi.org/10.1088/1126-6708/2006/08/045). arXiv: [hep-th/0605073](https://arxiv.org/abs/hep-th/0605073).
- [25] Mark Van Raamsdonk. “Comments on quantum gravity and entanglement”. In: (July 2009). arXiv: [0907.2939](https://arxiv.org/abs/0907.2939) [hep-th].
- [26] Mark Van Raamsdonk. “Building up spacetime with quantum entanglement”. In: *Gen. Rel. Grav.* 42 (2010), pp. 2323–2329. DOI: [10.1007/s10714-010-1034-0](https://doi.org/10.1007/s10714-010-1034-0), [10.1142/S0218271810018529](https://doi.org/10.1142/S0218271810018529).
- [27] Nima Lashkari, Michael B. McDermott, and Mark Van Raamsdonk. “Gravitational dynamics from entanglement “thermodynamics””. In: *JHEP* 04 (2014), p. 195. DOI: [10.1007/JHEP04\(2014\)195](https://doi.org/10.1007/JHEP04(2014)195). arXiv: [1308.3716](https://arxiv.org/abs/1308.3716) [hep-th].
- [28] Thomas Faulkner, Monica Guica, Thomas Hartman, Robert C. Myers, and Mark Van Raamsdonk. “Gravitation from Entanglement in Holographic CFTs”. In: *JHEP* 03 (2014), p. 051. DOI: [10.1007/JHEP03\(2014\)051](https://doi.org/10.1007/JHEP03(2014)051). arXiv: [1312.7856](https://arxiv.org/abs/1312.7856) [hep-th].
- [29] ChunJun Cao, Sean M. Carroll, and Spyridon Michalakis. “Space from Hilbert Space: Recovering Geometry from Bulk Entanglement”. In: *Phys. Rev. D* 95.2 (2017), p. 024031. DOI: [10.1103/PhysRevD.95.024031](https://doi.org/10.1103/PhysRevD.95.024031). arXiv: [1606.08444](https://arxiv.org/abs/1606.08444) [hep-th].
- [30] Jacob D. Bekenstein. “Black holes and entropy”. In: *Phys. Rev. D* 7 (1973), pp. 2333–2346. DOI: [10.1103/PhysRevD.7.2333](https://doi.org/10.1103/PhysRevD.7.2333).
- [31] S. W. Hawking. “Particle Creation by Black Holes”. In: *Commun. Math. Phys.* 43 (1975). Ed. by G. W. Gibbons and S. W. Hawking. [Erratum: *Commun. Math. Phys.* 46, 206 (1976)], pp. 199–220. DOI: [10.1007/BF02345020](https://doi.org/10.1007/BF02345020).

- [32] S. W. Hawking. “Breakdown of predictability in gravitational collapse”. In: *Phys. Rev. D* 14 (10 Nov. 1976), pp. 2460–2473. DOI: [10.1103/PhysRevD.14.2460](https://doi.org/10.1103/PhysRevD.14.2460). URL: <https://link.aps.org/doi/10.1103/PhysRevD.14.2460>.
- [33] Don N. Page. “Information in black hole radiation”. In: *Phys. Rev. Lett.* 71 (1993), pp. 3743–3746. DOI: [10.1103/PhysRevLett.71.3743](https://doi.org/10.1103/PhysRevLett.71.3743). arXiv: [hep-th/9306083](https://arxiv.org/abs/hep-th/9306083).
- [34] Gerard 't Hooft. “Dimensional reduction in quantum gravity”. In: *Conf. Proc. C* 930308 (1993), pp. 284–296. arXiv: [gr-qc/9310026](https://arxiv.org/abs/gr-qc/9310026).
- [35] Leonard Susskind. “The World as a hologram”. In: *J. Math. Phys.* 36 (1995), pp. 6377–6396. DOI: [10.1063/1.531249](https://doi.org/10.1063/1.531249). arXiv: [hep-th/9409089](https://arxiv.org/abs/hep-th/9409089).
- [36] Raphael Bousso. “The Holographic principle”. In: *Rev. Mod. Phys.* 74 (2002), pp. 825–874. DOI: [10.1103/RevModPhys.74.825](https://doi.org/10.1103/RevModPhys.74.825). arXiv: [hep-th/0203101](https://arxiv.org/abs/hep-th/0203101).
- [37] Andrew Strominger and Cumrun Vafa. “Microscopic origin of the Bekenstein-Hawking entropy”. In: *Phys. Lett. B* 379 (1996), pp. 99–104. DOI: [10.1016/0370-2693\(96\)00345-0](https://doi.org/10.1016/0370-2693(96)00345-0). arXiv: [hep-th/9601029](https://arxiv.org/abs/hep-th/9601029).
- [38] Andrew Strominger. “Black hole entropy from near horizon microstates”. In: *JHEP* 02 (1998), p. 009. DOI: [10.1088/1126-6708/1998/02/009](https://doi.org/10.1088/1126-6708/1998/02/009). arXiv: [hep-th/9712251](https://arxiv.org/abs/hep-th/9712251).
- [39] Steven Carlip. “Black hole entropy from conformal field theory in any dimension”. In: *Phys. Rev. Lett.* 82 (1999), pp. 2828–2831. DOI: [10.1103/PhysRevLett.82.2828](https://doi.org/10.1103/PhysRevLett.82.2828). arXiv: [hep-th/9812013](https://arxiv.org/abs/hep-th/9812013).
- [40] Steven Carlip. “Near horizon conformal symmetry and black hole entropy”. In: *Phys. Rev. Lett.* 88 (2002), p. 241301. DOI: [10.1103/PhysRevLett.88.241301](https://doi.org/10.1103/PhysRevLett.88.241301). arXiv: [gr-qc/0203001](https://arxiv.org/abs/gr-qc/0203001).
- [41] T. Padmanabhan. “General Relativity from a Thermodynamic Perspective”. In: *Gen. Rel. Grav.* 46 (2014), p. 1673. DOI: [10.1007/s10714-014-1673-7](https://doi.org/10.1007/s10714-014-1673-7). arXiv: [1312.3253](https://arxiv.org/abs/1312.3253) [gr-qc].
- [42] T. Padmanabhan. “Gravity and/is Thermodynamics”. In: *Curr. Sci.* 109 (2015), pp. 2236–2242. DOI: [10.18520/v109/i12/2236-2242](https://doi.org/10.18520/v109/i12/2236-2242). arXiv: [1512.06546](https://arxiv.org/abs/1512.06546) [gr-qc].
- [43] Kirill Krasnov and Carlo Rovelli. “Black holes in full quantum gravity”. In: *Class. Quant. Grav.* 26 (2009), p. 245009. DOI: [10.1088/0264-9381/26/24/245009](https://doi.org/10.1088/0264-9381/26/24/245009). arXiv: [0905.4916](https://arxiv.org/abs/0905.4916) [gr-qc].
- [44] Fotini Markopoulou and Lee Smolin. “Quantum geometry with intrinsic local causality”. In: *Phys. Rev. D* 58 (1998), p. 084032. DOI: [10.1103/PhysRevD.58.084032](https://doi.org/10.1103/PhysRevD.58.084032). arXiv: [gr-qc/9712067](https://arxiv.org/abs/gr-qc/9712067).
- [45] Etera R. Livine. “From Coarse-Graining to Holography in Loop Quantum Gravity”. In: *EPL* 123.1 (2018), p. 10001. DOI: [10.1209/0295-5075/123/10001](https://doi.org/10.1209/0295-5075/123/10001). arXiv: [1704.04067](https://arxiv.org/abs/1704.04067) [gr-qc].
- [46] J. Eisert, M. Cramer, and M. B. Plenio. “Area laws for the entanglement entropy - a review”. In: *Rev. Mod. Phys.* 82 (2010), pp. 277–306. DOI: [10.1103/RevModPhys.82.277](https://doi.org/10.1103/RevModPhys.82.277). arXiv: [0808.3773](https://arxiv.org/abs/0808.3773) [quant-ph].
- [47] Shi-Ju Ran, Emanuele Tirrito, Cheng Peng, Xi Chen, Luca Tagliacozzo, Gang Su, and Maciej Lewenstein. “Lecture Notes of Tensor Network Contractions”. In: *arXiv e-prints*, arXiv:1708.09213 (Aug. 2017). arXiv: [1708.09213](https://arxiv.org/abs/1708.09213) [physics.comp-ph].
- [48] D. Perez-Garcia, F. Verstraete, M. M. Wolf, and J. I. Cirac. “Matrix Product State Representations”. In: *arXiv e-prints*, quant-ph/0608197 (Aug. 2006). arXiv: [quant-ph/0608197](https://arxiv.org/abs/quant-ph/0608197) [quant-ph].
- [49] Roman Orus. “A Practical Introduction to Tensor Networks: Matrix Product States and Projected Entangled Pair States”. In: *Annals Phys.* 349 (2014), pp. 117–158. DOI: [10.1016/j.aop.2014.06.013](https://doi.org/10.1016/j.aop.2014.06.013). arXiv: [1306.2164](https://arxiv.org/abs/1306.2164) [cond-mat.str-el].
- [50] Jacob C. Bridgeman and Christopher T. Chubb. “Hand-waving and Interpretive Dance: An Introductory Course on Tensor Networks”. In: *J. Phys. A* 50.22 (2017), p. 223001. DOI: [10.1088/1751-8121/aa6dc3](https://doi.org/10.1088/1751-8121/aa6dc3). arXiv: [1603.03039](https://arxiv.org/abs/1603.03039) [quant-ph].

- [51] Brian Swingle. “Entanglement Renormalization and Holography”. In: *Phys. Rev. D* 86 (2012), p. 065007. DOI: [10.1103/PhysRevD.86.065007](https://doi.org/10.1103/PhysRevD.86.065007). arXiv: [0905.1317](https://arxiv.org/abs/0905.1317) [[cond-mat.str-el](#)].
- [52] Wolfram Helwig, Wei Cui, Arnau Riera, José I. Latorre, and Hoi-Kwong Lo. “Absolute Maximal Entanglement and Quantum Secret Sharing”. In: *Phys. Rev. A* 86 (2012), p. 052335. DOI: [10.1103/PhysRevA.86.052335](https://doi.org/10.1103/PhysRevA.86.052335). arXiv: [1204.2289](https://arxiv.org/abs/1204.2289) [[quant-ph](#)].
- [53] Patrick Hayden, Sepehr Nezami, Xiao-Liang Qi, Nathaniel Thomas, Michael Walter, and Zhao Yang. “Holographic duality from random tensor networks”. In: *JHEP* 11 (2016), p. 009. DOI: [10.1007/JHEP11\(2016\)009](https://doi.org/10.1007/JHEP11(2016)009). arXiv: [1601.01694](https://arxiv.org/abs/1601.01694) [[hep-th](#)].
- [54] Sukhwinder Singh and Guifre Vidal. “Tensor network states and algorithms in the presence of a global SU(2) symmetry”. In: *Phys. Rev. B* 86 (2012), p. 195114. DOI: [10.1103/PhysRevB.86.195114](https://doi.org/10.1103/PhysRevB.86.195114). arXiv: [1208.3919](https://arxiv.org/abs/1208.3919) [[cond-mat.str-el](#)].
- [55] Sukhwinder Singh, Robert N. C. Pfeifer, and Guifré Vidal. “Tensor network decompositions in the presence of a global symmetry”. In: *Phys. Rev. A* 82 (5 Nov. 2010), p. 050301. DOI: [10.1103/PhysRevA.82.050301](https://doi.org/10.1103/PhysRevA.82.050301). arXiv: [0907.2994](https://arxiv.org/abs/0907.2994) [[cond-mat.str-el](#)]. URL: <https://link.aps.org/doi/10.1103/PhysRevA.82.050301>.
- [56] Goffredo Chirco, Daniele Oriti, and Mingyi Zhang. “Group field theory and tensor networks: towards a Ryu–Takayanagi formula in full quantum gravity”. In: *Class. Quant. Grav.* 35.11 (2018), p. 115011. DOI: [10.1088/1361-6382/aabf55](https://doi.org/10.1088/1361-6382/aabf55). arXiv: [1701.01383](https://arxiv.org/abs/1701.01383) [[gr-qc](#)].
- [57] E. Joos, H.D. Zeh, C. Kiefer, D.J.W. Giulini, J. Kupsch, and I.O. Stamatescu. *Decoherence and the Appearance of a Classical World in Quantum Theory*. Springer, 2003. ISBN: 9783540003908.
- [58] W.H. Zurek. “Decoherence, einselection, and the quantum origins of the classical”. In: *Rev. Mod. Phys.* 75 (3 May 2003), pp. 715–775. DOI: [10.1103/RevModPhys.75.715](https://doi.org/10.1103/RevModPhys.75.715). URL: <https://link.aps.org/doi/10.1103/RevModPhys.75.715>.
- [59] M.A. Schlosshauer. “Decoherence, the measurement problem, and interpretations of quantum mechanics”. In: *Rev. Mod. Phys.* 76 (4 Feb. 2005), pp. 1267–1305. DOI: [10.1103/RevModPhys.76.1267](https://doi.org/10.1103/RevModPhys.76.1267). URL: <https://link.aps.org/doi/10.1103/RevModPhys.76.1267>.
- [60] M.A. Schlosshauer. *Decoherence And the Quantum-To-Classical Transition*. The Frontiers Collection. Springer, 2007. ISBN: 9783540357735. URL: <https://books.google.co.uk/books?id=1qrJUS5zNbEC>.
- [61] F.G.S.L. Brandão, M. Piani, and P. Horodecki. “Generic emergence of classical features in quantum Darwinism”. In: *Nat. Commun.* 6 (2015), p. 7908. DOI: [10.1038/ncomms8908](https://doi.org/10.1038/ncomms8908).
- [62] P.A. Knott, T. Tufarelli, M. Piani, and G. Adesso. “Generic Emergence of Objectivity of Observables in Infinite Dimensions”. In: *Phys. Rev. Lett.* 121 (16 Oct. 2018), p. 160401. DOI: [10.1103/PhysRevLett.121.160401](https://doi.org/10.1103/PhysRevLett.121.160401). URL: <https://link.aps.org/doi/10.1103/PhysRevLett.121.160401>.
- [63] Lee Smolin. “The Future of spin networks”. In: (Jan. 1997). arXiv: [gr-qc/9702030](https://arxiv.org/abs/gr-qc/9702030).
- [64] Robert Oeckl and Hendryk Pfeiffer. “The Dual of pure nonAbelian lattice gauge theory as a spin foam model”. In: *Nucl. Phys. B* 598 (2001), pp. 400–426. DOI: [10.1016/S0550-3213\(00\)00770-7](https://doi.org/10.1016/S0550-3213(00)00770-7). arXiv: [hep-th/0008095](https://arxiv.org/abs/hep-th/0008095).
- [65] Thomas Thiemann. *Modern Canonical Quantum General Relativity*. Cambridge Monographs on Mathematical Physics. Cambridge University Press, 2007. ISBN: 978-0-511-75568-2, 978-0-521-84263-1. DOI: [10.1017/CB09780511755682](https://doi.org/10.1017/CB09780511755682).
- [66] Alejandro Corichi. “Comments on area spectra in loop quantum gravity”. In: *Rev. Mex. Fis.* 50 (2005), pp. 549–552. arXiv: [gr-qc/0402064](https://arxiv.org/abs/gr-qc/0402064).
- [67] Etera R. Livine and Daniel R. Terno. “Reconstructing quantum geometry from quantum information: Area renormalisation, coarse-graining and entanglement on spin networks”. In: (Mar. 2006). arXiv: [gr-qc/0603008](https://arxiv.org/abs/gr-qc/0603008).

- [68] Laurent Freidel and Simone Speziale. “Twisted geometries: A geometric parametrisation of $SU(2)$ phase space”. In: *Phys. Rev. D* 82 (2010), p. 084040. DOI: [10.1103/PhysRevD.82.084040](https://doi.org/10.1103/PhysRevD.82.084040). arXiv: [1001.2748](https://arxiv.org/abs/1001.2748) [gr-qc].
- [69] Bianca Dittrich and James P. Ryan. “Simplicity in simplicial phase space”. In: *Phys. Rev. D* 82 (2010), p. 064026. DOI: [10.1103/PhysRevD.82.064026](https://doi.org/10.1103/PhysRevD.82.064026). arXiv: [1006.4295](https://arxiv.org/abs/1006.4295) [gr-qc].
- [70] Laurent Freidel and Etera R. Livine. “Bubble networks: framed discrete geometry for quantum gravity”. In: *Gen. Rel. Grav.* 51.1 (2019), p. 9. DOI: [10.1007/s10714-018-2493-y](https://doi.org/10.1007/s10714-018-2493-y). arXiv: [1810.09364](https://arxiv.org/abs/1810.09364) [gr-qc].
- [71] Alejandro Perez. “Spin foam models for quantum gravity”. In: *Class. Quant. Grav.* 20 (2003), R43. DOI: [10.1088/0264-9381/20/6/202](https://doi.org/10.1088/0264-9381/20/6/202). arXiv: [gr-qc/0301113](https://arxiv.org/abs/gr-qc/0301113).
- [72] Herbert W. Hamber. “Quantum Gravity on the Lattice”. In: *Gen. Rel. Grav.* 41 (2009), pp. 817–876. DOI: [10.1007/s10714-009-0769-y](https://doi.org/10.1007/s10714-009-0769-y). arXiv: [0901.0964](https://arxiv.org/abs/0901.0964) [gr-qc].
- [73] J. Ambjorn, A. Goerlich, J. Jurkiewicz, and R. Loll. “Nonperturbative Quantum Gravity”. In: *Phys. Rept.* 519 (2012), pp. 127–210. DOI: [10.1016/j.physrep.2012.03.007](https://doi.org/10.1016/j.physrep.2012.03.007). arXiv: [1203.3591](https://arxiv.org/abs/1203.3591) [hep-th].
- [74] Vincent Rivasseau. “Random Tensors and Quantum Gravity”. In: *SIGMA* 12, 069 (July 2016), p. 069. DOI: [10.3842/SIGMA.2016.069](https://doi.org/10.3842/SIGMA.2016.069). arXiv: [1603.07278](https://arxiv.org/abs/1603.07278) [math-ph].
- [75] Razvan Gurau and James P. Ryan. “Colored Tensor Models - a review”. In: *SIGMA* 8 (2012), p. 020. DOI: [10.3842/SIGMA.2012.020](https://doi.org/10.3842/SIGMA.2012.020). arXiv: [1109.4812](https://arxiv.org/abs/1109.4812) [hep-th].
- [76] Etera R. Livine and Daniel R. Terno. “Quantum black holes: Entropy and entanglement on the horizon”. In: *Nucl. Phys. B* 741 (2006), pp. 131–161. DOI: [10.1016/j.nuclphysb.2006.02.012](https://doi.org/10.1016/j.nuclphysb.2006.02.012). arXiv: [gr-qc/0508085](https://arxiv.org/abs/gr-qc/0508085).
- [77] Etera R. Livine and Daniel R. Terno. “Bulk Entropy in Loop Quantum Gravity”. In: *Nucl. Phys. B* 794 (2008), pp. 138–153. DOI: [10.1016/j.nuclphysb.2007.10.027](https://doi.org/10.1016/j.nuclphysb.2007.10.027). arXiv: [0706.0985](https://arxiv.org/abs/0706.0985) [gr-qc].
- [78] Alexandre Feller and Etera R. Livine. “Ising Spin Network States for Loop Quantum Gravity: a Toy Model for Phase Transitions”. In: *Class. Quant. Grav.* 33.6 (2016), p. 065005. DOI: [10.1088/0264-9381/33/6/065005](https://doi.org/10.1088/0264-9381/33/6/065005). arXiv: [1509.05297](https://arxiv.org/abs/1509.05297) [gr-qc].
- [79] Etera R. Livine. “Intertwiner Entanglement on Spin Networks”. In: *Phys. Rev. D* 97.2 (2018), p. 026009. DOI: [10.1103/PhysRevD.97.026009](https://doi.org/10.1103/PhysRevD.97.026009). arXiv: [1709.08511](https://arxiv.org/abs/1709.08511) [gr-qc].
- [80] William Donnelly. “Entanglement entropy in loop quantum gravity”. In: *Phys. Rev. D* 77 (2008), p. 104006. DOI: [10.1103/PhysRevD.77.104006](https://doi.org/10.1103/PhysRevD.77.104006). arXiv: [0802.0880](https://arxiv.org/abs/0802.0880) [gr-qc].
- [81] William Donnelly. “Decomposition of entanglement entropy in lattice gauge theory”. In: *Phys. Rev. D* 85 (2012), p. 085004. DOI: [10.1103/PhysRevD.85.085004](https://doi.org/10.1103/PhysRevD.85.085004). arXiv: [1109.0036](https://arxiv.org/abs/1109.0036) [hep-th].
- [82] Clement Delcamp, Bianca Dittrich, and Aldo Riello. “On entanglement entropy in non-Abelian lattice gauge theory and 3D quantum gravity”. In: *JHEP* 11 (2016), p. 102. DOI: [10.1007/JHEP11\(2016\)102](https://doi.org/10.1007/JHEP11(2016)102). arXiv: [1609.04806](https://arxiv.org/abs/1609.04806) [hep-th].
- [83] Alexandre Feller and Etera R. Livine. “Entanglement entropy and correlations in loop quantum gravity”. In: *Class. Quant. Grav.* 35.4 (2018), p. 045009. DOI: [10.1088/1361-6382/aaa27c](https://doi.org/10.1088/1361-6382/aaa27c). arXiv: [1710.04473](https://arxiv.org/abs/1710.04473) [gr-qc].
- [84] Eugenio Bianchi, Hal M. Haggard, and Carlo Rovelli. “The boundary is mixed”. In: *Gen. Rel. Grav.* 49.8 (2017), p. 100. DOI: [10.1007/s10714-017-2263-2](https://doi.org/10.1007/s10714-017-2263-2). arXiv: [1306.5206](https://arxiv.org/abs/1306.5206) [gr-qc].
- [85] Bekir Baytaş, Eugenio Bianchi, and Nelson Yokomizo. “Gluing polyhedra with entanglement in loop quantum gravity”. In: *Phys. Rev. D* 98.2 (2018), p. 026001. DOI: [10.1103/PhysRevD.98.026001](https://doi.org/10.1103/PhysRevD.98.026001). arXiv: [1805.05856](https://arxiv.org/abs/1805.05856) [gr-qc].
- [86] Eugenio Bianchi, Pietro Donà, and Ilya Vilensky. “Entanglement entropy of Bell-network states in loop quantum gravity: Analytical and numerical results”. In: *Phys. Rev. D* 99.8 (2019), p. 086013. DOI: [10.1103/PhysRevD.99.086013](https://doi.org/10.1103/PhysRevD.99.086013). arXiv: [1812.10996](https://arxiv.org/abs/1812.10996) [gr-qc].

- [87] John W. Essam and Michael E. Fisher. “Some Basic Definitions in Graph Theory”. In: *Reviews of Modern Physics* 42.2 (Apr. 1970), pp. 271–288. DOI: [10.1103/RevModPhys.42.271](https://doi.org/10.1103/RevModPhys.42.271).
- [88] Daniele Oriti. “Group field theory as the 2nd quantization of Loop Quantum Gravity”. In: *Class. Quant. Grav.* 33.8 (2016), p. 085005. DOI: [10.1088/0264-9381/33/8/085005](https://doi.org/10.1088/0264-9381/33/8/085005). arXiv: [1310.7786](https://arxiv.org/abs/1310.7786) [gr-qc].
- [89] Daniele Oriti, Daniele Pranzetti, James P. Ryan, and Lorenzo Sindoni. “Generalized quantum gravity condensates for homogeneous geometries and cosmology”. In: *Class. Quant. Grav.* 32.23 (2015), p. 235016. DOI: [10.1088/0264-9381/32/23/235016](https://doi.org/10.1088/0264-9381/32/23/235016). arXiv: [1501.00936](https://arxiv.org/abs/1501.00936) [gr-qc].
- [90] Daniele Oriti, Lorenzo Sindoni, and Edward Wilson-Ewing. “Emergent Friedmann dynamics with a quantum bounce from quantum gravity condensates”. In: *Class. Quant. Grav.* 33.22 (2016), p. 224001. DOI: [10.1088/0264-9381/33/22/224001](https://doi.org/10.1088/0264-9381/33/22/224001). arXiv: [1602.05881](https://arxiv.org/abs/1602.05881) [gr-qc].
- [91] Daniele Oriti, Daniele Pranzetti, and Lorenzo Sindoni. “Black Holes as Quantum Gravity Condensates”. In: *Phys. Rev. D* 97.6 (2018), p. 066017. DOI: [10.1103/PhysRevD.97.066017](https://doi.org/10.1103/PhysRevD.97.066017). arXiv: [1801.01479](https://arxiv.org/abs/1801.01479) [gr-qc].
- [92] Daniele Oriti, Daniele Pranzetti, and Lorenzo Sindoni. “Horizon entropy from quantum gravity condensates”. In: *Phys. Rev. Lett.* 116.21 (2016), p. 211301. DOI: [10.1103/PhysRevLett.116.211301](https://doi.org/10.1103/PhysRevLett.116.211301). arXiv: [1510.06991](https://arxiv.org/abs/1510.06991) [gr-qc].
- [93] Carlo Rovelli. “Partial observables”. In: *Phys. Rev. D* 65 (2002), p. 124013. DOI: [10.1103/PhysRevD.65.124013](https://doi.org/10.1103/PhysRevD.65.124013). arXiv: [gr-qc/0110035](https://arxiv.org/abs/gr-qc/0110035).
- [94] B. Dittrich. “Partial and complete observables for canonical general relativity”. In: *Class. Quant. Grav.* 23 (2006), pp. 6155–6184. DOI: [10.1088/0264-9381/23/22/006](https://doi.org/10.1088/0264-9381/23/22/006). arXiv: [gr-qc/0507106](https://arxiv.org/abs/gr-qc/0507106).
- [95] B. Dittrich. “Partial and complete observables for Hamiltonian constrained systems”. In: *Gen. Rel. Grav.* 39 (2007), pp. 1891–1927. DOI: [10.1007/s10714-007-0495-2](https://doi.org/10.1007/s10714-007-0495-2). arXiv: [gr-qc/0411013](https://arxiv.org/abs/gr-qc/0411013).
- [96] Johannes Tambornino. “Relational Observables in Gravity: a Review”. In: *SIGMA* 8 (2012), p. 017. DOI: [10.3842/SIGMA.2012.017](https://doi.org/10.3842/SIGMA.2012.017). arXiv: [1109.0740](https://arxiv.org/abs/1109.0740) [gr-qc].
- [97] Martin Bojowald, Philipp A Hoehn, and Artur Tsobanjan. “An Effective approach to the problem of time”. In: *Class. Quant. Grav.* 28 (2011), p. 035006. DOI: [10.1088/0264-9381/28/3/035006](https://doi.org/10.1088/0264-9381/28/3/035006). arXiv: [1009.5953](https://arxiv.org/abs/1009.5953) [gr-qc].
- [98] Martin Bojowald, Philipp A Hohn, and Artur Tsobanjan. “Effective approach to the problem of time: general features and examples”. In: *Phys. Rev. D* 83 (2011), p. 125023. DOI: [10.1103/PhysRevD.83.125023](https://doi.org/10.1103/PhysRevD.83.125023). arXiv: [1011.3040](https://arxiv.org/abs/1011.3040) [gr-qc].
- [99] Philipp A. Hoehn, Alexander R.H. Smith, and Maximilian P.E. Lock. “Equivalence of approaches to relational quantum dynamics in relativistic settings”. In: (July 2020). arXiv: [2007.00580](https://arxiv.org/abs/2007.00580) [gr-qc].
- [100] Esteban Castro-Ruiz, Flaminia Giacomini, Alessio Belenchia, and Časlav Brukner. “Quantum clocks and the temporal localisability of events in the presence of gravitating quantum systems”. In: *Nature Commun.* 11.1 (2020), p. 2672. DOI: [10.1038/s41467-020-16013-1](https://doi.org/10.1038/s41467-020-16013-1). arXiv: [1908.10165](https://arxiv.org/abs/1908.10165) [quant-ph].
- [101] Flaminia Giacomini, Esteban Castro-Ruiz, and Časlav Brukner. “Quantum mechanics and the covariance of physical laws in quantum reference frames”. In: *Nature Commun.* 10.1 (2019), p. 494. DOI: [10.1038/s41467-018-08155-0](https://doi.org/10.1038/s41467-018-08155-0). arXiv: [1712.07207](https://arxiv.org/abs/1712.07207) [quant-ph].
- [102] Flaminia Giacomini, Esteban Castro-Ruiz, and Časlav Brukner. “Relativistic Quantum Reference Frames: The Operational Meaning of Spin”. In: *Phys. Rev. Lett.* 123.9 (2019), p. 090404. DOI: [10.1103/PhysRevLett.123.090404](https://doi.org/10.1103/PhysRevLett.123.090404). arXiv: [1811.08228](https://arxiv.org/abs/1811.08228) [quant-ph].

- [103] Luca Marchetti and Daniele Oriti. “Effective relational cosmological dynamics from Quantum Gravity”. In: *JHEP* 05 (2021), p. 025. DOI: [10.1007/JHEP05\(2021\)025](https://doi.org/10.1007/JHEP05(2021)025). arXiv: [2008.02774](https://arxiv.org/abs/2008.02774) [gr-qc].
- [104] Yang Li, Daniele Oriti, and Mingyi Zhang. “Group field theory for quantum gravity minimally coupled to a scalar field”. In: *Class. Quant. Grav.* 34.19 (2017), p. 195001. DOI: [10.1088/1361-6382/aa85d2](https://doi.org/10.1088/1361-6382/aa85d2). arXiv: [1701.08719](https://arxiv.org/abs/1701.08719) [gr-qc].
- [105] Marcin Domagala, Kristina Giesel, Wojciech Kaminski, and Jerzy Lewandowski. “Gravity quantized: Loop Quantum Gravity with a Scalar Field”. In: *Phys. Rev. D* 82 (2010), p. 104038. DOI: [10.1103/PhysRevD.82.104038](https://doi.org/10.1103/PhysRevD.82.104038). arXiv: [1009.2445](https://arxiv.org/abs/1009.2445) [gr-qc].
- [106] Marcin Kisielowski and Jerzy Lewandowski. “Spin-foam model for gravity coupled to massless scalar field”. In: *Class. Quant. Grav.* 36.7 (2019), p. 075006. DOI: [10.1088/1361-6382/aafcc0](https://doi.org/10.1088/1361-6382/aafcc0). arXiv: [1807.06098](https://arxiv.org/abs/1807.06098) [gr-qc].
- [107] Fernando Pastawski, Beni Yoshida, Daniel Harlow, and John Preskill. “Holographic quantum error-correcting codes: Toy models for the bulk/boundary correspondence”. In: *JHEP* 06 (2015), p. 149. DOI: [10.1007/JHEP06\(2015\)149](https://doi.org/10.1007/JHEP06(2015)149). arXiv: [1503.06237](https://arxiv.org/abs/1503.06237) [hep-th].
- [108] Kenneth G. Wilson. “The Renormalization Group: Critical Phenomena and the Kondo Problem”. In: *Rev. Mod. Phys.* 47 (1975), p. 773. DOI: [10.1103/RevModPhys.47.773](https://doi.org/10.1103/RevModPhys.47.773).
- [109] A. Weichselbaum, F. Verstraete, U. Schollwöck, J. I. Cirac, and Jan von Delft. “Variational matrix product state approach to quantum impurity models”. In: *arXiv e-prints*, cond-mat/0504305 (Apr. 2005), cond-mat/0504305. arXiv: [cond-mat/0504305](https://arxiv.org/abs/cond-mat/0504305) [cond-mat.str-el].
- [110] J. Ignacio Cirac and Frank Verstraete. “Renormalization and tensor product states in spin chains and lattices”. In: *Journal of Physics A Mathematical General* 42.50, 504004 (Dec. 2009), p. 504004. DOI: [10.1088/1751-8113/42/50/504004](https://doi.org/10.1088/1751-8113/42/50/504004). arXiv: [0910.1130](https://arxiv.org/abs/0910.1130) [cond-mat.str-el].
- [111] Patrick Hayden, Sepehr Nezami, Xiao-Liang Qi, Nathaniel Thomas, Michael Walter, and Zhao Yang. “Holographic duality from random tensor networks”. In: *JHEP* 11 (2016), p. 009. DOI: [10.1007/JHEP11\(2016\)009](https://doi.org/10.1007/JHEP11(2016)009). arXiv: [1601.01694](https://arxiv.org/abs/1601.01694) [hep-th].
- [112] Xiao-Liang Qi, Zhao Yang, and Yi-Zhuang You. “Holographic coherent states from random tensor networks”. In: *JHEP* 08 (2017), p. 060. DOI: [10.1007/JHEP08\(2017\)060](https://doi.org/10.1007/JHEP08(2017)060). arXiv: [1703.06533](https://arxiv.org/abs/1703.06533) [hep-th].
- [113] Luca Tagliacozzo and Guifre Vidal. “Entanglement Renormalization and Gauge Symmetry”. In: *Phys. Rev. B* 83 (2011), p. 115127. DOI: [10.1103/PhysRevB.83.115127](https://doi.org/10.1103/PhysRevB.83.115127). arXiv: [1007.4145](https://arxiv.org/abs/1007.4145) [cond-mat.str-el].
- [114] Luca Tagliacozzo, Alessio Celi, and Maciej Lewenstein. “Tensor Networks for Lattice Gauge Theories with continuous groups”. In: *Phys. Rev. X* 4.4 (2014), p. 041024. DOI: [10.1103/PhysRevX.4.041024](https://doi.org/10.1103/PhysRevX.4.041024). arXiv: [1405.4811](https://arxiv.org/abs/1405.4811) [cond-mat.str-el].
- [115] Mark Van Raamsdonk. “Building up spacetime with quantum entanglement”. In: *Gen. Rel. Grav.* 42 (2010), pp. 2323–2329. DOI: [10.1142/S0218271810018529](https://doi.org/10.1142/S0218271810018529). arXiv: [1005.3035](https://arxiv.org/abs/1005.3035) [hep-th].
- [116] Brian Swingle. “Constructing holographic spacetimes using entanglement renormalization”. In: (Sept. 2012). arXiv: [1209.3304](https://arxiv.org/abs/1209.3304) [hep-th].
- [117] Ning Bao, Geoffrey Penington, Jonathan Sorce, and Aron C. Wall. “Beyond Toy Models: Distilling Tensor Networks in Full AdS/CFT”. In: *JHEP* 11 (2019), p. 069. DOI: [10.1007/JHEP11\(2019\)069](https://doi.org/10.1007/JHEP11(2019)069). arXiv: [1812.01171](https://arxiv.org/abs/1812.01171) [hep-th].
- [118] Pablo Arrighi, Marios Christodoulou, and Amélia Durbec. “Quantum superpositions of graphs”. In: (Oct. 2020). arXiv: [2010.13579](https://arxiv.org/abs/2010.13579) [gr-qc].
- [119] A. Barbieri. “Quantum tetrahedra and simplicial spin networks”. In: *Nucl. Phys. B* 518 (1998), pp. 714–728. DOI: [10.1016/S0550-3213\(98\)00093-5](https://doi.org/10.1016/S0550-3213(98)00093-5). arXiv: [gr-qc/9707010](https://arxiv.org/abs/gr-qc/9707010).
- [120] Qian Chen and Etera R. Livine. “Loop Quantum Gravity’s Boundary Maps”. In: (Mar. 2021). arXiv: [2103.08409](https://arxiv.org/abs/2103.08409) [gr-qc].

- [121] W. H. Zurek. “Pointer basis of quantum apparatus: Into what mixture does the wave packet collapse?” In: *Phys. Rev. D* 24 (6 Sept. 1981), pp. 1516–1525. DOI: [10.1103/PhysRevD.24.1516](https://doi.org/10.1103/PhysRevD.24.1516). URL: <https://link.aps.org/doi/10.1103/PhysRevD.24.1516>.
- [122] W. H. Zurek. “Environment-induced superselection rules”. In: *Phys. Rev. D* 26 (8 Oct. 1982), pp. 1862–1880. DOI: [10.1103/PhysRevD.26.1862](https://doi.org/10.1103/PhysRevD.26.1862). URL: <https://link.aps.org/doi/10.1103/PhysRevD.26.1862>.
- [123] W. H. Zurek. “Decoherence and the transition from quantum to classical – REVISITED”. In: *Physics Today* 44 (July 2003). DOI: [10.1063/1.881293](https://doi.org/10.1063/1.881293).
- [124] Wojciech Hubert Zurek. “Quantum darwinism”. In: *Nature physics* 5.3 (2009), p. 181.
- [125] Harold Ollivier, David Poulin, and Wojciech H. Zurek. “Objective Properties from Subjective Quantum States: Environment as a Witness”. In: *Phys. Rev. Lett.* 93 (22 Nov. 2004), p. 220401. DOI: [10.1103/PhysRevLett.93.220401](https://doi.org/10.1103/PhysRevLett.93.220401). URL: <https://link.aps.org/doi/10.1103/PhysRevLett.93.220401>.
- [126] Harold Ollivier, David Poulin, and Wojciech H. Zurek. “Environment as a witness: Selective proliferation of information and emergence of objectivity in a quantum universe”. In: *Phys. Rev. A* 72 (4 Oct. 2005), p. 042113. DOI: [10.1103/PhysRevA.72.042113](https://doi.org/10.1103/PhysRevA.72.042113). URL: <https://link.aps.org/doi/10.1103/PhysRevA.72.042113>.
- [127] R. Blume-Kohout and W.H. Zurek. “Quantum Darwinism: Entanglement, branches, and the emergent classicality of redundantly stored quantum information”. In: *Phys. Rev. A* 73 (6 June 2006), p. 062310. DOI: [10.1103/PhysRevA.73.062310](https://doi.org/10.1103/PhysRevA.73.062310). URL: <https://link.aps.org/doi/10.1103/PhysRevA.73.062310>.
- [128] R. Horodecki, J. K. Korbicz, and P. Horodecki. “Quantum origins of objectivity”. In: *Phys. Rev. A* 91 (3 Mar. 2015), p. 032122. DOI: [10.1103/PhysRevA.91.032122](https://doi.org/10.1103/PhysRevA.91.032122). URL: <https://link.aps.org/doi/10.1103/PhysRevA.91.032122>.
- [129] Thao P. Le and Alexandra Olaya-Castro. “Strong Quantum Darwinism and Strong Independence are Equivalent to Spectrum Broadcast Structure”. In: *Phys. Rev. Lett.* 122 (1 Jan. 2019), p. 010403. DOI: [10.1103/PhysRevLett.122.010403](https://doi.org/10.1103/PhysRevLett.122.010403). URL: <https://link.aps.org/doi/10.1103/PhysRevLett.122.010403>.
- [130] Robin Blume-Kohout and Wojciech H. Zurek. “Quantum Darwinism in Quantum Brownian Motion”. In: *Phys. Rev. Lett.* 101 (24 Dec. 2008), p. 240405. DOI: [10.1103/PhysRevLett.101.240405](https://doi.org/10.1103/PhysRevLett.101.240405). URL: <https://link.aps.org/doi/10.1103/PhysRevLett.101.240405>.
- [131] M. Zwolak, H.T. Quan, and W.H. Zurek. “Quantum Darwinism in a Mixed Environment”. In: *Phys. Rev. Lett.* 103 (11 Sept. 2009), p. 110402. DOI: [10.1103/PhysRevLett.103.110402](https://doi.org/10.1103/PhysRevLett.103.110402). URL: <https://link.aps.org/doi/10.1103/PhysRevLett.103.110402>.
- [132] C. Jess Riedel and Wojciech H. Zurek. “Quantum Darwinism in an Everyday Environment: Huge Redundancy in Scattered Photons”. In: *Phys. Rev. Lett.* 105 (2 July 2010), p. 020404. DOI: [10.1103/PhysRevLett.105.020404](https://doi.org/10.1103/PhysRevLett.105.020404). URL: <https://link.aps.org/doi/10.1103/PhysRevLett.105.020404>.
- [133] C.J. Riedel, W.H. Zurek, and M. Zwolak. “The rise and fall of redundancy in decoherence and quantum Darwinism”. In: *New J. Phys.* 14.8 (2012), p. 083010. DOI: [10.1088/1367-2630/14/8/083010](https://doi.org/10.1088/1367-2630/14/8/083010). URL: <http://stacks.iop.org/1367-2630/14/i=8/a=083010>.
- [134] F. Galve, R. Zambrini, and S. Maniscalco. “Non-Markovianity hinders Quantum Darwinism”. In: *Sci. Rep.* 6 (2015), p. 19607. DOI: [10.1038/srep19607](https://doi.org/10.1038/srep19607).
- [135] N. Balaneskovic. *Random Unitary Evolution Model of Quantum Darwinism with pure decoherence*. arXiv:1510.02386. 2015. eprint: [1510.02386](https://arxiv.org/abs/1510.02386).
- [136] J. Tuziemiński and J. K. Korbicz. “Dynamical objectivity in quantum Brownian motion”. In: *Europhys. Lett.* 112.4 (2015), p. 40008. DOI: [10.1209/0295-5075/112/40008](https://doi.org/10.1209/0295-5075/112/40008). URL: <http://stacks.iop.org/0295-5075/112/i=4/a=40008>.

- [137] J. Tuziemski and J.K. Korbicz. “Objectivisation In Simplified Quantum Brownian Motion Models”. In: *Photonics* 2.1 (2015), p. 228. DOI: [10.3390/photonics2010228](https://doi.org/10.3390/photonics2010228). URL: <http://www.mdpi.com/2304-6732/2/1/228>.
- [138] J Tuziemski and J K Korbicz. “Analytical studies of spectrum broadcast structures in quantum Brownian motion”. In: *J. Phys. A: Math. Theor.* 49.44 (2016), p. 445301. DOI: [10.1088/1751-8113/49/44/445301](https://doi.org/10.1088/1751-8113/49/44/445301). URL: <http://stacks.iop.org/1751-8121/49/i=44/a=445301>.
- [139] N. Balaneskovic and M. Mendler. “Dissipation, dephasing and quantum Darwinism in qubit systems with random unitary interactions”. In: *Eur. Phys. J. D* 70.9 (2016), p. 177. ISSN: 1434-6079. DOI: [10.1140/epjd/e2016-70174-9](https://doi.org/10.1140/epjd/e2016-70174-9). URL: <https://doi.org/10.1140/epjd/e2016-70174-9>.
- [140] Aniello Lampo, Jan Tuziemski, Maciej Lewenstein, and Jarosław K. Korbicz. “Objectivity in the non-Markovian spin-boson model”. In: *Phys. Rev. A* 96 (1 July 2017), p. 012120. DOI: [10.1103/PhysRevA.96.012120](https://doi.org/10.1103/PhysRevA.96.012120). URL: <https://link.aps.org/doi/10.1103/PhysRevA.96.012120>.
- [141] Graeme Pleasance and Barry M. Garraway. “Application of quantum Darwinism to a structured environment”. In: *Phys. Rev. A* 96 (6 Dec. 2017), p. 062105. DOI: [10.1103/PhysRevA.96.062105](https://doi.org/10.1103/PhysRevA.96.062105). URL: <https://link.aps.org/doi/10.1103/PhysRevA.96.062105>.
- [142] T.P. Le and A. Olaya-Castro. “Objectivity (or lack thereof): Comparison between predictions of quantum Darwinism and spectrum broadcast structure”. In: *Phys. Rev. A* 98 (3 2018), p. 032103. DOI: [10.1103/PhysRevA.98.032103](https://doi.org/10.1103/PhysRevA.98.032103). URL: <https://link.aps.org/doi/10.1103/PhysRevA.98.032103>.
- [143] Ming-Cheng Chen, Han-Sen Zhong, Yuan Li, Dian Wu, Xi-Lin Wang, Li Li, Nai-Le Liu, Chao-Yang Lu, and Jian-Wei Pan. “Emergence of classical objectivity of quantum Darwinism in a photonic quantum simulator”. In: *Science Bulletin* 64.9 (2019), pp. 580–585.
- [144] Mario A. Ciampini, Giorgia Pinna, Paolo Mataloni, and Mauro Paternostro. “Experimental signature of quantum Darwinism in photonic cluster states”. In: *Phys. Rev. A* 98 (2 Aug. 2018), p. 020101. DOI: [10.1103/PhysRevA.98.020101](https://doi.org/10.1103/PhysRevA.98.020101). URL: <https://link.aps.org/doi/10.1103/PhysRevA.98.020101>.
- [145] T. K. Unden, D. Louzon, M. Zwolak, W. H. Zurek, and F. Jelezko. “Revealing the Emergence of Classicality Using Nitrogen-Vacancy Centers”. In: *Phys. Rev. Lett.* 123 (14 Oct. 2019), p. 140402. DOI: [10.1103/PhysRevLett.123.140402](https://doi.org/10.1103/PhysRevLett.123.140402). URL: <https://link.aps.org/doi/10.1103/PhysRevLett.123.140402>.
- [146] X. Qi and D. Ranard. *Emergent classicality in general multipartite states and channels*. 2020. arXiv: [2001.01507](https://arxiv.org/abs/2001.01507) [quant-ph].
- [147] G. Aubrun, L. Lami, C. Palazuelos, S.J. Szarek, and A. Winter. “Universal gaps for XOR games from estimates on tensor norm ratios”. In: *Preprint arXiv:1809.10616* (2018).
- [148] H. Ollivier and W.H. Zurek. “Quantum discord: a measure of the quantumness of correlations”. In: *Phys. Rev. Lett.* 88.1 (2001), p. 017901.
- [149] L. Henderson and V. Vedral. “Classical, quantum and total correlations”. In: *J. Phys. A* 34.35 (2001), p. 6899.
- [150] M.E. Shirokov. “On the Energy-Constrained Diamond Norm and Its Application in Quantum Information Theory”. In: *Problems Inform. Transmission* 54.1 (2018), pp. 20–33. ISSN: 1608-3253. DOI: [10.1134/S0032946018010027](https://doi.org/10.1134/S0032946018010027).
- [151] A. Winter. “Energy-constrained diamond norm with applications to the uniform continuity of continuous variable channel capacities”. In: *Preprint arXiv:1712.10267* (2017).
- [152] D. Aharonov, A. Kitaev, and N. Nisan. “Quantum Circuits with Mixed States”. In: *Proceedings of the Thirtieth Annual ACM Symposium on Theory of Computing*. STOC ’98. Dallas, Texas, USA: ACM, 1998, pp. 20–30. ISBN: 0-89791-962-9. DOI: [10.1145/276698.276708](https://doi.org/10.1145/276698.276708).

- [153] M.F. Sacchi. “Optimal discrimination of quantum operations”. In: *Phys. Rev. A* 71 (6 2005), p. 062340. DOI: [10.1103/PhysRevA.71.062340](https://doi.org/10.1103/PhysRevA.71.062340).
- [154] J. Watrous. “Semidefinite Programs for Completely Bounded Norms”. In: *Theory Comput.* 5.11 (2009), pp. 217–238. DOI: [10.4086/toc.2009.v005a011](https://doi.org/10.4086/toc.2009.v005a011).
- [155] S. Weis and M. Shirokov. “Extreme points of the set of quantum states with bounded energy”. In: *Preprint arXiv:2002.03969* (2020).
- [156] A. Winter. “Tight Uniform Continuity Bounds for Quantum Entropies: Conditional Entropy, Relative Entropy Distance and Energy Constraints”. In: *Commun. Math. Phys.* 347.1 (2016), pp. 291–313. ISSN: 1432-0916. DOI: [10.1007/s00220-016-2609-8](https://doi.org/10.1007/s00220-016-2609-8).
- [157] J. Watrous. “Lecture Notes – Theory of Quantum Information”. In: (2011). eprint: <https://cs.uwaterloo.ca/~watrous/LectureNotes.html>.
- [158] A.S. Holevo. *Quantum Systems, Channels, Information: A Mathematical Introduction*. De Gruyter Studies in Mathematical Physics. De Gruyter, 2012. ISBN: 9783110273403.
- [159] R. Koenig. “The conditional entropy power inequality for Gaussian quantum states”. In: *J. Math. Phys.* 56.2 (2015), p. 022201. DOI: [10.1063/1.4906925](https://doi.org/10.1063/1.4906925).
- [160] G. De Palma and D. Trevisan. “The Conditional Entropy Power Inequality for Bosonic Quantum Systems”. In: *Commun. Math. Phys.* 360.2 (2018), pp. 639–662. ISSN: 1432-0916. DOI: [10.1007/s00220-017-3082-8](https://doi.org/10.1007/s00220-017-3082-8).
- [161] K.K. Sabapathy and A. Winter. “Non-Gaussian operations on bosonic modes of light: Photon-added Gaussian channels”. In: *Phys. Rev. A* 95 (6 2017), p. 062309. DOI: [10.1103/PhysRevA.95.062309](https://doi.org/10.1103/PhysRevA.95.062309).
- [162] L. Lami, K.K. Sabapathy, and A. Winter. “All phase-space linear bosonic channels are approximately Gaussian dilatable”. In: *New J. Phys.* 20.11 (2018), p. 113012.
- [163] Y. Lim, S. Lee, J. Kim, and K. Jeong. “Upper bounds on the quantum capacity for a general attenuator and amplifier”. In: *Phys. Rev. A* 99 (5 2019), p. 052326. DOI: [10.1103/PhysRevA.99.052326](https://doi.org/10.1103/PhysRevA.99.052326).
- [164] S. Becker, N. Datta, L. Lami, and C. Rouzé. “Convergence rates for the quantum central limit theorem”. In: *Preprint arXiv:1912.06129* (2019).
- [165] K. Modi, A. Brodutch, H. Cable, T. Paterek, and V. Vedral. “The classical-quantum boundary for correlations: discord and related measures”. In: *Rev. Mod. Phys.* 84.4 (2012), p. 1655.
- [166] G. Adesso, T.R. Bromley, and M. Cianciaruso. “Measures and applications of quantum correlations”. In: *J. Phys. A* 49.47 (2016), p. 473001.
- [167] Daniele Oriti. “Levels of spacetime emergence in quantum gravity”. In: (July 2018). arXiv: [1807.04875 \[physics.hist-ph\]](https://arxiv.org/abs/1807.04875).
- [168] Xiao-Liang Qi. “Does gravity come from quantum information?” In: *Nature Phys.* 14.10 (2018), pp. 984–987. DOI: [10.1038/s41567-018-0297-3](https://doi.org/10.1038/s41567-018-0297-3).
- [169] Xiao-Liang Qi, Zhao Yang, and Yi-Zhuang You. “Holographic coherent states from random tensor networks”. In: *JHEP* 08 (2017), p. 060. DOI: [10.1007/JHEP08\(2017\)060](https://doi.org/10.1007/JHEP08(2017)060). arXiv: [1703.06533 \[hep-th\]](https://arxiv.org/abs/1703.06533).
- [170] Fabio Anzà and Goffredo Chirco. “Fate of the Hoop Conjecture in Quantum Gravity”. In: *Phys. Rev. Lett.* 119.23 (2017), p. 231301. DOI: [10.1103/PhysRevLett.119.231301](https://doi.org/10.1103/PhysRevLett.119.231301). arXiv: [1703.05241 \[gr-qc\]](https://arxiv.org/abs/1703.05241).
- [171] Daniele Oriti, Daniele Pranzetti, James P Ryan, and Lorenzo Sindoni. “Generalized quantum gravity condensates for homogeneous geometries and cosmology”. In: *Class. Quant. Grav.* 32.23 (2015), p. 235016. DOI: [10.1088/0264-9381/32/23/235016](https://doi.org/10.1088/0264-9381/32/23/235016). arXiv: [1501.00936 \[gr-qc\]](https://arxiv.org/abs/1501.00936).

- [172] Daniele Oriti, Daniele Pranzetti, and Lorenzo Sindoni. “Black Holes as Quantum Gravity Condensates”. In: *Phys. Rev. D* 97.6 (Mar. 2018), p. 66017. ISSN: 2470-0010. DOI: [10.1103/PhysRevD.97.066017](https://doi.org/10.1103/PhysRevD.97.066017). arXiv: [1801.01479 \[gr-qc\]](https://arxiv.org/abs/1801.01479). URL: <http://arxiv.org/abs/1801.01479%20http://dx.doi.org/10.1103/PhysRevD.97.066017%20https://link.aps.org/doi/10.1103/PhysRevD.97.066017>.
- [173] Donald Marolf. “Unitarity and Holography in Gravitational Physics”. In: *Phys. Rev. D* 79 (2009), p. 044010. DOI: [10.1103/PhysRevD.79.044010](https://doi.org/10.1103/PhysRevD.79.044010). arXiv: [0808.2842 \[gr-qc\]](https://arxiv.org/abs/0808.2842).
- [174] Chandramouli Chowdhury, Victor Godet, Olga Papadoulaki, and Suvrat Raju. “Holography from the Wheeler-DeWitt equation”. In: (July 2021). arXiv: [2107.14802 \[hep-th\]](https://arxiv.org/abs/2107.14802).
- [175] Laurent Freidel. “Gravitational Energy, Local Holography and Non-equilibrium Thermodynamics”. In: *Class. Quant. Grav.* 32.5 (2015), p. 055005. DOI: [10.1088/0264-9381/32/5/055005](https://doi.org/10.1088/0264-9381/32/5/055005). arXiv: [1312.1538 \[gr-qc\]](https://arxiv.org/abs/1312.1538).
- [176] William Donnelly, Laurent Freidel, Seyed Farooq Moosavian, and Antony J. Speranza. “Gravitational edge modes, coadjoint orbits, and hydrodynamics”. In: *JHEP* 09 (2021), p. 008. DOI: [10.1007/JHEP09\(2021\)008](https://doi.org/10.1007/JHEP09(2021)008). arXiv: [2012.10367 \[hep-th\]](https://arxiv.org/abs/2012.10367).
- [177] Aram W. Harrow. “The Church of the Symmetric Subspace”. In: arXiv:1308.6595 (Aug. 2013), arXiv:1308.6595. arXiv: [1308.6595 \[quant-ph\]](https://arxiv.org/abs/1308.6595).
- [178] Michael Tinkham. *Group theory and quantum mechanics*. Courier Corporation, 2003.
- [179] W. Matthews, S. Wehner, and A. Winter. “Distinguishability of Quantum States Under Restricted Families of Measurements with an Application to Quantum Data Hiding”. In: *Commun. Math. Phys.* 291.3 (2009), pp. 813–843.
- [180] L. Lami, C. Palazuelos, and A. Winter. “Ultimate Data Hiding in Quantum Mechanics and Beyond”. In: *Commun. Math. Phys.* 361.2 (2018), pp. 661–708. DOI: [10.1007/s00220-018-3154-4](https://doi.org/10.1007/s00220-018-3154-4).
- [181] R. Bhatia. *Matrix Analysis*. Graduate Texts in Mathematics. Springer New York, 2013.
- [182] L. Lami, S. Khatri, G. Adesso, and M.M. Wilde. “Extendibility of Bosonic Gaussian States”. In: *Phys. Rev. Lett.* 123 (5 2019), p. 050501. DOI: [10.1103/PhysRevLett.123.050501](https://doi.org/10.1103/PhysRevLett.123.050501).